Aus der Klinik and Poliklinik für Psychatrie und Psychotherapie

Klinik der Ludwig-Maximilians-Universität München

Vostand: Prof Dr. med. Peter Falkai

Thousand and one amino acid kinase 2 (TAOK2) modulates Hippo pathway activity and impacts on synaptic plasticity

Dissertation

zum Erwerb des Doktorgrades der Humanbiologie

an der Medizinischen Fakultät der

Ludwig-Maximilians-Universität zu München

vorgelegt von

Xiao Ma

aus

Shangqiu

2021

Mit Genehmigung der Medizinischen Fakultät
der Universität München

Berichterstatter: PD Dr. Michael Wehr

Mitberichterstatter: Prof. Dr. Thomas Gudermann

Prof. Dr. Andreas Dendorfer

Mitbetreuung durch

denpromovierten Mitarbeiter:

Dekan: Prof. Dr. med. Thomas Gudermann

Tag der mündlichen Prüfung: 16.12.2021

Affidavit

Herewith I declare that I prepared the thesis entitled: “Thousand and one amino acid kinase 2 (TAOK2) modulates Hippo pathway activity and impacts on synaptic plasticity” on my own and with no other sources and aids than quoted.

Xiao Ma

12th May,2021

Munich

Table of content

Zusammenfassung (Deutsch)

Der Hippo-Signalweg ist ein evolutionär konservierter Signalweg und spielt eine entscheidende Rolle bei der Kontrolle der Gewebehomöostase, der Zelldifferenzierung und der richtigen Entwicklung der Organgröße durch die Regulierung der Zellproliferation und Apoptose. Der Hippo-Signalweg wurde als Tumoursuppressor-Signalweg identifiziert und ist an verschiedenen Krebsarten beteiligt. Darüber hinaus deutet Vieles darauf hin, dass der Hippo-Signalweg in mehreren Stadien an der neuronalen Entwicklung beteiligt ist, von der Proliferation neuronaler Stammzellen (NSCs) bis zur Apoptose neuronaler Zelltypen. Dieser Signalweg kann nicht nur auf Signale reagieren, die das Wachstum fördern oder begrenzen, sondern auch verschiedene zelluläre Signale integrieren, einschließlich mechano-sensorischer Stimuli und Stresssignale. Auf molekularer Ebene reguliert der Hippo-Signalweg die Aktivität des Co-Transkriptionsaktivators YAP1, der der Haupteffektor des Signalwegs ist. Der Kern des Weges besteht aus einer sog. Kinasekassette, die die Kinasen STK3/4 und LATS1/2 umfasst, die wiederum die Aktivität von YAP1 einschränken. Die Aktivität des Signalwegs wird darüber hinaus durch Polaritätsproteine wie Mitglieder der WWC-Familie oder Proteine der AMOT-Familie und weitere Kinasen und Strukturproteine, aber auch Membranrezeptoren gesteuert.

Im ersten Teil der Studie verwendete ich das zellbasierte genetisch kodierte Split-TEV-Testsystem, um Protein-Protein-Wechselwirkungen zwischen Kernkomponenten und Hauptregulatoren des Hippo-Signalwegs zu analysieren. Das Ziel war es, bisher verborgene Wechselwirkungen zwischen Komponenten zu identifizieren, die die Aktivität des Hippo-Signalwegs modulieren könnten. Als zentralen Modulator der Hippo-Signalisierung habe ich TAOK2 identifiziert. TAOK2 bindet an LATS1 und phosphoryliert dieses. Die Überexpression von TAOK2 erhöhte die Phosphorylierung von LATS1, verringerte die YAP1-Transkriptionsaktivität und führte zu einer verringerten Proliferation von HEK293-Zellen. Dagegen führte eine Herunterregulierung von TAOK2 zu einer Reduzierung der LATS1-Phosphorylierung und einer erhöhten Proliferationsrate. Diese Beobachtungen aus der Zellkultur korrelieren mit einer reduzierten TAOK2- Expression und einer reduzierten Überlebensrate von Patienten, die an bestimmten Krebsarten, wie

z.B. Lungen- und Pankreas-Adenokarzinome oder Gliome niedrigen Malignitätsgrades, gelitten haben.

Da der Hippo-Signal-Weg auch an der Proliferation neuronaler Vorläufer und der Entwicklung von Neuronen beteiligt ist, beschreibt der zweite Teil der Studie mögliche Rollen von TAOK2 in synaptischen Signalnetzwerken. Vorarbeiten aus unserem Labor an Mäusen, bei denen Taok2 spezifisch in Neuronen im Gehirn während der frühen Phasen der Nervenentwicklung mit einer Emx1-Cre-Line ausgeschaltet wurde, zeigten mit einem milden Hyperaktivitätsphänotyp und leichten kognitiven Defizite ein verändertes Verhaltensprofil. Darüber hinaus haben Kollegen in Mäusen, die einen kompletten Taok2-Knockout (Taok2-ko) tragen, einen eindeutigen Hyperaktivitätsphänotyp sowie Defizite in der Kognition und im Angst- und Sozialverhalten beschrieben. Um diese Phänotypen auf zellulärer Ebene besser zu verstehen, habe ich in meiner Arbeit den Effekt einer Taok2-Inaktivierung in primären kortikalen Neuronenkulturen aus der Maus untersucht. Eine zelluläre Profilierung anhand des multiparametrischen cisProfiler-Assays in Taok2-ko-Neuronen zeigte, dass die genetische Deletion von Taok2 die Aktivität von MAP-Kinase-Signalwegen verringerte, die nach synaptischer Aktivität, z.B. durch Stimulation mit AMPA, aktiviert werden. RNAseq-Analysen in primären Maus-Neuronen mit TAOK2-Überexpression und shRNA-vermittelter Taok2-Inaktivierung wiesen gemeinsame differentiell regulierte Gene (DEGs) auf, die für den Zellzyklus und den Notch-Signalweg angereichert waren. Auf Proteinebene verursachte die Inaktivierung von Taok2 in primären Mausneuronen, die mit AMPA bzw. NMDA stimuliert wurden, eine Verringerung des Phosphorylierungsniveaus der MAP-Kinase Erk. Eine Inaktivierung von Taok2 in Neuronen führt somit unter definierten Bedingungen zu einer verringerten Weiterleitung der synaptischen Aktivität in Neuronen, was die in Taok2-ko-Mäusen beobachteten Verhaltensdefizite auf molekularer Ebene erklären könnte.

Abstract (English)

The Hippo-signaling pathway, which is an evolutionarily conserved pathway, has a crucial function in the field of controlling the homeostasis of different tissues, cell differentiation across diverse organisms, and coordinates the proper size of organ during development by regulating the proliferation process and the apoptosis of cells. It has been identified that Hippo-signaling is a tumor-suppressing pathway and has been related with various types of cancers. In addition, accumulating researchers indicate that Hippo-signaling pathway participates the neuronal development at multiple stages, involving in the proliferation process of neural stem cells (NSCs) and neuronal death. This pathway not only responds to signals promoting or limiting growth, but also integrates diverse cellular cues including mechano-sensory inputs and energy stress. At the molecular level, Hippo signaling regulates the activity of the co-transcriptional activator YAP1, which is the main effector of the pathway. Two kinases: STK3/4 and LATS1/2, which can moderate the activity of YAP1, comprise a kinase cassette that composes the key component of the Hippo pathway. Upstream, the polarity proteins, such as WWC family members or AMOT family proteins, other kinases, scaffolding proteins, and transmembrane receptors control the activity of the pathway.

In the first part of the study, I used the cell-based genetically encoded split TEV assay method to profile protein-protein interactions among Hippo pathway core components and major regulators to identify so far hidden interactions among components that may modulate Hippo pathway activity. I identified TAOK2 as central modulator of Hippo signaling. TAOK2 binds to and phosphorylate LATS1. Overexpression of TAOK2 reduced YAP1 transcriptional activity and led to decreased proliferation of HEK293 cells. In contrast, downregulation of TAOK2 led to a reduction in LATS1 phosphorylation levels and an increased proliferation. These observations from cell culture correlate with reduced TAOK2 expression and survival in patients who have suffered from certain cancers, such as lung and pancreatic adenocarcinomas or low-grade gliomas.

Due to the involvement of this pathway in the proliferation of neural precursors and development of neurons as well, the second part of this study describes the potential role

of TAOK2 in synaptic signaling networks. Preliminary work from our lab in mice in which Taok2 was specifically inactivated in neurons in the brain during early neurodevelopment using an Emx1-Cre driver line showed an altered behavioral profile with a mild hyperactivity phenotype and mild cognitive deficits. In addition, colleagues have described a distinct hyperactivity phenotype in mice carrying a complete Taok2 knockout (Taok2-ko), as well as deficits in social behavior, cognition and anxiety. To better understand these phenotypes at the molecular level, my work investigated the effect of Taok2 inactivation in primary murine cortical neuron cultures. A cellular profiling using the multiparametric cisProfiler assay in Taok2-ko neurons showed that the genetic inactivation of Taok2 reduced the activity of MAP kinase signaling which is, e.g., after AMPA stimulation, activated upon synaptic transmission. RNAseq-based analyses for neurons either with overexpressed human TAOK2 or shRNA-depleted Taok2 shared differentially regulated genes (DEGs) that were enriched for the cell cycle and Notch signaling. At the protein level, an inactivation of Taok2 in neurons, stimulated with AMPA or NMDA, caused a reduction in the phosphorylation levels of the MAP kinase Erk1/2. An inactivation of Taok2 in neurons thus led to reduced transmission of synaptic activity in neurons under defined conditions, which could explain the behavioral deficits observed in Taok2-ko mice at the molecular level.

List of Figures

List of Tables

List of Abbreviations

A	Amygdala
AA	Amino acids
AAV	Adeno-associated viruses
AMOT	Angiomotin
AMOTL1/2	AMOT-like proteins 1 and 2
AMPAR	α-amino-3-hydroxy-5-methyl-4-isoxazolepropionic acid receptors
ATM	Ataxia telangiectasia mutated
AU	Arbitrary units
AUC	Area under curve
BC	Barcode
bHLH	Basic helix-loop-helix
BIC	Bicuculline
Bim	Bcl-2 interacting mediator
BMP2	Bone morphogenetic protein2
CaMKII	Calcium/calmodulin dependent protein kinase II
CCK-8	Cell counting kit-8
ccnd1	Cyclin D1
CK1δ/ε	Casein kinase 1 delta/epsilon
Co-IP	Co-immunoprecipitation
Cre	Cyclization recombinase
CRISPR	Clusters of regularly interspaced short palindromic repeats
CTEV	C-terminal TEV moiety
Cx	Cortex
dCas9-KRAB	Dead Cas9-KRAB
DEGs	Differentially expressed genes
DIV	Day in vitro
DPK	Dendritic cell-derived protein kinase
DVL	Disheveled
ER	Endoplasmic reticulum
FC	Fear conditioning
floxed	loxP flanked
GC	Genomic copies
GO	Gene ontology
GPCRs	G protein-coupled receptors
GV	GAL4-VP16
HD	Huntington's disease
Het	Heterozygous
HIF1α	Hypoxia-inducible factor 1-alpha
hNPCs	Human neural progenitor cells

Hpc	Hippocampus
HPIN	Hippo pathway interaction network
Hrk	Harakiri
hUbC	Human ubiquitin C
ID	Intellectual disability
IEG	Immediate early gene
IL-17RA	Interleukin-17 receptor A
KO	Knockout
LATS1/2	Large tumour suppressor 1/2
loxP	Locus of x-over, P1
LPA	Lysophosphatidic acid
LTD	Long-term depression
LTP	Long-term potentiation
LTR	Long terminal repeats
luc	Luciferase
MAP3K	MAP kinase kinase kinase
MLP	Major late promoter
MOB1/2	MOB kinase activator 1A/B
STK3/4	Sterile 20-like protein kinase 1/2
NDR	Nuclear Dbf2-realted
NF2	Neurofibromin 2
NGS	Next-generation sequencing
NMDAR	N-methyl-d-aspartate receptors
NSCs	Neural stem cells
NTB	Neurocognitive test battery
NTEV	N-terminal moiety of the TEV protease
ORF	Open reading frame
pA	Poly A
PARP	Poly ADP-ribose polymerase
PEI	Polyethlyenimin
PLL	Poly-L-lysine
PPI	Prepulse inhibition
PPIs	Protein-protein interactions
PSD	Postsynaptic density
RNAseq	RNA sequencing
ROCK-1	Rho kinase 1
RRID	Research resource identifiers
rtTA	Reverse tetracycline-controlled transactivator
S1P	Sphingosine 1-phosphate
SAPK	Stress-activated protein kinase
SARAH	Sav/Rassf/Hpo
SAV1	Salvador 1

SBD	Substrate-binding domain
Scr	Scramble
SEPT7	Septin 7
SZ	Schizophrenia
TAOK2-KD	TAOK2 kinase dead
TAOKs	Thousand and one amino acid kinases
TAZ	Transcriptional co-activator with PDZ-binding motif
tcs	TEV cleavage site
TEAD	Transcriptional enhanced associate domain
TEV	Tobacco etch virus
tg	Transgenic
TRAF	Necrosis factor receptor-associated factor
TRE	rtTA element
T-SSRs	Tyrosine site specific recombinases
TST	Tail suspension test
UAS	Upstream activated sequences
WPRE	Woodchuck hepatitis virus posttranscriptional response element
WT	Wild type
WTIP	Wilms tumour protein 1-interacting protein
WWTR1	WW domain containing transcription regulator 1
YAP	Yes-associated protein

1. Introduction

1.1 TAOK2 and Hippo signaling

1.1.1 TAOK family

It is known that mitogen-activated protein kinases (MAPKs) can activate or de-activate their downstream targets by phosphorylating the serine residues and threonine residues on their substrates (Pearson et al., 2001). For the thousand and one protein kinases (TAOKs) which belong to a protein family named as the MAP kinase kinase kinase (MAP3K), in mammals, there are three members TAOK 1, 2, and 3 (Yustein et al., 2003). TAOK1 (also named as microtubule affinity regulating kinase kinase, MARKK) has a length of 1001 amino acid residues. The gene encoding it is situated on 16q11.2 (Zihni et al., 2006). TAOK2, the largest of the three proteins, is also encoded by a gene situated on 16q11.2. It is also called PSK1. It has two isoforms, TAOK2-α has a length of 1235 residues and TAOK2-β has a length of 1049 residues (Moore et al., 2000). Both TAOK1 and TAOK2 hold a specific residue:Ser181, which could be phosphorylated (Figure 1) (Wojtala et al., 2011). TAOK3 has 898 amino acid residues. It is also named as JIK: JNK/SAPK-Inhibitory Kinase. It is encoded by a gene situated on 12q24.23 (Tassi et al., 1999; Yustein et al., 2003; W. Zhang et al., 2000). The activation of TAOK3 is correlated with its phosphorylation at Ser324 (Figure 1.) (Raman et al., 2007). According to the studies, the TAOKs have functions in regulating various signaling pathways, which include the JNK-SAPK pathway, p38-MAPK pathway, and the Hippo signaling pathway, as shown in Table 1 (Ye et al., 2020).

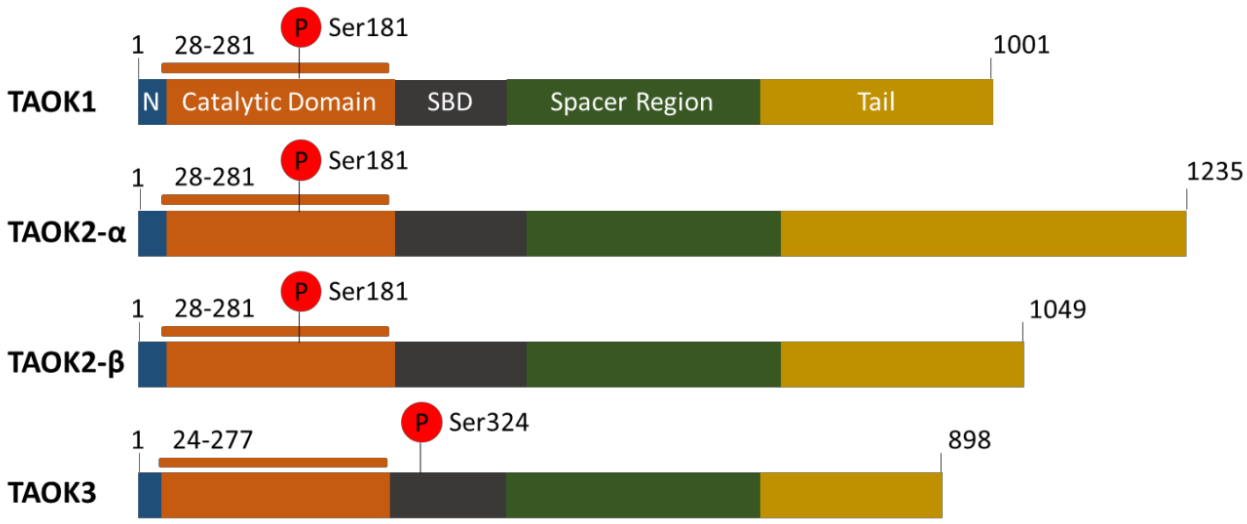

Figure 1. Structure features of TAOKs.

TAOK1-3, have similar structures. Each of them begins with an N-terminal head, following by a catalytic domain, a substrate-binding domain (SBD), and spacer region. The number of amino acid residues of their spacer regions are nearly equal, despite their distinct tails. TAOK1 is composed of 1001 amino acids (AA), TAOK2 1235 or 1049 AA, while TAOK3 898 AA. Adapted from (Ye et al., 2020).

Table 1. Related biological processes and effectors downstream of TAOKs.

Kinases	Biological Processes	Effectors Downstream	References
TAOK1	MAPK Signaling Pathway	MEK3/4/6, JNK, p38 MAPK	(Chen et al., 2003; Hutchison et al., 1998; Raman et al., 2007; Zihni et al., 2006)
	DNA Damage Stress Response	MEK3/6, p38 MAPK	(Raman et al., 2007)
	Hippo Signaling Pathway	STK3/4 (STK3/4), LATS1/2, MAP4Ks	(Boggiano et al., 2011; Plouffe et al., 2016; Poon et al., 2011)
	Limit Filopodia of Dendritic	Myosin Va	(Ultanir et al., 2014)
	IL-17 Signal Transduction	IL-17RA	(Z. Zhang et al., 2018)
	Apoptosis	ROCK1, Caspase 3, JNK	(Zihni et al., 2006)
TAOK2	MAPK Signaling Pathway	MEK3/4/6, JNK, p38 MAPK, Sap1, Elk1	(Calderon de Anda et al., 2012; Chen et al., 1999; Chen & Cobb,

			2001; Moore et al., 2000; Raman et al., 2007)
	DNA Damage Stress Response	MEK3/6, p38 MAPK	(Raman et al., 2007)
	Ethanol Response	JNK, p38 MAPK	(Calderon de Anda et al., 2012; Chen & Cobb, 2001)
	Axon and Dendritic Formation	JNK, SEPT7, PSD95	(Calderon de Anda et al., 2012; Yadav et al., 2017)
	Filopodia of Dendrites	Myosin Va	(Ultanir et al., 2014)
	Cytoskeleton Stability	α/β-tubulin	(Mitsopoulos et al., 2003)
	Apoptosis	JNK, PARP	(Zihni et al., 2007)
TAOK3	MAPK Pathway	MEK1/2/3/6, JNK, ERK1/2, p38 MAPK	(Kapfhamer et al., 2012; Ormonde et al., 2018; Raman et al., 2007; Tassi et al., 1999; Yoneda et al., 2001; W. Zhang et al., 2000)
	DNA Damage Stress Response	MEK3/6, p38 MAPK	(Raman et al., 2007)
	TCR Signal Transduction	MEK1/2, ERK1/2, LCK	(Ormonde et al., 2018)
	Hippo Pathway	STK3/4, LATS1/2, MAP4Ks	(Plouffe et al., 2016)
	Notch Pathway	ADAM10	(Hammad et al., 2017)
	Ethanol Response	JNK	(Kapfhamer et al., 2012)
	Post-Axotomy Apoptosis	BimEL, Hrk	(Wakabayashi et al., 2005)
	ER Stress Response	JNK, caspase 12, IRE1α, TRAF2	(Yoneda et al., 2001)

TAOKs can activate the p38 MAPK pathways through their activity as MAP3Ks (Figure. 2) (Chen et al., 2003; Chen & Cobb, 2001; Hutchison et al., 1998; Yustein et al., 2003). It has been found that phosphorylation of ATM (ataxia telangiectasia mutated) can activate TAOKs to modulate DNA damage responses mediated by p38. Additionally, it is also

reported that TAOK2 and p38 cascades can be activated by the heterotrimeric G protein $G\alpha_0$, which suggested that TAOKs play a role as intermediates and connect certain G protein-coupled receptors (GPCRs) with the p38 MAPK pathway (Figure. 2) (Chen et al., 2003). Besides, activated TAOKs can phosphorylate MKK3/6 (the MAP2Ks) as well, which can phosphorylate p38 kinases further (Chen et al., 1999; Hutchison et al., 1998). TAOK1 and TAOK2 were found to phosphorylate not only MKK3/6, but also the MKK4/MMK7, and activate JNK signaling (Figure. 2) (Chen et al., 1999; Zihni et al., 2006, 2007). Paclitaxel and staurosporine, the apoptosis-inducing agent, can activate endogenous TAOK1, TAOK2 and JNK pathway. A study in HEK293 cells found that endogenous JNK/SAPK cascade was activated by TAOK2 overexpression (Chen & Cobb, 2001). As to the role of TAOK3 playing in SAPK/JNK pathway, this is disputable to some extent. While a research in NIH-3T3 cells found TAOK3 activated SAPK/JNK (W. Zhang et al., 2000), another study in Hela cells demonstrated that rapid activation of JNK1/2 and caspase-9 was caused by TAOK3 downregulation, which suggested that TAOK3 regulated the SAPK/JNK cascade negatively (MacKeigan et al., 2005).

TAOKs have been found to modulate Hippo-signaling pathway and YAP/TAZ trans-activation can be suppressed by the activation of TAOKs. The TAOK1/2/3-knockout model in HEK293A cells showed that TAOK1/3 can act upstream of STK3/4. Besides, TOAK1/3 could activate LATS1/2 in parallel. The elimination of TAOKs can decrease YAP/TAZ phosphorylation significantly, which resulted in the reduction of their cytoplasmic retention (Plouffe et al., 2016). Additionally, a combined knockout of three MAP4K family members: MAP4K4, 6, and 7, was reported to significantly block YAP1 phosphorylation induced by TAOK1 , which indicates that TAOK1 could activate LATS1/2 vis three MAP4K family members: MAP4K4/6/7 (Meng et al., 2015). In summary, TAOKs regulate Hippo signaling pathway, the activation of which can suppress the ability of YAP1/TAZ trans-activation (Figure 2.).

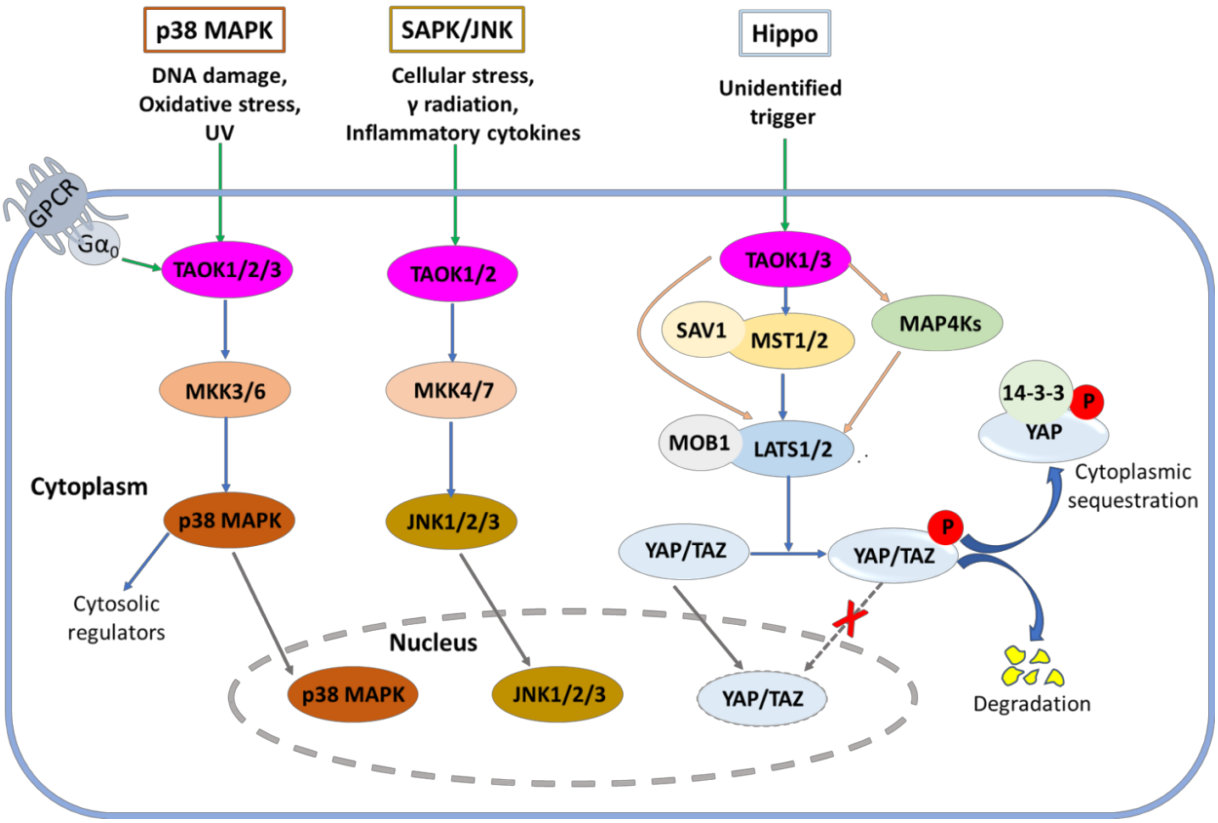

Figure 2. TAOK1/2/3 regulates various kinase cascades.

TAO kinases (TAOKs) regulate MAPK-signaling pathway and Hippo-signaling cascades. Note that both p38 and SAPK/JNK MAPK pathways are regulated by TAOKs. Furthermore, Ga_0 was reported to activate TAOK2, linking GPCR and TAOK biology. Green-colored arrows indicate upstream stimuli; blue-colored arrows represent canonical pathways; orange-colored arrows indicate the pathways that bypass the core kinase cassette in Hippo signaling; grey-colored arrows point to nuclear translocation. GPCR, G protein-coupled receptor; SAV1, Salvador 1. Adapted from (Fang et al., 2020).

1.1.2 **Mechanisms of activation and inactivation of Hippo-signaling pathway**

The Hippo pathway is evolutionarily conserved signaling cascade and is involved in tissue homeostasis maintenance, cell differentiation of diverse organisms, and proper development of organ size by regulating proliferation process and apoptosis process of cells (Di Cara et al., 2015; Pan, 2010; F.-X. Yu & Guan, 2013). Over the last two decades, Hippo signaling has been identified as tumor suppressor pathway in numerous studies. More recent studies has also implicated Hippo signaling components in tumorigenesis and cancer progression through regulation of cancer stem cells, where Hippo signaling acts as antagonist of growth (Moon et al., 2018; F.-X. Yu et al., 2015; Zygulska et al.,

2017). Additionally, accumulating evidence suggests that the Hippo pathway exerts an important role in the neuronal development at multiple stages, including proliferation process and neuronal death process of neural stem cells (NSCs) (Gee et al., 2011; D. Han et al., 2015; Milewski et al., 2004; Sanphui & Biswas, 2013). In mammals, sterile 20-like protein kinase 1 and 2 (STK3/4) together with its adaptor proteins Salvador homolog 1 (SAV1), large tumor suppressor 1 and 2 (LATS 1/2) with its adaptor protein MOB kinase activator 1A and B (MOB1/2) comprise the key components of the Hippo pathway (Pan, 2010). These kinases can phosphorylate downstream effectors of Hippo pathway directly. They can phosphorylate the yes-associated protein (YAP1) on residues including S61, S109, S127, S164, and S381, and the transcriptional co-activator with PDZ-binding motif (TAZ, HGNC symbol: WWTR1) on serine residues of S66, S89, S117, and S311 (Huang et al., 2005; Lei et al., 2008; Zhao et al., 2007; Zhao, Li, Tumaneng, et al., 2010a). Canonically, autophosphorylation or activation mediated by kinase domain dimerization of STK3/4 can activate Hippo-signaling (Deng et al., 2003; Glantschnig et al., 2002). Once activated, STK3/4 form heterodimers with SAV1 by the C-terminal SARAH domains and phosphorylate SAV1 and MOB1A (Chan et al., 2005; Hergovich et al., 2006; Praskova et al., 2008). To recruit STK3/4 to the membrane, it requires SAV1 to bring about the interaction of STK3/4 with other proteins mediated by SARAH domain. Meanwhile, MOB1A/B is required to facilitate the interaction of STK3/4 with LATS1/2 (Huang et al., 2005). Activation of STK3/4 and the adaptor proteins can further activate LATS1 by phosphorylating it at Thr1079 and activate LATS2 by phosphorylating it at Thr1041 (E. Kim et al., 2020). Furthermore, LATS kinases can phosphorylate YAP1/TAZ at different serine residues, which enforces the YAP1/TAZ towards different fates. When YAP1 is phosphorylated by LATS at Ser127 and TAZ is phosphorylated by LATS at Ser89 in mammals, they get a binding site for 14-3-3, which results in their retention in cytoplasm (Y. Han, 2019) (Figure 3.A). On the contrary, when the phosphorylation of YAP1 happens at Ser381 and TAZ at Ser311, SCF-β-TrCP proteins can recognize them. This can cause their degradation which is E3 ubiquitination-dependent (Zhao, Li, Tumaneng, et al., 2010a) (Figure 3.A). Thus, YAP1's nuclear translocation is restricted by Hippo pathway activation and the expression of genes dependent on YAP is inhibited. However, if the Hippo-

signaling pathway is inhibited, YAP/TAZ are not phosphorylated by LATS kinases. Then YAP/TAZ translocate into the nucleus, where they interact with different transcriptional co-activators, including TEAD family proteins to activate the genes which are related to cell survival and proliferation (Figure 3.B). Notably, a diverse range of genes can be transcribed by the YAP1-TEAD complex. These genes include regulators of cell-cycle such as CycE; genes related to growth promoting such as c-Myc and inhibitors of apoptosis process, such as Birc3 (Happé et al., 2011; Nishimoto et al., 2019). Thus, active cell proliferation process and tissue overgrowth are the primary transcriptional outputs of YAP-TEAD (Bae & Luo, 2018). The interaction between YAP1 and P73 that occurs inside the nucleus has been described in some non-canonical contexts as well. This interaction is mainly implicated in apoptosis process promoting through transcribing pro-apoptotic genes such as PUMA and BAX (Matallanas et al., 2007; Strano et al., 2005).

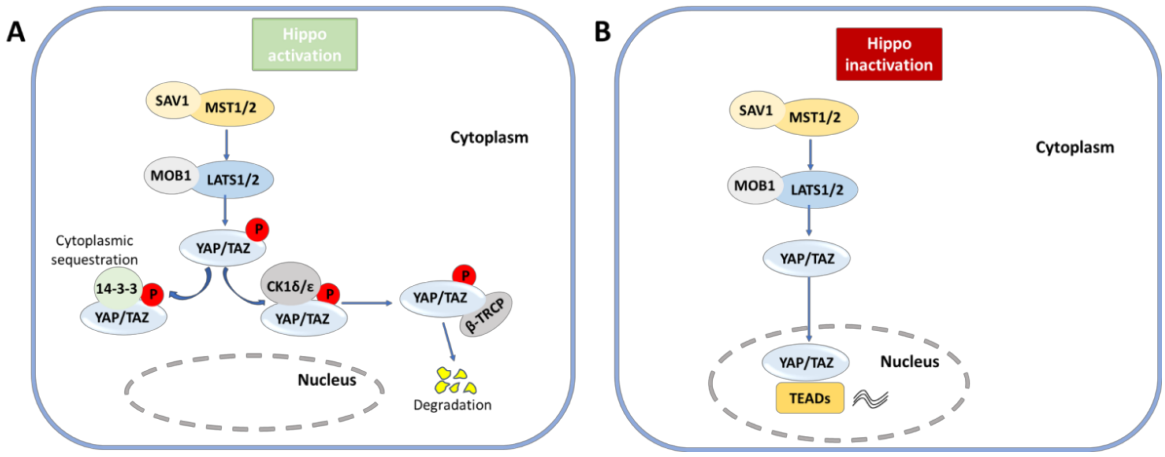

Figure 3. Mechanisms of Hippo-signaling activation and inactivation.

(**A**) Hippo-signaling activation causes the phosphorylation of YAP/TAZ at different sites, which leads to their binding with 14-3-3 or CK1δ/ε. Binding with 14-3-3 results in the cytoplasmic sequestration of YAP/TAZ, while CK1δ/ε leads to the degradation of them. (**B**) Inactivation of Hippo-signaling facilitates the translocation of YAP/TAZ inside the nucleus. YAP/TAZ talk with various co-activators including TEAD to transcribe various genes related with cell survival and proliferation.

1.1.3 **Upstream regulatory molecules and crosstalk with other signaling pathways**

A large number of regulators which have functions on the upstream of the Hippo pathway have been described as well. Hippo pathway reacts to various signals from upstream including cell polarity, adhesion proteins, junctional proteins, GPCRs and its ligands,

cellular stress, and various other kinases (F.-X. Yu & Guan, 2013; Zhao, Li, & Guan, 2010). The interactions among Hippo signaling and polarity proteins like WWC family proteins WWC1/2/3, result in a reduced transcriptional outcome of the genes which are the targets of YAP1/TAZ, including CYR61 and CTGF (Rong et al., 2019; Zhao et al., 2008). It was reported that α-catenin, which plays a role in adhere junction formation can regulate YAP1 negatively. Molecular and gene analysis for mouse models in the skin epidermis have identified that α-catenin can inhibit YAP nuclear localization, which further inhibits YAP transcriptional activity, thus playing an anti-tumor role (Schlegelmilch et al., 2011; Silvis et al., 2011). The angiomotin (AMOT) family proteins, which localize to actin cytoskeleton and tight junctions, can recruit Hippo core components and YAP1 to the plasma membrane and further promote their phosphorylation, thus inhibiting the transcriptional activities of YAP1 and TAZ (Paramasivam et al., 2011; Zhao et al., 2011). Besides, Hippo-signaling pathway activity can also be regulated by a variety of GPCRs and the correlated heterotrimer G protein signals through Rho GTPases. LATS1/2 can be inhibited by ligands for Gα12/13-coupled receptor (F.-X. Yu et al., 2012). Gα12/13 can polymerize actin in a Rho GTPase dependent manner, thus inhibiting LATS1/2 and further activating YAP/TAZ. In a similar way, GPCR ligands for Gαq/11-coupled receptor, like endothelin-1 and estrogen, can trigger YAP/TAZ in the Rho GTPase dependent manner as well (Wang et al., 2017; X. Zhou et al., 2015). Cellular stress signals, which include energy stress, osmotic stress, and hypoxia, also play roles in regulating Hippo pathway (Meng et al., 2016). For example, hypoxia causes the activation of YAP/TAZ through inhibiting Hippo pathway. In terms of mechanism, hypoxia can stimulate SIAH2, an E3 ubiquitin ligase that can bind to and destabilize LATS2. The loss of SIAH2 can suppress tumorigenesis dependent on LATS2. Moreover, YAP1 can form a complex with Hypoxia-inducible factor 1-alpha (HIF1α), which plays a significant role in HIF1α stability and function (B. Ma et al., 2015). In *Drosophila*, Thousand and one (Tao) kinase could initiate the Hippo kinase cascade through phosphorylating Hippo (Hpo) at its activation loop. Merlin and Expanded (Ex), the upstream components of Hpo, promoted Hpo phosphorylation and their effects on Hippo-Salvador-Warts (HSW) signaling were mediated by Tao (Boggiano et al., 2011; Poon et al., 2011). Recently, Tao has also been

found to phosphorylate Misshapen (Msn), the homolog of MAP4K4/6/7, at its activation loop in the *Drosophila* gut. It is in consistence with the high homology of Msn and Hpo kinase domains (Q. Li et al., 2018). In mammalian cells, TAOK1 and TAOK3, but not TAOK2 can bypass STK3/4 and directly phosphorylate hydrophobic motif of LATS1/2, thus activating them (Plouffe et al., 2016).

Hippo pathway also interact with several other signaling pathways intricately, including Wnt/β-catenin, Notch, and MAPK pathways (Ouyang et al., 2020). Because of the key roles in tumorigenesis, how the Wnt/β-catenin (Wnt pathway) interacts with the Hippo pathway has become the focus of many studies. Hippo pathway activation can inhibit the phosphorylation level of disheveled (DVL) protein which is regulated by CK1δ/ε, thus promoting cytoplasmic TAZ to inhibit Wnt/β-catenin pathway (Varelas et al., 2010). The interaction between Hippo and Notch pathways has been widely studied in the maintenance of tissue homeostasis in mammals. YAP plays vital roles in smooth muscle differentiation, intestinal dilatation, and liver cell fate regulation via Notch signaling, which is shown by genetic analysis (Camargo et al., 2007; Manderfield et al., 2015; Yimlamai et al., 2014; D. Zhou et al., 2011). Notch signaling is activated in the trophectoderm during the process of embryonic development, and YAP and the NICD activate Cdx2 transcription synergistically for the specification of trophectoderm lineage (Rayon et al., 2014). Mechanically, the Notch receptor and it's ligand Jagged1 act as the direct target genes of YAP, while NICD can enhance YAP/TAZ activity by intensifying its stability, thus creating a positive feedback circle (W. Kim et al., 2017; Tschaharganeh et al., 2013; D. Zhou et al., 2011). In addition, stress response is linked to Hippo signaling by MAPK pathway, which includes JNK and p38. In both Drosophila and mammalian, researches revealed that JNK promotes Ajuba family proteins to bind to Warts and LATS, thus increasing Yki and YAP1 activity (Sun & Irvine, 2013). As to p38, it is reported that TEAD cytoplasmic translocation can be promoted by environmental stress through p38 MAPK, which can selectively inhibit YAP1-driven cancer cell growth (Lin et al., 2017).

1.1.4 **Hippo Signaling and dendrite maintenance**

Establishing a dendritic tree is a highly dynamic process, which is characterized with extending and retracting branches, and stabilizing current dendrites and synaptic connections (Jan & Jan, 2010). In order to guarantee the proper coverage of the receptive fields, it is important to coordinate all of the above processes strictly at every timepoints. Typically, dendrite arbors are formed through adding and extending branches. These branches develop from the cell body and their expansion forms secondary and tertiary dendrites (Emoto, 2011a). Actually, a neuron's final branching pattern is established not only by adding, but also via retracting and eliminating branches. Once the dendrite coverage of the neurons' receptive field is established, many of them can maintain this coverage for the rest of their life. As to the question how dendrite fields of neurons are established and maintained during development, dendrite tiling process provides a good example. To guarantee coverage of the receptive filed to be complete but non-overlapping, neurons of some functional groups tile their dendrites through dendrite repulsion (Yip & Heiman, 2016). The NDR kinase Trc and its activator Fry have been identified as key regulators for establishing dendritic tiling by genetic screens of Drosophila sensory neurons (Emoto et al., 2004). However, Warts/Lats (Wts), which is also a NDR family kinase and functions as a tumour suppressor, also plays roles in maintaining mature dendrite (Emoto et al., 2006). It is well known that Wts kinase (also known as Lats) can maintain organ size through coordinating cell growth and apoptosis (Xu et al., 1995). However, dendrite maintenance also requires Wts activity. Function loss of the Wts kinase leads to a gradual defect in maintaining dendrite trees in Drosophila sensory neurons. This can lead to large gaps in receptive fields of neurons. Furthermore, Trc as well as Wts can be phosphorylated by the upstream kinase Hippo directly in their C-terminal hydrophobic motifs, which enables the activation of them (Emoto et al., 2006). In addition, defects in establishing and maintaining of dendritic fields can result from the *hpo* gene mutations (Emoto et al., 2006). Therefore, the Hippo-NDR Signaling pathway may play a potential role in the coordination of establishing and maintaining receptive fields. This control system for dendritic field size is strikingly analogous to that of the organ size. As to the regulation of organ size, the Hippo pathway can maintain organ size

through limiting cell growth and promoting apoptosis (Halder & Johnson, 2011). Although in the vertebrate brain, Hippo and NDR kinases are conserved evolutionarily and expressed abundantly, it is still worth investigating the role of the related Signaling pathways in mammals.

1.1.5 **Hippo Signaling in neurodevelopmental and neurodegenerative diseases**

During the neuro-developmental process, Hippo pathway has a key function in maintaining the proper balance between proliferation and death of neurons. Dysregulation of Hippo Signaling is involved in a variety of neuro-developmental diseases, which can be reflected by diverse brain deformations. Analysis found there exist the mutations of CDK5RAP2 in patients with microcephaly disorder, which is characterized by premature differentiation and apoptosis. Notably, CDK5RAP2 interacts actively with proteins associated Hippo Signaling pathway (Fong et al., 2008; Sukumaran et al., 2017). Hydrocephalus, which is a common neurodevelopmental defect, is characterized with expanded intracerebral ventricles and intellectual retardation. It was reported to be caused by the loss of YAP1 in neurons and the ependymal cells of the ventricular surfaces (Park et al., 2016). In addition, mutations in YAP1 can also result in the congenital malformations such as orofacial clefting and mental retardation during human brain development (Williamson et al., 2014). A study demonstrated that reduced cerebellar size, defects of foliation and fissure formation can be caused by the loss of Yap1/Taz in cerebellum. This study was carried out with a double knockout mouse model (Hughes et al., 2020). Recently, it has been revealed that there exist alteration in the pattern of DNA methylation of certain crucial pathway genes like Hippo Signaling in human neuronal progenitor cells (hNPCs) under the high glucose condition, which could explain the neuro-developmental deformities of the offspring from diabetic pregnancy (Kandilya et al., 2020). It is also found that transient expression of exogenous YAP can turn neurons into neural stem cell like cells (Panciera et al., 2016). Moreover, YAP can also facilitates embryonic neural stem cell proliferation by elevating their responsiveness to fibroblast growth factor 2 (FGF2), one of the major growth factors for neural stem cells, both in vivo and in vitro (D. Han et al., 2020).

In the brain, Hippo pathway plays a binary role in cell survival, which means hypo-or hyper-activation of Hippo can lead to different pathological conditions such as glioma and neurodegeneration. Recently, the soaring role of hyper-activation of Hippo pathway in inflaming neurodegeneration diseases has been emphasized. The neurodegeneration diseases are characterized by abnormal neuronal death and the corresponding abnormality of cognition and phenotype (Misra & Irvine, 2018). Indeed, Hippo pathway has been found to be involved in diverse neurodegenerative disorders, like Alzheimer's disease (AD) and Huntington's disease (HD). As the main cause for dementia, AD is linked to progressive neurodegeneration of the brain cortex and hippocampus (Haque & Levey, 2019). In the process of AD progression, amyloid precursor protein (APP) can promote the interaction between transcription factor FOXO3a and MST1, which can further trigger intrinsic apoptotic pathway mediated by Bcl-2 (Sanphui & Biswas, 2013). It has been reported that YAP1/TAZ could interact with APP directly and act as a regulator for downstream transcription. And expression of proteins related to apoptosis can be induced by the complex of YAP/TAZ which is transcriptionally active (Swistowski et al., 2009). HD is also a neurodegenerative disease, which is typified by motor movement disability, abnormal behavior and impaired cognition (Labbadia & Morimoto, 2013). A current research has reported the dysregulation of Hippo pathway in HD. Both in the postmortem brain samples and NSCs from HD patients, the researchers found an increased level of p-MST and p-YAP and a significant reduction of YAP levels in the neuronal nuclear (Mueller et al., 2018). In the same study, the researchers also observed a similar trend of nuclear YAP levels in the cortex of HD mouse model with CAG knock in. Moreover, reduced nuclear YAP levels was found to be associated with the decrease in YAP-TEAD interaction, which resulted in the subsequent dysregulation of transcription. The disturbance of the transcriptional activity of YAP was suggested to be the main cause of neuronal damage and death in HD patients (Mueller et al., 2018).

1.2 Role of Hippo signaling in neuronal stem cells and neurogenesis

1.2.1 Role of Hippo Signaling in neuronal stem cells

During the development of embryos, NSCs are self-renewing and multipotent in the vertebrate brain. They can differentiate into neurons and glial cells (Beattie & Hippenmeyer, 2017). Notably, in the subgranular and subventricular zones there persist some NSCs, which can produce neurons throughout lifespan. Therefore, there exist diverse states of NSCs in the brain, which are tightly regulated. It has been found that Hippo pathway is implicated in regulation of NSC physiology. Inactivation of LATS1/2 kinases in *Lats1/2* conditional knockout (KO) mice via *Nestin-Cre,* causes global hypertranscription driven by YAP/TAZ in neural progenitors. This can upregulate various genes related to cell proliferation process(Lavado et al., 2018). However, in neural progenitors, hypertranscription can also lead to extensive apoptosis by inhibiting differentiation and inducing replication stress of DNA and damage of DNA (Lavado et al., 2018). In addition, in the mouse embryonic brain, overexpression of YAP/TAZ can increase stemness, thus inducing cell localization in the ventricular zone (D. Han et al., 2015). Moreover, bone treatment with bone morphogenetic protein2 (BMP2) has been demonstrated to inhibit embryonic NSCs proliferation (Yao et al., 2014). However, BMP2 did not reduce formation of neurosphere further when knocking down YAP1, which suggested the crosstalk between BMP2 and the Hippo-YAP Signaling. Additionally, it was found that BMP2 didn't show inhibitory effect on the proliferation of mouse NSC when knocking down cyclin D1 (ccnd1), which is a target gene downstream of the YAP-TEAD Signaling (Yao et al., 2014). Furthermore, Ding et al. showed that Hippo Signaling exerts a key role in the maintenance of NSC quiescence in *Drosophila*, as the loss of *Hpo* or *Wts* leads to premature nuclear localization of Yorkie, which results in the premature initiation of NSCs growth process and proliferation process in the nervous system of *Drosophila* (Ding et al., 2016).

1.2.2 **Role of Hippo Signaling in neurogenesis**

The coordinated control of cell cycle exit and upregulation of various genes related to neuronal differentiation is an essential aspect of neurogenesis. Both processes can be initiated by proneural transcription factors with basic helix-loop-helix, like Atoh1 (Math1), *Ascl1* (*Mash1*), *Neurog1-3* (*Neurogenin 1-3*), or *Neurod1-4*. Recently, it has been demonstrated in multiple types of stem cells that Hippo pathway makes an important impact on promoting the cell cycle exit and terminating neuronal differentiation (H. Zhang et al., 2012). When activating Hippo Signaling, Lats1/2 kinases can be activated by the core Stk3/4 kinases, which further causes the phosphorylation and inhibition of the transcriptional co-factor Yap1 (Hiemer & Varelas, 2013). Gene knockout mice which lack *Sav1*, exhibited impaired formation of retinal epithelium during the process of neurogenesis (J.-H. Lee et al., 2008). However, it was reported that knockdown of Yap in zebrafish embryos could decrease neuron production and reduce the populations of progenitor cell in the central nervous system (Jiang et al., 2009). Zhang et al. also found the expression of *Yap1* in mammalian retinal progenitor cells, which was regulated by Hippo Signaling, and the retinal proliferation and differentiation can be modulated by the activity of *Yap1*. They further found that *Yap1* function can be antagonized by proneural bHLH proteins, both at YAP1 expression level and through the LATS1/2 kinases. Interestingly, the cell cycle exit which is propelled by proneural bHLH proteins can be prevented by YAP1. All of the above observations demonstrate that the reciprocally inhibitory interactions between bHLH proteins and YAP1 plays a crucial role in regulating neurogenesis (H. Zhang et al., 2012).

1.3 **TAOKs and neurodevelopmental disorders**

1.3.1 **Dendrite spine and synapse plasticity**

Dendrite spines are small membranous postsynaptic protrusions from the dendrite, and the majority of the excitatory synaptic input could be received by them in the brain (Shepherd, 1996). Spines can compartmentalize calcium (Ca^{2+}) and serve as biochemically Signaling compartments which could isolate synaptic input from each other

(Sabatini et al., 2002; Yuste & Denk, 1995). Notably, dendrite spines are essential substrate for Ca^{2+}-dependent Signaling pathways, which are important for synaptic plasticity. Synaptic plasticity is an important cellular mechanism for learning process and memory process. Many researches have suggested that the morphology of spine is closely correlated with synaptic function. In detail, long-term depression (LTD) and long-term potentiation (LTP), the two key forms of synaptic plasticity, are associated with the shrinkage and enlargement of dendritic spines (Matsuzaki et al., 2004; Q. Zhou et al., 2004). At the molecular level, the postsynaptic density (PSD) plays a role as organizer for the postsynaptic Signaling machinery, which is composed with cell adhesion molecules, cytoskeletal proteins and receptors containing α-amino-3-hydroxy-5-methyl-4-isoxazolepropionic acid receptors (AMPAR). PSD is a large complex electron-dense structure which is attached to the postsynaptic dendrite membrane (Emes et al., 2008; Frank & Grant, 2017; J. Li et al., 2016). It has been revealed that the amplitude of the AMPAR-mediated currents, the number of synaptic AMPAR, the area of PSD, and the presynaptic area of AMPAR's synaptic partner are proportional to the spine volume (Matsuzaki et al., 2001; Takumi et al., 1999). Thus, spine morphology and synaptic function are tightly associated with each other.

1.3.2 **Dendrite spines in neurodevelopmental disease**

It is thought that the fine adjustment of dendritic spine density and its morphology is the structural basis for learning, synaptic plasticity and memory. Therefore, the disturbance of dendritic spine plasticity can result in cognitive defect of the human brain (Caroni et al., 2012; Yang et al., 2009). Indeed, current studies have demonstrated that abnormal dendritic spine plasticity is the common character shared by different neuropsychiatric disorders, like intellectual disability (ID), schizophrenia, and autism spectrum disorder (ASD) (Forrest et al., 2018; Yan et al., 2016). Mutations in spine excitatory and regulation have been correlated to psychiatric disorders in many behavioural and cellular aspects. The mutations mainly happen in genes which encode glutamate receptors (e.g., AMPAR), cell adhesion molecules (e.g., neuroligin-3), scaffolding proteins (e.g., SH3), and calcium regulated proteins (e.g., Calcium/calmodulin dependent protein kinase II (CaMKII)) (Araki

et al., 2015; Etherton et al., 2011; Liu et al., 2017; Stephenson et al., 2017; Y. Zhou et al., 2016). Apart from mutations, chromosomal microdeletions and microduplications, which make up a fraction of copy-number variants (CNVs), have long been related to aberrant neurodevelopmental outcomes (Watson et al., 2014). Several recent publications on both CNVs and genome-wide association studies have focused on the role of single nucleotide polymorphisms (SNPs) and genes which are situated on deletion or duplication area on chromosome related to neuropsychiatric diseases (Bray & O'Donovan, 2018). Through these analyses, TAOK2 was identified as candidate risk gene for ASD and schizophrenia (Pardiñas et al., 2018). Notably, TAOK2 is located in the CNV 16p11.2 that occurs as heterozygous deletion or duplication in patients (Steinman et al., 2016; Weiss et al., 2008).

1.3.3 **TAOK2 and neurodevelopmental diseases**

As introduced before, TAOK2 protein belongs to MAP3K family. It is also a serine/threonine kinase of the Ste20-like family and is located at the chromosomal locus 16p11.2 (Moore et al., 2000; Yadav et al., 2017). A heterozygous deletion of the 16p11.2 locus is linked to autism spectrum disorders (Weiss et al., 2008), while a duplication of the same chromosomal region is associated with bipolar disorder, autism, and schizophrenia (McCarthy et al., 2009; Steinberg et al., 2014; Weiss et al., 2008). A study inhibiting TAOK2 expression in mouse found that TAOK2 was essential for development of basal dendrite in cortical neurons (Calderon de Anda et al., 2012), whereas in Drosophila neurons it was found that Tao protein, the fly homologue, was involved in axonal development (King et al., 2011). In addition, TAOK was reported to be a MST3 phosphorylation target in mouse brain by the analog-specific approach, in which the phospho-mutant and phospho-mimetic forms of TAOK were expressed. It was found that expression of phospho-mutant TAOK1 or TAOK2 was enough to increase dendrite filopodia and spines loss, reminiscent of the phenotype of MST2 function loss (Ultanir et al., 2014). Similar with MST3, TAOK2 is also associated with the development of dendritic spine (Yasuda et al., 2007) and synchronous loss of TAOK1 and TAOK2 results in the increase of immature and thin dendritic filopodia (Ultanir et al., 2014). In mouse brain lysates, Septin7 has been recently identified as one of the direct substrates of TAOK2. It

is reported that TAOK2 phosphorylates cytoskeletal GTPase Septin-7. The phosphorylation of Septin-7 can stimulate it's spine localization and also interaction with PSD95, which is needed for the maturation of spine (Yadav et al., 2017). Interestingly, global and nervous system-specific disturbance of the Taok2 gene in mouse model demonstrated that loss of Taok2 affects many behaviours after ethanol exposure. For example, both conditional and global Taok2 deficient mice consumed more ethanol, whereas only full knockout Taok2 mice displayed a hyperactivity phenotype (Kapfhamer et al., 2013). Another study recently has tried to dissected the function of TAOK2 in the development of neural circuit through integrating ASD sequence with a Taok2 heterozygous (Het) and knockout (KO) mouse model (Richter et al., 2019). Taok2 Het and KO mice exhibited impairments in synapse formation and excitatory neurotransmission, cognition defect, social interaction defeat and anxiety. Interesting, enhancing RhoA activity, which was decreased by TAOK2 loss, could rescue the Taok2 KO mice from synaptic phenotypes pharmacologically. In addition, 2 de novo mutations: A135P and P1022*, which were found in ASD families, were identified to affect the kinase activity of TAOK2 and the development of spine (Richter et al., 2019). All of the above discoveries suggest that TAOK2 is involved in neurodevelopmental disorders.

1.4 Genetically encoded cell-based assay techniques to study the function of TAOK2

1.4.1 PPI (split TEV)

Hippo pathway activity is controlled by a plethora of proteins, either promoting or inhibiting the transcriptional activity mediated by YAP1 (Boopathy & Hong, 2019). For many of these regulators, defined interactions with core kinase cassette components are described. For example, WWC proteins bind to LATS kinases to increase phospho-YAP1 levels and thus inhibit YAP1 activity (Genevet et al., 2010; Wennmann et al., 2014). Conversely, Ajuba family proteins, such as Ajuba and Wilms tumour protein 1-interacting protein (WTIP), bind to LATS kinases and SAV1 to inhibit LATS kinases to promote nuclear, i.e., active YAP1 (Das Thakur et al., 2010). To gain further insight on physical

interactions, and the relative strength of associations, and to better characterize modulators, we performed a focused interaction screen among core components and major regulators of the pathway with the usage of special system: the split TEV, which allows the robust and quantitative assessment of PPIs in living cells (Wehr et al., 2006). This method is built on the foundation of the split N1a protease of the tobacco etch virus (TEV), with the N-terminal moiety fused to a bait protein candidate. The C-terminal TEV moiety is fused to the prey protein candidate (Figure 4.). Further, all bait-NTEV proteins were linked to a TEV cleavage site (tcs) and the transcriptional co-activator GAL4-VP16 (GV). Once an interaction between a bait and a prey has occurred, the TEV protease fragments functionally complement to restore TEV protease activity. In turn, GV is cleaved off. Then, GV moves the location to the nucleus and GV further initiates the transcription of a special gene which is a firefly luciferase reporter through binding to upstream activating sequences (UAS). Thus, increased firefly luciferase activity indicates an occurred interaction event. In this experimental setup, bait-NTEV-tcs-GV fusions must be either membrane, membrane-associated or strictly cytosolically localized proteins.

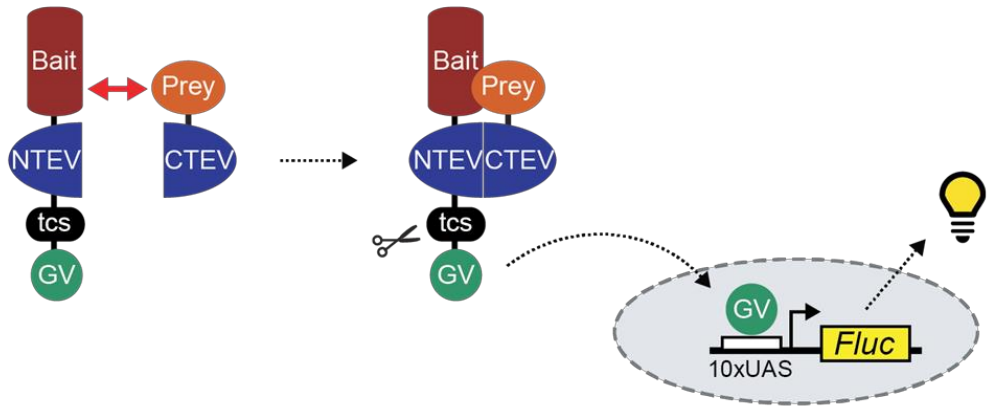

Figure 4. Principle of the split TEV PPI interaction assay.

Bait candidates are fused to the N-terminal moiety of the TEV protease (NTEV), a TEV protease cleavage site (tcs), and the artificial co-transcriptional transactivator GAL4-VP16 (GV). Prey candidates are fused the C-terminal TEV moiety (CTEV). If a bait associates with a prey, NTEV and CTEV complement to form a functionally active TEV protease, resulting in the release of GV. GV migrates into the nucleus where it binds to clustered upstream activating sequences (UAS) to activate a firefly luciferase gene. Firefly luciferase activity is converted into light signals that correspond to the strength of an observed protein-protein interaction.

1.4.2 **Cre/loxP-Generation of Knockout mice**

TAOK2 is situated on the chromosomal locus 16p11.2, duplication of which is related to schizophrenia, while deletion of the same chromosomal region is strongly correlated with autism spectrum disorders (Bristow et al., 2020; Weiss et al., 2008). Additionally, the study by Richter et al. has shown the behavioural changes in mice with a complete Taok2 knockout, like hyperactivity and changes in working memory, which are typical for neuropsychiatric disorders (i.e., autism and schizophrenia) (Richter et al., 2019). Therefore, it's necessary to analyze a broad spectrum of psychiatric symptoms by behavioural profiling of transgenic mouse-models. The Cre-loxP system is a strong technology which is widely used for generating genetically engineered mouse models and allows region-specific and temporally controlled inactivation of candidate genes. Cre is a 38-kDa DNA recombinase and it is tyrosine site specific (T-SSRs). It includes D6 specific recombinase (Dre) and flipase (Flp). There is a special DNA fragment motif with 34 bp called loxP (locus of x-over, P1) site. The loxP site includes a 8 bp core sequences and two 13 bp special DNA motif which is named as inverted and palindromic repeats. Two directly repeated loxP site can be recognized by a single Cre recombinase, then loxP flanked (floxed) DNA can be excised, which creates inactivated gene X (Figure 5.A). The Cre-loxP can not only be applied in excising DNA, but also induce the translocation and inversion of DNA. In Cre-loxP, it needs two necessary elements to create the spatiotemporally controlled mutant mice. Firstly, Cre-driver mouse line needs to be generated. In this line, a promoter specifically targeting the tissue or cell of interest can express Cre recombinase. Secondly, mouse line containing loxP flanked (floxed) DNA needs to be generated. Then the conditional knockout mice can be created by the breeding of Cre-driver line with a floxed line (Figure 5.B). The used promoter and /or enhancer could control the timing and specificity of the recombination (H. Kim et al., 2018). As the efficiency of the Cre/loxP system decreases when genetic distance increases, the floxed sequences of TAOK2 only includes several exons instead of the whole gene sequence. To achieve a tissue-specific inactivation of TAOK2, the murine *Taok2* gene is homozygously floxed between exons 4/5 and 8/9 (fl/fl) (Figure 6.A). For an efficient inactivation of Taok2 at early stages during neurodevelopment in the murine cortex, a

Cre-driver line which expresses *Cre* recombinase regulated by the *Emx1* promoter is used. *Emx1* encodes a homeodomain protein whose expression is restricted in the developing and adult cortex as well as in the hippocampus and amygdala. *Emx1* is expressed in both progenitor cells and postmitotic neurons of the dorsal, medial, and lateral pallia during early stages of neurogenesis beginning at embryonal stage day 10 (E10.5) (Cocas et al., 2009; Gorski et al., 2002; Guo et al., 2000) (Figure 6.B).

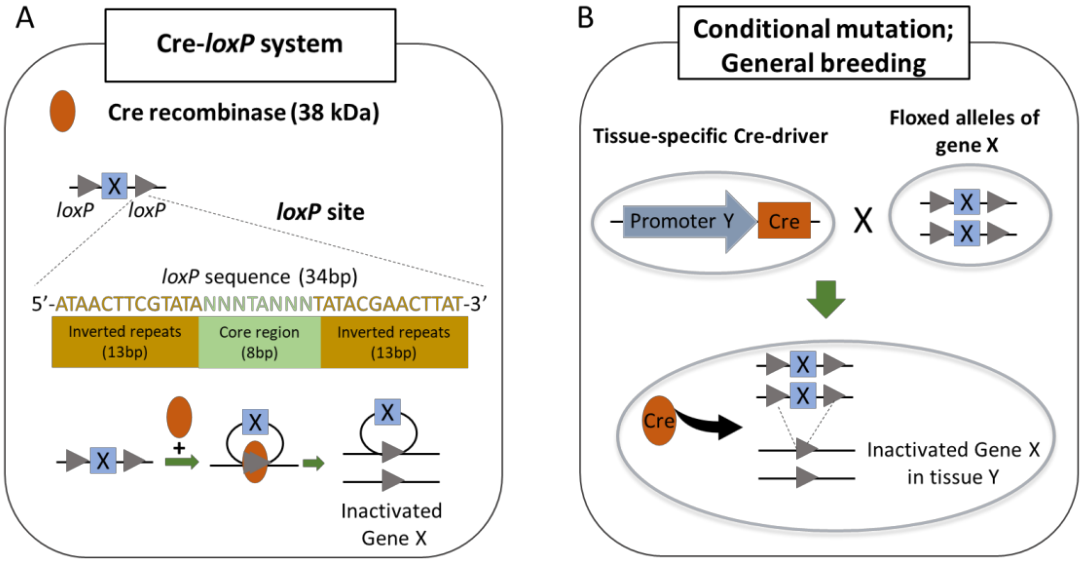

Figure 5. Mechanism of Cre-loxP system.

(**A**) An overview of Cre-loxP system. The loxP sites on DNA, which has a specific 34 bp DNA motif, is recognized by a protein named 38 kDa Cre recombinase. (**B**) General breeding strategy for obtaining a conditional inactivation of a gene of interest X using loxP-flanked (floxed) alleles and a *Cre* driver mouse line. Expression of *Cre* recombinase excises floxed loci and inactivates the gene X. Adapted from (H. Kim et al., 2018)

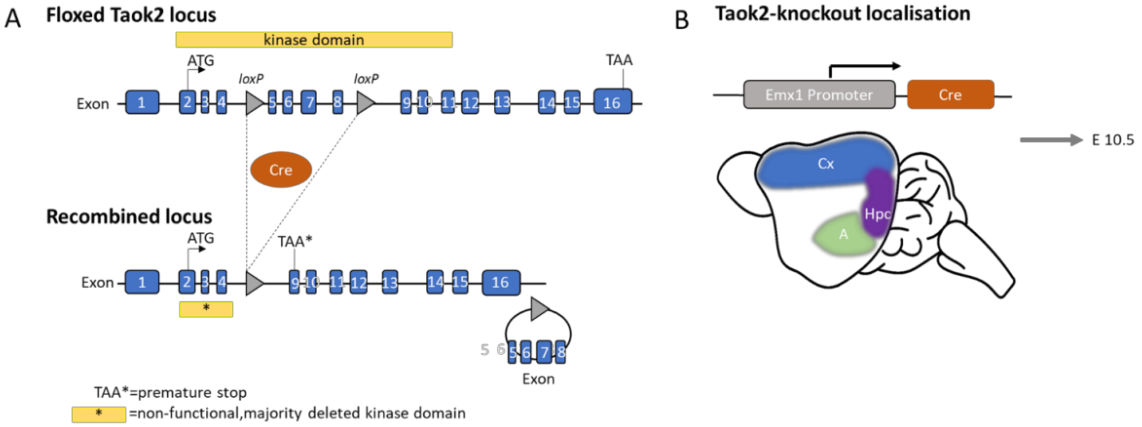

Figure 6. Conditional Taok2 knockout in the mouse brain using an Emx1-Cre driver line.

(**A**) Taok2-knockout: Excision of Taok2 exons 5-8 using the Cre/loxP system, resulting in a premature stop of the Taok2 gene. Excised exons 5-8 form a loop, which is degraded. (**B**) Emx-1 driven *Cre* recombinase is expressed in the murine cortex (Cx), the hippocampus (Hpc), and the amygdala (A) from embryonic day E10.5 onwards.

1.4.3 **PsyCop platform - behavioural profiling of mice**

Behavioural differences (e.g., wild type vs. transgenic animal) can be analyzed through a series of various behavioural tests which covers different symptom domains of psychiatric diseases (Stephan et al., 2019). The system called Research Domain Criteria (RDoC) can classify the following domains: arousal and regulatory systems, sensorimotor systems, cognition, and social processes and positive and negative valence (Insel et al., 2010; Morris & Cuthbert, 2012). Our behavioural profiling was performed using the PsyCoP platform, which is designed according to the RDoC concept (Volkmann et al., 2021). Behavioural tests were arranged following an optimized order, beginning with low to non-aversive tests and ending with clearly aversive tests to minimize interference between paradigms.

The general workflow of PsyCop platform and assigned order of behavioural tests is shown in Figure 7. Positive symptoms can be observed by hyperactivity and prepulse inhibition (PPI). As an indicator of overshooting dopaminergic Signaling, hyperactivity is measured redundantly during the first three tests of the platform: Open Field, Y-Maze, and general activity in the Intellicage (Stephan et al., 2019). Prepulse inhibition (PPI) is used for analyzing the sensorimotor gating, the disruption of which is a common endophenotype of SZ (Karl & Arnold, 2014). Open Field test, Tail Suspension test and Sucrose Preference test are used to observe the negative symptoms like loss of motivation, adhedonia and anxiety-like behaviour. Cognitive systems including working memory or fear memory can be monitored by the Intellicage, a fear conditioning setup, or Y-Maze test.

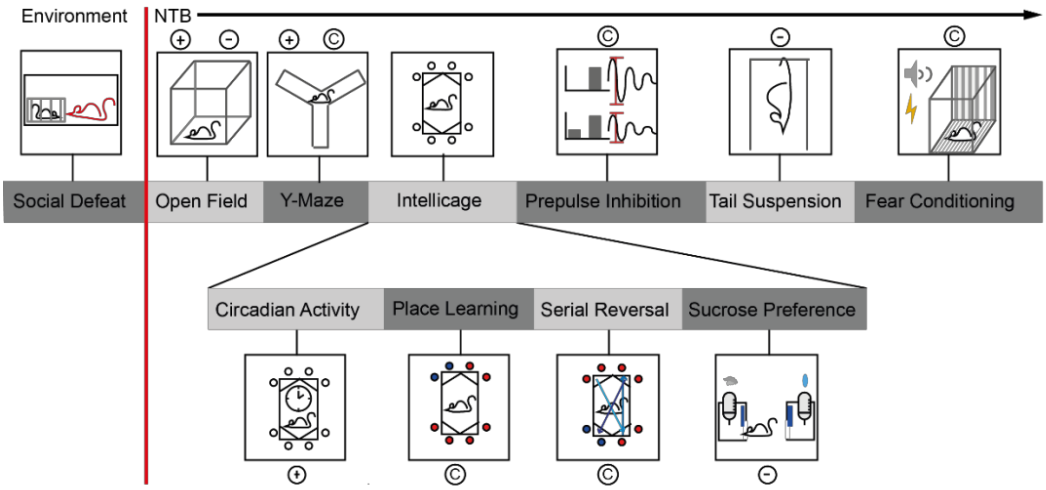

Figure 7. Platform for the behavioural and cognitive profiling of mice to analyze psychosis-related phenotypes.

The PsyCop platform consists of various tests which can assess phenotypes in mice that can be correlated to symptom domains (positive, negative and cognitive) of psychiatric diseases. The tests are arranged in an optimized manner and start with non-aversive tests (i.e., Open field test and Y-Maze test) and end in aversive tests (i.e., Fear Conditioning). Open Field, Y-Maze and Circadian Activity are used to analyze positive symptoms, while negative symptoms are analyzed by Open Filed, Tail suspension, and Sucrose Preference. Y-Maze, Prepulse Inhibition, Fear Conditioning, and Placing Learning & Serial Reversal cover the analysis of cognitive symptoms. Circadian Activity, Place Learning, Serial Reversal, and Sucrose Preference are tested in the automated Intellicage system (graphics provided by P. Volkmann and M. Stephan).

1.5 Aim/Goal of the study

Hippo pathway has been identified as a tumour suppressor pathway, and is involved in maintaining tissue homeostasis, proper development of organ size, and various types of cancers. Also, it is critical for the maintenance of stemness and the development of neural cells, including the differentiation of neurons.

Therefore, the **first aim/part** of this thesis is to use the cell-based genetically encoded split TEV assay system to profile protein-protein interactions among Hippo pathway core components and major regulators, and to identify so far hidden interactions among components that exert a direct modulatory effect on Hippo pathway activity.

As I have identified TAOK2 as modulator of Hippo Signaling in the first part of this study, and as TAOK2 is reported to be implicated in the development of synapses, synaptic

plasticity, and synaptic transmission, and impacts on mouse behaviour, I addressed in the **second part** how TAOK2 regulates synaptic activity at the cellular level.

2. Materials and Methods

2.1 Materials

2.1.1 Plasmids

OF ID	Name	Application
V188	pMD2.G (VSVG envelope protein)	Lentivirus production
V763	psPAX2 (packaging proteins)	Lentivirus production
V1474	pAAV-TEAD-RE-v4-MLP-E01356-S110	Luciferase assay; Split-TEV screen
V66	phRL-TK	Luciferase assay
V1200	pcDNA3.1_FLAG-YAP1	Luciferase assay
V663	pCMV7.1_3xFLAG-LATS1	Luciferase assay
V669	pCMV7.1_3xFLAG-LATS2	Luciferase assay
V697	pCMV7.1_3xFLAG-STK3	Luciferase assay
V696	pCMV7.1_3xFLAG-STK4	Luciferase assay
Hs515	pCMV7.1_3xFLAG-TAOK1	Luciferase assay
V1681	pCMV7.1_3xFLAG-TAOK2	Luciferase assay
Hs527	pCMV7.1_3xFLAG-TAOK3	Luciferase assay
V1682	pcDNA3.1_nV5-TAOK2	co-IP
V1463	pCMV7.1_3xFLAG-MOB1A	co-IP
V607	pCMV7.1_3xFLAG-SAV1	co-IP
V1305	pcDNA3.1_Zeo_2xHA-AMOT-var1	co-IP
V1315	pcDNA3.1_Zeo_2xHA-AMOT-var2	co-IP
V1325	pcDNA3.1_Zeo_2xHA-AMOTL1	co-IP
V1430	pcDNA3.1_Zeo_2xHA-AMOTL2	co-IP
V64	pCMV7.1_3xFLAG-X_DEST	co-IP
V702	pCMV7.1_3xFLAG-KIBRA	co-IP
V1287	pCMV7.1_3xFLAG-WWC2-var1	co-IP

V1717	pCMV7.1_3xFLAG-WWC3	co-IP
V1832	pInducer21-puro_TAOK2	pInducer construct
V2207	pInducer21-puro_TAOK2-KD	pInducer construct
V3115	pLV_hU6-sgRNA_hUbC-dCas9-ZIM3-KRAB-T2a-PuroR	CRISPR-Cas9 construct
V3118	pLV_dCas9-ZIM3-KRAB_sgTAOK2_CRISPRi_1	CRISPR-Cas9 construct
V3119	pLV_dCas9-ZIM3-KRAB_sgTAOK2_CRISPRi_2	CRISPR-Cas9 construct
V3120	pLV_dCas9-ZIM3-KRAB_sgTAOK2_CRISPRi_3	CRISPR-Cas9 construct

2.1.2 **Oligonucleotides**

Oligonucleotides were purchased from Eurofins in Munich.

cDNA synthesis:	
Oligo(dT)	PHO-TTTTTTTTTTTTTTTTTTTT
Randome nonamer(N9)	NNNNNNNNN
qRT-PCR:	
CTGF fwd (human)	AGCTGACCTGGAAGAGAACATT
CTGF rev (human)	GCTCGGTATGTCTTCATGCTG
CYR61 fwd (human)	CCAGTGTACAGCAGCCTGAA
CYR61 rev (human)	GGCCGGTATTTCTTCACACTC
TAOK2 fwd (human)	ACAGTCACCTCTCACAGCTC
TAOK2 rev (human)	TATCTCTGGCTGGTAGGGGT
18S fwd (human)	CTCAACACGGGAAACCTCAC
18S rev (human)	CGCTCCACCAACTAAGAACG
Rplp0 fwd (human)	TCTACAACCCTGAAGTGCTTGAT
Rplp0 rev (human)	CAATCTGCAGACAGACACTGG
Genotyping:	
senseECMV_IRES (mouse)	ATTTTCCACCATATTGCCGTCT
asenseECMV_IRES (mouse)	AGCCATTTGACTCTTTCCACAAC

oIMR4170 (mouse)	AAGGTGTGGTTCCAGAATCG
oIMR4171 (mouse)	CTCTCCACCAGAAGGCTGAG
Taok2_5arm_loxP_fwd_1 (mouse)	GACCAGTCTGGACTACCTAGTG
Taok2_critical region_rev_1 (mouse)	GAAGCTGAGCCCAGGCAATAC
Taok2_3arm_rev_1 (mouse)	CAGAATCTAGCACACTGGGCAG

2.1.3 **Antibodies**

Antibodies	Company	IDENTIFIER
Rabbit polyclonal anti-TAOK2	ProteinTech	21188-1-AP; RRID: AB_10755293
Rabbit monoclonal anti-pYAP (Ser127) (D9W2I)	Cell Signaling Technology	Cat# 13008; RRID: AB_2650553
Rabbit monoclonal anti-pYAP (Ser397) (D1E7Y)	Cell Signaling Technology	Cat# 13619; RRID: AB_2650554
Mouse monoclonal anti-YAP (M01), clone 2F12	Abnova	Cat# H00010413-M01; RRID: AB_535096
Rabbit monoclonal anti pLATS1 (Thr1079) (D57D3)	Cell Signaling Technology	Cat# 8654; RRID: AB_10971635
Rabbit monoclonal anti LATS1 (C66B5)	Cell Signaling Technology	Cat# 3477; RRID: AB_2133513
Rabbit monoclonal anti-pMOB1 (Thr35) (D2F10)	Cell Signaling Technology	Cat# 8699; RRID: AB_11139998
Rabbit monoclonal anti-MOB1 (E1N9D)	Cell Signaling Technology	Cat# 13730; RRID: AB_2783010
Mouse monoclonal anti-alpha-Tubulin	Sigma-Aldrich	Cat# T5168; RRID: AB_477579

2.1.4 **Baterial and virus strains, enzymes**

Name	Manufacturer	Identifier
Escherichia coli One Shot™ Mach1™ T1 competent cells	ThermoFisher	Cat# C862003

2.1.5 **Organisms**

2.1.5.1 Cell lines

Experimental Models: Cell Lines	Source	Identifier
Human: HEK293-A cells	ATCC	RRID: CVCL_6910
Human: HEK293-FT cells	ATCC	Cat# PTA-5077; RRID: CVCL_6911
Human: HEK293-TAOK2 cells	This paper	N/A
Human: HEK293-TAOK2 KD cells	This paper	N/A

2.1.5.2 Mouse

Line	Genotype	Genetic background	Experiment
Taok2xEmx 1-Cre	Taok2tm1c fl/fl; Emx1-Cre tg/0 (Knockout) Taok2tm1c fl/fl; Emx1-Cre + (control, wt) Taok2tn1c fl/+; Emx1-Cre+ (control, wt)	C57Bl/6N	cisProfiler; RNAseq

2.1.6 **Chemicals, peptides, recombinant proteins, enzymes,and polymerase**

Chemicals, Peptides, and Recombinant Proteins	Source	Identifier
Lipofectamine	Invitrogen	Cat#L3000015
SYBR Green Master Mix with ROX	ThermoFisher	Cat#A25777
QiaZol lysis buffer	Qiagen	Cat#79306
Direct-zol RNA MiniPrep	Zymo	Cat#R2052
High-Capacity c-DNA Reverse Transcription Kit	ThermoFisher	Cat#4368813
Passive lysis buffer	Promega	Cat# E1941
Firefly luciferase substrate: D-Luciferin, free acid	PJK GmbH	Cat# 102112
Renilla luciferase substrate: h-Coelenterazine	PJK GmbH	Cat# 102182
HotStarTaq Plus DNA Polymerase	Qiagen	Cat# 203605
Restriction enzyme BsmBI	NEB	Cat# R0739S
T4 DNA ligase	NEB	Cat# M0202L

Proteinase K	Roth	Cat# 7528.2
Pwo Master	Roche	Cat# 3789403001
Pfu Ultra II Fusion HotStart DNA Polymerase	Agilent Genomics	Cat# 600670
AccuPrime™ GC-Rich DNA Polymerase	ThermoFisher	Cat# 12337016
Benzonase	Sigma	Cat# E1014
Go Tag G2 Flexi	Promega	Cat#598761
Red Tag	Sigma	Cat#D4309-250UN

2.1.7 **Critical commercial assay kit**

Critical Commercial Assays	Source	Identifier
Protein assay Dye reagent concentrate	Bio Rad	Cat# 500-0006
Cell Counting Kit-8	Dojindo	Cat# CK04-11

2.1.8 **Equipment**

Equipment	Manufacturer	Device/Catalog No.
Safe 2020 Workbench	ThermoScientific	475663
Centrifuge 5810R	Eppendorf	5820850078
Mini Centrifuge Model sprout	ThermoScientific	-
BioPhotometer	Eppendorf	6131 000.012
Thermocycler T3000	Biometra	050-801
UV Gel documentation system	INTAS	-
Microscope Axiovert 25	Zeiss	-
Microscope Observer Z1	Zeiss	-
Water bath	GFL	1500946
Autoclave	Systec	HX-430
Arium 611 Water Purification System	Sartorius	85032-536-36
Microplate Reader Mithras	Berthold Technologies	38099BA1
Delfia Plateshake	WALLAC	1296-001

StepOnePlus Real-Time PCR System	ThermoFisher Scientific	-
Mini Trans-Blot Electrophoretic Transfer Cell	Bio Rad	170-3930
Mini Trans-Blot Module	Bio Rad	170-3935
Blotting Roller, 8.6 cm wide	ThermoFisher Scientific	LC2100
ECL ChemoCam Imager	INTAS	-
Cell strainer 40 µm	BD Falcon	352340
Millex HF-Filter 0,45µm, 33mm	Millipore	SLHa033SS
Discardit II Syringe; 10 ml	Biosciences	309110 BD
PCR 96-well Plate, klar	Biozym	712220
White 96-Well-Plate	Falcon	353296

2.1.9 **Software and Algorithms**

Software and Algorithms	Source	Link
R studio	RStudio	https://rstudio.com/
ImageJ	National Institutes of Health	https://imagej.nih.gov/ij
Universal ProbeLibrary Assay Design Center	Roche	https://lifescience.roche.com/en_de/brands/universal-probe-library.html#assay-design-center
Illustrator CS5	Adobe	-
Lumicycle Version 1.4	ActiMetrics	-
Zotero	Zotero	https://www.zotero.org/

2.1.10 **Media**

Neuron Culture medium
Neurobasal medium, 2% B27, 1% GlutaMax
HEK293-A/FT
DMEM (4.5 g/l glucose), 10% FBS, 1% GlutaMax (maintenance medium)
HEK293-TAOK2/TAOK2 KD/sgTAOK2
DMEM (4.5 g/l glucose), 10% FBS, 1% GlutaMax,700ng/ml Puromycin

2.1.10.1 Buffers and solutions

Buffer for genotyping
Lysis buffer:

EDTA-Na_2-$2H_2O$ EDTA f.c. 0.2mM

NaOH f.c. 25mM

74.4 mg EDTA is added to 1 L of Millipore water in a beaker with a magnetic stirring bar and is stirred until dissolved. 1 g NaOH is added and dissolved under stirring.

Neutralization buffer:

Tris· HCl f.c. 40mM

1 g Tris · HCl is added to 159 mL Millipore water in a beaker and stirred on a magnetic stirring bar until dissolved

Buffer for western blotting

10x Running buffer:

Components	Concentration	g/1L
Glycine	1.92 M	144
Tris base	0.25 M	30.3
SDS	1%	10

Dilute 10-fold before use.

10x Transfer (blotting) buffer:

Components	Concentration	g/1L
Tris	0.25 M	30.3
Glycine	1.92 M	144

Dilute 10-fold before use, and add 200ml Methanol/1L + 0.2% SDS

➔ for 1L, take 100ml 10x stock, 680ml H_2O, 200ml Methanol, 20ml 10% SDS.

Solutions for cisProfiler (lysis/binding buffer(500ml))

50 ml	1 M TRIS/HCl pH7,5	=>	100 mM
10,6 g	LiCl	=>	500 mM
50 ml	100 mM EDTA pH 8	=>	10 mM
385,63 mg	DTT	=>	5 mM
5 g (complete can)	LiDS	=>	1 %

Add H_2O dd to 500 ml

2.2 Methods

2.2.1 **Cloning**

For all 28 components tested in the interaction screen, recombination-based Gateway cloning (ThermoFisher) was used to clone the corresponding open reading frame (ORF). Amplify each ORF by PCR using DNA proofreading polymerases (Pwo, Roche; Pfu Ultra, Agilent Genomics; AccuPrime™ GC-Rich, ThermoFisher) and BP-recombine them in the pDONR/Zeo plasmid (ThermoFisher) to generate an Entry plasmid. Then it was control-digested with BsrGI (testing successful cloning of insert) and sequence-verified. RefSeq IDs for each ORF cloned is provided in the material part for plasmids. For split TEV assays, C-terminally open ORFs (i.e. containing no stop codon) are fused to NTEV-tcs-GV and CTEV moieties. Split TEV-based Gateway pDEST vectors were described previously (Wehr et al., 2006). Cloning of STK4 (Wehr et al., 2013) as well as PIK3R1, GRB2, SHC1, SRC and ERBB4 (Wehr et al., 2017) was described before. All oligonucleotides used for Gateway-based BP cloning of ORFs are listed in Table S1.

For the time-controlled gene expression, we used the pInducer plasmid carrying a human ubiquitin C (hUbC) promotor-driven reversed tetracycline-controlled transactivator (rTta) gene, an IRES-controlled puromycin resistance gene, and an tetracycline response element-driven expression cassette for genes of interest (Wennmann et al., 2014). The ORF for TAOK2 was cloned using recombination-based Gateway cloning. The TAOK2 kinase-dead mutant (TAOK2-var1_D151A) was generated using site-directed mutagenesis, which was conducted using a whole plasmid PCR followed by a DpnI digest to remove the parental plasmid DNA. PCR primers for the mutagenesis are provided in material part.

For the inactivation of TAOK2, we applied the CRISPR inhibition (CRISPRi) technology (Gilbert et al., 2014). We used a lentiviral approach to simultaneously express an sgRNA under the control of the hU6 promotor and a hUbC promoter-driven dead Cas9-KRAB fusion (dCas9-KRAB). A puromycin resistance gene for stable selection is linked to dCas9-KRAB via a T2A cleavage site (Addgene plasmid # 71236, pLV hU6-sgRNA hUbC-dCas9-KRAB-T2a-Puro) (Thakore et al., 2015). For improved CRISPRi

performance, the existing KRAB domain was replaced in this vector by the ZIM3-KRAB domain (Alerasool et al., 2020) using NheI, yielding the plasmid pLV_hU6-sgRNA_hUbC-dCas9-ZIM3-KRAB-T2a-PuroR. Sequences for CRISPRi sgRNAs were designed using the Broad Institute GPP sgRNA Designer site (https://portals.broadinstitute.org/gpp/public/analysis-tools/sgrna-design-crisprai).
sgRNAs were cloned using BsmBI. Oligonucleotides used to clone sgRNAs are listed in the material part.

2.2.2 **Culturing of eukaryotic cell lines**

HEK293-A and HEK293-FT cell lines were cultured in DMEM (4,5g/L) supplemented with 10% FCS, 1% GlutaMAX, and 1 % Pen/Strep in a humidified incubator with 5% CO_2 at 37°C. To generate HEK293-TAOK2/TAOK2 KD and HEK293-Ctrl CRISPRi /sgTAOK2-CRISPRi stable cell lines, HEK293-A cells were infected with lentivirus particles carrying a puromycin resistance gene (either pInducer or sgTAOK2-CRISPRi constructs). Two days after infection, cells were selected using DMEM (4.5g/L) supplemented with 10% FCS, 1% GlutaMAX and 700 ng/ml puromycin to obtain polygenic clones with stable integrates. Maintenance medium containing puromycin was replaced with fresh medium every 2-3 days. Polygenic clones were obtained 10-14 days after the selection was initiated. These stable cell lines were maintained in the same medium as above at 37°C and 5% CO_2. To induce the overexpression of TAOK2/TAOK2 KD, doxycyclin (f.c.125ng/ml) was added to each cell line for 6 hours. When cells are 80-90% confluent, they were passaged according to standard protocol.

2.2.3 **Primary neuron culture**

E15.5 Taok2xEmx1-Cre mice embryos with C57Bl/6N genetic background were used to prepare primary mouse cortical neurons. Before neuron preparation, genotyping for each mice embryo was performed as following:
A small piece of tail tissue from each embryo was cut off and put into the PCR tubes. 75 µl lysis buffer was added into one PCR tube, which was subsequently transferred to a thermocycler. The closed tube was heated for 20min at 95 °C. Afterwards, the tube was

removed from the heat block and cooled down to room temperature. Then 75 µl neutralization buffer was added into it. Typically, 1~2µl supernatant was used for the genotyping PCR. The PCR mix was prepared, as shown in Table 2 with different primers for each target gene (Table 3). The PCR program was ran as described in Table 4. For the agarose gel electrophoreses a 1.5% gel was used for Cre and Emx1-Cre.

Table 2. PCR master-mix for floxed Taok2 and Cre

Floxed Taok2	Stock	1x(µl)	Cre	1x(µl)
DNA	1x	1	DNA	2
H_2O	1x	1,175	H_2O	6,05
Flexi 5X	5x	3	REDTaq buffer	1,5
$MgCl_2$	25mM	1.8	dNTP each	1,6
dNTP each	2mM	1.5	O1848	0,77
O1053	10µM	0,15	O1849	0,77
O1054	10µM	0,15	O1850	0,77
O1056	10µM	0,15	O1851	0,77
GoTag	5U/µl	0,075	REDTag	0,77
Total		15		15

Table 3. PCR primer for floxed Taok2 and Cre

Primer	Sequence	ID	Protein
Taok2_5arm_loxP_fwd_1	GACCAGTCTGGACTACCTAGTG	O1053	flox
Taok2_critical region_rev_1	GAAGCTGAGCCCAGGCAATAC	O1054	flox
Taok2_3arm_rev_1	CAGAATCTAGCACACTGGGCAG	O1056	flox
senseECMV_IRES	ATTTTCCACCATATTGCCGTCT	O1848	Cre
asenseECMV_IRES	AGCCATTTGACTCTTTCCACAAC	O1849	Cre
oIMR4170	AAGGTGTGGTTCCAGAATCG	O1850	Cre
oIMR4171	CTCTCCACCAGAAGGCTGAG	O1851	Cre

Table 4. PCR program for floxed Taok2 and Cre

Program: Floxed Taok2	time	cycle	Program: Cre	time	cycle
95°C	break	-	94°C	break	-
95°C	1min	-	94°C	3min	-
95°C	10sec	36	94°C	30sec	36
65°C	20sec		55°C	30sec	
72°C	30sec		72°C	30sec	
72°C	2min	-	72°C	7min	-
4°C	break	-	12°C	break	-

Plate medium with half of the final volume to the plates coated with poly-L-lysine (PLL, 0.1 mg/ml in dH2O), which were kept in the incubator until dissection. Dissect mouse cortices in cold HBSS supplemented with 5mM HEPES. Next, they were dissociated in 1 ml activated papain (1 ml DMEM + 40 µl Papain + 40 µl DNaseI + 10 µl L-cysteine) with 13 min under the room temperature. Terminate papain treatment with 10 ml pH equilibrated and pre-warmed plating medium [DMEM (4.5 g/l glucose) +10 % FBS]. The medium was discarded and another 10 ml plating medium was added and aspirated again. Later 2 ml medium was added to the cortices. Subsequently, P1000 pipette was used to triturate the cortices. Then to separate any cell clusters, we transferred cell suspension through a 40 µm cell strainer (BD). After this, cell density was determined with a cell counting chamber by counting trypan blue-negative cells. Finally, dilute cells with plating medium for the desired cell density, plate cells and incubate them in the incubator. During the whole experiment process, we set the cell density to be ~500 cells/mm^2. On DIV1, completely replace plating medium with serum-free neuronal culture medium. On DIV6-7, for the first time, we feed the neuronal cultures through replacing half volume with pH equilibrated neuronal culture medium. Afterwards, in next 3-4 days, we feed neuronal cultures again.

2.2.4 **AAV generation**

AAV generation was conducted according to the instruction provided in A. Herholt's PhD thesis (page 35-36, Section 4.3 AAV production)(Alexander Herholt, 2016), which included 3 main steps: transfection, AAV harvest and quantification.

Transfection

HEK293FT cells were used to generate AAVs. For one virus prep in 15cm dish, the transfection DNA was mixed as following table:

Table 5. Mix DNA for AAV production

Plasmid name	Amount
AAV transfer plasmid	x µg (1pmol)
pSerotype*	7,5 µg (1pmol)
pFdelta6 (V1739)	10 µg (1pmol)

- Calculate the amount of AAV transfer plasmid based on following formula:

$$\mu g\ (DNA) = \left(\frac{660\ pg}{1\ pmol}\right) \times \left(\frac{1\ \mu g}{10^6\ pg}\right) \times N \times 1\ pmol\ (DNA)$$

N = Number of base pairs of AAV transfer plasmid

AAV harvest and quantification

After 3 days incubation, AAV particles was harvested, aliquoted and stored at -80°C.The AAV genomic copies (GC) quantification was performed by PCR to control the infection rate during experiments. Usually, AAV GC titers were obtained in the range of 1e+09-1e+10 GC/µl finally.

2.2.5 **Lentivirus production**

The production of Lentivirus was performed according to the general published guidelines, which included 2 main steps: transfection and lentivirus harvest.

Transfection

HEK293FT cells were used to generate lentivirus. Make the transfection DNA mix with the following ratio: Lentivirus Transfer Vector 6 µg + psPAX2 (V763) 4.5 µg + pMD2.G (V188) 1.5 µg.

Lentivirus harvest

After two days incubation, supernatant was collected, centrifuged at 3000 x g for 15 minutes and filtered through a 0.45 µM PVDF filter, then the purified virus was obtained.

It was aliquoted and stored at -80°C for future usage. Virus cannot be quantified. During experiment, 500 µl of filter-purified virus was added into one well of HEK293 cells in 6-well plate (400,000 cells/well) according to the rule of thumb for infections.

2.2.6 **Luciferase assays for split TEV-based protein-protein interaction screening**

The constructs used for split TEV screening are presented in detail and graphically as Figure 8. All assays were run in 96-well plates using six replicates per condition. On each plate, a WWC1 homodimerization assay and a WWC1::R1-noSARAH assay served as positive and negative controls, respectively. For each bait (i.e. NTEV fusions), we assessed the basal activity in the split TEV interaction assay when co-expressed with the control R1-noSARAH-CTEV. For interaction screening, 20 000 HEK293 cells were plated per 96-well. The following day, plasmids encoding bait-NTEV-tcs-GV, prey-CTEV, 10xUAS-Fluc, and TK-Renilla were transiently transfected into HEK293 cells using Lipofectamine 2000 (Thermo Fisher) and plasmids were allowed to express 20h. Lyse cell with passive lysis buffer (Promega) and subject them to a dual luciferase assay (Promega). For data processing, resulting firefly values were divided by Renilla values to yield firefly/Renilla ratios. For each interaction, the six replicates were averaged. To normalize interaction data for each bait/prey interaction pair, the averaged Firefly/Renilla ratio was divided by the corresponding averaged Firefly/Renilla ratio of the bait/RASSF1-noSARAH negative control to yield a fold change value. A detailed plate layout of the screening assays and a summary on data processing is provided in Figure 9. Screening data (fold change values and log2-transformed values for all bait-prey interactions measured) are provided in Table S2.

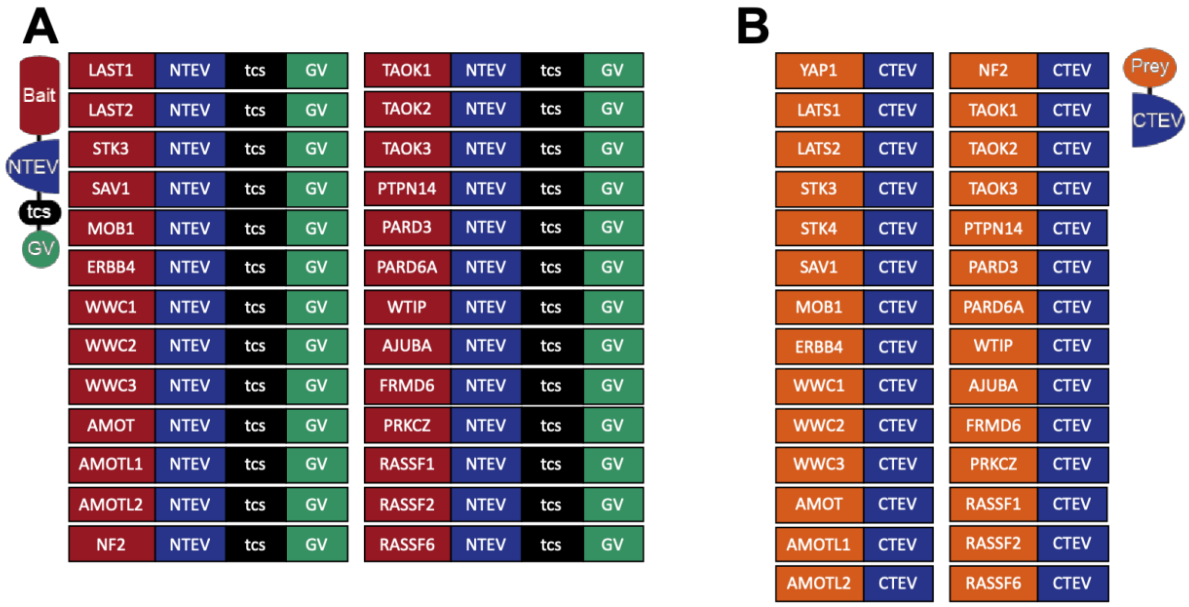

Figure 8. Constructs used for split TEV screening.

(**A**) 26 constructs expressing the bait-NTEV-tcs-GV fusions. (**B**) 28 constructs expressing the prey-CTEV fusions.

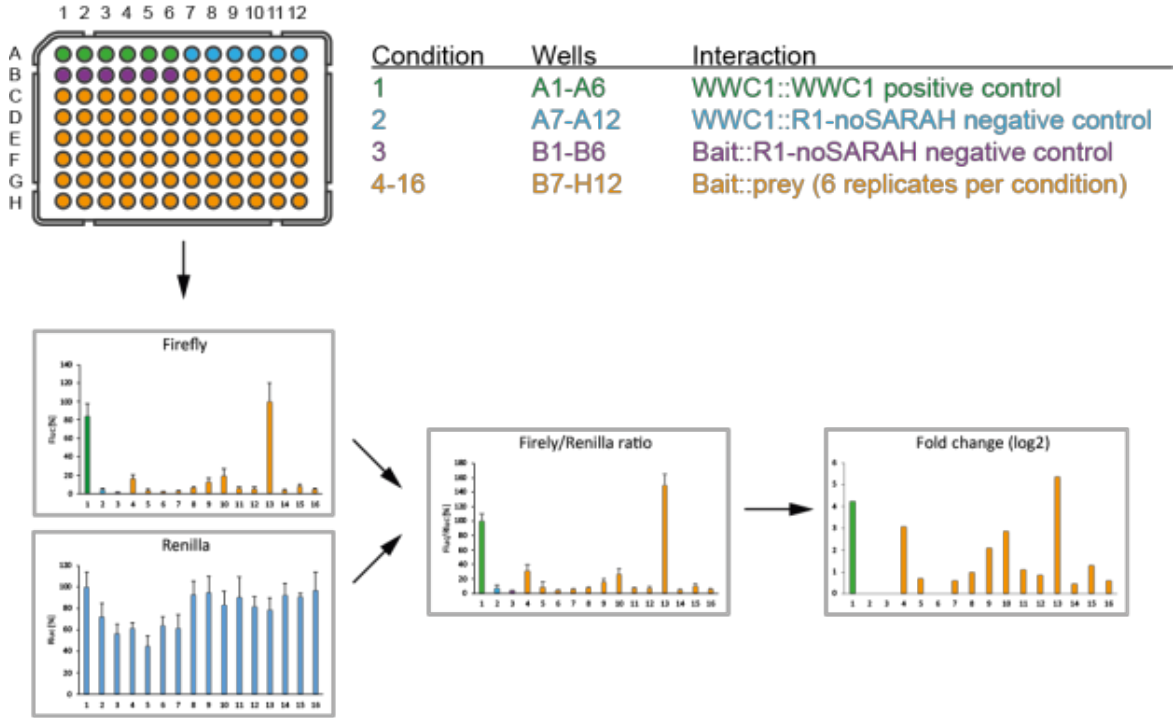

Figure 9. Plate layout and data processing of the focused protein-protein interaction screen.

Upper panel: The screen was performed in 96-well plates, with six replicates per condition. All plates contained identical positive and negative interaction controls. In positions A1-A6 (dark green colored wells), a positive protein-protein interaction control comprising the constitutive dimer formation of WWC1 was applied (condition 1). In positions A7-A12 (light blue colored wells), a negative protein-protein interaction control comprising WWC1 and RASSF1 that lacks the C-terminal SARAH domain (R1-noSARAH) was used (condition 2). For each bait, a bait negative control was added to positions B1-B6 (light purple-colored wells, condition 3). In positions B7-H12 (orange-colored wells), the bait-prey combinations were tested (conditions 4 – 16). Lower panel: For each condition, firefly luciferase and *Renilla* luciferase values were collected and averaged. From these data, a ratio of Firefly/*Renilla* was calculated. For calculation of log2-transformed fold changes, the positive control ratio was divided by the negative control ratio, and each bait-prey ratio was divided by the bait negative control ratio to obtain fold change values. Fold change values were log2-transformed. Averaged firefly luciferase, firefly/*Renilla* ratios, and log2-transformed fold changes are shown according to the color scheme introduced above (i.e., dark green for condition 1, light blue for condition 2, light purple for condition 3, and orange for conditions 4 – 16). Averaged *Renilla* luciferase values are depicted in blue. Error bars represent SD, n=6.

For visualizing screening data in hierarchically clustered heatmaps, log2-transformed fold change values of protein-protein interactions were plotted using the heatmap function of the R package gplots. Weighted interaction networks were constructed using R packages tidygraph, graphlayouts, and ggraph. Nodes were assigned as source and target. Weights of edges were calculated from (1) log2-transformed fold change values obtained from our split TEV interaction data and (2) from an interaction score downloaded from the Mentha database (https://mentha.uniroma2.it/beta-tools/index.php) that contains primary interaction data.

2.2.7 **Luciferase assay for TEAD reporters**

This assay was run in 96-well plates using six replicates per condition. 20 000 HEK293 cells were plated per 96-well. The following day, plasmids encoding TEAD reporter, core Hippo Signaling components, 10xUAS-Fluc, and TK-*Renilla* were transiently transfected into HEK293 cells using Lipofectamine 3000 (Thermo Fisher). 20h later, lyse cells with passive lysis buffer (Promega) and subject them to a dual luciferase assay (Promega). For data processing, resulting firefly values were divided by Renilla values to yield firefly/*Renilla* ratios. For each condition, the six replicates were averaged.

2.2.8 **Quantitative real-time PCR**

Wash $6x10^5$ HEK293 cells with PBS and lyse them in 300µl QIAzol Lysis Reagent (Qiagen). Isolate total RNA using Direct-zol RNA MiniPrep kit (Zymo Research). cDNA

was synthesized from 500 ng total RNA with the High Capacity cDNA Reverse Transcription Kit (Applied Biosystems, Foster City, USA) in a 20 µl reaction mixture (S. Ma et al., 2020). Perform Real-time PCR in the Applied Biosystems™ StepOnePlus™ Real-Time PCR System (ThermoFisher Scientific). Primers were designed with Roche's Universal Probe Library Assay Design Center (https://lifescience.roche.com/en_de/brands/universal-probe-library.html#assay-design-center) and the sequences used are listed in 2.1.2 Oligonucleotide. Efficiency of designed primers were assessed individually and the primer pairs with efficiency ~98% and single peak in the melting curves were selected for further studies (using Applied Biosystems software). Fold change of the targets in stimulated samples was calculated relative to control-treated cells using standard DDCT method after normalizing to housekeeping genes RPLP0 and 18S.

2.2.9 **Co-immunoprecipitations and Western blotting**

Plate HEK293 cells with $6x10^5$ cells/well in 6-well plates. Transfect cells with selected plasmids using Lipofectamine 3000 (Life Technologies ThermoFisher) the next day. 18h later, cells were lysed in lysis buffer (1% Triton-X) supplemented with PhosSTOP (Roche) and cOmplete™ Mini Protease Inhibitor Cocktail (Roche). For co-immunoprecipitaions, spin cell extracts at 4℃ at 14000 rpm for 10 mins. Purify FLAG-tagged proteins by anti-FLAG M2 affinity gel (Sigma). After 2h of incubation at 4°C, wash the FLAG immunoprecipitates four times in lysis buffer and denature them at 70°C for 10min. Protein gels were run using the PowerPac™ HC Electrophoresis System (Bio-Rad), and gels were blotted either using the same chambers or applying a wet blotting approach. Detect proteins was performed using chemiluminescence (ECL Plus Western Blotting Substrate, ThermoScientific). Analysis of western blots was done by ImageJ, following a protocol available on lukemiller.org. Significance was calculated by GraphPad Prism with 1-way ANOVA, followed by Bonferroni posthoc tests.

2.2.10 **Cell proliferation**

Cell proliferation was assessed for 96 hours using the CCK-8 kit (Dojindo, Munich, Germany). Measurements were performed at 8h, 24 h, 48h, 72h, and 96h after seeding. In brief, 5000 HEK293 (i.e., HEK293_TAOK2-dox, HEK293_sgScr, HEK293_sgTAOK2i) cells/well were divided into a 96-well plate, respectively. Each condition was run in 6 replicates. As values were acquired at 5 different time points, five 96-well plates with the same layout were prepared for each cell line. HEK293 cells of the doxycycline-inducible TAOK2 inducible cell line (HEK293_TAOK2-dox) were grown in medium containing 125 ng/ml doxycycline. 3 hours prior to measurement, 10µl of the CCK-8 solution was put to each well and incubated in the dark at 37°C. The absorbance was measured at 450nm wavelength with a LB940 Mithras plate reader (Berthold Technologies). Optical density (OD) values obtained at all time points were normalized to 8h time points, for which the mean was set to 1. Each experiment was replicated three times.

2.2.11 **Patient Survival Analysis**

Overall survival of patients and TAOK2 expression data of 28 different types of cancers were extracted from the TCGA database (pan-cancer atlas project 2018) using the R package cgdsr. We assessed the association between TAOK2 expression with patients' survival time. The log-rank test was used to compare the overall survival of patients between high and low TAOK2 expression samples (separated by the median value), considering $p \leq 0.05$ as significant statistically. Survfit function from R package survival was used to performed survival analysis.

2.2.12 **Multiparametric cisProfiler assay for pathway profiling**

Cortex primary neurons from wild type and TAOK2 ko mice were plated into 96-well plates coated with poly-L-lysine (20,000/well) with neuronal maintenance medium. On DIV2, neurons were fed and then infected with the AAV-based cis-regulatory sensor library (5000 AAV GCs/cell). The detailed information of these cis-regulatory sensors was listed in Table S3. On DIV7, neurons were fed again. Then on DIV 12, neurons were stimulated with different stimuli (concentration 0.1,1, 10, and 100 µM（or ng/ml）) for 4h, 24h, and

48h, respectively. After stimulation, neurons were lysed with Tag&Pool lysis/binding buffer and stored in -80°C freezer. Then RNA would be purified with Dynabeads™ mRNA Direct Kit™ (Thermo fisher) and cDNA would be synthesized using the High-capacity c-DNA reverse Transcription Kit (Applied Biosystems).

For barcode amplification and sequencing, it was conducted according to the instruction described in A. Herholt's PhD thesis (page 38-39, Section 4.5 Multiplexed cis-regulatory sensor assay) (Alexander Herholt, 2016). It was performed as following: After the cDNA synthesis, barcodes were amplified. The input of cDNA was 1 µl of cDNA (1/10 dilution) into a 20 µl PCR reaction. Perform PCR for 30 cycles with an annealing temperature of 59°C. Verify PCR product by agarose gel-electrophoresis. Then barcodes were fused with the adapter sequences for Ion Torrent sequencing in a second PCR. HotStar Taq plus DNA polymerase (Qiagen) were used to do the PCR, whose product was further verified using agarose gel-electrophoresis. Barcode libraries were sequenced by the PI chip on the Ion Torrent Proton sequencer. Sequencing was performed with Ion PI Sequencing 200 v3 kit. Raw data was processed using custom shell and R scripts with the help of Dr. Sven Wichert (Alexander Herholt, 2016).

2.2.13 **Next-Generation Sequence (RNAseq)**

RNA extraction

Extract total RNA from primary neurons infected with different AAVs (i.e. pAAV_EFSp_hTAOK2-var1; pAAV_ EFSp_EGFP; pAAV_shRNA-mTaok2_ 3_Syn1p_EGFP_Mm114; pAAV_shCtrl) with RLT (Qiagen Micro-Rneasy Kit). Then purify RNA with a NucleoSpin RNA Clean-up kit (MachereyNagel, NucleoSpin®, Germany).

Library construction for RNA sequencing

450 ng of RNA was used for RNA-Seq library preparation. The libraries were prepared using Quantseq 3'mRNA Sequencing (FWD) kit (Lexogen, Austria). Briefly, first strand cDNA was generated using a poly-T tagged primer and then the second strand cNDA was synthesized. The samples were indexed for multiplexing. The libraries were quantified using KAPA library quantification kit (Roche, Switzerland) and equimolar

concentrations were pooled for sequencing. The libraries were then sequenced on a HiSeq2500 Platform (Illumina, USA).

Sequencing data analysis

Quality control for the raw data was performed by using FASTQC (de Sena Brandine & Smith, 2021). Then map the filtered reads to Mouse Genome (Mus musculus 10 Genome) using STAR aligner. Reads that map unambiguously to single loci on the genome were retained and counted using the HTSeq Count function (Anders et al., 2015). DESeq2 was used to find differential expressed gene (Love et al., 2014).

Pathway enrichment analysis

GOseq was used to execute Gene Ontology (GO) enrichment analysis. Terms with KS value < 0.05 (Kolmogorov–Smirnov) were regarded as enriched with significance. The KEGG enriched pathways of the DEGs was done by KOBAS.

2.2.14 **Generation of Taok2 conditional knockout mice**

Taok2 was inactivated in the brain using the Cre/loxP system. Floxed Taok2-mice were generated from mouse embryonic stem cells obtained from EUCOMM (M. Wehr, personal communication). They carried with two inserted loxP sites between exon four and five, as well as exon eight and nine of the Taok2 gene (fl/fl). The Emx1-Cre driver line was mated to floxed Taok2 mice to inactivate Taok2 early during development and to target a rather large area within the brain. To establish mouse cohorts for behavioural profiling, Taok2 (fl/fl) and Emx1-Cre (tg/0) mice were mated.

2.2.15 **Behavioural profiling using the PsyCop platform**

The PsyCop platform consists of several consecutively performed experiments to analyze behavioural difference between genetically modified mice and wildtype mice. First, a cohort should be established by mating male and female mice with an appropriate genotype 12 weeks before the actual behavioural test experiments. Averagely, a female mouse needs 1 week to get pregnant and 3 more weeks to give birth to pups (6-8 pups on average). When reaching 3 weeks old, the pups can be separated from their mother (a process termed wean) and genotyped by a selective PCR using a small piece of tail

tissue. To study psychosocial stress and to precipitate psychosis-related phenotypes in a mouse model, resident-intruder paradigm (or social defeat paradigm) can be performed in mice of 3-5 weeks old. It takes 3 weeks to complete this paradigm. Afterwards, every mouse needs to be chipped with an animal transponder for intellicage-based tests, which are part of the PsyCop platform. To allow the mice to recover, they should not be in an experiment for the next three days after chipping.

Usually, a test cohort consists of 12-20 knock-out mice and 12-20 littermate controls. The knock-out mice contain both the homozygous floxed Taok2 alleles and the Cre recombinase under the control of the Emx1 promoter (Taok2 fl/fl; Emx1-Cre tg/0, referred as Taok2 knock-out (Taok2 ko)), while the littermate controls only contain the homozygous floxed Taok2 alleles (Taok2 fl/fl, referred as wildtype(wt) controls). To avoid extraordinary aggression among the male mice, they need to be put together into their new home cage after weaning, which happens around 3-4 weeks after birth. Within a cohort, 8-14 mice per “Type 4 cage” are group-housed, in which wt control and Taok2 ko mice are mixed. Every mouse can access food and water unrestrictedly and should be checked for injuries or sickness daily. Their bedding is changed every week. A Perspex tunnel is put into each cage so as to make the mice accustomed to the handling device. When mice reach 8-16 weeks old, experiments can be started on them. Ideally, the mice should have a similar age, which is not always possible due to breeding logistics. However, it is important to guarantee that all mice are tested under similar conditions, e.g., daytime and light intensity. Notably, a protocol sheet needs to be filed to document results for each behavioural test. Behavioural experiments were performed by Celestine Dutta and Elisabeth Voggenreiter, both of them were Master students in Michael Wehr’s lab.

3. Results

3.1 TAOK2 modulates Hippo Signaling to regulate growth

3.1.1 Characterization of a Hippo pathway interaction network using a split TEV-based protein-protein interaction screening in living cells

Hippo pathway activity is controlled by a plethora of proteins, either promoting or inhibiting the transcriptional activity of the YAP1 (Boopathy & Hong, 2019). For many of these regulators, defined interactions with core kinase cassette components are described. For example, WWC proteins bind to LATS kinases to increase phospho-YAP1 levels and thus inhibit YAP1 activity (Genevet et al., 2010; Wennmann et al., 2014; J. Yu et al., 2010). Conversely, Ajuba family proteins, such as Ajuba and Wilms tumour protein 1-interacting protein (WTIP), bind to LATS kinases and SAV1 to inhibit LATS kinases to promote nuclear, i.e., active YAP1 (Das Thakur et al., 2010). To gain further insight on physical interactions, and the relative strength of associations, and to better characterize modulators, we performed a focused interaction screen among core components and major regulators of the pathway using the split TEV technique, which allows the robust and quantitative assessment of PPIs in living cells (Wehr et al., 2006).

To identify potentially hidden interactions, we conducted a pairwise interaction analysis of 28 Signaling components (Table S1) using the split TEV assay system. For YAP1, which shuttles between the cytosol and the nucleus, we used a CTEV fusion only as an NTEV-tcs-GV fusion is likely to cause artificially high background signals due to a nuclear localization. To further exclude any other bait-NTEV-tcs-GV fusion that may produce high background activity during interaction screening, all other bait-NTEV-tcs-GV fusions were first functionally tested in HEK293 cells. Each bait-NTEV-tcs-GV fusion was transfected into HEK293 cells with a 10x clustered UAS firefly luciferase reporter plasmid (10xUAS-luc2) and a thymidine kinase promoter-driven *Renilla* luciferase plasmid (TK-*Renilla*) that is used for normalization (Figure 10.A). Cells were lysed 20hrs later and subjected to a dual luciferase assay. Each experimental condition was performed in six replicates. A homodimer formation of WWC1 (WWC1-NTEV-tcs-GV and WWC1-CTEV), which is

known to provide a strong signal in a split TEV assay (Genevet et al., 2010), served as positive control readout and its readings were used to define the activity of the assay to 100% (Figure 10.B). Notably, the STK4-NTEV-tcs-GV fusion resulted in high background signals (Figure 10.B), likely caused by caspase-mediated cleavage resulting in the release of GV and concomitant reporter activation (Graves et al., 2001; K.-K. Lee et al., 2001). Therefore, STK4-NTEV-tcs-GV was removed from the bait collection and used as CTEV fusion in the prey collection only. For the focused interaction screen, 26 baits (fused to NTEV-tcs-GV) were tested against 28 preys (fused to CTEV) (Figure 11.A) (Table S1 for listing baits and preys). A mutant RASSF1 that lacks the C-terminal SARAH interaction domain (residues 1-289 of RASSF1, denoted R1-noSARAH) and was fused to the CTEV moiety was used as negative control in the split TEV assays. Bait and prey constructs were co-transfected with 10xUAS-luc2 and TK-Renilla plasmids into HEK293 cells, in six replicates per condition. Luciferase readings for each interaction tested (e.g., bait-X-NTEV-tcs-GV::prey-Y-CTEV) were normalized to the corresponding background control (i.e., bait-X-NTEV-tcs-GV::R1-noSARAH-CTEV interaction) to yield a log2-transformed fold change value for each interaction tested (Figure 11.B). Unsupervised hierarchical clustering of log2-transformed fold changes of interaction data produced a heatmap of a split TEV-based Hippo pathway interaction network (HPIN) formed of 28 components (Figure 11.C). The heatmap of clustered interactions measured by the split TEV assays indicates the existence of Hippo signalosome cluster, polarity cluster and SARAH cluster (Figure 11.C). Each pathway component that was either fused as bait or prey to NTEV-tcs-GV or CTEV, respectively, was validated for expression in HEK293 cells (Figure 12.A&B).

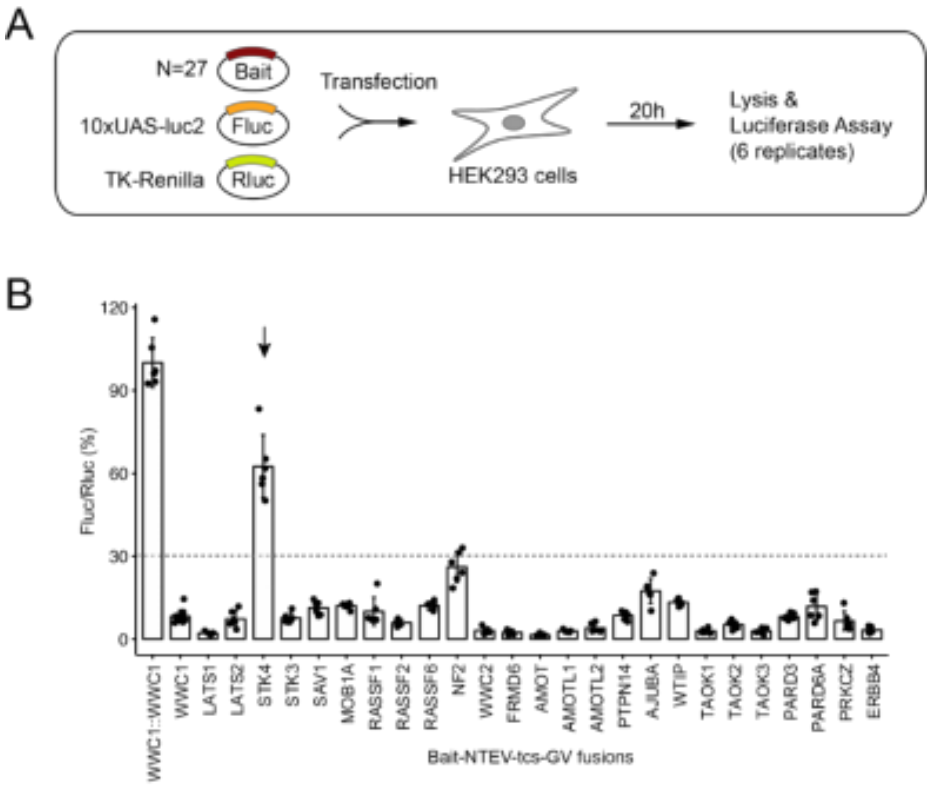

Figure 10. Functional analysis of bait-NTEV-tcs-GV fusions.

(**A**) 26 plasmids expressing the bait-NTEV-tcs-GV fusions were co-transfected with the RASSF1-noSARAH-CTEV control, along with the 10xUAS-Fluc reporter plasmid and the TK-Rluc plasmid, which served as transfection control. Cells were lyses 20hr later, followed by lysis and a dual luciferase assay. Each experimental condition was performed in six replicates. (**B**) Activities of bait-NTEV-tcs-GV fusions without simultaneous transfection of a prey-CTEV plasmid.

Data information: tcs, TEV protease cleavage site; GV, GAL4-VP16; UAS, upstream activating sequences; Fluc, firefly luciferase; TK, thymidine kinase; Rluc, Renilla luciferase. Ratio activity is calculated by Fluc/Rluc; n = 6; data are shown as mean, and error bars represent SD.

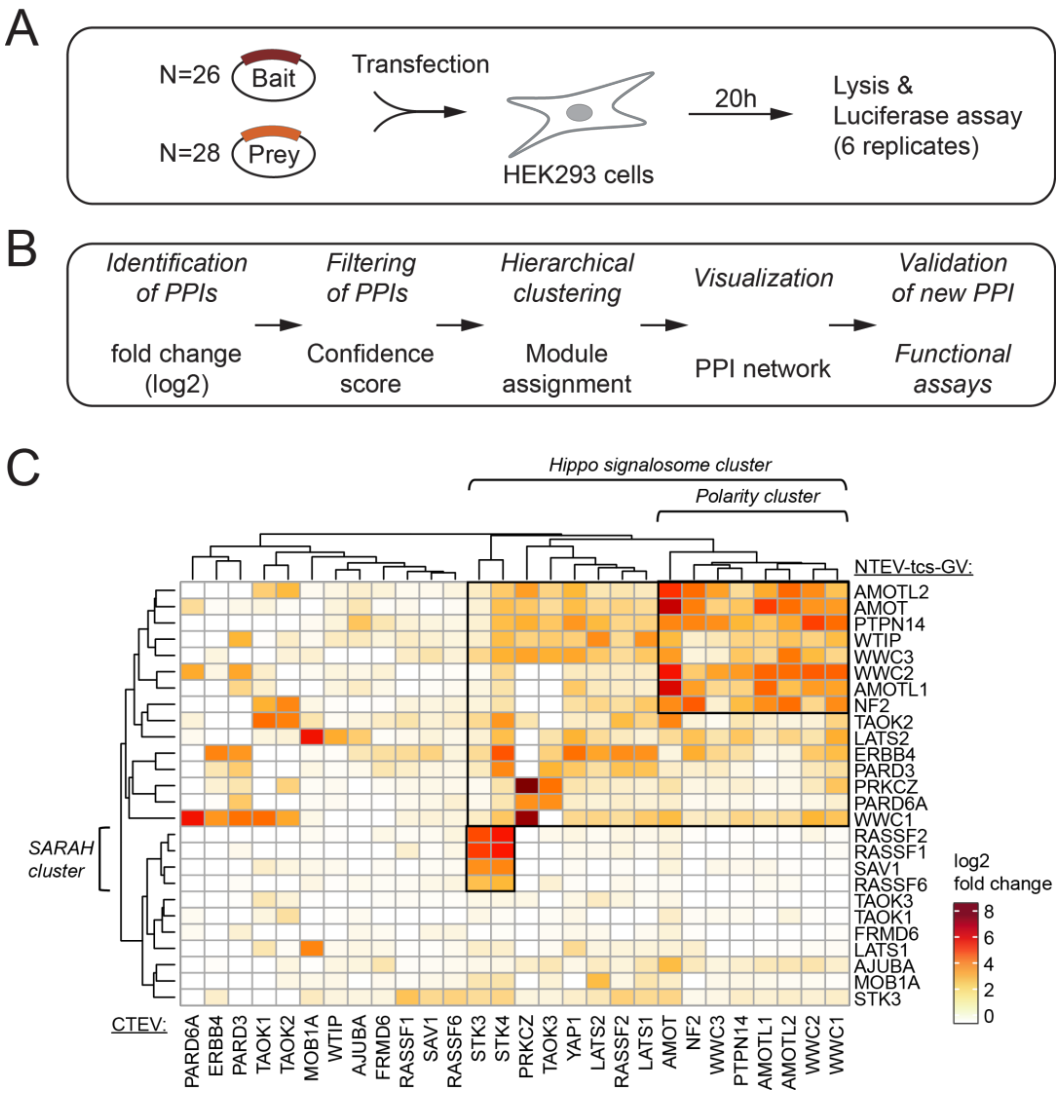

Figure 11. A focused split TEV protein-protein interaction screen identifies so far hidden interactions among Hippo pathway components.

(**A**) Concept of the focused split TEV protein-protein interaction screen. 26 baits were tested against 28 prey proteins. Baits (fused to NTEV-tcs-GV) and preys (fused to CTEV) were co-transfected with 10xUAS-firefly luciferase and TK-Renilla luciferase reporter constructs into HEK293 cells and were allowed to express for 20h, followed by lysis and a dual luciferase assay. Each bait-prey assay was conducted in six replicates. (**B**) Workflow for processing primary data to construct a Hippo pathway interaction network. For each bait-prey assay, a log2-transformed fold change value was calculated to identifying protein-protein interactions (PPIs) among Hippo pathway components. PPIs with confidence score of a log2-transformed fold change value of equal or above 1.6 were subjected to a hierarchical cluster analysis to assign modules of PPIs, followed by visualizing PPIs as network graphs. (**C**) Heatmap of hierarchically clustered protein-protein interactions monitored by split TEV assays. Among the components tested, clustering suggests three main modules for the Hippo pathway, the polarity protein cluster, the Hippo signalosome cluster covering polarity proteins and core kinase cassette components, and the SARAH interaction domain cluster. Values for interactions are given as log2-transformed fold changes relative to baseline controls (Table S2).

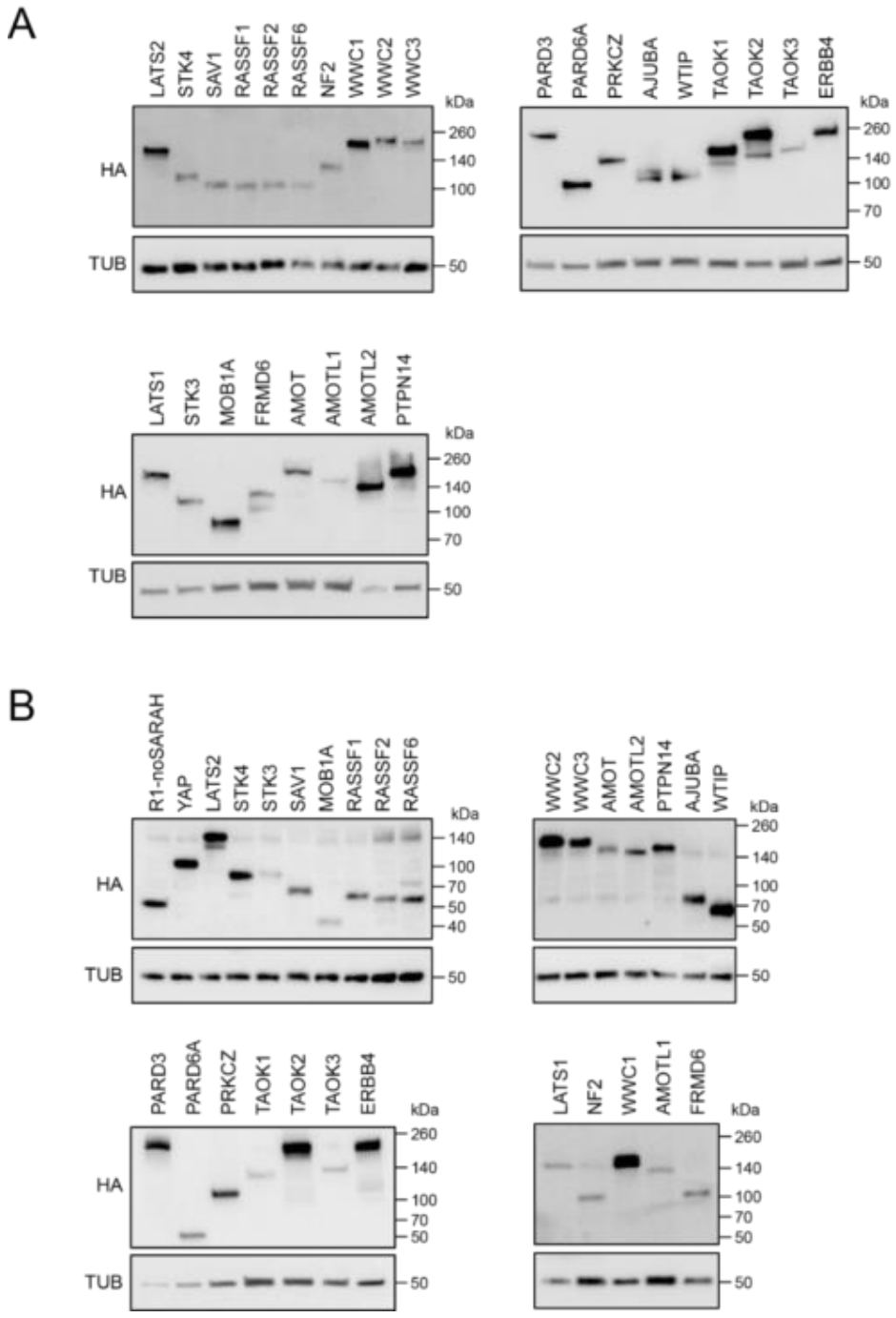

Figure 12. Validation of split TEV fusion proteins.

(**A, B**) Expression analysis of bait-NTEV-tcs-GV (**A**) and prey-CTEV fusions (**B**). Bait proteins fused to NTEV-tcs-GV-2HA tags and prey proteins fused to CTEV-2HA were transfected into in HEK293 cells. Cells were lysed after 20 h of incubation, and lysates were subjected to Western Blot analysis using the indicated antibodies.

When setting the high confidence interaction score for this network to a threshold of a log2-transformed fold change of 1.6 (corresponds to a fold change of 3) (Dembélé & Kastner, 2014), we identified 244 pairwise interactions above threshold (of 728 interactions monitored in total). Next, we compared our findings from the split TEV-based screen with physical interaction data deposited in the Mentha database (Calderone et al., 2013) that is fed by relevant databases such as BioGRID (Stark, 2006) and IntAct (Orchard et al., 2014). Interaction data curated in the Mentha database did overlap by 28.1% (72 interactions), while 67.2% (172 interactions) were newly identified PPIs by split TEV screen only and 4.7% (12 interactions) were only covered by Mentha database (Figure 13.A).

An in-depth analysis focusing on each Signaling component revealed new interactions for all components tested, except for RASSF6 (Figure 13.B). For some Signaling components, i.e., FRMD6, TAOK2, TAOK3, no interactions among the components tested were previously reported. Notably, protein-protein interactions for components of the Hippo core network (comprising the core kinase cassette and YAP1) as well as polarity proteins NF2, WWC family proteins, and AMOT family proteins the largely overlap between split TEV-based data and published interactions retrieved from Mentha database (Figure 13.B). Thus, we conclude that split TEV captures relevant known protein interactions in the Hippo Signaling network (Zhao, Li, Tumaneng, et al., 2010b).

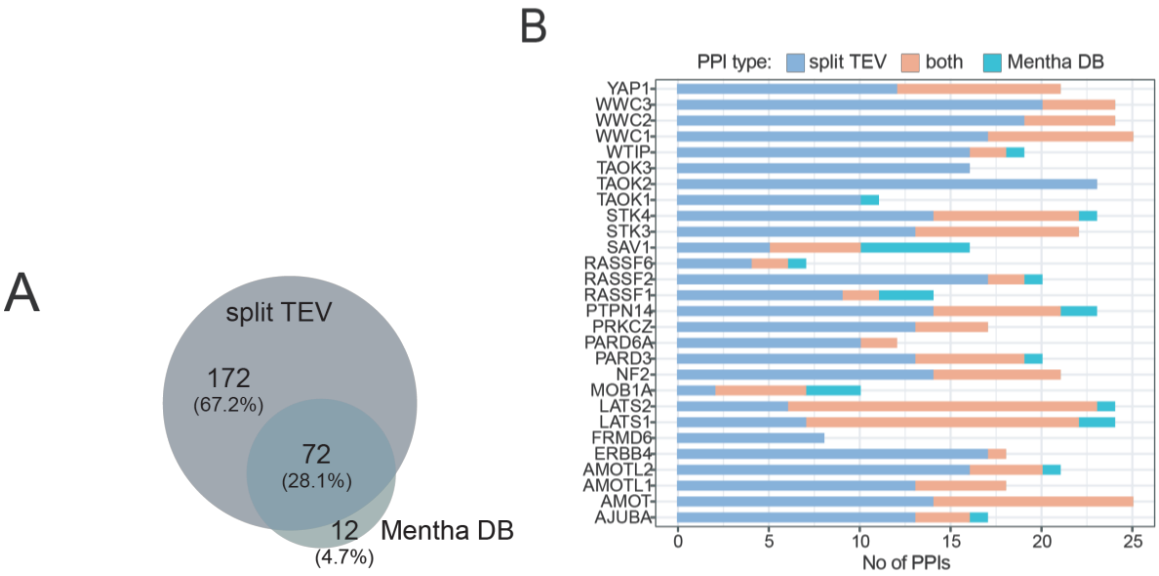

Figure 13. Distribution of newly identified and validated interactions for each component.

(**A**) Percentage Venn diagram showing the coverage of PPIs identified in the focused split TEV screen and PPI data provided by the Mentha database (Mentha DB). (**B**) Stacked bar graphs displaying newly identified PPIs (blue, covered by split TEV screen only) known and split TEV-validated PPIs (orange, both covered by split TEV screen and Mentha database), and known PPIs (green, covered by Mentha database only) for each candidate protein tested.

3.1.2 **Split TEV-based screen verifies module formation within Hippo Signaling**

Hippo Signaling is organized in Signaling modules that are formed by defined signaling proteins aggregating into these modules (Couzens et al., 2013; Hao et al., 2008; Hauri et al., 2013; Y. Li et al., 2015; Wennmann et al., 2014; Yin et al., 2013; J. Zhang et al., 2008). Major modules within Hippo Signaling are the (i) core kinase cassette, which comprises STK3/4 kinases, LATS1/2 kinases, and adapter proteins SAV1 and MOB1A, (ii) a SARAH interaction domain module (proteins with a SARAH interaction domain, e.g., STK3/4, SAV1, RASSF1-6), and (iii) the polarity protein module, which e.g., comprises WWC family proteins (WWC1/2/3), AMOT family proteins (AMOT and AMOT-like proteins 1 and 2 (AMOTL1/2)), and NF2. For visualization of these modules, we extracted protein-protein interaction data from the entire network and produced weighted network graphs (Figure 14.A). We visualized the interaction modules for the core kinase cassette (Figure 14.B, indicated in red), the SARAH domain module (Figure 14.B indicated in green), and the polarity cluster. In detail, LATS1 and LATS2 strongly associate with MOB1A, and to a lesser extent, with STK3 and STK4 (Figure 14.B). Likewise, STK3 and STK4 strongly associate with SAV1. The Hippo pathway also hosts the SARAH interaction domain, which promotes homophilic interactions and is present in STK3, STK4, SAV1, and RASSF family proteins (Genevet & Tapon, 2011; Sánchez-Sanz et al., 2016). In the split TEV-based HPIN, SARAH domain-containing components specifically interact and cluster. Further, LATS1/2 associate with the polarity proteins of the WWC family (WWC1/2/3), the AMOT family (AMOT, AMOTL1/2), NF2, PTPN14, as well as YAP1 to form a polarity cluster (Figure 14.B).

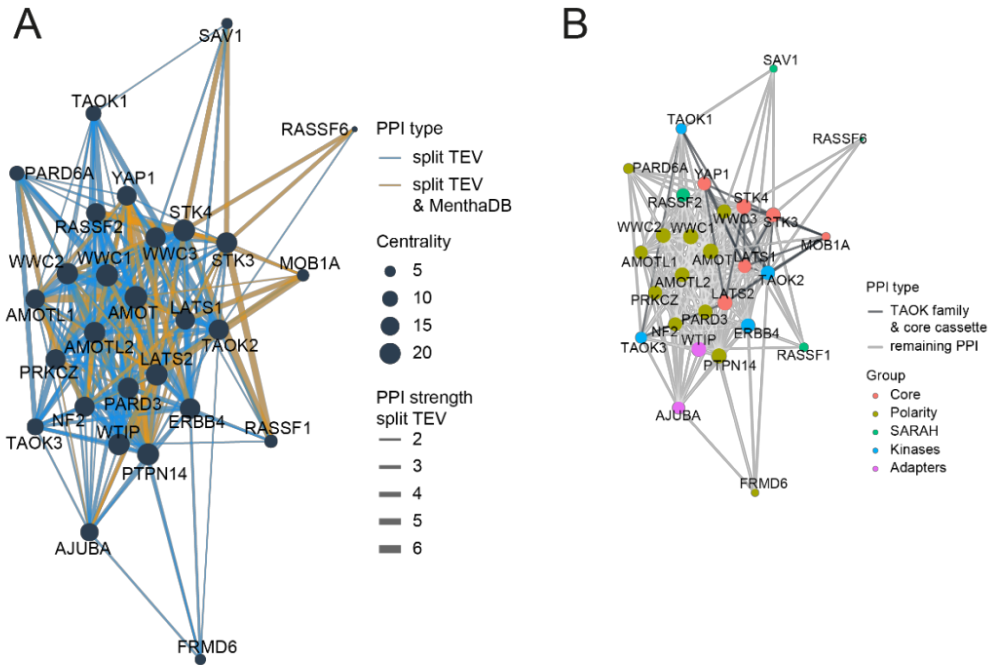

Figure 14. Visualization of major modules within Hippo Signaling.

(**A**) Weighted network map of the Hippo pathway network for all components tested using the *tidygraph* package in R bioconductor. Blue edges (denoted as PPI type) represent interactions only detected with split TEV, orange edges represent interactions both identified with split TEV and Mentha database. Edge thickness (denoted as PPI strength split TEV) correlates to log2-transformed fold changes for given interactions. The size of each node indicates centrality within the network. (**B**) Network map plotted in the same orientation as in (A) and highlighting edges for the TAOK family (TAOK1, TAOK2, TAOK3, blue nodes) and core kinase cassette components (Core, red nodes). 'Group' denotes the classifier for each component.

To show fidelity of our split TEV approach for identifying protein-protein interactions and to visualize cluster formation within the Hippo network, we extracted interaction data for selected Hippo pathway components and plotted a hierarchical heatmap of the core kinase cassette (STK3/4 and LATS1/2 kinases, including adapters SAV1 and MOB1A), WWC family proteins (WWC1-3), AMOT family proteins (AMOT and AMOT-like proteins 1 and 2 (AMOTL1/2)), NF2, and YAP1 (Figure 15.A). Next, we constructed network maps for the split-TEV based interactions (Figure 15.B) and the published interaction data deposited in the Mentha database (Figure 15.C), and we observed a similar module formation for both the core kinase cassette and the polarity proteins. When comparing interaction data from our split TEV-based approach and the Mentha database, we noticed a substantial overlap of nearly 50% to our Hippo network (Figure 15.D). Further, we

identified novel interactions in this network using our split TEV-based approach. For example, interactions between WWC family proteins (WWC1, WWC2, and WWC3) and AMOT family proteins (AMOT, AMOTL1, and AMOTL2) were only described for WWC1 AMOT and WWC1 AMOTL1 (Couzens et al., 2013; Hauri et al., 2013; Toloczko et al., 2017). Our split TEV results indicate that all WWC family proteins can interact with all AMOT family proteins. Using co-immunoprecipitation experiments performed in HEK293 cells, we validated these pairwise associations between WWC family proteins and AMOT family proteins biochemically (Figure 16.A&B). Taken together, we conclude from these analyses that the split TEV-based HPIN can validate known and identify new interactions that were hidden so far and provides a tool to characterize module formation within signaling pathways.

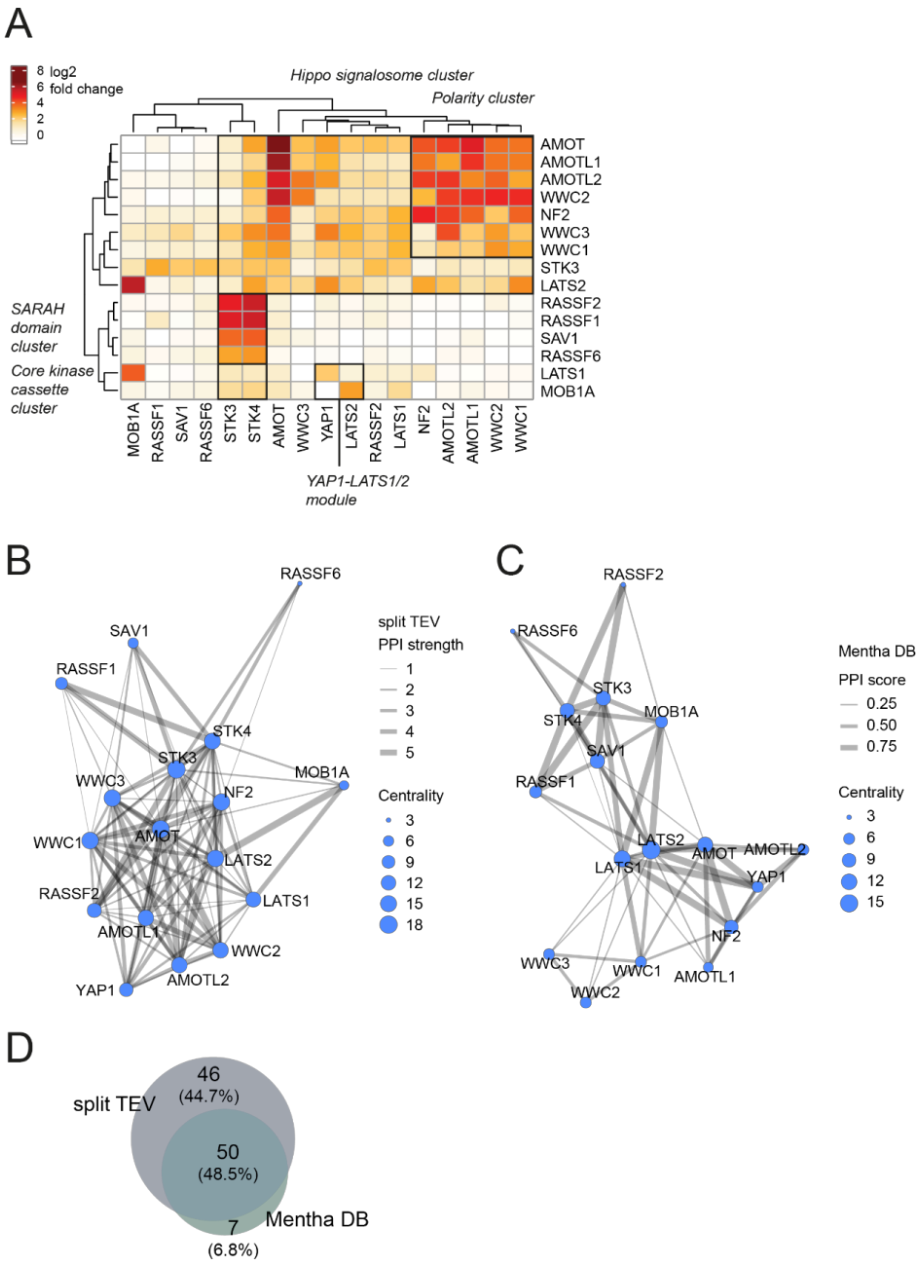

Figure 15. Interactions of selected core components of the Hippo pathway.

(**A**) Heatmap of hierarchically clustered protein-protein interactions of selected Hippo pathway core components monitored by split TEV. Interactions are given as log2-transformed fold changes relative to baseline controls. Note cluster formation of the core kinase cassette (comprising the kinases STK3, STK4, LATS1, LATS2 and the adapter protein SAV1 and MOB1A), of the SARAH domain-containing proteins (i.e., STK3, STK4, SAV1, RASSF1, RASSF2), and of the polarity proteins (WWC1, WWC2, WWC3, NF2, AMOT, AMOTL1, AMOTL2). (**B**) Weighted network map of the core components, SARAH domain containing components, and polarity proteins depicted in (A) using the *tidygraph* package in R bioconductor. Edge thickness (denoted as PPI strength split TEV) correlates to log2-transformed fold changes for given interactions. (**C**) Weighted network map of the core components, SARAH domain containing components,

and polarity proteins using interaction scores downloaded from the Mentha database (Mentha DB). Node thickness correlates to the scores provided by the Mentha DB. (**D**) Venn diagram showing the overlap between PPIs identified in the focused split TEV screen and PPI data provided by the Mentha DB for selected core Hippo pathway components depicted in (A).

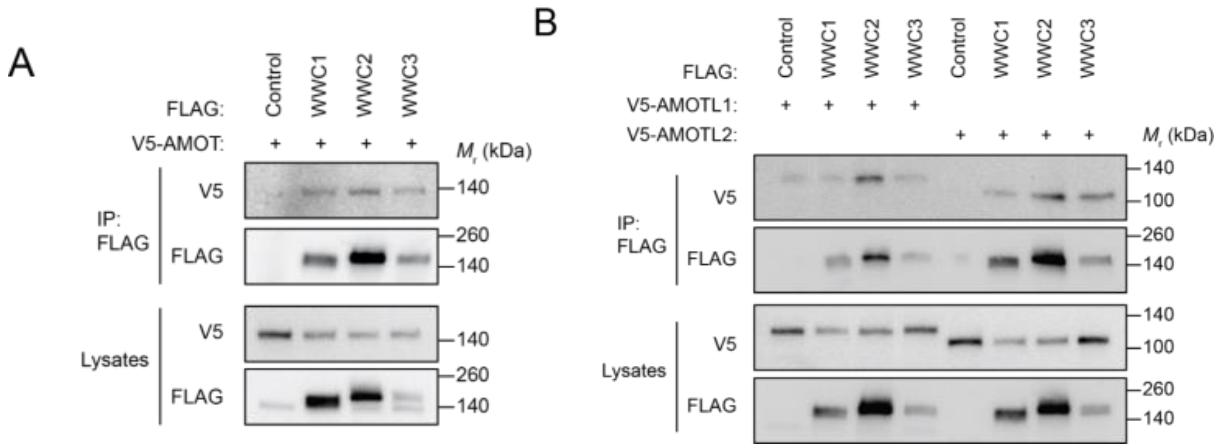

Figure 16. Pairwise associations between WWC family proteins and AMOT family proteins. WWC family proteins interact with AMOT family proteins.

(**A**) WWC1/2/3 interact with AMOT. (**B**) WWC1/2/3 interact with AMOTL1 and AMOTL2. HEK293 cells were transfected with FLAG-tagged and V5-tagged plasmids as indicated. FLAG-co-immunoprecipitation assays were followed by Western blotting and probing for V5-tagged proteins, followed by FLAG-tagged proteins. IP denotes FLAG-precipitated samples, lysate denotes regular whole-cell lysates.

3.1.3 **TAOK2 controls YAP transcriptional activity and promotes the phosphorylation of MOB1A**

For TAOK2 and TAOK3, no physical interactions with Hippo pathway components were previously reported (c.f. e.g., BioGRID, IntAct, and Mentha databases). For TAOK3, however, it is known that it can phosphorylate STK4 and LATS1, as is the case for TAOK1 (Boggiano et al., 2011; Plouffe et al., 2016; Poon et al., 2011). For TAOK2 neither binding nor phosphorylation of Hippo targets is reported so far. However, our split TEV data indicate that both TAOK2 and TAOK3 physically interact with components of the Hippo Signaling pathway, implicating a possible role for these two proteins in modulating Hippo pathway activity (Figure 17.A). To test whether all TAOKs control Hippo pathway activity, we performed a luciferase assay that monitors YAP1 transcriptional activity and uses 18 clustered binding sites for the TEAD transcription factor (18xTEAD-luc), which is more sensitive and robust than the 8xTEAD reporter in HEK293 cells (Dupont et al., 2011). When YAP1 was co-transfected with the 18xTEAD-luc reporter plasmid into HEK293 cells,

we observed a strong induction of luciferase activity (Figure 17.A). Co-expression of validated Hippo pathway components, such as LATS1 and STK4, efficiently inhibited YAP1 activity. Interestingly, all TAO kinases, including TAOK2, inhibited YAP1 transcriptional activity (Figure 17.A). In addition, the TAOK2-mediated inhibitory effect on YAP1 transcriptional activity was validated in a dose-dependent manner, suggesting that TAOK2 is an efficient inhibitor of YAP1 activity.

Phosphorylation of MOB1A can be used as a readout to monitor activities of upstream Hippo pathway modulators. MOB1A is phosphorylated by STK3/STK4 to fully activate LATS1/2 (Hirabayashi et al., 2008; Praskova et al., 2008), and this process can be induced by TAOK1 (Poon et al., 2011). Therefore, we tested whether TAO kinases when overexpressed increase MOB1 phosphorylation in HEK293 cells. Here, we show that all TAO kinases, including TAOK2, induces MOB1A phosphorylation in these cells (Figure 17.B). Our results suggest that TAOK2 also plays a central role in modulating Hippo pathway activity.

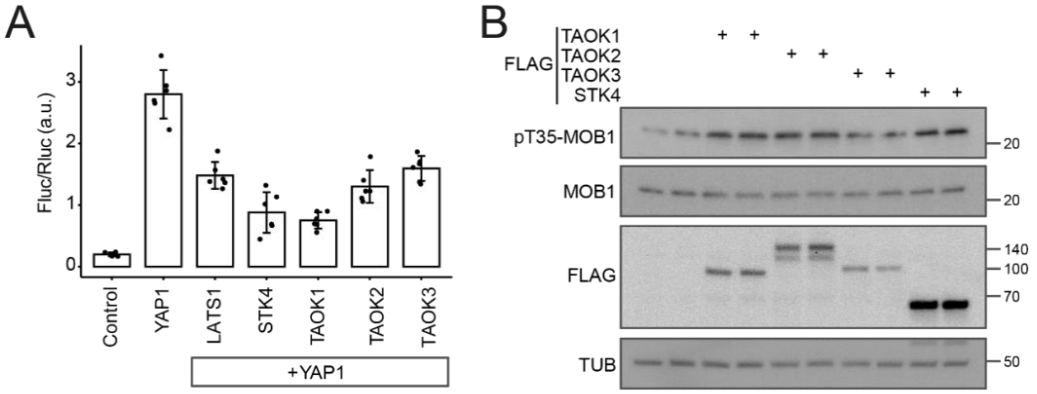

Figure 17. TAOK2 controls YAP transcriptional activity and promotes the phosphorylation of MOB1A.

(**A**) TAOK2 inhibits YAP1 transcriptional activity. Plasmids expressing indicating genes and a 18x clustered TEAD firefly luciferase reporter were transfected into HEK293 cells, lysed 20 hrs later, and subjected to a dual luciferase assay. Firefly readings were normalized to a constitutive Renilla control and averaged. Error bars represent SD, n=6. (**B**) TAOK1 and TAOK2 upregulate phospho-MOB1A levels in HEK293 cells. TAOK1, TAOK2, and TAOK3 expressing plasmids were transfected into HEK293 cells. Cells were lysed 20h later and subjected to a Western blotting analysis using the indicated antibodies.

3.1.4 **TAOK2 interacts with and phosphorylates LATS1 kinase**

As TAOK2 clustered to LATS1 in the weighted network graph (Figure 14.A&B), we focused on this interaction to further investigate. To test whether TAOK2 phosphorylates

LATS1, we established a HEK293 cell line with a stably integrated and doxycycline-controlled expression of TAOK2 (HEK293-TAOK2 cells). To do this, we applied a lentivirus-based polyclonal selection approach, which uses the pInducer plasmid harboring the TAOK2 ORF under the control of a reverse tetracycline-controlled transactivator (rtTA) element (TRE), an rtTA ORF under the control of a constitutively active EF1 promoter, and a puromycin resistance gene linked through an internal ribosome entry site (IRES) element to the EF1 promoter-dependent expression (Figure 18.A) (Wennmann et al., 2014). As rtTA only binds to the TRE in a doxycycline-bound state, addition of doxycycline initiates transcription of TAOK2. A time course analysis revealed that TAOK2 protein levels were substantially increased 6h after addition of doxycycline, both for wild type TAOK2 (Figure 18.B&C) and a kinase dead form of TAOK2 (TAOK2-KD) that bears a D151A mutation (Figure 18.D&E). For TAOK2, physical associations with Hippo pathway components have not been described so far, prompting us to further investigate TAOK2 interactions. Our split TEV based interaction data suggests that TAOK2 associates with the core kinase cassette components STK3/4 and LATS1 (Figure 19.A). Using co-immunoprecipitation, we next tested whether TAOK2 binds to core Hippo pathway components as indicated from the split TEV-based screen. We confirmed that TAOK2 binds to LATS1 and LATS2 in HEK293 cells (Figure 19.B). Doxycycline-induced TAOK2 overexpression resulted in significantly increased phosphorylation levels of endogenous LATS1 (Figure 19.C&D). By contrast, doxycycline-induced overexpression of TAOK2-KD did not change phosphorylation levels of LATS1 (Figure 19.C&D). As TAOK2 associates with LATS1, this suggests that LATS1 is a direct target of TAOK2.

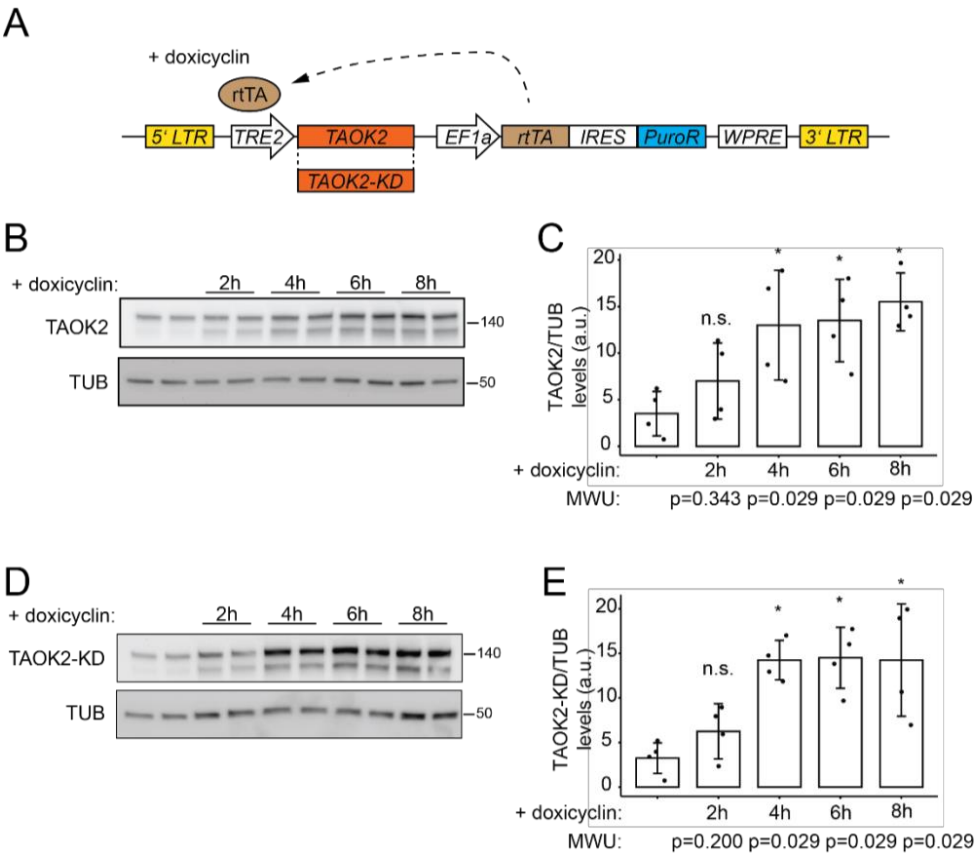

Figure 18. Lentiviral system for a stably integrated and doxycycline inducible TAOK2.

(**A**) Scheme of lentiviral vector used for polyclonal selection to obtain a stably integrated and doxycycline inducible TAOK2. Arrows indicate promoters/enhancers. LTR, long terminal repeats; rtTA, reverse tetracycline-controlled transactivator; TRE, rtTA element; IRES, internal ribosome entry site; WPRE, woodchuck hepatitis virus posttranscriptional response element. (**B**) Doxycycline-induced TAOK2 reaches a plateau 6 hours after stimulation. HEK293 cells with stably integrated and doxycycline inducible TAOK2 were stimulated with 125ng/ml doxycycline for indicated hours. Assay was run in duplicates. (**C**) Quantification of TAOK2 levels shown in (B). For each condition, four data points from two independent experiments were used. Error bars represent SD. (**D**) Doxycycline-induced TAOK2-KD reaches a plateau 6 hours after stimulation. HEK293 cells with stably integrated and doxycycline inducible TAOK2-KD were stimulated with 125ng/ml doxycycline for indicated hours. Assay was run in duplicates. (**E**) Quantification of TAOK2-KD levels shown in (D). MWU, Mann Whitney U test. Error bars represent SD.

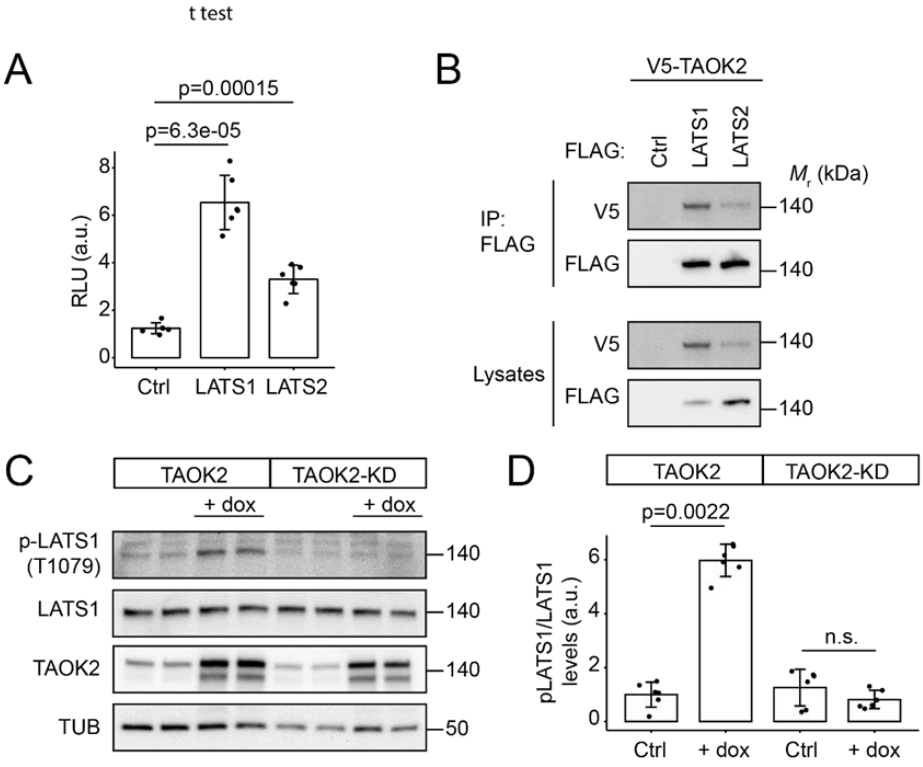

Figure 19. TAOK2 overexpression increases the phosphorylation level of LATS1.

(**A**) Split TEV luciferase assays for TAOK2 and LATS1 and LATS2. Single luciferase data was extracted from the focused split TEV interaction screen shown in Figure11C. RLU, relative luciferase units. Error bars represent SD. Two-sided t-test was conducted with unequal variance (**B**) TAOK2 associates with LATS1 and LATS2 in a co-immunoprecipitation assay that was performed in HEK293 cells. (**C**) Doxycycline-induced TAOK2 increased phosphorylation levels of LATS1, while doxycycline-induced TAOK2-KD did not increase phosphorylation levels of LATS1. HEK293 cells that harbor a stably integrated TAOK2/TAOK2-KD that is under the control of the reverse tetracycline-controlled transactivator (rtTA) element (TRE) were stimulated for 6h with 125ng/ml doxycycline. (**D**) Quantification of p-LATS1 levels shown in (C). For each condition, six data points from three independent experiments were used. A Mann-Whitney-U test was conducted. Error bars represent SD.

3.1.5 TAOK2 depletion and phosphorylation of LATS1

To also assess the effect of depleted TAOK2 protein levels on Hippo Signaling, we applied the CRISPRi technique and generated HEK293 cell lines that each stably expresses an sgRNA directed against TAOK2 (sgTAOK2) and a dead Cas9-ZIM3 -KRAB fusion (dCas9-ZIM3- KRAB). In all three cell lines, termed HEK293-sgTAOK2i#1, #2 and #3, we observed a strong reduction of TAOK2 protein levels (Figure 20. A&B). In contrast to the overexpression situation, reduced TAOK2 protein levels in HEK293-sgTAOK2i#3 caused decreased phospho-LATS1 levels (t-test, p=0.0018, Figure 20.C&D).

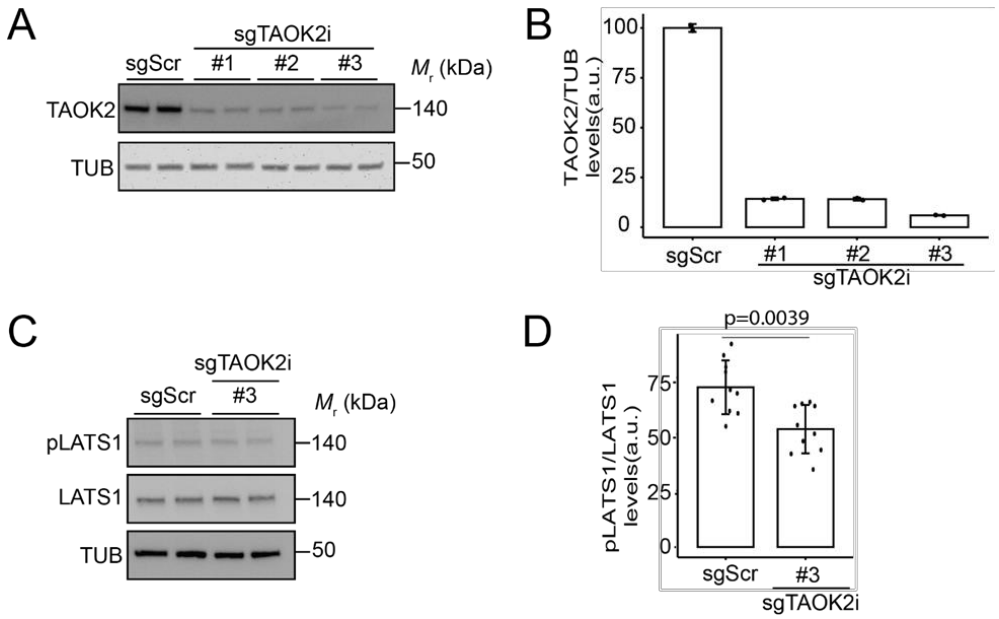

Figure 20. TAOK2 depletion decreases the phosphorylation level of LATS1.

(**A**) HEK293-sgTAOK2i#1, #2, and #3 were generated with CRISPRi technique which can stably express an sgRNA directed against TAOK2 (sgTAOK2) and result in strong reduction of TAOK2 protein level. (**B**). Quantification of TAOK2 levels in (A). (**C**) Reduced TAOK2 protein levels in HEK293 cells reduces phosphorylation levels of LATS1. (**D**) Quantification of p-LATS1 levels shown in (C). For each condition, 10 data points from 5 independent experiments were used. Significance levels were assessed using a Mann Whitney U test. Error bars represent SD.

3.1.6 **TAOK2 regulates phosphorylation levels of YAP1**

Activated LATS1 phosphorylates YAP1 and primes it for cytoplasmic retention (Zhao et al., 2007) or ubiquitin-mediated protein degradation (Zhao, Li, Tumaneng, et al., 2010b). Therefore, we next tested whether increased levels of TAOK2 also lead to increased phospho-YAP1 levels. Indeed, doxycycline-induced TAOK2 increased phospho-YAP1 levels both at residues S127 (triggers cytoplasmic retention) and S397 (triggers ubiquitin-mediated protein degradation) in HEK293 cells (Figure 21), supporting our previous finding that TAOK2 reduces transcriptionally active YAP1 (Figure 17.A).

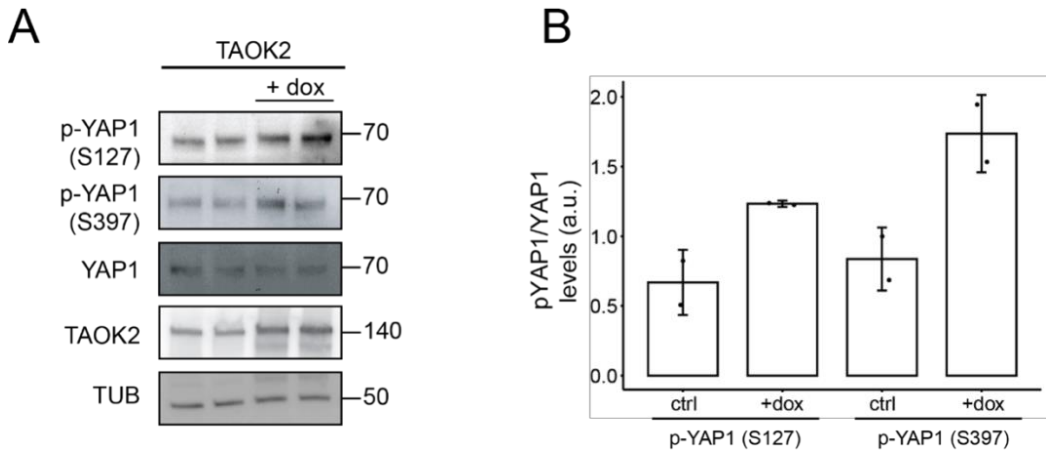

Figure 21. TAOK2 overexpression increases the phosphorylation level of YAP1.

(**A**) When inducing TAOK2 overexpression with doxycycline in HEK293-pIND-hTAOK2 stable cell line, phospho-YAP1 levels both at residues S127 (triggers cytoplasmic retention) and S397 (triggers ubiquitin-mediated protein degradation) increase. (**B**) Quantification of p-YAP1 (S127) and p-YAP1 (S397) levels shown in (A). Error bars represent SD, n=2.

3.1.7 **TAOK2 modulates YAP transcriptional targets CTGF and CYR61**

Nuclear YAP activates the transcription of CTGF and CYR61, both of which are well established transcriptional targets of YAP (Zhao et al., 2008). To confirm that TAOK2 modulates YAP transcriptional activity, we performed RT-qPCR experiments to assess levels of CTGF and CYR61 transcripts. As described before, CTGF and CYR61 are strongly activated in HEK293 cells upon serum stimulation. In contrast, doxycycline induced TAOK2 overexpression resulted in a significant decrease of CTGF, but not CYR61, 24h post induction of TAOK2 expression (Figure 22.A). To also assess the effect of TAOK2 inactivation on CTGF and CYR61 transcripts, we reduced TAOK2 protein levels in HEK293 cells using the CRISPRi technique by generating HEK293 cell lines that stably express an sgRNA directed against TAOK2 (sgTAOK2) and a dead Cas9-KRAB fusion (dCas9-KRAB). In both cell lines, termed HEK293-sgTAOK2#1 and #2, we observed a significant increase of CTGF transcription levels (Figure 22.B). However, a significant increase of CYR61 transcription levels was not observed in these cells, but rather an unexpected decrease in HEK293-sgTAOK2#2 cells (Figure 22.B). Together, these findings support the notion that TAOK2 controls YAP-dependent transcription in a LATS-dependent manner.

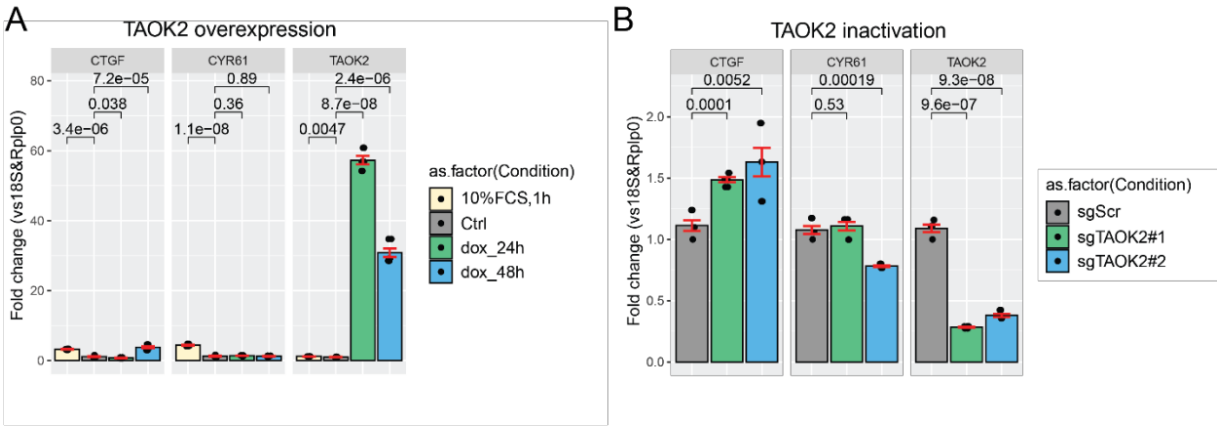

Figure 22. TAOK2 modulates the YAP1 transcriptional target CTGF.

(**A**). Doxycycline-induced TAOK2 overexpression results in a significant decrease of CTGF. Serum stimulation which results in strong activation of CTGF and CYR61 was used as a positive control. (**B**) TAOK2 inactivation causes significant increase of CTGF (both in HEK293-sgTAOK2#1 and #2) and CYR61 (HEK293-sgTAOK2#2). Significance was assessed using t test. Error bars represent SD, n=3.

3.1.8 **TAOK2 impacts on proliferation**

To assess whether TAOK2 also controls proliferation of cells, we compared growth rates of HEK293-TAOK2 cells that were induced with doxycycline to overexpress TAOK2 with control HEK293-TAOK2 cells that were not induced for 96 hours. Indeed, doxycycline induced HEK293-TAOK2 cells proliferated slower than controls (Figure 23.A). This finding is in line with our observation that induced TAOK2 overexpression increases phospho-LATS1 and phospho-YAP1 levels, supporting the notion that nuclear YAP1 drives proliferation.

Meanwhile, we compared HEK293_dCas9_ZIM3_KRAB_sgTAOK2 cells with control HEK293 cells that harbor a stably integrated scrambled control HEK293_dCas9_ZIM3_KRAB_sgScr cells) for 96 hours. Indeed, HEK293_dCas9_ZIM3_KRAB_sgTAOK2#3 cells proliferated faster (Figure 23.B). This finding is in line with our observation that TAOK2 downregulation decreases phospho-LATS1 levels and supports the notion that TAOK2 modulates nuclear YAP to regulate proliferation.

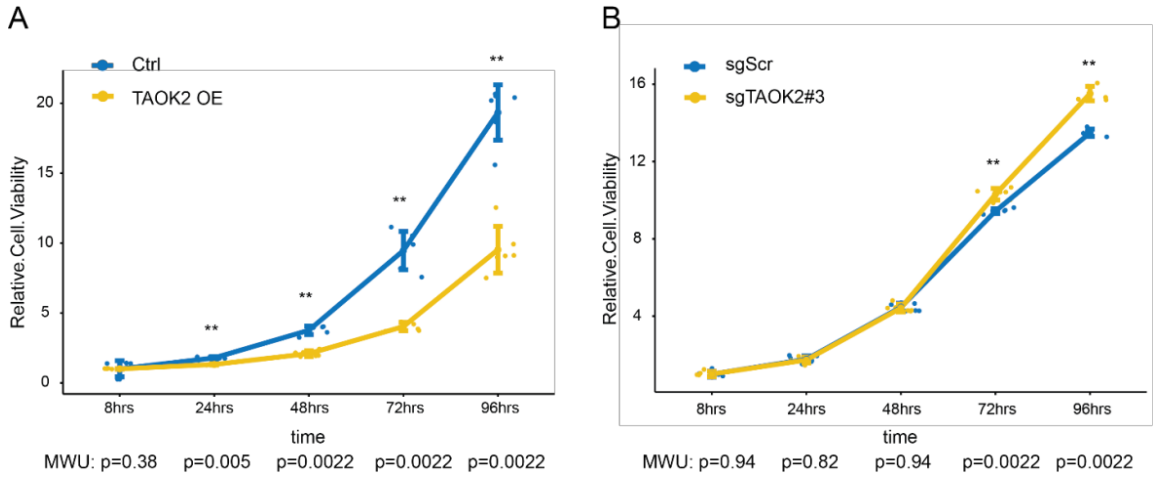

Figure 23. TAOK2 regulates proliferation.

(**A**) HEK293 cells stably carrying a doxycycline inducible TAOK2 gene were continuously treated with 125ng/ml doxycycline (TAOK2 OE, magenta) and cell proliferation was measured at 8h, 24h, 48h, 72, and 96h after plating using a CCK-8 assay. Control cells (Ctrl, red) were not stimulated. (**B**) HEK293 cells stably carrying dCas9_ZIM3_KRAB_sgTAOK2#3 and a scramble control (sgScr) were assayed for proliferation at 8h, 24h, 48h, 72, and 96h after plating using a CCK-8 assay. Line graphs are calculated as mean, error bars represent SD, n=6. p values were calculated using a Mann-Whitney U (MWU) test.

3.1.9 **TAOK2 is downregulated in various types of cancer**

TAOK2 is a tumour suppressor gene and downregulation of TAOK2 is thus expected to promote tumour progression. To identify the clinical impact for downregulation of TAOK2, we extracted TAOK2 expression data of 28 different types of cancers and overall survival of patients from the TCGA database. It was found that there is a significant positive correlation between TAOK2 expression and overall survival of patients in 5 cancer types. Reduced TAOK2 expression correlated with reduced survival in patients with head and neck squamous cell carcinoma (HNSC), kidney chromophobe (KICH), brain lower grade glioma (LGG), lung adenocarcinoma (LUAD), and pancreatic adenocarcinoma (PAAD) (Figure 24.A). However, in colorectal adenocarcinoma (COADREAD) patients, reduced TAOK2 expression correlated with increased survival (Figure 24.B).

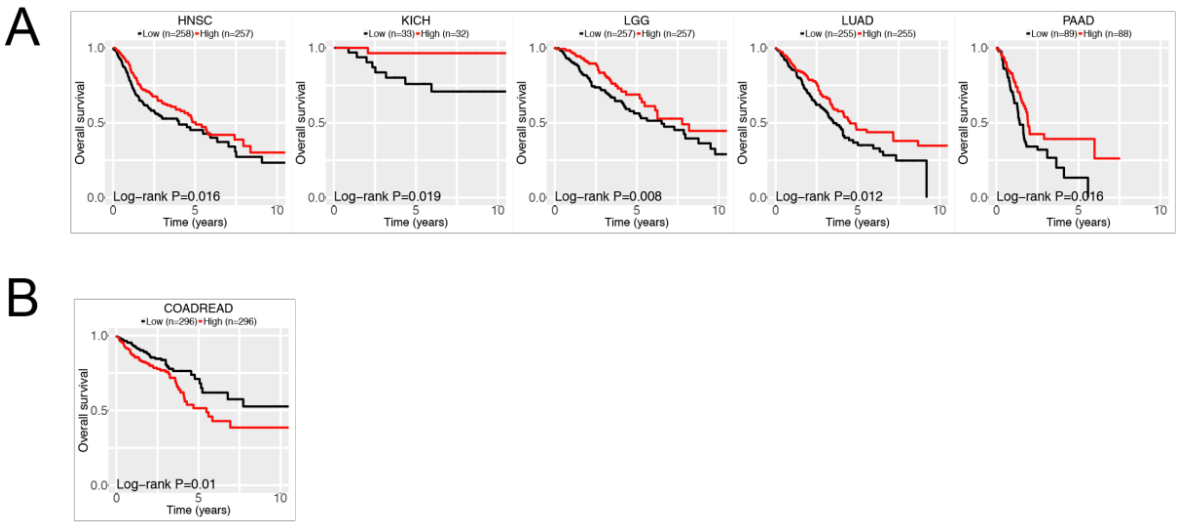

Figure 24. Kaplan-Meier analysis with a log-rank test was performed in patients grouped by TAOK2 expression in individual cancer types.

(**A**) Reduced TAOK2 expression correlated with reduced survival in patients with HNSC, KICH, LGG, LUAD and PAAD. (**B**) Reduced TAOK2 expression correlated with increased survival in patients with COADREAD.

3.2 TAOK2 impacts on synaptic plasticity

It is known that TAOK2 is located in the 16p11.2 chromosomal deletion region which has a relationship with autism spectrum disorder (ASD) and schizophrenia (Maillard et al., 2015; Weiss et al., 2008). TAOK2 is also associated with other neurodevelopmental phenotypes (Steinman et al., 2016). In mice, full inactivation of Taok2 in the forebrain caused a hyperactivity phenotype (Kapfhamer et al., 2013) and deficits in cognition, anxiety, and social interaction (Richter et al., 2019). However, a profound behavioural profiling of TAOK2 in mice with respect to psychosis-relevant phenotypes is elusive. Therefore, Celestine Dutta and Elisabeth Voggenreiter performed behavioural profiling experiments to test for potential for psychosis-relevant phenotypes in Taok2 conditional knockout mice, in which Taok2 was inactivated in the brain using the Emx1-Cre driver line. The description of their findings is presented in the next section. At the molecular and cellular level, TAOK2 regulates actin dynamics to promote arborization of neurons (Calderon de Anda et al., 2012). Phosphorylation of TAOK2 by the serine-threonine kinase 24 regulates the development of synapse via interaction with Myosin Va (Ultanir

et al., 2014). In addition, TAOK2 also promotes the formation of mature spines by associating with septin 7 (SEPT7), which in turn stabilizes PSD-95; conversely, inactivation of TAOK2 leads to mis-localization of synapses onto the dendritic shaft and defects in calcium compartmentalization (Yadav et al., 2017). Furthermore, Tao kinases activate Hippo Signaling, a pathway that also controls cell fate decision, cell polarity maintenance, and actin cytoskeleton dynamics in neurons (Hansen et al., 2015). These findings show that TAOK2 has function in arborization of dendrite and maturation of synapse, suggesting that any changes in TAOK2 activity may cause aberrant synaptic connectivity and behavioural phenotypes. Therefore, I investigated the impact of TAOK2 on synaptic plasticity in the context of physiological signaling.

3.2.1 **Behavioural profiling of brain specific Taok2 knockout mice**

Behavioural profiling was performed by Celestine Dutta and Elisabeth Voggenreiter. It was carried out in 3 cohorts of Taok2 fl/fl x Emx1-Cre mice using the tests that are part of PsyCop (Fig. 7): Open Field, Y-Maze, Intellicage experiments (activity, nocturnality, place learning, reversal learning and anhedonia tests), prepulse inhibition, and tail suspension. Two cohorts were tested for potential behavioural differences caused by the Taok2 genotype. A third cohort was additionally subjected to a social defeat paradigm at the age of 5-8 weeks to assess gene x environment interactions. Each cohort containing both brain specific Taok2 knockouts and littermate controls, and mice were tested at the age of 8 -12 weeks.

Overall phenotypes observed in these conditional Taok2 ko mice were rather subtle (Dutta, 2019; Voggenreiter, 2020). Here, the findings of the experiments that provided significant differences, or at least a substantially trend were summarized. First, Open Field test was performed to analyze novelty-induced activity and anxiety/curiosity related behaviour. In this test, mean speed (calculated as meters a mouse travels in the box per seconds) and the rotation rate (i.e., hecticness, that is defined by the number of direction changes per meter) were assessed. Anxiety/curiosity is monitored by measuring the time a mouse stays in the center of the box. Typically, the behavioural movement pattern of mice is to stay more time close to the wall than in the center. In Dutta's cohort, the results

showed that transgenic mice had a significant different speed comparing with wild type controls (p=0.044), while in Voggenreiter's cohort, the difference was not significant (p=0.8618). Also only in Dutta's cohort, transgenic mice had significant different anxiety-related behaviour comparing with wild type controls (p=0.02202).

In the Y-maze test, the number of choices each mouse made to explore the three arms of the Y-Maze was measured to analyze the activity. It was shown in the activity plot of Dutta's cohort that transgenic mice had a significant different activity comparing with wild type mice (p=0.019). Meanwhile, spontaneous alterations (exploring the three arms in the right order: A, B, C, A…) was counted to measure the working memory. In both cohorts, the result showed that transgenic and wild type mice had no significant difference in spontaneous alterations.

Then, mice were placed into the Intellicage for 20 days, in which activity (number of visits), nocturnality (circadian preference), place learning, (serial) reversal learning, and anhedonia tests were analyzed using the transponders implanted in the mice and the heat and RFID-sensors of the Intellicage. Only in Voggenreiter's cohort, the transgenic mice showed significantly higher activity than the wild type mice (p=0.032). Transgenic mice has a non-significant different nocturnality comparing with the wild type mice. As to place learning, reversal learning and serial reversal learning, the difference between transgenic and wild type mice was not significant. For the analysis of sucrose preference, the result indicated that there was no difference for the sucrose preference between transgenic mice and wild type mice.

In the pre-pulse inhibition test (PPI), the functioning sensorimotor gating of mice was analyzed by assessing whether they could pre-cognitively link pre-pulse and pulse. In this test, mice are exposed to a loud acoustic signal (main pulse: 115 dB) with or without a preceding stimulus (weaker acoustic signal: 70, 75, 80 dB), then the different strengths of reactions (jumping, twitching) of each mouse are measured. As expected, the wt controls show an inhibited startle response after playing the prepulses. The stronger the pulse was applied the stronger the inhibition was observed. The tg mice showed similar trends. There was no significant difference between wt controls and transgenic mice.

Tail suspension test (TST) was the fifth test, which analyzed possible depression-like behaviour by recording the escape-oriented behaviour of the mice. If the mouse showed less motivation to release itself than a healthy littermate control (significantly decreased mobility), it is regarded as depression-like behaviour (Can et al., 2011). The immobile time of the mouse is the parameter to analyze the escape-oriented behaviour and intrinsic motivation. Analysis of the immobility time of mice shows that there exists no significant difference for the immobility time between transgenic and wild type mice.

Fear conditioning (FC) was the last test. It measured the freezing behaviour of mice as response to a cue and context, on which the mice were conditioned, to analyze their function of fear memory. The test lasted three days in total: day 1. conditioning day; day 2. context memory day; day 3. cue memory day. Plot showed that both transgenic and wildtype mice displayed the slightest freezing behaviour on the first day before shock and there was significant difference between them. On the second day after conditioning, the freezing time increased, but as to context response, there existed no significant difference between transgenic and wildtype mice. Regarding to cue memory, there was also no significant difference in freezing behaviour after hearing the tone between transgenic and wildtype mice.

In order to visualize the behavioural profile of the animals in just two dimensions, canonical discriminant analysis (CDA) for dimension reduction was used (Volkmann et al., 2021). CDA optimizes linear combinations of all variables to output latent variables called canonical components or canonical scores. They can be treated very much like principal components and visualized in a dimension plot (Figure 25.A). The weights of the single variables in these components, called canonical coefficients, were plotted as vectors (Figure 25.B). The main advantage of the canonical discriminant analysis over more commonly used dimension reduction techniques such as principal component analysis is that it optimizes for group separation. Therefore, the canonical coefficients represent the importance of the respective variable for the optimal group separation in phenotypic space. In order to find variables contributing to the differences between experimental groups, a CDA for each single term of the experiment design's linear model was computed and used for the ANOVA procedure, and the canonical coefficients were

visualized in a heatmap (Figure 25.C). In the dimension plot, all four groups segregate in phenotypic space, which confirms that there is a biological difference in their behavioural and cognitive profile. Moreover, both ways of visualizing the canonical coefficients can immediately tell the impacted traits in the disease model and the respective research domain. In short, with the help of this analysis, a researcher can get an overview of the neurocognitive and behavioural profile in one glance.

In the GxE model, canonical component one separated the experimental groups by the environmental factor and accounted for 79% of the total canonical correlation. The second component separated groups by genotype and accounted for 16.1% of the total canonical correlation. Notably, there was no overlap of the data ellipses between the disease model (tg_sd) and healthy control (wt_hc) (Figure 25.A). However, there was a large overlap between genotypes, suggesting that the impact of the Taok2 conditional knockout is minor. In contrast, there is just a small overlap along the environment axis, underlining the bigger effect of psychosocial stress on the behavioural profile. Moreover, the structure of each canonical component gives insights in the importance of each variable to the separation of groups along the respective axis. The canonical coefficients of each variable in the first two canonical components is represented by the coordinates of the vector tips in the second dimension plot (Figure 25.B). The coefficients' absolute values are weights of the contribution to the canonical score by the respective variable. In phenotypic space, the vectors' magnitude represents the importance of the variable for segregating the groups in this space, because the canonical components represent the optimal solution for this segregation (Figure 25.B).

Furthermore, the CDA of each term of the linear model was used to find variables that separate the groups along the genotype and environmental factor, respectively. The canonical coefficients were visualized in a heatmap with the results of the respective univariate ANOVA (Figure 25.C). Notably, the interaction term was not statistically significant for all behavioural and cognitive phenotypes, suggesting that the conditional knockout of Taok2 with Emx1-Cre line used, does not interact with social defeat-induced psychosocial stress on a behavioural level. Detailed ANOVA analysis data is provided in Supplementary TableS4.

Overall, the changes in the behavioural phenotypes were rather subtle, which is in contrast to findings published previously (Richter et al., 2019) where strong phenotypes have been observed in full Taok2 ko mice for cognition, anxiety, and social interaction. Given these finding from our colleagues, I still believe that inactivation of Taok2 in neurons leads to phenotypes that should also become apparent on a molecular level. Therefore, I continued to study the role of Taok2-dependent signaling in neuron cultures.

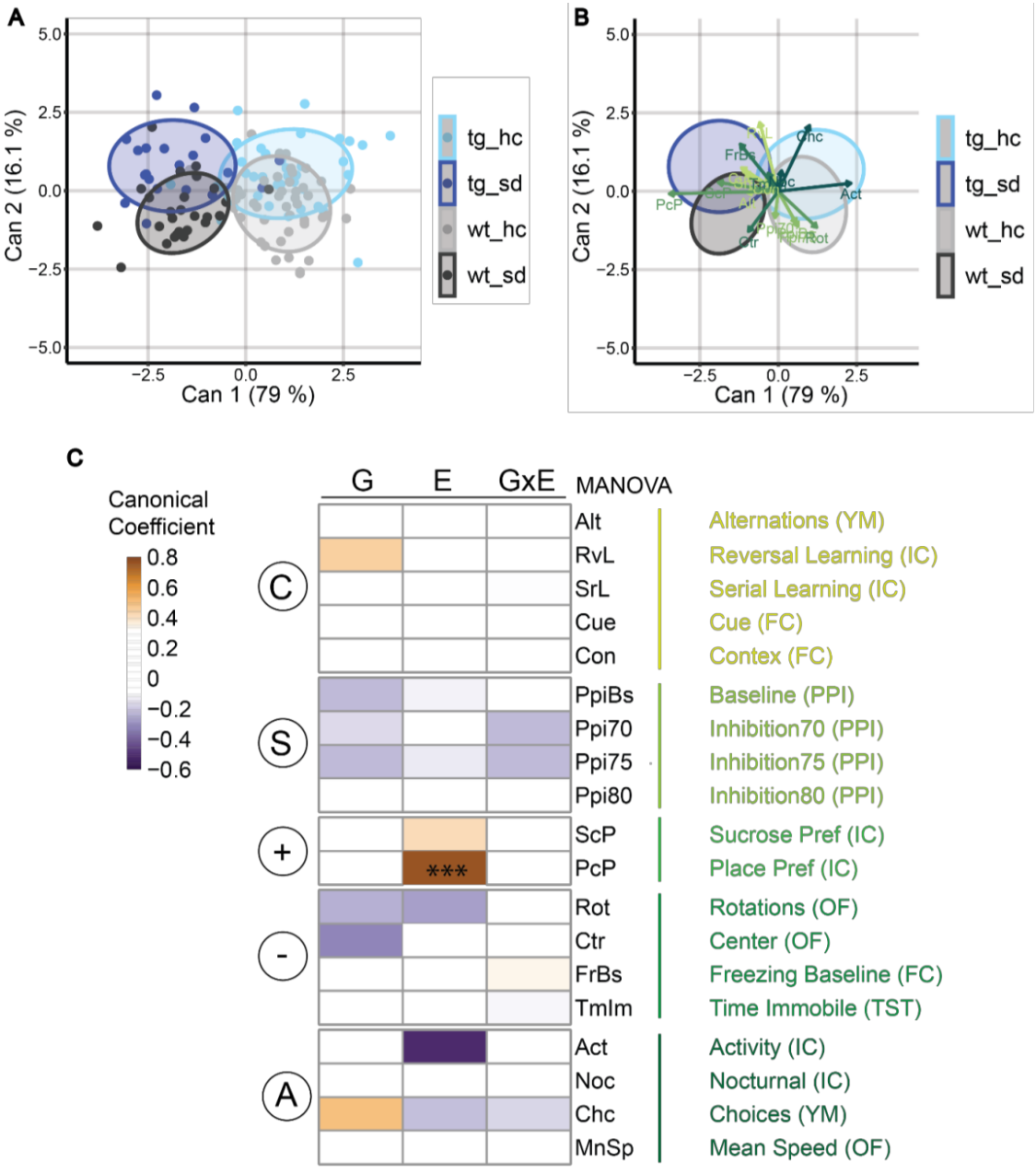

Figure 25. Psychosocial stress but not the Emx1-Cre-driven Taok2 conditional knockout genotype segregates groups well in CDA dimension reduced phenotypic space.

(**A**). The Canonical Discriminant Analysis (CDA) dimension plot showed that separation of the datapoints along the stronger canonical component 1 (Can1) is driven by social defeat, while the second component represents the effect of Taok2 gene dosage. 75% coverage of each group is visualized with ellipsoids and each animal is represented by a dot in the respective groups colour. (**B**). The same dimension plot without single datapoints was superimposed with vectors visualizing the weights (canonical coefficients) represented by the coordinates of the vector tips. This plot reveals how individual variable contributes to the structure of each canonical component. (**C**). A heatmap displays the canonical coefficients for each individual term of the multivariate model: Genotype (G), Environment (E) and their interaction (GxE). This heatmap presents the variables categorized in RDoC domains, showing differences in the impact of genotype and environment on different domains. In summary, variables grouping according to RDoC domains reveals a subtle impact of social defeat on the positive valence ("+") and arousal systems ("A"). Only the environment term showed significant effects on place preference (p_adj = 4.41E-06). The p-values of significant differences after FDR-adjustment are indicated with asterisks.

3.2.2 **Impact of TAOK2 on cellular Signaling (cisPRO data)**

Knock-down of synaptic TAOK2 results in non-mature spines and causes altered morphology and electrophysiological signatures (Calderon de Anda et al., 2012), a defect in calcium compartmentalization (Yadav et al., 2017), and altered neuronal Signaling (Richter et al., 2019). To better understanding the underlying complex biological processes that occur in neurons after Taok2 inactivation, I used the multiparametric cell-based cisProfiler assay that can address 100 individual Signaling events in parallel. The cisProfiler assay is a barcoded pathway profiling platform that uses genetically encoded pathway sensors and molecular barcodes to profile Signaling activities in living cells (Herholt et al., 2018). Importantly, these sensors are linked to molecular barcodes that are short strings of nucleotide sequences, can be analyzed by Next-generation sequencing (NGS), and enable the simultaneous tracking of multiple individual Signaling events in parallel. Sensors consist of either repetitive DNA sequences that recruit single transcription factors or promoters of pathway-indicative genes that recruit multiple transcription factors (Figure 26.A). Thus, transcription factors are used as distal endpoints of Signaling pathways. Pathway sensors available in the cisProfiler assay are divided into seven major Signaling categories covering synaptic activity & calcium Signaling, cell fate, regulation of cellular stress, immune response, metabolism, immediate early gene (IEG) response and stem cell pluripotency (Figure 26.B) (Herholt et al., 2018).

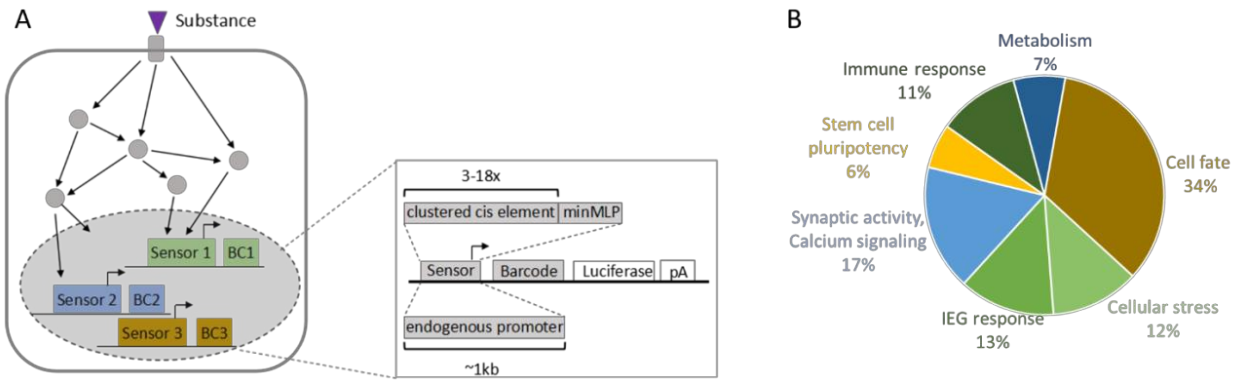

Figure 26. Principle of the multiparametric cell-based cisProlifer assay.

(**A**). Scheme of the multiparametric cisProfiler assay. Inset: Structure of clustered cis element and endogenous promoter reporters; BC, barcode; minMLP, minimal major late promoter; luc, luciferase; pA, polyA sequence. (**B**). Pie chart depicting classes of Signaling categories covered by the cisProfiler assay.

I performed the cisProfiler assay in primary neurons extracted from the cortex of Taok2 (fl/fl) x Emx1-Cre knockout mice and littermate controls to analyze the impact of Taok2 inactivation on synapse-to-nucleus Signaling in synaptic plasticity. We treated neurons (Taok2 ko vs. wild type) with different concentrations of AMPA (agonist for the AMPA receptor), BDNF, bicuculline (BIC, blocks GABA-A receptors), forskolin (forsk, cAMP agonist) and NMDA (agonist of the NMDA receptor) treatment for 4hrs, 24hrs, and 48hrs, respectively. For AMPA, BIC, forskolin and NMDA, the concentrations were 0.1, 1, 10, and 100 µM; for BDNF, the concentrations were 0.1, 1, 10, and 100 ng/ml. From the analysis of statistically significant sensor activities, it became clear that after 4hrs stimuli treatment, sensors for MAPK/IEG, calcium, cAMP Signaling displayed the strongest activation both in wt and Taok2 ko neurons, which links synapse activity to transcriptional activation (Figure 27.A). However, the activity of some sensors decreased in Taok2 ko neurons, which suggested that Taok2 inactivation decreased synaptic activity. In addition, sensor activity also increased after 24hrs and 48hrs stimuli treatment, but it was not as robust as after 4hrs, which suggested that sensors had an early response to these stimuli (Figure 27.A). Furthermore, after selecting the sensors (UPRE-v2, SARE, NR4A1p, CRE, EGR1p, EGR2p, FOSBp, FOSp, SRE, AP-v1 and DUSP5p), which showed a robust response to the stimuli after 4hrs treatment, I plotted line graphs of their activity to better

visualize the effects on the various stimuli and Taok2 genotype, i.e., wt vs. Taok2 ko (Figure 27.B). For AMPA, a concentration of 1 µM was sufficient to induce the strongest senor activity, while for BDNF, it required 100 ng/ml to induce the strongest response for many (i.e. SARE and EGR1p) of the selected sensors. For BIC, forskolin, and NMDA, 10 µM induced the strongest sensor activity. For all the stimuli with different concentrations, Taok2 inactivation reduced the sensor activity (Figure 27.B).

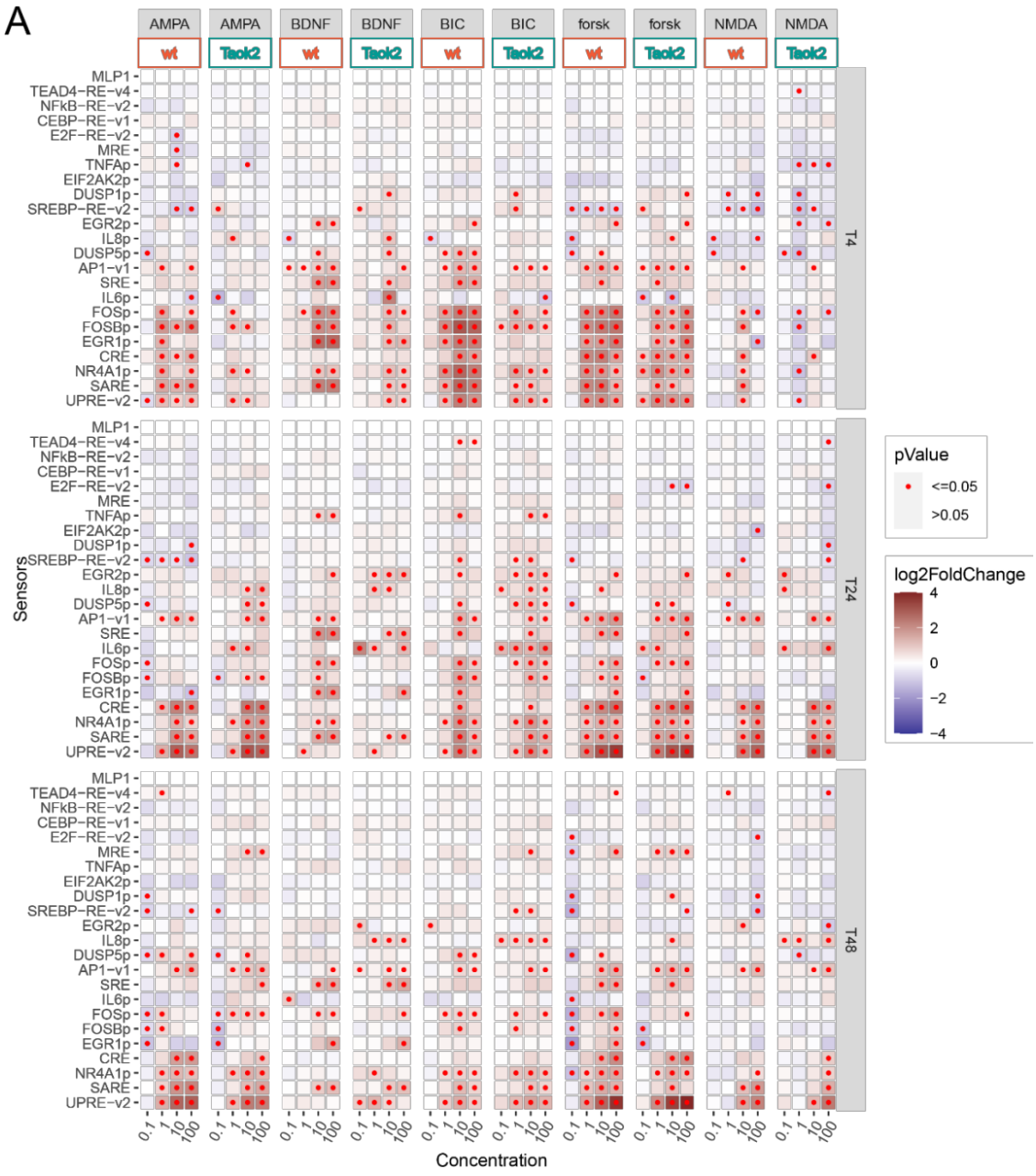

B

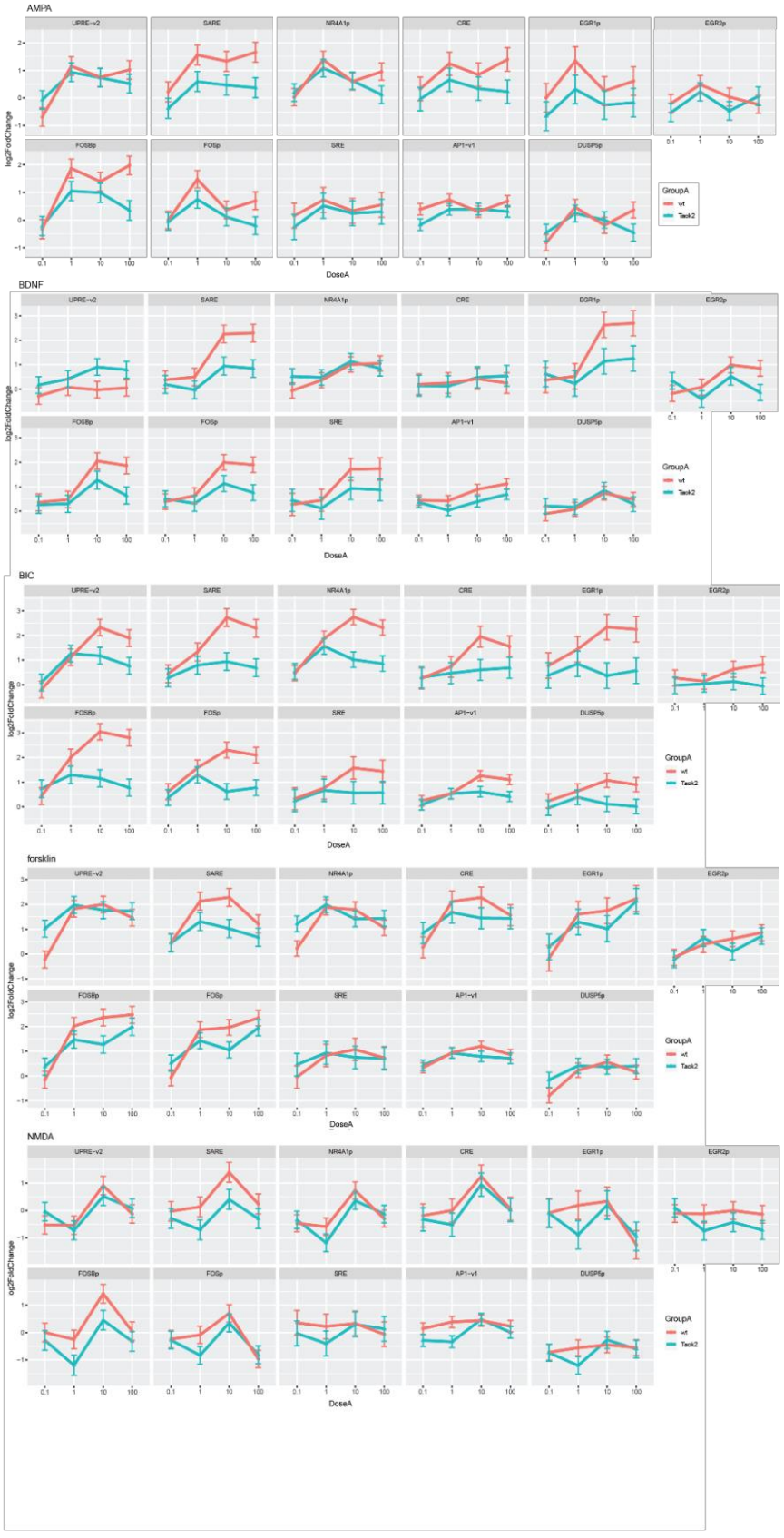
AMPA
BDNF
BIC
forsklin
NMDA
UPRE−v2
SARE
NR4A1p
CRE
EGR1p
EGR2p
FOSBp
FOSp
SRE
AP1−v1
DUSP5p
log2FoldChange
DoseA
GroupA
wt
Task2

Figure 27. Taok2 inactivation reduces synaptic activity.

Data obtained from the cisProfiler assay was modelled to get a single estimate for each condition, and this estimate was used to calculate fold changes for each condition. (**A**). Heatmap of 23 cisProfiler sensor responses with significance at the indicated time points in primary cortical neurons (wt vs. Taok2 ko) as log2 fold-changes between treated (AMPA, BDNF, BIC, forskolin, and NMDA) and untreated samples, measured by barcode sequencing. Significant levels, indicted by red dots, correspond to $p \leqslant 0.05$. (**B**). Line graphs of selected sensor activities in wt and Taok2 ko neurons after 4hrs treatment with AMPA, BDNF, bicuculline, forskolin, and NMDA. Error bars represent SD, n=4. SD represent a single estimate of a posterior SD, which is calculated for each feature (i.e., a sensor), giving a dynamic range of the deviation one can expect for that feature (sensor).

3.2.3 **Impact of TAOK2 on cellular Signaling (RNA-seq data)**

To study the impact of TAOK2 on targets and pathway signatures in neurons, we also performed RNA-seq in primary murine cortical neurons infected with different adeno-associated viruses (AAV) that either overexpress human TAOK2 or inactivate endogenous murine Taok2. Besides, neuronal activity in vitro was evoked when using GABAA receptor antagonist BIC to block inhibitory synaptic transmission.

3.2.3.1 Differentially expressed genes (DEGs) for TAOK2 overexpression and Taok2 inactivation

RNAseq data and determination of DEGs

To study the effects of TAOK2 overexpression, primary mouse cortical neurons were infected with AAVs that overexpress human TAOK2 (EFSp_hTAOK2-var1). AAVs that express EFSp_EGFP were used as control for overexpression conditions. Each condition has 4 replicates and was successfully sequenced. In total, 230 transcripts were determined to be expressed differentially with log2 (Foldchange) ≥ 1 and filtered p-value ≤ 0.05 in neurons upon TAOK2 overexpression (hTaok2_OE) based on RNA-Seq analysis. Among those genes, 214 were upregulated and 16 were downregulated (Figure 28.A). For Taok2 inactivation, primary mouse cortical neurons were infected with AAVs that inactivate endogenous Taok2 (pAAV_shRNA-mTaok2_Syn1p_EGFP), and AAVs expressing a non-targeting shRNA (shCtrl) were used as control for inactivation. Totally, 182 transcripts were differentially expressed with logFoldchange ≥ 1 and filtered p-value ≤ 0.05 in neurons with Taok2 inactivation (shTaok2). Among those genes, 154 were

upregulated and 28 were downregulated in neurons with shTaok2 compared to the control condition (shCtrl) (Figure 28.B).

GO and KEGG analysis of the DEGs

GO, which includes the major ontology of biological process, was used to analyze the obtained DEGs for TAOK2 overexpression and Taok2 inactivation, respectively. The most enriched top 10 GO terms for TAOK2 overexpression are depicted in Figure 28.C. KEGG enrichment analysis revealed that the 230 DEGs caused by TAOK2 overexpression were annotated with 3 pathways, including “cell cycle”, “Notch Signaling pathway”, and “Proximal tubule bicarbonate reclamation” ($p \leq 0.05$, hypergeometic test, as shown in Figure 28.E). For example, the upregulated genes Fringe, Delta, Senate, MAML and Hes1/5 are enriched in Notch Signaling pathway (Figure 28.G). For Taok2 inactivation, the top 10 GO terms are shown in Figure 27.D. KEGG enrichment anlaysis showed genes modulated by Taok2 inactivation were involved in “cell cycle”, “oocyte meiosis”, “DNA replication”, “p53 Signaling pathway”, “progesterone-mediated oocyte maturation” and “Notch Signaling pathway” ($p \leq 0.05$, hypergeometic test, as shown in Figure 28.F). Still, taking the Notch Signaling pathway as an example, we found the upregulated genes Senate, Numb, MAML and Hes1/5 are enriched in this pathway (Figure 28.H).

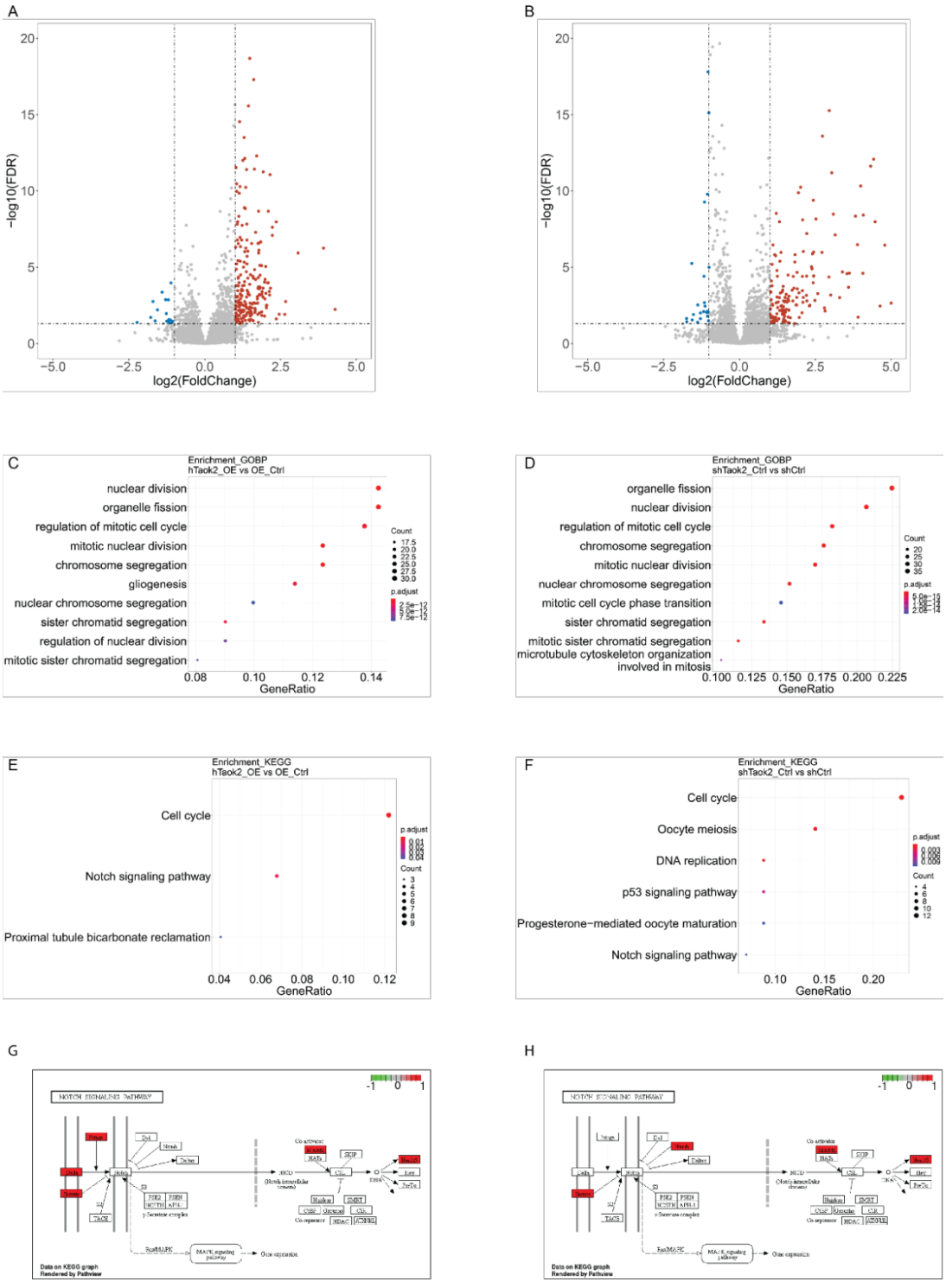

Figure 28. Genes were differentially expressed in neurons with Taok2 overexpression and Taok2 inactivation.

(**A**). Volcano plot of DEGs between hTaok2_OE and OE_Ctrl. FDR: false discovery rate. The red dots and blue dots represented up-regulated genes (214) and down-regulated genes (16), respectively. The gray dots indicated genes with no significantly differential expression. (**B**). Volcano plot of DEGs between shTaok2_Ctrl and shCtrl. FDR: false discovery rate. The red dots and blue dots represented up-regulated genes (154) and down-regulated genes (28), respectively. The gray dots indicated genes with no significantly differential expression. (**C**). The most enriched top 10 GO terms for Taok2 overexpression. (**D**). The most enriched top 10 GO terms for Taok2 inactivation. (**E**). KEGG annotation for the 230 DEGs between hTaok2_OE and OE_Ctrl. (**F**). KEGG annotation for the 182 DEGs between shTaok2_Ctrl and shCtrl. (**G**). An example of upregulated genes enriched in Notch Signaling pathway when overexpressing Taok2. (**H**). An example of upregulated genes enriched in Notch Signaling pathway when inactivating Taok2.

3.2.3.2 DEGs in neurons stimulated with bicuculine

When the neuronal cultures are stimulated with BIC for 4hrs, they showed changed synaptic activity, which allows analysis of modulatory impact of Taok2. For primary mouse cortical neurons infected with AAV of EFSp_EGFP (control for overexpression), 765 transcripts were differentially expressed in neurons treated with BIC (logFoldchange ≥ 1 and filtered pValue ≤ 0.05). Among those genes, 546 were upregulated and 219 downregulated in neurons treated with BIC compared with control condition. KEGG annotation of the pathways of the 765 DEGs involves in “MAPK Signaling pathway”, “p53 Signaling pathway”, “cell cycle” and “neuroactive ligand-receptor interaction” ($p \leq 0.05$, hypergeometic test). For neurons infected with AAV of shCtrl (control for inactivation), there are 619 differentially expressed transcripts (logFoldchange ≥ 1 and filtered pValue ≤ 0.05) in neurons treated with BIC compared to control condition. Among those genes, 470 were upregulated and 149 were downregulated. KEGG annotation of these 619 DEGs involves in the following pathways: “MAPK Signaling pathway”, “neurotrophin Signaling pathway”, “neuroactive ligand-receptor interaction”, “osteoclast differentiation”, “p53 Signaling pathway” and “prostate cancer” ($p < 0.05$, hypergeometic test).

3.2.3.3 DEGs in TAOK2 overexpressing and bicuculine stimulated neurons

For primary mouse cortical neurons infected with AAV of EFSp_EGFP (control for overexpression), 765 transcripts were differentially expressed in neurons treated with BIC (logFoldchange ≥ 1 and filtered pValue < 0.05). For primary mouse cortical neurons infected with AAV of EFSp_hTAOK2-var1, 495 transcripts were differentially expressed in neurons treated with BIC (logFoldchange ≥ 1 and filtered pValue < 0.05).Venn diagram of OE_Ctrl_BIC_vs_OE_Ctrl and hTAOK2_OE_BIC_vs_hTAOK2_OE highlighted 358

overlapping genes (Figure 29.A), and KEGG annotation of these genes involves in the following pathways: “MAPK Signaling pathway”, “p53 Signaling pathway” and “neuroactive ligand-receptor interaction” (Figure 29.B) ($p < 0.05$, hypergeometic test).Then KEGG annotation of the 137 genes which were TAOK2-specific differentially regulated genes involves in the “Notch Signaling pathway” (Figure 29.C) ($p < 0.05$, hypergeometic test).

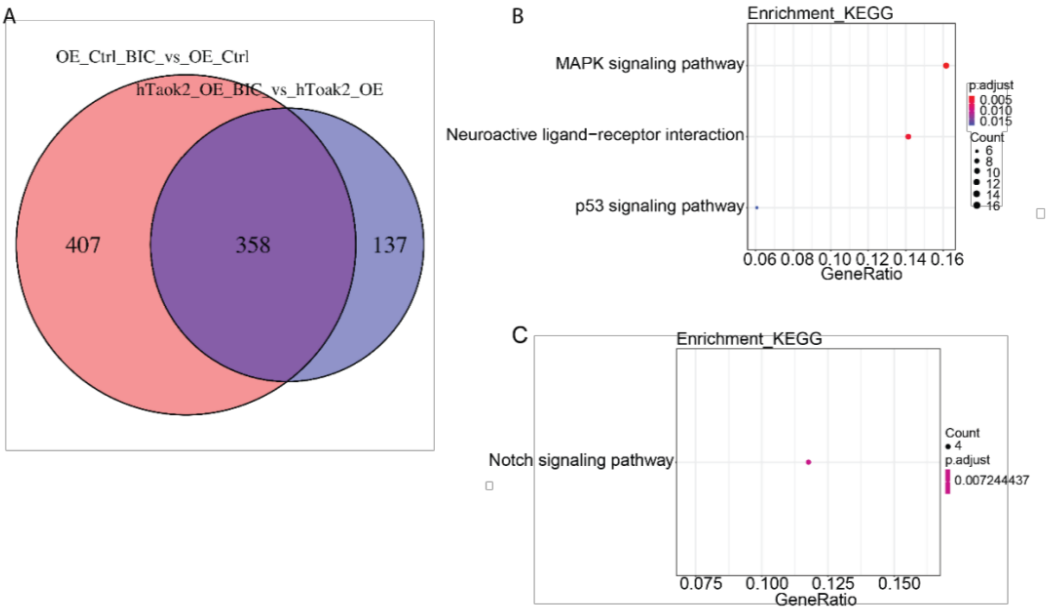

Figure 29. Pathway analysis of DEGs in neurons that overexpressed TAOK2 and were stimulated with bicuculine.

(**A**). Venn diagram of OE_Ctrl_BIC_vs_OE_Ctrl and hTaok2_OE_BIC_vs_hTaok2_OE highlighted 358 overlapping and 137 Taok2-specific DEGs in this analysis. (**B**). KEGG annotation of overlapping DEGs. (**C**). KEGG annotation of Taok2-specific DEGs.

3.2.3.4 DEGs in neurons with downregulated Taok2 and stimulated with bicuculine

For neurons infected with AAV of shCtrl (control for inactivation), 619 transcripts were differentially expressed in neurons treated with BIC (logFoldchange ≥ 1 and filtered pValue < 0.05). For primary mouse cortical neurons infected with AAV of pAAV_shRNA-mTaok2_Syn1p_EGFP, 348 transcripts were differentially expressed in neurons treated with BIC (logFoldchange ≥ 1 and filtered p-vvalue < 0.05).Venn diagram of ShCtrl_BIC_vs_ShCtrl and ShTaok2_BIC_vs_ShTaok2_Ctrl highlighted 292 overlapping

genes (Figure 30.A), and KEGG annotation of these genes involves in the following pathways: “MAPK Signaling pathway”, “p53 Signaling pathway”, “Neuroactive ligand-receptor interaction”, “Neurotrophin Signaling pathway”, “JAK-STAT Signaling pathway” and “Osteoclast differentiation” (Figure 30.B) ($p < 0.05$, hypergeometic test). Then KEGG annotation of the 56 genes which were Taok2-specific differentially regulated genes involves in the “Neuroactive ligand-receptor interaction” (Figure 30.C) ($p < 0.05$, hypergeometic test).

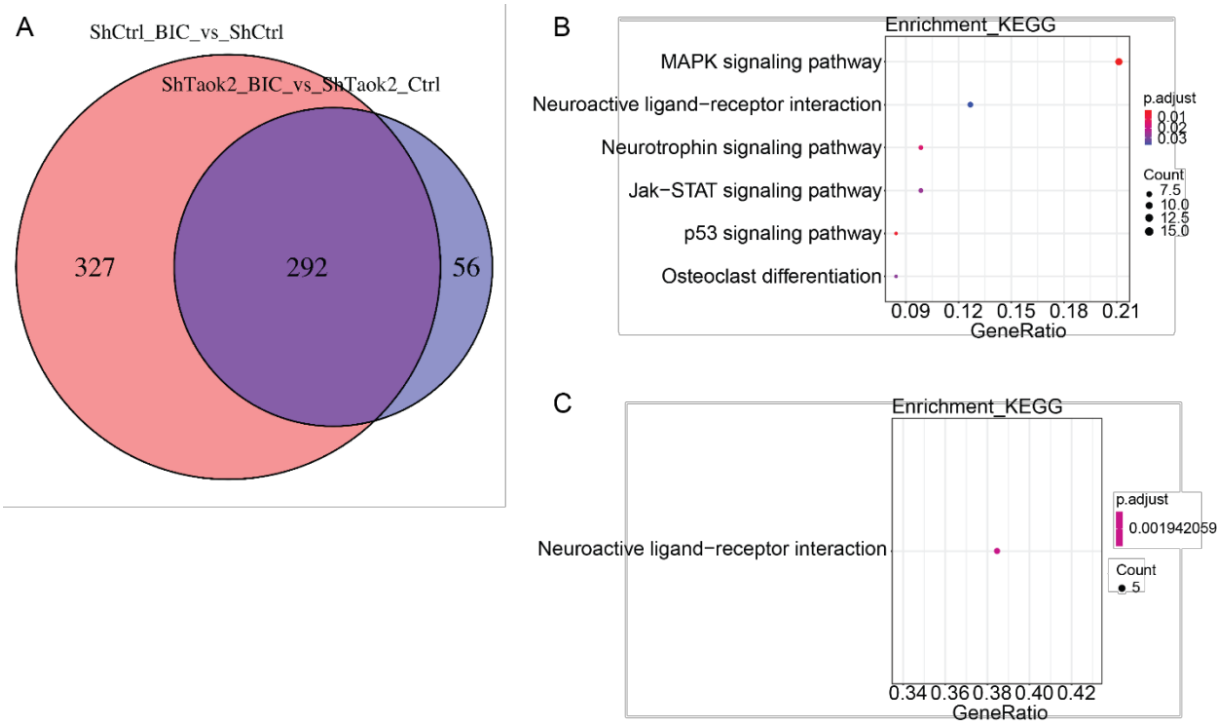

Figure 30. Pathway analysis of DEGs for Taok2 downregulation and bicuculine stimulated neurons.

(**A**). Venn diagram of ShCtrl_BIC_vs_ShCtrl and ShTaok2_BIC_vs_ShTaok2_Ctrl highlighted 292 overlapping and 56 Taok2-specific DEGs in this analysis. (**B**). KEGG annotation of overlapping DEGs. (**C**). KEGG annotation of Taok2-specific DEGs.

3.2.4 **Validation of molecular phenotypes in Taok2 KO neurons**

TAOK2 kinase has been demonstrated to activate MAP/ERK kinases (MEKs) 3,4, and 6 in vitro, which further activate JNK/SAPK and p38 MAP kinase (Zihni et al., 2007). Recently, a study using a heterozygous (Het) and knockout (KO) mouse model shows that A135P mutation (loss of function mutation) reduces Taok2 activity, thus decreasing

JNK1 activation, while P1022* mutation (gain of function mutation) increases JNK1 activation which is TAOK2-dependent (Richter et al., 2019). Therefore, we would like to examine the effect of TAOK2 on endogenous MAPKs in neurons. We analyzed the impact of TAOK2 on ERK1/2, one of the downstream components of MAPK Signaling. I stimulated both wt primary murine cortical neurons and Taok2 ko neurons with AMPA (10 µM) and NMDA (10 µM) for 5 minutes, respectively. Then, I assessed the changes of phosphorylation levels of Erk1/2 on their Thr202 and Tyr204 sites. I found that in wt neurons, AMPA increased the phosphorylation level of Erk1/2 significantly (p=0.026, *t* test). However, in Taok2 ko neurons, AMPA didn't increase the phosphorylation level of Erk1/2 (p=0.407, *t* test) (Figure 31.A&B). For NMDA, I also found that NMDA increased the phosphorylation levels of Erk1/2 significantly in wt neurons (p=0.004, *t* test), while in Taok2 ko neurons, the NMDA effect on phosphorylation level of Erk1/2 was comprised (p=0.156, *t* test) (Figure 31.C&D). As MAPK activation can phosphorylate cAMP response element binding protein (CREB), which can regulate the transcription of many important genes and proteins like the brain-derived neurotrophic factor (BDNF), I further analyzed the effect of Taok2 on Creb (Wu et al., 2020). I found that AMPA did not increase the phosphorylation level of Creb significantly in both wt and Taok2 ko neurons (wt: p=0.168, *t* test; Taok2 ko: p=0.307, *t* test) (Figure 32.A&B). Likewise, NMDA did not increase the phosphorylation levels of Creb significantly in both wt and Taok2 ko neurons (wt: p=0.258, *t* test; Taok2 ko: p=0.206, *t* test) (Figure 32.C&D).

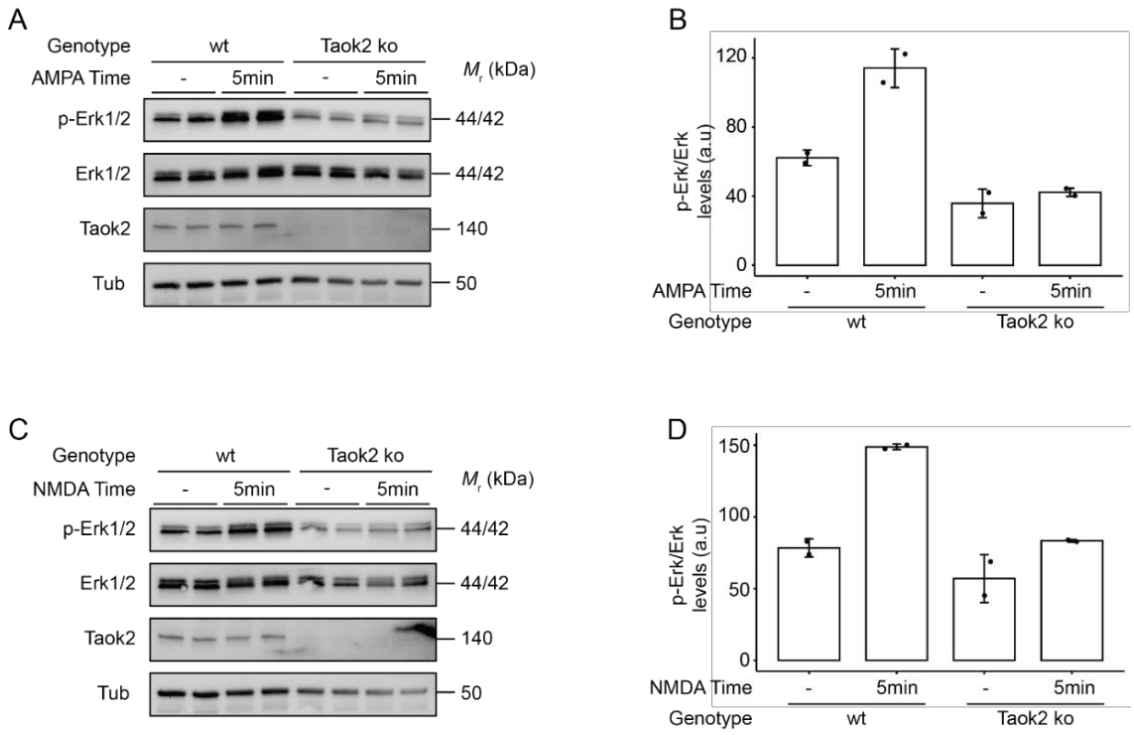

Figure 31. Taok2 inactivation decreases Erk1/2 phosphorylation (Thr202 and Tyr204 sites) in neurons stimulated with AMPA and NMDA.

(**A, B**). Western blot and quantification analysis show that AMPA treatment (10 μM, 5min) increased the phosphorylation level of Erk1/2 in wt neurons (p=0.026, *t* test), while it didn't increase phosphorylation level of Erk1/2 in Taok2 ko neurons (p=0.407, *t* test). (**C, D**). Western blot and quantification analysis show that NMDA treatment (10 μM, 5min) increased the phosphorylation level of Erk1/2 in wt neurons (p=0.004, t test), while it did not increase phosphorylation level of Erk1/2 in Taok2 ko neurons (p=0.156, *t* test). Error bars represent SD, n=2.

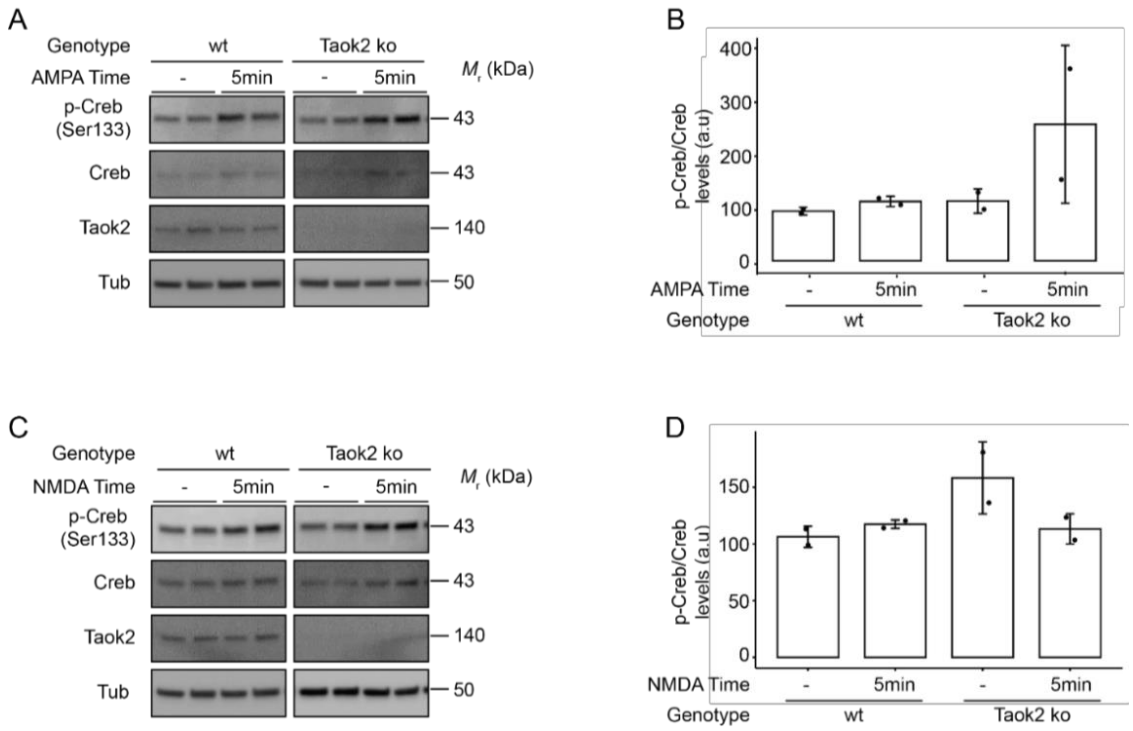

Figure 32. Taok2 inactivation does not change Creb phosphorylation in neurons stimulated with AMPA and NMDA.

(**A, B**). Western blot and quantification analysis show that AMPA treatment (10 μM, 5min) didnot increase the phosphorylation levels of Creb significantly in both wt and Taok ko neurons (wt: p=0.168, *t* test; Taok2 ko: p=0.307, *t* test). (**C, D**). Western blot and quantification analysis show that NMDA treatment (10 μM, 5min) did not increase the phosphorylation levels of Creb significantly in both wt and Taok2 ko neurons (wt: p=0.258, *t* test; Taok2 ko: p=0.206, *t* test). Error bars represent SD, n=2.

4. Discussion

4.1 TAOK2 is a new upstream regulator of Hippo Signaling pathway

For the TAOK family, TAOK1 and TAOK3, but not TAOK2, were functionally linked to Hippo Signaling. They can promote the activity of the core cassette kinases STK3/4 and LATS1/2 (Boggiano et al., 2011; Poon et al., 2011). TAOK2, however, was reported to have no impact on Hippo Signaling, as only TAOK1 and TAOK3 phosphorylated LATS1/2 in an in vitro kinase assay (Plouffe et al., 2016). Here, I identified TAOK2 as a new regulator of Hippo Signaling. My split TEV interaction screen identified the interactions between TAOK2 and the core components of Hippo pathway (STK3/4, LATS1/2, MOB1A). The co-immunoprecipitation assay validated the screen results. Compared to a previous study that suggested that only TAOK1/3 act both upstream of and in parallel to STK3/4 and MAP4Ks to phosphorylate and activate LAST/2, we found that TAOK2 also interacts with and phosphorylates LATS1 and further modulates the activity and phosphorylation of YAP, the most downstream effector of the Hippo pathway (Plouffe et al., 2016).

4.1.1 **TAOK2 modulates Hippo Signaling pathway to regulate cell growth**

Previous study found Hippo Signaling can regulate the proliferation of cells by modulating cell number (W. Kim et al., 2018; Moon et al., 2018). In my study, doxycycline induced overexpression of TAOK2 was found to increase phospho-YAP1 levels and further leads to decreased expression levels of YAP1 transcriptional targets CTGF. In addition, strong reduction of TAOK2 expression using the CRISPRi technique increased the transcription levels of both CTGF and CYR61. Notably, proliferation assays conducted in HEK293 cells showed that cells overexpressing TAOK2 (i.e., activating Hippo Signaling) proliferated slower than controls, whereas cells depleted of TAOK2 (i.e., reducing Hippo Signaling) proliferated faster than controls (Figure 23. A&B). Thus, TAOK2 exerts similar mechanisms on Hippo Signaling as previously reported for TAOK1 and TAOK3 (Bian et al., 2019; Torrini et al., 2019). My findings demonstrate the clear role of TAOK2 in mediating growth signals to the Hippo pathway and illustrates how activating and

inactivating TAOK2 can result in pathological changes of YAP and its transcriptional targets.

4.1.2 TAOK2 associates with the prognosis of cancer through Hippo signaling pathway

My findings from cell culture are consistent with the role of TAOK2 in cancer progression, where altered expression levels of TAOK2 are correlated with cancer progression. I analyzed the clinical impact of TAOK2 and found that reduced TAOK2 expression was correlated with reduced survival time in patients with HNSC, KICH, LGG, LUAD, and PAAD. Furthermore, my finding that TAOK2 antagonizes proliferation is supported by studies in human tissue, as TAOK2 expression was reduced in lung adenocarcinoma tissue using a transcriptome analysis (Transcriptome analysis in lung adenocarcinoma reveals gender-specific differences in the overall metabolic response of female and male patients) (Y. Li et al., 2020). By contrast, TAOK2 activity was increased in melanoma drug resistant cells. It has been thought that the activation of the JNK by TAOK2 contributes to the resistance of BRAF inhibitor (Sharma et al., 2016). TAOK2 can signal either through JNK or Hippo Signaling, which could result in tumour promotion or inhibition consequences, respectively. These diverse regulatory for TAOK2 raise the notion that TAOK2 may have tissue- and cell-specific functions. Notably, studies on growth control and tumour biology were mostly performed in cell lines. Therefore, the impact of those studies to clinical manifestation remains to be elucidated thoroughly.

In summary, these findings support the notion that TAOK2 interacts with core Hippo pathway components to regulate YAP1-dependent transcription and cell proliferation. Furthermore, TAOK2 is implicated in cancer progression as a tumour suppressor gene, since TAOK2 expression levels are reduced in a set of cancers. Therefore, TAOK2 can be a potentially new biomarker for cancer. As a serine/threonine protein kinase which has been identified as a potential cancer therapeutic target, TAOK2 provides new treatment strategy for pharmacology intervention studies of cancers.

4.2 TAOK2 impacts on synaptic plasticity and mouse behaviour

As TAOK2 has been reported to be a risk gene of mental disorders, e.g., for schizophrenia and autism, and as the Hippo pathway is involved in neuron development as well, I further studied the role of TAOK2 in neurons (Emoto, 2011a, 2011b; Pardiñas et al., 2018; Weiss et al., 2008).

4.2.1 **Behavioural deficits of brain specific Taok2 knockout mice**

In neurons, TAOK2 is implicated in the development of synapses, synaptic plasticity and synaptic transmission and is regarded as key contributor to the pathophysiology of neurodevelopmental disorders (Calderon de Anda et al., 2012; Fang et al., 2020; Kapfhamer et al., 2013; Yadav et al., 2017). TAOK2 is located on chromosomal locus 16p 11.2, duplication of which is associated with schizophrenia (Bristow et al., 2020), while deletion of the same chromosomal region is strongly linked to autism spectrum disorders (Weiss et al., 2008). TAOK2 has been identified as schizophrenia risk gene in genome-wide association studies (Pardiñas et al., 2018). A genetic deletion of Taok2 in mice lead to impairments in social interaction, cognition, and anxiety at the behavioural level, as well as aberrations in neural connectivity and brain size at the structural level, which are dosage-dependent (Richter et al., 2019). Furthermore, Richter et al identified TAOK2 de novo mutations in autism families, strengthening the link between TAOK2 biology and autism. At the molecular level, these deficits are linked to altered RhoA Signaling and F-actin stability as mediators of TAOK2-dependent synaptic development (Richter et al., 2019). However, behavioural profiling of our conditional Taok2 ko mouse model (conducted by Celestine Dutta and Elisabeth Voggenreiter) showed that conditional Taok2 ko mice only showed very limited behavioural abnormalities compared with wild type controls. One reason may be that behavioural tests were performed by different researchers. For example, conditional Taok2 ko mice of cohort 1, with tests conducted by Celestine Dutta, displayed both a significant increase of mean speed (Open Field test) ($p=0.044$) and choices (Y-Maze test) ($p=0.019$). However, these findings were not replicated in cohort 2, with tests conducted by Elisabeth Voggenreiter. A second reason may be contributed by the brain-specific inactivation of Taok2 mediated by Emx1-Cre,

which is not sufficient to cause similar behavioural deficits as observed for full Taok2 ko mice. Furthermore, behavioural deficits can be due to the dosage of Taok2, as impairments in social interaction, cognition, and anxiety shown in Taok2 heterozygous (Het) and knockout (KO) mice was dosage-dependent (Richter et al., 2019). The third reason may be due to a compensatory role of TAOK1 and TAOK3. TAOK2 is involved in the pathophysiology of Alzheimer's disease as well, as TAOK2 can phosphorylate microtubule-associated protein tau to modulate tau-microtubule interactions (Tavares et al., 2013). Abnormal physiology for Alzheimer's disease may also be inferred by TAOK1, as TAOK1 modulates synapse formation and can phosphorylate tau. Likewise, TAOK1 de novo mutations were also linked to neurodevelopmental disorders and may thus contribute to autism phenotypes (Dulovic-Mahlow et al., 2019). Therefore, roles in the pathophysiology of neurodevelopmental disorders for TAOK1 and TAOK2 may overlap, and deficits may be mutually compensated by each protein.

4.2.2 **Impact of Taok2 on cellular Signaling**

Preliminary work from our lab in conditional Taok2 ko mice only showed very mild behavioural phenotypes. Colleagues have, however, described distinct phenotypes, including hyperactivity and deficits in cognition, anxiety, and social behaviour, in mice carrying a complete Taok2 knockout (Taok2-ko), as well as structural and electrophysiological impairments of neurons. Therefore, I was still convinced that the conditional inactivation of Taok2 in neurons has a strong impact on cellular Signaling in these cells per se. To better understand these phenotypes at the molecular level, I investigated the effect of Taok2 inactivation in primary murine cortical neuron cultures.
Pathway profiling using the multiparametric and cell-based cisProfiler assay indicates that Taok2 inactivation leads to decreased synaptic activity, which is reflected by the reduced activity of sensors for MAPK/IEG, calcium, and cAMP Signaling (Figure 27.A&B). This suggested that Taok2 inactivation reduces MAPK pathway activity. TAOK2, a MAPKKK, has already been reported to activates MEK3, a MAPKK, thus phosphorylating p38, a MAPK (Yasuda et al., 2007). However, the activation of p38 can in turn feed-back on TAOK2, which phosphorylates a critical serine that is needed for triggering N-cadherin

endocytosis at the synapse. SiRNA knockdown of N-cadherin can rescue the phenotype of increased number of dendritic spines caused by arcadlin knockout. The regulation of endocytosis of N-cadherin by protocadherin/TAOK2/MEK3/p38 provides a molecular mechanism, which explains the transduction of neuronal activity to synaptic morphology changes (Yasuda et al., 2007). Furthermore, Richter et.al. only detected the role of TAOK2 on JNK1, another branch of MAPK Signaling (Richter et al., 2019). In sum, it was previously reported that TAOK2 regulates the p38 and JNK branches of MAPK Signaling. However, the cisProfiler assay indicated that the ERK1/ERK2 branch of MAPK Signaling is strongly implicated in TAOK2 mediated Signaling in neuron as well. My biochemical results verified that Taok2 inactivation reduced the phosphorylation levels of Erk1/2 (Thr202 and Tyr204 sites) in neurons (Figure 31).

Analyses from the RNA-seq experiments in primary neurons also indicated that MAPK Signaling is the Signaling pathway that is most significantly modulated. Together with the data obtained from the cisProfiler assay and the biochemistry validation experiments, this supports the notion that Taok2 predominantly modulates MAPK Signaling in neurons. However, other Signaling pathways including RhoA and F-actin Signaling (Richter et al., 2019) and neuro-active ligand receptor interactions ((Yasuda et al., 2007), own data from RNA-seq) may well be contributing to the synaptic plasticity regulated by TAOK2.

5. Outlook

It is known that cell migration and invasion exert a significant role in cancer development. Therefore, future work should detect the impact of TAOK2 expression level on cell migration. My hypothesis is that TAOK2 overexpression will decrease cell migration ability, while TAOK2 depletion will increase migration ability.

Notably, Taok2 protein levels in lysates from cortex and hippocampus were absent (Voggenreiter,2019). However, an immunocytological staining of key brain regions is required to address whether Taok2 is absent in all (glutamatergic) neurons. Additionally, to better investigate the impact of the Emx1-Cre-driven conditional Taok2 knockout, we should also detect the change of brain size, neural connectivity in cortex, hippocampus and amygdala, excitatory neurotransmission, dendrite and synapse formation, and cortical layering (Calderon de Anda et al., 2012).

Results from the cisProfiler assay and the RNA-seq experiments provided correlating data. However, the RNA-seq experiment was performed in shRNA-depleted neurons, while the cisProfiler assay was conducted in knockout neurons from embryos that harbored a conditional Emx1-Cre driven Taok2 knockout. To better compare the results from the cisProfiler assay with the RNA-seq data set, I am currently conducting another RNA-seq experiment in primary neurons that bear the conditional Taok2 knockout. Furthermore, I will stimulate the neurons in this experiment with BIC and AMPA, the two stimuli that provided the largest differences in sensor response between wt and Taok2 ko conditions in the cisProfiler assay. This way, I hope to further investigate the Signaling mechanisms of Taok2 in neurons.

To also better map the protein-protein interaction profile of Taok2 in neurons, future work may also imply mass spectrometry-based proteomics in neurons that, for example, overexpress HA-tagged human TAOK2. By identifying druggable targets that bind to TAOK2 directly, such an approach may pave the way to targeted pharmacology interventions, which could finally lead to treatment options within the framework of personalized medicine.

References

Alerasool, N., Segal, D., Lee, H., & Taipale, M. (2020). An efficient KRAB domain for CRISPRi applications in human cells. *Nature Methods*, *17*(11), 1093–1096. https://doi.org/10.1038/s41592-020-0966-x

Alexander Herholt. (2016). *Development of a multiplexed RNAi-coupled sensor assay to study neuronal function on the large-scale* [Georg-August-University Göttingen]. PhD Thesis.

Anders, S., Pyl, P. T., & Huber, W. (2015). HTSeq—A Python framework to work with high-throughput sequencing data. *Bioinformatics*, *31*(2), 166–169. https://doi.org/10.1093/bioinformatics/btu638

Araki, Y., Zeng, M., Zhang, M., & Huganir, R. L. (2015). Rapid Dispersion of SynGAP from Synaptic Spines Triggers AMPA Receptor Insertion and Spine Enlargement during LTP. *Neuron*, *85*(1), 173–189. https://doi.org/10.1016/j.neuron.2014.12.023

Bae, S. J., & Luo, X. (2018). Activation mechanisms of the Hippo kinase signaling cascade. *Bioscience Reports*, *38*(4), BSR20171469. https://doi.org/10.1042/BSR20171469

Beattie, R., & Hippenmeyer, S. (2017). Mechanisms of radial glia progenitor cell lineage progression. *FEBS Letters*, *591*(24), 3993–4008. https://doi.org/10.1002/1873-3468.12906

Bian, Y., Teper, Y., Mathews Griner, L. A., Aiken, T. J., Shukla, V., Guha, R., Shinn, P., Xin, H.-W., Pflicke, H., Powers, A. S., Li, D., Jiang, J., Patel, P., Rogers, S. A., Aubé, J., Ferrer, M., Thomas, C. J., & Rudloff, U. (2019). Target Deconvolution of a Multikinase Inhibitor with Antimetastatic Properties Identifies TAOK3 as a Key Contributor to a Cancer Stem Cell–Like Phenotype. *Molecular Cancer Therapeutics*, *18*(11), 2097–2110. https://doi.org/10.1158/1535-7163.MCT-18-1011

Boggiano, J. C., Vanderzalm, P. J., & Fehon, R. G. (2011). Tao-1 Phosphorylates Hippo/MST Kinases to Regulate the Hippo-Salvador-Warts Tumor Suppressor Pathway. *Developmental Cell*, *21*(5), 888–895. https://doi.org/10.1016/j.devcel.2011.08.028

Boopathy, G. T. K., & Hong, W. (2019). Role of Hippo Pathway-YAP/TAZ Signaling in Angiogenesis. *Frontiers in Cell and Developmental Biology*, *7*, 49. https://doi.org/10.3389/fcell.2019.00049

Bray, N. J., & O'Donovan, M. C. (2018). The genetics of neuropsychiatric disorders. *Brain and Neuroscience Advances*, *2*, 239821281879927. https://doi.org/10.1177/2398212818799271

Bristow, G. C., Thomson, D. M., Openshaw, R. L., Mitchell, E. J., Pratt, J. A., Dawson, N., & Morris, B. J. (2020). 16p11 Duplication Disrupts Hippocampal-Orbitofrontal-Amygdala Connectivity, Revealing a Neural Circuit Endophenotype for Schizophrenia. *Cell Reports*, *31*(3), 107536. https://doi.org/10.1016/j.celrep.2020.107536

Calderon de Anda, F., Rosario, A. L., Durak, O., Tran, T., Gräff, J., Meletis, K., Rei, D., Soda, T., Madabhushi, R., Ginty, D. D., Kolodkin, A. L., & Tsai, L.-H. (2012). Autism spectrum disorder susceptibility gene TAOK2 affects basal dendrite formation in the neocortex. *Nature Neuroscience*, *15*(7), 1022–1031. https://doi.org/10.1038/nn.3141

Calderone, A., Castagnoli, L., & Cesareni, G. (2013). mentha: A resource for browsing integrated protein-interaction networks. *Nature Methods*, *10*(8), 690–691. https://doi.org/10.1038/nmeth.2561

Camargo, F. D., Gokhale, S., Johnnidis, J. B., Fu, D., Bell, G. W., Jaenisch, R., & Brummelkamp, T. R. (2007). YAP1 Increases Organ Size and Expands Undifferentiated Progenitor Cells. *Current Biology*, *17*(23), 2054–2060. https://doi.org/10.1016/j.cub.2007.10.039

Can, A., Dao, D. T., Terrillion, C. E., Piantadosi, S. C., Bhat, S., & Gould, T. D. (2011). The Tail Suspension Test. *Journal of Visualized Experiments*, *58*, 3769. https://doi.org/10.3791/3769

Caroni, P., Donato, F., & Muller, D. (2012). Structural plasticity upon learning: Regulation and functions. *Nature Reviews Neuroscience*, *13*(7), 478–490. https://doi.org/10.1038/nrn3258

Chan, E. H. Y., Nousiainen, M., Chalamalasetty, R. B., Schäfer, A., Nigg, E. A., & Silljé, H. H. W. (2005). The Ste20-like kinase Mst2 activates the human large tumor suppressor kinase Lats1. *Oncogene*, *24*(12), 2076–2086. https://doi.org/10.1038/sj.onc.1208445

Chen, Z., & Cobb, M. H. (2001). Regulation of Stress-responsive Mitogen-activated Protein (MAP) Kinase Pathways by TAO2. *Journal of Biological Chemistry*, *276*(19), 16070–16075. https://doi.org/10.1074/jbc.M100681200

Chen, Z., Hutchison, M., & Cobb, M. H. (1999). Isolation of the Protein Kinase TAO2 and Identification of Its Mitogen-activated Protein Kinase/Extracellular Signal-regulated Kinase Kinase Binding Domain. *Journal of Biological Chemistry*, *274*(40), 28803–28807. https://doi.org/10.1074/jbc.274.40.28803

Chen, Z., Raman, M., Chen, L., Lee, S. F., Gilman, A. G., & Cobb, M. H. (2003). TAO (Thousand-and-one Amino Acid) Protein Kinases Mediate Signaling from Carbachol to p38 Mitogen-activated Protein Kinase and Ternary Complex Factors. *Journal of Biological Chemistry*, *278*(25), 22278–22283. https://doi.org/10.1074/jbc.M301173200
Cocas, L. A., Miyoshi, G., Carney, R. S. E., Sousa, V. H., Hirata, T., Jones, K. R., Fishell, G., Huntsman, M. M., & Corbin, J. G. (2009). Emx1-Lineage Progenitors Differentially Contribute to Neural Diversity in the Striatum and Amygdala. *Journal of Neuroscience*, *29*(50), 15933–15946. https://doi.org/10.1523/JNEUROSCI.2525-09.2009
Couzens, A. L., Knight, J. D. R., Kean, M. J., Teo, G., Weiss, A., Dunham, W. H., Lin, Z.-Y., Bagshaw, R. D., Sicheri, F., Pawson, T., Wrana, J. L., Choi, H., & Gingras, A.-C. (2013). Protein Interaction Network of the Mammalian Hippo Pathway Reveals Mechanisms of Kinase-Phosphatase Interactions. *Science Signaling*, *6*(302), rs15–rs15. https://doi.org/10.1126/scisignal.2004712
Das Thakur, M., Feng, Y., Jagannathan, R., Seppa, M. J., Skeath, J. B., & Longmore, G. D. (2010). Ajuba LIM proteins are negative regulators of the Hippo signaling pathway. *Current Biology: CB*, *20*(7), 657–662. https://doi.org/10.1016/j.cub.2010.02.035
de Sena Brandine, G., & Smith, A. D. (2021). Falco: High-speed FastQC emulation for quality control of sequencing data. *F1000Research*, *8*, 1874. https://doi.org/10.12688/f1000research.21142.2
Dembélé, D., & Kastner, P. (2014). Fold change rank ordering statistics: A new method for detecting differentially expressed genes. *BMC Bioinformatics*, *15*(1), 14. https://doi.org/10.1186/1471-2105-15-14
Deng, Y., Pang, A., & Wang, J. H. (2003). Regulation of mammalian STE20-like kinase 2 (MST2) by protein phosphorylation/dephosphorylation and proteolysis. *The Journal of Biological Chemistry*, *278*(14), 11760–11767. https://doi.org/10.1074/jbc.M211085200
Di Cara, F., Maile, T. M., Parsons, B. D., Magico, A., Basu, S., Tapon, N., & King-Jones, K. (2015). The Hippo pathway promotes cell survival in response to chemical stress. *Cell Death & Differentiation*, *22*(9), 1526–1539. https://doi.org/10.1038/cdd.2015.10
Ding, R., Weynans, K., Bossing, T., Barros, C. S., & Berger, C. (2016). The Hippo Signaling pathway maintains quiescence in Drosophila neural stem cells. *Nature Communications*, *7*(1), 10510. https://doi.org/10.1038/ncomms10510
Dulovic-Mahlow, M., Trinh, J., Kandaswamy, K. K., Braathen, G. J., Di Donato, N., Rahikkala, E., Beblo, S., Werber, M., Krajka, V., Busk, Ø. L., Baumann, H., Al-Sannaa, N. A., Hinrichs, F., Affan, R., Navot, N., Al Balwi, M. A., Oprea, G., Holla, Ø. L., Weiss, M. E. R., … Lohmann, K. (2019). De Novo Variants in TAOK1 Cause Neurodevelopmental Disorders. *The American Journal of Human Genetics*, *105*(1), 213–220. https://doi.org/10.1016/j.ajhg.2019.05.005
Dupont, S., Morsut, L., Aragona, M., Enzo, E., Giulitti, S., Cordenonsi, M., Zanconato, F., Le Digabel, J., Forcato, M., Bicciato, S., Elvassore, N., & Piccolo, S. (2011). Role of YAP/TAZ in mechanotransduction. *Nature*, *474*(7350), 179–183. https://doi.org/10.1038/nature10137
Emes, R. D., Pocklington, A. J., Anderson, C. N. G., Bayes, A., Collins, M. O., Vickers, C. A., Croning, M. D. R., Malik, B. R., Choudhary, J. S., Armstrong, J. D., & Grant, S. G. N. (2008). Evolutionary expansion and anatomical specialization of synapse proteome complexity. *Nature Neuroscience*, *11*(7), 799–806. https://doi.org/10.1038/nn.2135
Emoto, K. (2011a). Dendrite remodeling in development and disease: Dendrite remodeling in development and disease. *Development, Growth & Differentiation*, *53*(3), 277–286. https://doi.org/10.1111/j.1440-169X.2010.01242.x
Emoto, K. (2011b). The growing role of the Hippo-NDR kinase Signaling in neuronal development and disease. *Journal of Biochemistry*, *150*(2), 133–141. https://doi.org/10.1093/jb/mvr080
Emoto, K., He, Y., Ye, B., Grueber, W. B., Adler, P. N., Jan, L. Y., & Jan, Y.-N. (2004). Control of Dendritic Branching and Tiling by the Tricornered-Kinase/Furry Signaling Pathway in Drosophila Sensory Neurons. *Cell*, *119*(2), 245–256. https://doi.org/10.1016/j.cell.2004.09.036
Emoto, K., Parrish, J. Z., Jan, L. Y., & Jan, Y.-N. (2006). The tumour suppressor Hippo acts with the NDR kinases in dendritic tiling and maintenance. *Nature*, *443*(7108), 210–213. https://doi.org/10.1038/nature05090
Etherton, M., Foldy, C., Sharma, M., Tabuchi, K., Liu, X., Shamloo, M., Malenka, R. C., & Sudhof, T. C. (2011). Autism-linked neuroligin-3 R451C mutation differentially alters hippocampal and cortical synaptic function. *Proceedings of the National Academy of Sciences*, *108*(33), 13764–13769. https://doi.org/10.1073/pnas.1111093108

Fang, C.-Y., Lai, T.-C., Hsiao, M., & Chang, Y.-C. (2020). The Diverse Roles of TAO Kinases in Health and Diseases. *International Journal of Molecular Sciences*, *21*(20), 7463. https://doi.org/10.3390/ijms21207463
Fong, K.-W., Choi, Y.-K., Rattner, J. B., & Qi, R. Z. (2008). CDK5RAP2 Is a Pericentriolar Protein That Functions in Centrosomal Attachment of the γ-Tubulin Ring Complex. *Molecular Biology of the Cell*, *19*(1), 115–125. https://doi.org/10.1091/mbc.e07-04-0371
Forrest, M. P., Parnell, E., & Penzes, P. (2018). Dendritic structural plasticity and neuropsychiatric disease. *Nature Reviews Neuroscience*, *19*(4), 215–234. https://doi.org/10.1038/nrn.2018.16
Frank, R. A., & Grant, S. G. (2017). Supramolecular organization of NMDA receptors and the postsynaptic density. *Current Opinion in Neurobiology*, *45*, 139–147. https://doi.org/10.1016/j.conb.2017.05.019
Gee, S. T., Milgram, S. L., Kramer, K. L., Conlon, F. L., & Moody, S. A. (2011). Yes-associated protein 65 (YAP) expands neural progenitors and regulates Pax3 expression in the neural plate border zone. *PloS One*, *6*(6), e20309. https://doi.org/10.1371/journal.pone.0020309
Genevet, A., & Tapon, N. (2011). The Hippo pathway and apico–basal cell polarity. *Biochemical Journal*, *436*(2), 213–224. https://doi.org/10.1042/BJ20110217
Genevet, A., Wehr, M. C., Brain, R., Thompson, B. J., & Tapon, N. (2010). Kibra is a regulator of the Salvador/Warts/Hippo signaling network. *Developmental Cell*, *18*(2), 300–308. https://doi.org/10.1016/j.devcel.2009.12.011
Gilbert, L. A., Horlbeck, M. A., Adamson, B., Villalta, J. E., Chen, Y., Whitehead, E. H., Guimaraes, C., Panning, B., Ploegh, H. L., Bassik, M. C., Qi, L. S., Kampmann, M., & Weissman, J. S. (2014). Genome-Scale CRISPR-Mediated Control of Gene Repression and Activation. *Cell*, *159*(3), 647–661. https://doi.org/10.1016/j.cell.2014.09.029
Glantschnig, H., Rodan, G. A., & Reszka, A. A. (2002). Mapping of MST1 kinase sites of phosphorylation. Activation and autophosphorylation. *The Journal of Biological Chemistry*, *277*(45), 42987–42996. https://doi.org/10.1074/jbc.M208538200
Gorski, J. A., Talley, T., Qiu, M., Puelles, L., Rubenstein, J. L. R., & Jones, K. R. (2002). Cortical Excitatory Neurons and Glia, But Not GABAergic Neurons, Are Produced in the Emx1-Expressing Lineage. *The Journal of Neuroscience*, *22*(15), 6309–6314. https://doi.org/10.1523/JNEUROSCI.22-15-06309.2002
Graves, J. D., Draves, K. E., Gotoh, Y., Krebs, E. G., & Clark, E. A. (2001). Both Phosphorylation and Caspase-mediated Cleavage Contribute to Regulation of the Ste20-like Protein Kinase Mst1 during CD95/Fas-induced Apoptosis. *Journal of Biological Chemistry*, *276*(18), 14909–14915. https://doi.org/10.1074/jbc.M010905200
Guo, H., Hong, S., Jin, X.-L., Chen, R.-S., Avasthi, P. P., Tu, Y.-T., Ivanco, T. L., & Li, Y. (2000). Specificity and Efficiency of Cre-Mediated Recombination in Emx1–cre Knock-in Mice. *Biochemical and Biophysical Research Communications*, *273*(2), 661–665. https://doi.org/10.1006/bbrc.2000.2870
Halder, G., & Johnson, R. L. (2011). Hippo signaling: Growth control and beyond. *Development*, *138*(1), 9–22. https://doi.org/10.1242/dev.045500
Hammad, H., Vanderkerken, M., Pouliot, P., Deswarte, K., Toussaint, W., Vergote, K., Vandersarren, L., Janssens, S., Ramou, I., Savvides, S. N., Haigh, J. J., Hendriks, R., Kopf, M., Craessaerts, K., de Strooper, B., Kearney, J. F., Conrad, D. H., & Lambrecht, B. N. (2017). Transitional B cells commit to marginal zone B cell fate by Taok3-mediated surface expression of ADAM10. *Nature Immunology*, *18*(3), 313–320. https://doi.org/10.1038/ni.3657
Han, D., Byun, S.-H., Park, S., Kim, J., Kim, I., Ha, S., Kwon, M., & Yoon, K. (2015). YAP/TAZ enhance mammalian embryonic neural stem cell characteristics in a Tead-dependent manner. *Biochemical and Biophysical Research Communications*, *458*(1), 110–116. https://doi.org/10.1016/j.bbrc.2015.01.077
Han, D., Lee, S. M., Kwon, M., Noh, H., Lee, J. H., Yoon, Y., Cho, J. Y., & Yoon, K. (2020). YAP Enhances FGF2-Dependent Neural Stem Cell Proliferation by Induction of FGF Receptor Expression. *Stem Cells and Development*, *29*(18), 1240–1246. https://doi.org/10.1089/scd.2019.0281
Han, Y. (2019). Analysis of the role of the Hippo pathway in cancer. *Journal of Translational Medicine*, *17*(1), 116. https://doi.org/10.1186/s12967-019-1869-4
Hansen, C. G., Moroishi, T., & Guan, K.-L. (2015). YAP and TAZ: A nexus for Hippo signaling and beyond. *Trends in Cell Biology*, *25*(9), 499–513. https://doi.org/10.1016/j.tcb.2015.05.002
Hao, Y., Chun, A., Cheung, K., Rashidi, B., & Yang, X. (2008). Tumor Suppressor LATS1 Is a Negative Regulator of Oncogene YAP. *Journal of Biological Chemistry*, *283*(9), 5496–5509. https://doi.org/10.1074/jbc.M709037200

Happé, H., van der Wal, A. M., Leonhard, W. N., Kunnen, S. J., Breuning, M. H., de Heer, E., & Peters, D. J. M. (2011). Altered Hippo Signaling in polycystic kidney disease. *The Journal of Pathology*, *224*(1), 133–142. https://doi.org/10.1002/path.2856
Haque, R. U., & Levey, A. I. (2019). Alzheimer's disease: A clinical perspective and future nonhuman primate research opportunities. *Proceedings of the National Academy of Sciences of the United States of America*. https://doi.org/10.1073/pnas.1912954116
Hauri, S., Wepf, A., Drogen, A., Varjosalo, M., Tapon, N., Aebersold, R., & Gstaiger, M. (2013). Interaction proteome of human Hippo signaling: Modular control of the co-activator YAP1. *Molecular Systems Biology*, *9*(1), 713. https://doi.org/10.1002/msb.201304750
Hergovich, A., Schmitz, D., & Hemmings, B. A. (2006). The human tumour suppressor LATS1 is activated by human MOB1 at the membrane. *Biochemical and Biophysical Research Communications*, *345*(1), 50–58. https://doi.org/10.1016/j.bbrc.2006.03.244
Herholt, A., Brankatschk, B., Kannaiyan, N., Papiol, S., Wichert, S. P., Wehr, M. C., & Rossner, M. J. (2018). Pathway sensor-based functional genomics screening identifies modulators of neuronal activity. *Scientific Reports*, *8*(1), 17597. https://doi.org/10.1038/s41598-018-36008-9
Hiemer, S. E., & Varelas, X. (2013). Stem cell regulation by the Hippo pathway. *Biochimica et Biophysica Acta (BBA) - General Subjects*, *1830*(2), 2323–2334. https://doi.org/10.1016/j.bbagen.2012.07.005
Hirabayashi, S., Nakagawa, K., Sumita, K., Hidaka, S., Kawai, T., Ikeda, M., Kawata, A., Ohno, K., & Hata, Y. (2008). Threonine 74 of MOB1 is a putative key phosphorylation site by MST2 to form the scaffold to activate nuclear Dbf2-related kinase 1. *Oncogene*, *27*(31), 4281–4292. https://doi.org/10.1038/onc.2008.66
Huang, J., Wu, S., Barrera, J., Matthews, K., & Pan, D. (2005). The Hippo signaling pathway coordinately regulates cell proliferation and apoptosis by inactivating Yorkie, the Drosophila Homolog of YAP. *Cell*, *122*(3), 421–434. https://doi.org/10.1016/j.cell.2005.06.007
Hughes, L. J., Park, R., Lee, M. J., Terry, B. K., Lee, D. J., Kim, H., Cho, S.-H., & Kim, S. (2020). Yap/Taz are required for establishing the cerebellar radial glia scaffold and proper foliation. *Developmental Biology*, *457*(1), 150–162. https://doi.org/10.1016/j.ydbio.2019.10.002
Hutchison, M., Berman, K. S., & Cobb, M. H. (1998). Isolation of TAO1, a Protein Kinase That Activates MEKs in Stress-activated Protein Kinase Cascades. *Journal of Biological Chemistry*, *273*(44), 28625–28632. https://doi.org/10.1074/jbc.273.44.28625
Insel, T., Cuthbert, B., Garvey, M., Heinssen, R., Pine, D. S., Quinn, K., Sanislow, C., & Wang, P. (2010). Research Domain Criteria (RDoC): Toward a New Classification Framework for Research on Mental Disorders. *American Journal of Psychiatry*, *167*(7), 748–751. https://doi.org/10.1176/appi.ajp.2010.09091379
Jan, Y.-N., & Jan, L. Y. (2010). Branching out: Mechanisms of dendritic arborization. *Nature Reviews Neuroscience*, *11*(5), 316–328. https://doi.org/10.1038/nrn2836
Jiang, Q., Liu, D., Gong, Y., Wang, Y., Sun, S., Gui, Y., & Song, H. (2009). Yap is required for the development of brain, eyes, and neural crest in zebrafish. *Biochemical and Biophysical Research Communications*, *384*(1), 114–119. https://doi.org/10.1016/j.bbrc.2009.04.070
Kandilya, D., Shyamasundar, S., Singh, D. K., Banik, A., Hande, M. P., Stünkel, W., Chong, Y. S., & Dheen, S. T. (2020). High glucose alters the DNA methylation pattern of neurodevelopment associated genes in human neural progenitor cells in vitro. *Scientific Reports*, *10*(1), 15676. https://doi.org/10.1038/s41598-020-72485-7
Kapfhamer, D., King, I., Zou, M. E., Lim, J. P., Heberlein, U., & Wolf, F. W. (2012). JNK Pathway Activation Is Controlled by Tao/TAOK3 to Modulate Ethanol Sensitivity. *PLoS ONE*, *7*(12), e50594. https://doi.org/10.1371/journal.pone.0050594
Kapfhamer, D., Taylor, S., Zou, M. E., Lim, J. P., Kharazia, V., & Heberlein, U. (2013). Taok2 controls behavioral response to ethanol in mice: Taok2 and ethanol behaviors. *Genes, Brain and Behavior*, *12*(1), 87–97. https://doi.org/10.1111/j.1601-183X.2012.00834.x
Karl, T., & Arnold, J. C. (2014). Schizophrenia: A consequence of gene-environment interactions? *Frontiers in Behavioral Neuroscience*, *8*. https://doi.org/10.3389/fnbeh.2014.00435
Kim, E., Kang, J. G., Kang, M. J., Park, J. H., Kim, Y. J., Kweon, T. H., Lee, H.-W., Jho, E.-H., Lee, Y.-H., Kim, S.-I., Yi, E. C., Park, H. W., Yang, W. H., & Cho, J. W. (2020). O-GlcNAcylation on LATS2 disrupts the Hippo pathway by inhibiting its activity. *Proceedings of the National Academy of Sciences of the United States of America*, *117*(25), 14259–14269. https://doi.org/10.1073/pnas.1913469117

Kim, H., Kim, M., Im, S.-K., & Fang, S. (2018). Mouse Cre-LoxP system: General principles to determine tissue-specific roles of target genes. *Laboratory Animal Research*, *34*(4), 147–159. https://doi.org/10.5625/lar.2018.34.4.147
Kim, W., Khan, S. K., Liu, Y., Xu, R., Park, O., He, Y., Cha, B., Gao, B., & Yang, Y. (2018). Hepatic Hippo signaling inhibits protumoural microenvironment to suppress hepatocellular carcinoma. *Gut*, *67*(9), 1692–1703. https://doi.org/10.1136/gutjnl-2017-314061
Kim, W., Khan, S. K., & Yang, Y. (2017). Interacting network of Hippo, Wnt/β-catenin and Notch signaling represses liver tumor formation. *BMB Reports*, *50*(1), 1–2. https://doi.org/10.5483/BMBRep.2017.50.1.196
King, I., Tsai, L. T.-Y., Pflanz, R., Voigt, A., Lee, S., Jackle, H., Lu, B., & Heberlein, U. (2011). Drosophila tao Controls Mushroom Body Development and Ethanol-Stimulated Behavior through par-1. *Journal of Neuroscience*, *31*(3), 1139–1148. https://doi.org/10.1523/JNEUROSCI.4416-10.2011
Labbadia, J., & Morimoto, R. I. (2013). Huntington's disease: Underlying molecular mechanisms and emerging concepts. *Trends in Biochemical Sciences*, *38*(8), 378–385. https://doi.org/10.1016/j.tibs.2013.05.003
Lavado, A., Park, J. Y., Paré, J., Finkelstein, D., Pan, H., Xu, B., Fan, Y., Kumar, R. P., Neale, G., Kwak, Y. D., McKinnon, P. J., Johnson, R. L., & Cao, X. (2018). The Hippo Pathway Prevents YAP/TAZ-Driven Hypertranscription and Controls Neural Progenitor Number. *Developmental Cell*, *47*(5), 576-591.e8. https://doi.org/10.1016/j.devcel.2018.09.021
Lee, J.-H., Kim, T.-S., Yang, T.-H., Koo, B.-K., Oh, S.-P., Lee, K.-P., Oh, H.-J., Lee, S.-H., Kong, Y.-Y., Kim, J.-M., & Lim, D.-S. (2008). A crucial role of WW45 in developing epithelial tissues in the mouse. *The EMBO Journal*, *27*(8), 1231–1242. https://doi.org/10.1038/emboj.2008.63
Lee, K.-K., Ohyama, T., Yajima, N., Tsubuki, S., & Yonehara, S. (2001). MST, a Physiological Caspase Substrate, Highly Sensitizes Apoptosis Both Upstream and Downstream of Caspase Activation. *Journal of Biological Chemistry*, *276*(22), 19276–19285. https://doi.org/10.1074/jbc.M005109200
Lei, Q.-Y., Zhang, H., Zhao, B., Zha, Z.-Y., Bai, F., Pei, X.-H., Zhao, S., Xiong, Y., & Guan, K.-L. (2008). TAZ promotes cell proliferation and epithelial-mesenchymal transition and is inhibited by the hippo pathway. *Molecular and Cellular Biology*, *28*(7), 2426–2436. https://doi.org/10.1128/MCB.01874-07
Li, J., Wilkinson, B., Clementel, V. A., Hou, J., O'Dell, T. J., & Coba, M. P. (2016). Long-term potentiation modulates synaptic phosphorylation networks and reshapes the structure of the postsynaptic interactome. *Science Signaling*, *9*(440), rs8–rs8. https://doi.org/10.1126/scisignal.aaf6716
Li, Q., Nirala, N. K., Nie, Y., Chen, H.-J., Ostroff, G., Mao, J., Wang, Q., Xu, L., & Ip, Y. T. (2018). Ingestion of Food Particles Regulates the Mechanosensing Misshapen-Yorkie Pathway in Drosophila Intestinal Growth. *Developmental Cell*, *45*(4), 433-449.e6. https://doi.org/10.1016/j.devcel.2018.04.014
Li, Y., He, C.-L., Li, W.-X., Zhang, R.-X., & Duan, Y. (2020). Transcriptome analysis reveals gender-specific differences in overall metabolic response of male and female patients in lung adenocarcinoma. *PLOS ONE*, *15*(4), e0230796. https://doi.org/10.1371/journal.pone.0230796
Li, Y., Zhou, H., Li, F., Chan, S. W., Lin, Z., Wei, Z., Yang, Z., Guo, F., Lim, C. J., Xing, W., Shen, Y., Hong, W., Long, J., & Zhang, M. (2015). Angiomotin binding-induced activation of Merlin/NF2 in the Hippo pathway. *Cell Research*, *25*(7), 801–817. https://doi.org/10.1038/cr.2015.69
Lin, K. C., Moroishi, T., Meng, Z., Jeong, H.-S., Plouffe, S. W., Sekido, Y., Han, J., Park, H. W., & Guan, K.-L. (2017). Regulation of Hippo pathway transcription factor TEAD by p38 MAPK-induced cytoplasmic translocation. *Nature Cell Biology*, *19*(8), 996–1002. https://doi.org/10.1038/ncb3581
Liu, S., Zhou, L., Yuan, H., Vieira, M., Sanz-Clemente, A., Badger, J. D., Lu, W., Traynelis, S. F., & Roche, K. W. (2017). A Rare Variant Identified Within the GluN2B C-Terminus in a Patient with Autism Affects NMDA Receptor Surface Expression and Spine Density. *The Journal of Neuroscience*, *37*(15), 4093–4102. https://doi.org/10.1523/JNEUROSCI.0827-16.2017
Love, M. I., Huber, W., & Anders, S. (2014). Moderated estimation of fold change and dispersion for RNA-seq data with DESeq2. *Genome Biology*, *15*(12), 550. https://doi.org/10.1186/s13059-014-0550-8
Ma, B., Chen, Y., Chen, L., Cheng, H., Mu, C., Li, J., Gao, R., Zhou, C., Cao, L., Liu, J., Zhu, Y., Chen, Q., & Wu, S. (2015). Hypoxia regulates Hippo Signaling through the SIAH2 ubiquitin E3 ligase. *Nature Cell Biology*, *17*(1), 95–103. https://doi.org/10.1038/ncb3073
Ma, S., Zhang, B., LaFave, L. M., Earl, A. S., Chiang, Z., Hu, Y., Ding, J., Brack, A., Kartha, V. K., Tay, T., Law, T., Lareau, C., Hsu, Y.-C., Regev, A., & Buenrostro, J. D. (2020). Chromatin Potential Identified by Shared Single-Cell Profiling of RNA and Chromatin. *Cell*, *183*(4), 1103-1116.e20. https://doi.org/10.1016/j.cell.2020.09.056

MacKeigan, J. P., Murphy, L. O., & Blenis, J. (2005). Sensitized RNAi screen of human kinases and phosphatases identifies new regulators of apoptosis and chemoresistance. *Nature Cell Biology*, *7*(6), 591–600. https://doi.org/10.1038/ncb1258
Maillard, A. M., Ruef, A., Pizzagalli, F., Migliavacca, E., Hippolyte, L., Adaszewski, S., Dukart, J., Ferrari, C., Conus, P., Männik, K., Zazhytska, M., Siffredi, V., Maeder, P., Kutalik, Z., Kherif, F., Hadjikhani, N., Beckmann, J. S., Reymond, A., Draganski, B., … 16p11.2 European Consortium. (2015). The 16p11.2 locus modulates brain structures common to autism, schizophrenia and obesity. *Molecular Psychiatry*, *20*(1), 140–147. https://doi.org/10.1038/mp.2014.145
Manderfield, L. J., Aghajanian, H., Engleka, K. A., Lim, L. Y., Liu, F., Jain, R., Li, L., Olson, E. N., & Epstein, J. A. (2015). Hippo signaling is required for Notch-dependent smooth muscle differentiation of neural crest. *Development*, *142*(17), 2962–2971. https://doi.org/10.1242/dev.125807
Matallanas, D., Romano, D., Yee, K., Meissl, K., Kucerova, L., Piazzolla, D., Baccarini, M., Vass, J. K., Kolch, W., & O'Neill, E. (2007). RASSF1A Elicits Apoptosis through an MST2 Pathway Directing Proapoptotic Transcription by the p73 Tumor Suppressor Protein. *Molecular Cell*, *27*(6), 962–975. https://doi.org/10.1016/j.molcel.2007.08.008
Matsuzaki, M., Ellis-Davies, G. C. R., Nemoto, T., Miyashita, Y., Iino, M., & Kasai, H. (2001). Dendritic spine geometry is critical for AMPA receptor expression in hippocampal CA1 pyramidal neurons. *Nature Neuroscience*, *4*(11), 1086–1092. https://doi.org/10.1038/nn736
Matsuzaki, M., Honkura, N., Ellis-Davies, G. C. R., & Kasai, H. (2004). Structural basis of long-term potentiation in single dendritic spines. *Nature*, *429*(6993), 761–766. https://doi.org/10.1038/nature02617
McCarthy, S. E., Makarov, V., Kirov, G., Addington, A. M., McClellan, J., Yoon, S., Perkins, D. O., Dickel, D. E., Kusenda, M., Krastoshevsky, O., Krause, V., Kumar, R. A., Grozeva, D., Malhotra, D., Walsh, T., Zackai, E. H., Kaplan, P., Ganesh, J., Krantz, I. D., … Sebat, J. (2009). Microduplications of 16p11.2 are associated with schizophrenia. *Nature Genetics*, *41*(11), 1223–1227. https://doi.org/10.1038/ng.474
Meng, Z., Moroishi, T., & Guan, K.-L. (2016). Mechanisms of Hippo pathway regulation. *Genes & Development*, *30*(1), 1–17. https://doi.org/10.1101/gad.274027.115
Meng, Z., Moroishi, T., Mottier-Pavie, V., Plouffe, S. W., Hansen, C. G., Hong, A. W., Park, H. W., Mo, J.-S., Lu, W., Lu, S., Flores, F., Yu, F.-X., Halder, G., & Guan, K.-L. (2015). MAP4K family kinases act in parallel to MST1/2 to activate LATS1/2 in the Hippo pathway. *Nature Communications*, *6*(1), 8357. https://doi.org/10.1038/ncomms9357
Milewski, R. C., Chi, N. C., Li, J., Brown, C., Lu, M. M., & Epstein, J. A. (2004). Identification of minimal enhancer elements sufficient for Pax3 expression in neural crest and implication of Tead2 as a regulator of Pax3. *Development (Cambridge, England)*, *131*(4), 829–837. https://doi.org/10.1242/dev.00975
Misra, J. R., & Irvine, K. D. (2018). The Hippo Signaling Network and Its Biological Functions. *Annual Review of Genetics*, *52*(1), 65–87. https://doi.org/10.1146/annurev-genet-120417-031621
Mitsopoulos, C., Zihni, C., Garg, R., Ridley, A. J., & Morris, J. D. H. (2003). The Prostate-derived Sterile 20-like Kinase (PSK) Regulates Microtubule Organization and Stability. *Journal of Biological Chemistry*, *278*(20), 18085–18091. https://doi.org/10.1074/jbc.M213064200
Moon, S., Yeon Park, S., & Woo Park, H. (2018). Regulation of the Hippo pathway in cancer biology. *Cellular and Molecular Life Sciences: CMLS*, *75*(13), 2303–2319. https://doi.org/10.1007/s00018-018-2804-1
Moore, T. M., Garg, R., Johnson, C., Coptcoat, M. J., Ridley, A. J., & Morris, J. D. H. (2000). PSK, a Novel STE20-like Kinase Derived from Prostatic Carcinoma That Activates the c-Jun N-terminal Kinase Mitogen-activated Protein Kinase Pathway and Regulates Actin Cytoskeletal Organization. *Journal of Biological Chemistry*, *275*(6), 4311–4322. https://doi.org/10.1074/jbc.275.6.4311
Morris, S. E., & Cuthbert, B. N. (2012). Research Domain Criteria: Cognitive systems, neural circuits, and dimensions of behavior. *Dialogues in Clinical Neuroscience*, *14*(1), 29–37.
Mueller, K. A., Glajch, K. E., Huizenga, M. N., Wilson, R. A., Granucci, E. J., Dios, A. M., Tousley, A. R., Iuliano, M., Weisman, E., LaQuaglia, M. J., DiFiglia, M., Kegel-Gleason, K., Vakili, K., & Sadri-Vakili, G. (2018). Hippo Signaling Pathway Dysregulation in Human Huntington's Disease Brain and Neuronal Stem Cells. *Scientific Reports*, *8*(1), 11355. https://doi.org/10.1038/s41598-018-29319-4
Nishimoto, M., Uranishi, K., Asaka, M. N., Suzuki, A., Mizuno, Y., Hirasaki, M., & Okuda, A. (2019). Transformation of normal cells by aberrant activation of YAP via cMyc with TEAD. *Scientific Reports*, *9*(1), 10933. https://doi.org/10.1038/s41598-019-47301-6

Orchard, S., Ammari, M., Aranda, B., Breuza, L., Briganti, L., Broackes-Carter, F., Campbell, N. H., Chavali, G., Chen, C., del-Toro, N., Duesbury, M., Dumousseau, M., Galeota, E., Hinz, U., Iannuccelli, M., Jagannathan, S., Jimenez, R., Khadake, J., Lagreid, A., … Hermjakob, H. (2014). The MIntAct project—IntAct as a common curation platform for 11 molecular interaction databases. *Nucleic Acids Research*, *42*(D1), D358–D363. https://doi.org/10.1093/nar/gkt1115

Ormonde, J. V. S., Li, Z., Stegen, C., & Madrenas, J. (2018). TAOK3 Regulates Canonical TCR Signaling by Preventing Early SHP-1–Mediated Inactivation of LCK. *The Journal of Immunology*, *201*(11), 3431–3442. https://doi.org/10.4049/jimmunol.1800284

Ouyang, T., Meng, W., Li, M., Hong, T., & Zhang, N. (2020). Recent Advances of the Hippo/YAP Signaling Pathway in Brain Development and Glioma. *Cellular and Molecular Neurobiology*, *40*(4), 495–510. https://doi.org/10.1007/s10571-019-00762-9

Pan, D. (2010). The Hippo Signaling Pathway in Development and Cancer. *Developmental Cell*, *19*(4), 491–505. https://doi.org/10.1016/j.devcel.2010.09.011

Panciera, T., Azzolin, L., Fujimura, A., Di Biagio, D., Frasson, C., Bresolin, S., Soligo, S., Basso, G., Bicciato, S., Rosato, A., Cordenonsi, M., & Piccolo, S. (2016). Induction of Expandable Tissue-Specific Stem/Progenitor Cells through Transient Expression of YAP/TAZ. *Cell Stem Cell*, *19*(6), 725–737. https://doi.org/10.1016/j.stem.2016.08.009

Paramasivam, M., Sarkeshik, A., Yates, J. R., Fernandes, M. J. G., & McCollum, D. (2011). Angiomotin family proteins are novel activators of the LATS2 kinase tumor suppressor. *Molecular Biology of the Cell*, *22*(19), 3725–3733. https://doi.org/10.1091/mbc.e11-04-0300

Pardiñas, A. F., Holmans, P., Pocklington, A. J., Escott-Price, V., Ripke, S., Carrera, N., Legge, S. E., Bishop, S., Cameron, D., Hamshere, M. L., Han, J., Hubbard, L., Lynham, A., Mantripragada, K., Rees, E., MacCabe, J. H., McCarroll, S. A., Baune, B. T., Breen, G., … Walters, J. T. R. (2018). Common schizophrenia alleles are enriched in mutation-intolerant genes and in regions under strong background selection. *Nature Genetics*, *50*(3), 381–389. https://doi.org/10.1038/s41588-018-0059-2

Park, R., Moon, U. Y., Park, J. Y., Hughes, L. J., Johnson, R. L., Cho, S.-H., & Kim, S. (2016). Yap is required for ependymal integrity and is suppressed in LPA-induced hydrocephalus. *Nature Communications*, *7*(1), 10329. https://doi.org/10.1038/ncomms10329

Pearson, G., Robinson, F., Beers Gibson, T., Xu, B., Karandikar, M., Berman, K., & Cobb, M. H. (2001). Mitogen-Activated Protein (MAP) Kinase Pathways: Regulation and Physiological Functions*. *Endocrine Reviews*, *22*(2), 153–183. https://doi.org/10.1210/edrv.22.2.0428

Plouffe, S. W., Meng, Z., Lin, K. C., Lin, B., Hong, A. W., Chun, J. V., & Guan, K.-L. (2016). Characterization of Hippo Pathway Components by Gene Inactivation. *Molecular Cell*, *64*(5), 993–1008. https://doi.org/10.1016/j.molcel.2016.10.034

Poon, C. L. C., Lin, J. I., Zhang, X., & Harvey, K. F. (2011). The Sterile 20-like Kinase Tao-1 Controls Tissue Growth by Regulating the Salvador-Warts-Hippo Pathway. *Developmental Cell*, *21*(5), 896–906. https://doi.org/10.1016/j.devcel.2011.09.012

Praskova, M., Xia, F., & Avruch, J. (2008). MOBKL1A/MOBKL1B phosphorylation by MST1 and MST2 inhibits cell proliferation. *Current Biology: CB*, *18*(5), 311–321. https://doi.org/10.1016/j.cub.2008.02.006

Raman, M., Earnest, S., Zhang, K., Zhao, Y., & Cobb, M. H. (2007). TAO kinases mediate activation of p38 in response to DNA damage. *The EMBO Journal*, *26*(8), 2005–2014. https://doi.org/10.1038/sj.emboj.7601668

Rayon, T., Menchero, S., Nieto, A., Xenopoulos, P., Crespo, M., Cockburn, K., Cañon, S., Sasaki, H., Hadjantonakis, A.-K., de la Pompa, J. L., Rossant, J., & Manzanares, M. (2014). Notch and Hippo Converge on Cdx2 to Specify the Trophectoderm Lineage in the Mouse Blastocyst. *Developmental Cell*, *30*(4), 410–422. https://doi.org/10.1016/j.devcel.2014.06.019

Richter, M., Murtaza, N., Scharrenberg, R., White, S. H., Johanns, O., Walker, S., Yuen, R. K. C., Schwanke, B., Bedürftig, B., Henis, M., Scharf, S., Kraus, V., Dörk, R., Hellmann, J., Lindenmaier, Z., Ellegood, J., Hartung, H., Kwan, V., Sedlacik, J., … Calderon de Anda, F. (2019). Altered TAOK2 activity causes autism-related neurodevelopmental and cognitive abnormalities through RhoA signaling. *Molecular Psychiatry*, *24*(9), 1329–1350. https://doi.org/10.1038/s41380-018-0025-5

Rong, X., Han, Q., Lin, X., Kremerskothen, J., & Wang, E. (2019). FRMPD1 activates the Hippo pathway via interaction with WWC3 to suppress the proliferation and invasiveness of lung cancer cells. *Cancer Management and Research*, *Volume 11*, 3395–3410. https://doi.org/10.2147/CMAR.S194512

Sabatini, B. L., Oertner, T. G., & Svoboda, K. (2002). The Life Cycle of Ca2+ Ions in Dendritic Spines. *Neuron*, *33*(3), 439–452. https://doi.org/10.1016/S0896-6273(02)00573-1
Sánchez-Sanz, G., Matallanas, D., Nguyen, L. K., Kholodenko, B. N., Rosta, E., Kolch, W., & Buchete, N.-V. (2016). MST2-RASSF protein–protein interactions through SARAH domains. *Briefings in Bioinformatics*, *17*(4), 593–602. https://doi.org/10.1093/bib/bbv070
Sanphui, P., & Biswas, S. C. (2013). FoxO3a is activated and executes neuron death via Bim in response to β-amyloid. *Cell Death & Disease*, *4*, e625. https://doi.org/10.1038/cddis.2013.148
Schlegelmilch, K., Mohseni, M., Kirak, O., Pruszak, J., Rodriguez, J. R., Zhou, D., Kreger, B. T., Vasioukhin, V., Avruch, J., Brummelkamp, T. R., & Camargo, F. D. (2011). Yap1 Acts Downstream of α-Catenin to Control Epidermal Proliferation. *Cell*, *144*(5), 782–795. https://doi.org/10.1016/j.cell.2011.02.031
Sharma, R., Fedorenko, I., Spence, P. T., Sondak, V. K., Smalley, K. S. M., & Koomen, J. M. (2016). Activity-Based Protein Profiling Shows Heterogeneous Signaling Adaptations to BRAF Inhibition. *Journal of Proteome Research*, *15*(12), 4476–4489. https://doi.org/10.1021/acs.jproteome.6b00613
Shepherd, G. M. (1996). The dendritic spine: A multifunctional integrative unit. *Journal of Neurophysiology*, *75*(6), 2197–2210. https://doi.org/10.1152/jn.1996.75.6.2197
Silvis, M. R., Kreger, B. T., Lien, W.-H., Klezovitch, O., Rudakova, G. M., Camargo, F. D., Lantz, D. M., Seykora, J. T., & Vasioukhin, V. (2011). -Catenin Is a Tumor Suppressor That Controls Cell Accumulation by Regulating the Localization and Activity of the Transcriptional Coactivator Yap1. *Science Signaling*, *4*(174), ra33–ra33. https://doi.org/10.1126/scisignal.2001823
Stark, C. (2006). BioGRID: A general repository for interaction datasets. *Nucleic Acids Research*, *34*(90001), D535–D539. https://doi.org/10.1093/nar/gkj109
Steinberg, S., de Jong, S., Mattheisen, M., Costas, J., Demontis, D., Jamain, S., Pietiläinen, O. P. H., Lin, K., Papiol, S., Huttenlocher, J., Sigurdsson, E., Vassos, E., Giegling, I., Breuer, R., Fraser, G., Walker, N., Melle, I., Djurovic, S., Agartz, I., … Stefansson, K. (2014). Common variant at 16p11.2 conferring risk of psychosis. *Molecular Psychiatry*, *19*(1), 108–114. https://doi.org/10.1038/mp.2012.157
Steinman, K. J., Spence, S. J., Ramocki, M. B., Proud, M. B., Kessler, S. K., Marco, E. J., Green Snyder, L., D'Angelo, D., Chen, Q., Chung, W. K., Sherr, E. H., & on behalf of the Simons VIP Consortium. (2016). 16p11.2 deletion and duplication: Characterizing neurologic phenotypes in a large clinically ascertained cohort. *American Journal of Medical Genetics Part A*, *170*(11), 2943–2955. https://doi.org/10.1002/ajmg.a.37820
Stephan, M., Volkmann, P., & Rossner, M. J. (2019). Assessing behavior and cognition in rodents, nonhuman primates, and humans: Where are the limits of translation? *Dialogues in Clinical Neuroscience*, *21*(3), 249–259. https://doi.org/10.31887/DCNS.2019.21.3/mrossner
Stephenson, J. R., Wang, X., Perfitt, T. L., Parrish, W. P., Shonesy, B. C., Marks, C. R., Mortlock, D. P., Nakagawa, T., Sutcliffe, J. S., & Colbran, R. J. (2017). A Novel Human *CAMK2A* Mutation Disrupts Dendritic Morphology and Synaptic Transmission, and Causes ASD-Related Behaviors. *The Journal of Neuroscience*, *37*(8), 2216–2233. https://doi.org/10.1523/JNEUROSCI.2068-16.2017
Strano, S., Monti, O., Pediconi, N., Baccarini, A., Fontemaggi, G., Lapi, E., Mantovani, F., Damalas, A., Citro, G., Sacchi, A., Del Sal, G., Levrero, M., & Blandino, G. (2005). The Transcriptional Coactivator Yes-Associated Protein Drives p73 Gene-Target Specificity in Response to DNA Damage. *Molecular Cell*, *18*(4), 447–459. https://doi.org/10.1016/j.molcel.2005.04.008
Sukumaran, S. K., Stumpf, M., Salamon, S., Ahmad, I., Bhattacharya, K., Fischer, S., Müller, R., Altmüller, J., Budde, B., Thiele, H., Tariq, M., Malik, N. A., Nürnberg, P., Baig, S. M., Hussain, M. S., & Noegel, A. A. (2017). CDK5RAP2 interaction with components of the Hippo signaling pathway may play a role in primary microcephaly. *Molecular Genetics and Genomics*, *292*(2), 365–383. https://doi.org/10.1007/s00438-016-1277-x
Sun, G., & Irvine, K. D. (2013). Ajuba Family Proteins Link JNK to Hippo Signaling. *Science Signaling*, *6*(292), ra81–ra81. https://doi.org/10.1126/scisignal.2004324
Swistowski, A., Zhang, Q., Orcholski, M. E., Crippen, D., Vitelli, C., Kurakin, A., & Bredesen, D. E. (2009). Novel Mediators of Amyloid Precursor Protein Signaling. *Journal of Neuroscience*, *29*(50), 15703–15712. https://doi.org/10.1523/JNEUROSCI.4351-09.2009
Takumi, Y., Ramírez-León, V., Laake, P., Rinvik, E., & Ottersen, O. P. (1999). Different modes of expression of AMPA and NMDA receptors in hippocampal synapses. *Nature Neuroscience*, *2*(7), 618–624. https://doi.org/10.1038/10172

Tassi, E., Biesova, Z., Di Fiore, P. P., Gutkind, J. S., & Wong, W. T. (1999). Human JIK, a Novel Member of the STE20 Kinase Family That Inhibits JNK and Is Negatively Regulated by Epidermal Growth Factor. *Journal of Biological Chemistry*, *274*(47), 33287–33295. https://doi.org/10.1074/jbc.274.47.33287
Tavares, I. A., Touma, D., Lynham, S., Troakes, C., Schober, M., Causevic, M., Garg, R., Noble, W., Killick, R., Bodi, I., Hanger, D. P., & Morris, J. D. H. (2013). Prostate-derived Sterile 20-like Kinases (PSKs/TAOKs) Phosphorylate Tau Protein and Are Activated in Tangle-bearing Neurons in Alzheimer Disease. *Journal of Biological Chemistry*, *288*(21), 15418–15429. https://doi.org/10.1074/jbc.M112.448183
Thakore, P. I., D'Ippolito, A. M., Song, L., Safi, A., Shivakumar, N. K., Kabadi, A. M., Reddy, T. E., Crawford, G. E., & Gersbach, C. A. (2015). Highly specific epigenome editing by CRISPR-Cas9 repressors for silencing of distal regulatory elements. *Nature Methods*, *12*(12), 1143–1149. https://doi.org/10.1038/nmeth.3630
Toloczko, A., Guo, F., Yuen, H.-F., Wen, Q., Wood, S. A., Ong, Y. S., Chan, P. Y., Shaik, A. A., Gunaratne, J., Dunne, M. J., Hong, W., & Chan, S. W. (2017). Deubiquitinating Enzyme USP9X Suppresses Tumor Growth via LATS Kinase and Core Components of the Hippo Pathway. *Cancer Research*, *77*(18), 4921–4933. https://doi.org/10.1158/0008-5472.CAN-16-3413
Torrini, C., Cubero, R. J., Dirkx, E., Braga, L., Ali, H., Prosdocimo, G., Gutierrez, M. I., Collesi, C., Licastro, D., Zentilin, L., Mano, M., Zacchigna, S., Vendruscolo, M., Marsili, M., Samal, A., & Giacca, M. (2019). Common Regulatory Pathways Mediate Activity of MicroRNAs Inducing Cardiomyocyte Proliferation. *Cell Reports*, *27*(9), 2759-2771.e5. https://doi.org/10.1016/j.celrep.2019.05.005
Tschaharganeh, D. F., Chen, X., Latzko, P., Malz, M., Gaida, M. M., Felix, K., Ladu, S., Singer, S., Pinna, F., Gretz, N., Sticht, C., Tomasi, M. L., Delogu, S., Evert, M., Fan, B., Ribback, S., Jiang, L., Brozzetti, S., Bergmann, F., … Breuhahn, K. (2013). Yes-Associated Protein Up-regulates Jagged-1 and Activates the NOTCH Pathway in Human Hepatocellular Carcinoma. *Gastroenterology*, *144*(7), 1530-1542.e12. https://doi.org/10.1053/j.gastro.2013.02.009
Ultanir, S. K., Yadav, S., Hertz, N. T., Oses-Prieto, J. A., Claxton, S., Burlingame, A. L., Shokat, K. M., Jan, L. Y., & Jan, Y.-N. (2014). MST3 Kinase Phosphorylates TAO1/2 to Enable Myosin Va Function in Promoting Spine Synapse Development. *Neuron*, *84*(5), 968–982. https://doi.org/10.1016/j.neuron.2014.10.025
Varelas, X., Miller, B. W., Sopko, R., Song, S., Gregorieff, A., Fellouse, F. A., Sakuma, R., Pawson, T., Hunziker, W., McNeill, H., Wrana, J. L., & Attisano, L. (2010). The Hippo Pathway Regulates Wnt/β-Catenin Signaling. *Developmental Cell*, *18*(4), 579–591. https://doi.org/10.1016/j.devcel.2010.03.007
Volkmann, P., Stephan, M., Krackow, S., Jensen, N., & Rossner, M. J. (2021). PsyCoP – A Platform for Systematic Semi-Automated Behavioral and Cognitive Profiling Reveals Gene and Environment Dependent Impairments of Tcf4 Transgenic Mice Subjected to Social Defeat. *Frontiers in Behavioral Neuroscience*, *14*, 618180. https://doi.org/10.3389/fnbeh.2020.618180
Wakabayashi, T., Kosaka, J., & Oshika, T. (2005). JNK inhibitory kinase is up-regulated in retinal ganglion cells after axotomy and enhances BimEL expression level in neuronal cells. *Journal of Neurochemistry*, *95*(2), 526–536. https://doi.org/10.1111/j.1471-4159.2005.03389.x
Wang, Z., Liu, P., Zhou, X., Wang, T., Feng, X., Sun, Y.-P., Xiong, Y., Yuan, H.-X., & Guan, K.-L. (2017). Endothelin Promotes Colorectal Tumorigenesis by Activating YAP/TAZ. *Cancer Research*, *77*(9), 2413–2423. https://doi.org/10.1158/0008-5472.CAN-16-3229
Watson, C. T., Tomas, M.-B., Sharp, A. J., & Mefford, H. C. (2014). The Genetics of Microdeletion and Microduplication Syndromes: An Update. *Annual Review of Genomics and Human Genetics*, *15*(1), 215–244. https://doi.org/10.1146/annurev-genom-091212-153408
Wehr, M. C., Hinrichs, W., Brzózka, M. M., Unterbarnscheidt, T., Herholt, A., Wintgens, J. P., Papiol, S., Soto-Bernardini, M. C., Kravchenko, M., Zhang, M., Nave, K., Wichert, S. P., Falkai, P., Zhang, W., Schwab, M. H., & Rossner, M. J. (2017). Spironolactone is an antagonist of NRG 1-ERBB4 signaling and schizophrenia-relevant endophenotypes in mice. *EMBO Molecular Medicine*, *9*(10), 1448–1462. https://doi.org/10.15252/emmm.201707691
Wehr, M. C., Holder, M. V., Gailite, I., Saunders, R. E., Maile, T. M., Ciirdaeva, E., Instrell, R., Jiang, M., Howell, M., Rossner, M. J., & Tapon, N. (2013). Salt-inducible kinases regulate growth through the Hippo Signaling pathway in Drosophila. *Nature Cell Biology*, *15*(1), 61–71. https://doi.org/10.1038/ncb2658
Wehr, M. C., Laage, R., Bolz, U., Fischer, T. M., Grünewald, S., Scheek, S., Bach, A., Nave, K.-A., & Rossner, M. J. (2006). Monitoring regulated protein-protein interactions using split TEV. *Nature Methods*, *3*(12), 985–993. https://doi.org/10.1038/nmeth967

Weiss, L. A., Shen, Y., Korn, J. M., Arking, D. E., Miller, D. T., Fossdal, R., Saemundsen, E., Stefansson, H., Ferreira, M. A. R., Green, T., Platt, O. S., Ruderfer, D. M., Walsh, C. A., Altshuler, D., Chakravarti, A., Tanzi, R. E., Stefansson, K., Santangelo, S. L., Gusella, J. F., … Daly, M. J. (2008). Association between Microdeletion and Microduplication at 16p11.2 and Autism. *New England Journal of Medicine*, *358*(7), 667–675. https://doi.org/10.1056/NEJMoa075974

Wennmann, D. O., Schmitz, J., Wehr, M. C., Krahn, M. P., Koschmal, N., Gromnitza, S., Schulze, U., Weide, T., Chekuri, A., Skryabin, B. V., Gerke, V., Pavenstädt, H., Duning, K., & Kremerskothen, J. (2014). Evolutionary and molecular facts link the WWC protein family to Hippo signaling. *Molecular Biology and Evolution*, *31*(7), 1710–1723. https://doi.org/10.1093/molbev/msu115

Williamson, K. A., Rainger, J., Floyd, J. A. B., Ansari, M., Meynert, A., Aldridge, K. V., Rainger, J. K., Anderson, C. A., Moore, A. T., Hurles, M. E., Clarke, A., van Heyningen, V., Verloes, A., Taylor, M. S., Wilkie, A. O. M., & FitzPatrick, D. R. (2014). Heterozygous Loss-of-Function Mutations in YAP1 Cause Both Isolated and Syndromic Optic Fissure Closure Defects. *The American Journal of Human Genetics*, *94*(2), 295–302. https://doi.org/10.1016/j.ajhg.2014.01.001

Wojtala, R. L., Tavares, I. A., Morton, P. E., Valderrama, F., Thomas, N. S. B., & Morris, J. D. H. (2011). Prostate-derived Sterile 20-like Kinases (PSKs/TAOKs) Are Activated in Mitosis and Contribute to Mitotic Cell Rounding and Spindle Positioning. *Journal of Biological Chemistry*, *286*(34), 30161–30170. https://doi.org/10.1074/jbc.M111.228320

Wu, D., Wu, F., Lin, R., Meng, Y., Wei, W., Sun, Q., & Jia, L. (2020). Impairment of learning and memory induced by perinatal exposure to BPA is associated with ERα-mediated alterations of synaptic plasticity and PKC/ERK/CREB signaling pathway in offspring rats. *Brain Research Bulletin*, *161*, 43–54. https://doi.org/10.1016/j.brainresbull.2020.04.023

Xu, T., Wang, W., Zhang, S., Stewart, R. A., & Yu, W. (1995). Identifying tumor suppressors in genetic mosaics: The Drosophila lats gene encodes a putative protein kinase. *Development (Cambridge, England)*, *121*(4), 1053–1063.

Yadav, S., Oses-Prieto, J. A., Peters, C. J., Zhou, J., Pleasure, S. J., Burlingame, A. L., Jan, L. Y., & Jan, Y.-N. (2017). TAOK2 Kinase Mediates PSD95 Stability and Dendritic Spine Maturation through Septin7 Phosphorylation. *Neuron*, *93*(2), 379–393. https://doi.org/10.1016/j.neuron.2016.12.006

Yan, Z., Kim, E., Datta, D., Lewis, D. A., & Soderling, S. H. (2016). Synaptic Actin Dysregulation, a Convergent Mechanism of Mental Disorders? *The Journal of Neuroscience*, *36*(45), 11411–11417. https://doi.org/10.1523/JNEUROSCI.2360-16.2016

Yang, G., Pan, F., & Gan, W.-B. (2009). Stably maintained dendritic spines are associated with lifelong memories. *Nature*, *462*(7275), 920–924. https://doi.org/10.1038/nature08577

Yao, M., Wang, Y., Zhang, P., Chen, H., Xu, Z., Jiao, J., & Yuan, Z. (2014). BMP2-SMAD Signaling Represses the Proliferation of Embryonic Neural Stem Cells through YAP. *Journal of Neuroscience*, *34*(36), 12039–12048. https://doi.org/10.1523/JNEUROSCI.0486-14.2014

Yasuda, S., Tanaka, H., Sugiura, H., Okamura, K., Sakaguchi, T., Tran, U., Takemiya, T., Mizoguchi, A., Yagita, Y., Sakurai, T., De Robertis, E. M., & Yamagata, K. (2007). Activity-Induced Protocadherin Arcadlin Regulates Dendritic Spine Number by Triggering N-Cadherin Endocytosis via TAO2β and p38 MAP Kinases. *Neuron*, *56*(3), 456–471. https://doi.org/10.1016/j.neuron.2007.08.020

Ye, J., Shi, M., Chen, W., Zhu, F., & Duan, Q. (2020). Research Advances in the Molecular Functions and Relevant Diseases of TAOKs, Novel STE20 Kinase Family Members. *Current Pharmaceutical Design*, *26*(26), 3122–3133. https://doi.org/10.2174/1381612826666200203115458

Yimlamai, D., Christodoulou, C., Galli, G. G., Yanger, K., Pepe-Mooney, B., Gurung, B., Shrestha, K., Cahan, P., Stanger, B. Z., & Camargo, F. D. (2014). Hippo Pathway Activity Influences Liver Cell Fate. *Cell*, *157*(6), 1324–1338. https://doi.org/10.1016/j.cell.2014.03.060

Yin, F., Yu, J., Zheng, Y., Chen, Q., Zhang, N., & Pan, D. (2013). Spatial Organization of Hippo Signaling at the Plasma Membrane Mediated by the Tumor Suppressor Merlin/NF2. *Cell*, *154*(6), 1342–1355. https://doi.org/10.1016/j.cell.2013.08.025

Yip, Z. C., & Heiman, M. G. (2016). Duplication of a Single Neuron in C. elegans Reveals a Pathway for Dendrite Tiling by Mutual Repulsion. *Cell Reports*, *15*(10), 2109–2117. https://doi.org/10.1016/j.celrep.2016.05.003

Yoneda, T., Imaizumi, K., Oono, K., Yui, D., Gomi, F., Katayama, T., & Tohyama, M. (2001). Activation of Caspase-12, an Endoplastic Reticulum (ER) Resident Caspase, through Tumor Necrosis Factor Receptor-

associated Factor 2-dependent Mechanism in Response to the ER Stress. *Journal of Biological Chemistry*, *276*(17), 13935–13940. https://doi.org/10.1074/jbc.M010677200
Yu, F.-X., & Guan, K.-L. (2013). The Hippo pathway: Regulators and regulations. *Genes & Development*, *27*(4), 355–371. https://doi.org/10.1101/gad.210773.112
Yu, F.-X., Zhao, B., & Guan, K.-L. (2015). Hippo Pathway in Organ Size Control, Tissue Homeostasis, and Cancer. *Cell*, *163*(4), 811–828. https://doi.org/10.1016/j.cell.2015.10.044
Yu, F.-X., Zhao, B., Panupinthu, N., Jewell, J. L., Lian, I., Wang, L. H., Zhao, J., Yuan, H., Tumaneng, K., Li, H., Fu, X.-D., Mills, G. B., & Guan, K.-L. (2012). Regulation of the Hippo-YAP Pathway by G-Protein-Coupled Receptor Signaling. *Cell*, *150*(4), 780–791. https://doi.org/10.1016/j.cell.2012.06.037
Yu, J., Zheng, Y., Dong, J., Klusza, S., Deng, W.-M., & Pan, D. (2010). Kibra Functions as a Tumor Suppressor Protein that Regulates Hippo Signaling in Conjunction with Merlin and Expanded. *Developmental Cell*, *18*(2), 288–299. https://doi.org/10.1016/j.devcel.2009.12.012
Yuste, R., & Denk, W. (1995). Dendritic spines as basic functional units of neuronal integration. *Nature*, *375*(6533), 682–684. https://doi.org/10.1038/375682a0
Yustein, J. T., Xia, L., Kahlenburg, J. M., Robinson, D., Templeton, D., & Kung, H.-J. (2003). Comparative studies of a new subfamily of human Ste20-like kinases: Homodimerization, subcellular localization, and selective activation of MKK3 and p38. *Oncogene*, *22*(40), 6129–6141. https://doi.org/10.1038/sj.onc.1206605
Zhang, H., Deo, M., Thompson, R. C., Uhler, M. D., & Turner, D. L. (2012). Negative regulation of Yap during neuronal differentiation. *Developmental Biology*, *361*(1), 103–115. https://doi.org/10.1016/j.ydbio.2011.10.017
Zhang, J., Smolen, G. A., & Haber, D. A. (2008). Negative Regulation of YAP by LATS1 Underscores Evolutionary Conservation of the Drosophila Hippo Pathway. *Cancer Research*, *68*(8), 2789–2794. https://doi.org/10.1158/0008-5472.CAN-07-6205
Zhang, W., Chen, T., Wan, T., He, L., Li, N., Yuan, Z., & Cao, X. (2000). Cloning of DPK, a Novel Dendritic Cell-Derived Protein Kinase Activating the ERK1/ERK2 and JNK/SAPK Pathways. *Biochemical and Biophysical Research Communications*, *274*(3), 872–879. https://doi.org/10.1006/bbrc.2000.3244
Zhang, Z., Tang, Z., Ma, X., Sun, K., Fan, L., Fang, J., Pan, J., Wang, X., An, H., & Zhou, J. (2018). TAOK1 negatively regulates IL-17-mediated signaling and inflammation. *Cellular & Molecular Immunology*, *15*(8), 794–802. https://doi.org/10.1038/cmi.2017.158
Zhao, B., Li, L., & Guan, K.-L. (2010). Hippo signaling at a glance. *Journal of Cell Science*, *123*(Pt 23), 4001–4006. https://doi.org/10.1242/jcs.069070
Zhao, B., Li, L., Lu, Q., Wang, L. H., Liu, C.-Y., Lei, Q., & Guan, K.-L. (2011). Angiomotin is a novel Hippo pathway component that inhibits YAP oncoprotein. *Genes & Development*, *25*(1), 51–63. https://doi.org/10.1101/gad.2000111
Zhao, B., Li, L., Tumaneng, K., Wang, C.-Y., & Guan, K.-L. (2010a). A coordinated phosphorylation by Lats and CK1 regulates YAP stability through SCF(beta-TRCP). *Genes & Development*, *24*(1), 72–85. https://doi.org/10.1101/gad.1843810
Zhao, B., Li, L., Tumaneng, K., Wang, C.-Y., & Guan, K.-L. (2010b). A coordinated phosphorylation by Lats and CK1 regulates YAP stability through SCF(beta-TRCP). *Genes & Development*, *24*(1), 72–85. https://doi.org/10.1101/gad.1843810
Zhao, B., Wei, X., Li, W., Udan, R. S., Yang, Q., Kim, J., Xie, J., Ikenoue, T., Yu, J., Li, L., Zheng, P., Ye, K., Chinnaiyan, A., Halder, G., Lai, Z.-C., & Guan, K.-L. (2007). Inactivation of YAP oncoprotein by the Hippo pathway is involved in cell contact inhibition and tissue growth control. *Genes & Development*, *21*(21), 2747–2761. https://doi.org/10.1101/gad.1602907
Zhao, B., Ye, X., Yu, J., Li, L., Li, W., Li, S., Yu, J., Lin, J. D., Wang, C.-Y., Chinnaiyan, A. M., Lai, Z.-C., & Guan, K.-L. (2008). TEAD mediates YAP-dependent gene induction and growth control. *Genes & Development*, *22*(14), 1962–1971. https://doi.org/10.1101/gad.1664408
Zhou, D., Zhang, Y., Wu, H., Barry, E., Yin, Y., Lawrence, E., Dawson, D., Willis, J. E., Markowitz, S. D., Camargo, F. D., & Avruch, J. (2011). Mst1 and Mst2 protein kinases restrain intestinal stem cell proliferation and colonic tumorigenesis by inhibition of Yes-associated protein (Yap) overabundance. *Proceedings of the National Academy of Sciences*, *108*(49), E1312–E1320. https://doi.org/10.1073/pnas.1110428108
Zhou, Q., Homma, K. J., & Poo, M. (2004). Shrinkage of Dendritic Spines Associated with Long-Term Depression of Hippocampal Synapses. *Neuron*, *44*(5), 749–757. https://doi.org/10.1016/j.neuron.2004.11.011

Zhou, X., Wang, S., Wang, Z., Feng, X., Liu, P., Lv, X.-B., Li, F., Yu, F.-X., Sun, Y., Yuan, H., Zhu, H., Xiong, Y., Lei, Q.-Y., & Guan, K.-L. (2015). Estrogen regulates Hippo signaling via GPER in breast cancer. *Journal of Clinical Investigation*, *125*(5), 2123–2135. https://doi.org/10.1172/JCI79573
Zhou, Y., Kaiser, T., Monteiro, P., Zhang, X., Van der Goes, Marie. S., Wang, D., Barak, B., Zeng, M., Li, C., Lu, C., Wells, M., Amaya, A., Nguyen, S., Lewis, M., Sanjana, N., Zhou, Y., Zhang, M., Zhang, F., Fu, Z., & Feng, G. (2016). Mice with Shank3 Mutations Associated with ASD and Schizophrenia Display Both Shared and Distinct Defects. *Neuron*, *89*(1), 147–162. https://doi.org/10.1016/j.neuron.2015.11.023
Zihni, C., Mitsopoulos, C., Tavares, I. A., Baum, B., Ridley, A. J., & Morris, J. D. H. (2007). Prostate-derived Sterile 20-like Kinase 1-α Induces Apoptosis: JNK- AND CASPASE-DEPENDENT NUCLEAR LOCALIZATION IS A REQUIREMENT FOR MEMBRANE BLEBBING. *Journal of Biological Chemistry*, *282*(9), 6484–6493. https://doi.org/10.1074/jbc.M608336200
Zihni, C., Mitsopoulos, C., Tavares, I. A., Ridley, A. J., & Morris, J. D. H. (2006). Prostate-derived Sterile 20-like Kinase 2 (PSK2) Regulates Apoptotic Morphology via C-Jun N-terminal Kinase and Rho Kinase-1. *Journal of Biological Chemistry*, *281*(11), 7317–7323. https://doi.org/10.1074/jbc.M513769200
Zygulska, A. L., Krzemieniecki, K., & Pierzchalski, P. (2017). Hippo pathway—Brief overview of its relevance in cancer. *Journal of Physiology and Pharmacology: An Official Journal of the Polish Physiological Society*, *68*(3), 311–335.
Alerasool, N., Segal, D., Lee, H., & Taipale, M. (2020). An efficient KRAB domain for CRISPRi applications in human cells. *Nature Methods*, *17*(11), 1093–1096. https://doi.org/10.1038/s41592-020-0966-x
Alexander Herholt. (2016). *Development of a multiplexed RNAi-coupled sensor assay to study neuronal function on the large-scale* [Georg-August-University Göttingen]. PhD Thesis.
Anders, S., Pyl, P. T., & Huber, W. (2015). HTSeq—A Python framework to work with high-throughput sequencing data. *Bioinformatics*, *31*(2), 166–169. https://doi.org/10.1093/bioinformatics/btu638
Araki, Y., Zeng, M., Zhang, M., & Huganir, R. L. (2015). Rapid Dispersion of SynGAP from Synaptic Spines Triggers AMPA Receptor Insertion and Spine Enlargement during LTP. *Neuron*, *85*(1), 173–189. https://doi.org/10.1016/j.neuron.2014.12.023
Bae, S. J., & Luo, X. (2018). Activation mechanisms of the Hippo kinase signaling cascade. *Bioscience Reports*, *38*(4), BSR20171469. https://doi.org/10.1042/BSR20171469
Beattie, R., & Hippenmeyer, S. (2017). Mechanisms of radial glia progenitor cell lineage progression. *FEBS Letters*, *591*(24), 3993–4008. https://doi.org/10.1002/1873-3468.12906
Bian, Y., Teper, Y., Mathews Griner, L. A., Aiken, T. J., Shukla, V., Guha, R., Shinn, P., Xin, H.-W., Pflicke, H., Powers, A. S., Li, D., Jiang, J., Patel, P., Rogers, S. A., Aubé, J., Ferrer, M., Thomas, C. J., & Rudloff, U. (2019). Target Deconvolution of a Multikinase Inhibitor with Antimetastatic Properties Identifies TAOK3 as a Key Contributor to a Cancer Stem Cell–Like Phenotype. *Molecular Cancer Therapeutics*, *18*(11), 2097–2110. https://doi.org/10.1158/1535-7163.MCT-18-1011
Boggiano, J. C., Vanderzalm, P. J., & Fehon, R. G. (2011). Tao-1 Phosphorylates Hippo/MST Kinases to Regulate the Hippo-Salvador-Warts Tumor Suppressor Pathway. *Developmental Cell*, *21*(5), 888–895. https://doi.org/10.1016/j.devcel.2011.08.028
Boopathy, G. T. K., & Hong, W. (2019). Role of Hippo Pathway-YAP/TAZ Signaling in Angiogenesis. *Frontiers in Cell and Developmental Biology*, *7*, 49. https://doi.org/10.3389/fcell.2019.00049
Bray, N. J., & O'Donovan, M. C. (2018). The genetics of neuropsychiatric disorders. *Brain and Neuroscience Advances*, *2*, 239821281879927. https://doi.org/10.1177/2398212818799271
Bristow, G. C., Thomson, D. M., Openshaw, R. L., Mitchell, E. J., Pratt, J. A., Dawson, N., & Morris, B. J. (2020). 16p11 Duplication Disrupts Hippocampal-Orbitofrontal-Amygdala Connectivity, Revealing a Neural Circuit Endophenotype for Schizophrenia. *Cell Reports*, *31*(3), 107536. https://doi.org/10.1016/j.celrep.2020.107536
Calderon de Anda, F., Rosario, A. L., Durak, O., Tran, T., Gräff, J., Meletis, K., Rei, D., Soda, T., Madabhushi, R., Ginty, D. D., Kolodkin, A. L., & Tsai, L.-H. (2012). Autism spectrum disorder susceptibility gene TAOK2 affects basal dendrite formation in the neocortex. *Nature Neuroscience*, *15*(7), 1022–1031. https://doi.org/10.1038/nn.3141
Calderone, A., Castagnoli, L., & Cesareni, G. (2013). mentha: A resource for browsing integrated protein-interaction networks. *Nature Methods*, *10*(8), 690–691. https://doi.org/10.1038/nmeth.2561
Camargo, F. D., Gokhale, S., Johnnidis, J. B., Fu, D., Bell, G. W., Jaenisch, R., & Brummelkamp, T. R. (2007). YAP1 Increases Organ Size and Expands Undifferentiated Progenitor Cells. *Current Biology*, *17*(23), 2054–2060. https://doi.org/10.1016/j.cub.2007.10.039

Can, A., Dao, D. T., Terrillion, C. E., Piantadosi, S. C., Bhat, S., & Gould, T. D. (2011). The Tail Suspension Test. *Journal of Visualized Experiments*, *58*, 3769. https://doi.org/10.3791/3769
Caroni, P., Donato, F., & Muller, D. (2012). Structural plasticity upon learning: Regulation and functions. *Nature Reviews Neuroscience*, *13*(7), 478–490. https://doi.org/10.1038/nrn3258
Chan, E. H. Y., Nousiainen, M., Chalamalasetty, R. B., Schäfer, A., Nigg, E. A., & Silljé, H. H. W. (2005). The Ste20-like kinase Mst2 activates the human large tumor suppressor kinase Lats1. *Oncogene*, *24*(12), 2076–2086. https://doi.org/10.1038/sj.onc.1208445
Chen, Z., & Cobb, M. H. (2001). Regulation of Stress-responsive Mitogen-activated Protein (MAP) Kinase Pathways by TAO2. *Journal of Biological Chemistry*, *276*(19), 16070–16075. https://doi.org/10.1074/jbc.M100681200
Chen, Z., Hutchison, M., & Cobb, M. H. (1999). Isolation of the Protein Kinase TAO2 and Identification of Its Mitogen-activated Protein Kinase/Extracellular Signal-regulated Kinase Kinase Binding Domain. *Journal of Biological Chemistry*, *274*(40), 28803–28807. https://doi.org/10.1074/jbc.274.40.28803
Chen, Z., Raman, M., Chen, L., Lee, S. F., Gilman, A. G., & Cobb, M. H. (2003). TAO (Thousand-and-one Amino Acid) Protein Kinases Mediate Signaling from Carbachol to p38 Mitogen-activated Protein Kinase and Ternary Complex Factors. *Journal of Biological Chemistry*, *278*(25), 22278–22283. https://doi.org/10.1074/jbc.M301173200
Cocas, L. A., Miyoshi, G., Carney, R. S. E., Sousa, V. H., Hirata, T., Jones, K. R., Fishell, G., Huntsman, M. M., & Corbin, J. G. (2009). Emx1-Lineage Progenitors Differentially Contribute to Neural Diversity in the Striatum and Amygdala. *Journal of Neuroscience*, *29*(50), 15933–15946. https://doi.org/10.1523/JNEUROSCI.2525-09.2009
Couzens, A. L., Knight, J. D. R., Kean, M. J., Teo, G., Weiss, A., Dunham, W. H., Lin, Z.-Y., Bagshaw, R. D., Sicheri, F., Pawson, T., Wrana, J. L., Choi, H., & Gingras, A.-C. (2013). Protein Interaction Network of the Mammalian Hippo Pathway Reveals Mechanisms of Kinase-Phosphatase Interactions. *Science Signaling*, *6*(302), rs15–rs15. https://doi.org/10.1126/scisignal.2004712
Das Thakur, M., Feng, Y., Jagannathan, R., Seppa, M. J., Skeath, J. B., & Longmore, G. D. (2010). Ajuba LIM proteins are negative regulators of the Hippo signaling pathway. *Current Biology: CB*, *20*(7), 657–662. https://doi.org/10.1016/j.cub.2010.02.035
de Sena Brandine, G., & Smith, A. D. (2021). Falco: High-speed FastQC emulation for quality control of sequencing data. *F1000Research*, *8*, 1874. https://doi.org/10.12688/f1000research.21142.2
Dembélé, D., & Kastner, P. (2014). Fold change rank ordering statistics: A new method for detecting differentially expressed genes. *BMC Bioinformatics*, *15*(1), 14. https://doi.org/10.1186/1471-2105-15-14
Deng, Y., Pang, A., & Wang, J. H. (2003). Regulation of mammalian STE20-like kinase 2 (MST2) by protein phosphorylation/dephosphorylation and proteolysis. *The Journal of Biological Chemistry*, *278*(14), 11760–11767. https://doi.org/10.1074/jbc.M211085200
Di Cara, F., Maile, T. M., Parsons, B. D., Magico, A., Basu, S., Tapon, N., & King-Jones, K. (2015). The Hippo pathway promotes cell survival in response to chemical stress. *Cell Death & Differentiation*, *22*(9), 1526–1539. https://doi.org/10.1038/cdd.2015.10
Ding, R., Weynans, K., Bossing, T., Barros, C. S., & Berger, C. (2016). The Hippo Signaling pathway maintains quiescence in Drosophila neural stem cells. *Nature Communications*, *7*(1), 10510. https://doi.org/10.1038/ncomms10510
Dulovic-Mahlow, M., Trinh, J., Kandaswamy, K. K., Braathen, G. J., Di Donato, N., Rahikkala, E., Beblo, S., Werber, M., Krajka, V., Busk, Ø. L., Baumann, H., Al-Sannaa, N. A., Hinrichs, F., Affan, R., Navot, N., Al Balwi, M. A., Oprea, G., Holla, Ø. L., Weiss, M. E. R., … Lohmann, K. (2019). De Novo Variants in TAOK1 Cause Neurodevelopmental Disorders. *The American Journal of Human Genetics*, *105*(1), 213–220. https://doi.org/10.1016/j.ajhg.2019.05.005
Dupont, S., Morsut, L., Aragona, M., Enzo, E., Giulitti, S., Cordenonsi, M., Zanconato, F., Le Digabel, J., Forcato, M., Bicciato, S., Elvassore, N., & Piccolo, S. (2011). Role of YAP/TAZ in mechanotransduction. *Nature*, *474*(7350), 179–183. https://doi.org/10.1038/nature10137
Emes, R. D., Pocklington, A. J., Anderson, C. N. G., Bayes, A., Collins, M. O., Vickers, C. A., Croning, M. D. R., Malik, B. R., Choudhary, J. S., Armstrong, J. D., & Grant, S. G. N. (2008). Evolutionary expansion and anatomical specialization of synapse proteome complexity. *Nature Neuroscience*, *11*(7), 799–806. https://doi.org/10.1038/nn.2135

Emoto, K. (2011a). Dendrite remodeling in development and disease: Dendrite remodeling in development and disease. *Development, Growth & Differentiation*, *53*(3), 277–286. https://doi.org/10.1111/j.1440-169X.2010.01242.x
Emoto, K. (2011b). The growing role of the Hippo-NDR kinase Signaling in neuronal development and disease. *Journal of Biochemistry*, *150*(2), 133–141. https://doi.org/10.1093/jb/mvr080
Emoto, K., He, Y., Ye, B., Grueber, W. B., Adler, P. N., Jan, L. Y., & Jan, Y.-N. (2004). Control of Dendritic Branching and Tiling by the Tricornered-Kinase/Furry Signaling Pathway in Drosophila Sensory Neurons. *Cell*, *119*(2), 245–256. https://doi.org/10.1016/j.cell.2004.09.036
Emoto, K., Parrish, J. Z., Jan, L. Y., & Jan, Y.-N. (2006). The tumour suppressor Hippo acts with the NDR kinases in dendritic tiling and maintenance. *Nature*, *443*(7108), 210–213. https://doi.org/10.1038/nature05090
Etherton, M., Foldy, C., Sharma, M., Tabuchi, K., Liu, X., Shamloo, M., Malenka, R. C., & Sudhof, T. C. (2011). Autism-linked neuroligin-3 R451C mutation differentially alters hippocampal and cortical synaptic function. *Proceedings of the National Academy of Sciences*, *108*(33), 13764–13769. https://doi.org/10.1073/pnas.1111093108
Fang, C.-Y., Lai, T.-C., Hsiao, M., & Chang, Y.-C. (2020). The Diverse Roles of TAO Kinases in Health and Diseases. *International Journal of Molecular Sciences*, *21*(20), 7463. https://doi.org/10.3390/ijms21207463
Fong, K.-W., Choi, Y.-K., Rattner, J. B., & Qi, R. Z. (2008). CDK5RAP2 Is a Pericentriolar Protein That Functions in Centrosomal Attachment of the γ-Tubulin Ring Complex. *Molecular Biology of the Cell*, *19*(1), 115–125. https://doi.org/10.1091/mbc.e07-04-0371
Forrest, M. P., Parnell, E., & Penzes, P. (2018). Dendritic structural plasticity and neuropsychiatric disease. *Nature Reviews Neuroscience*, *19*(4), 215–234. https://doi.org/10.1038/nrn.2018.16
Frank, R. A., & Grant, S. G. (2017). Supramolecular organization of NMDA receptors and the postsynaptic density. *Current Opinion in Neurobiology*, *45*, 139–147. https://doi.org/10.1016/j.conb.2017.05.019
Gee, S. T., Milgram, S. L., Kramer, K. L., Conlon, F. L., & Moody, S. A. (2011). Yes-associated protein 65 (YAP) expands neural progenitors and regulates Pax3 expression in the neural plate border zone. *PloS One*, *6*(6), e20309. https://doi.org/10.1371/journal.pone.0020309
Genevet, A., & Tapon, N. (2011). The Hippo pathway and apico–basal cell polarity. *Biochemical Journal*, *436*(2), 213–224. https://doi.org/10.1042/BJ20110217
Genevet, A., Wehr, M. C., Brain, R., Thompson, B. J., & Tapon, N. (2010). Kibra is a regulator of the Salvador/Warts/Hippo signaling network. *Developmental Cell*, *18*(2), 300–308. https://doi.org/10.1016/j.devcel.2009.12.011
Gilbert, L. A., Horlbeck, M. A., Adamson, B., Villalta, J. E., Chen, Y., Whitehead, E. H., Guimaraes, C., Panning, B., Ploegh, H. L., Bassik, M. C., Qi, L. S., Kampmann, M., & Weissman, J. S. (2014). Genome-Scale CRISPR-Mediated Control of Gene Repression and Activation. *Cell*, *159*(3), 647–661. https://doi.org/10.1016/j.cell.2014.09.029
Glantschnig, H., Rodan, G. A., & Reszka, A. A. (2002). Mapping of MST1 kinase sites of phosphorylation. Activation and autophosphorylation. *The Journal of Biological Chemistry*, *277*(45), 42987–42996. https://doi.org/10.1074/jbc.M208538200
Gorski, J. A., Talley, T., Qiu, M., Puelles, L., Rubenstein, J. L. R., & Jones, K. R. (2002). Cortical Excitatory Neurons and Glia, But Not GABAergic Neurons, Are Produced in the Emx1-Expressing Lineage. *The Journal of Neuroscience*, *22*(15), 6309–6314. https://doi.org/10.1523/JNEUROSCI.22-15-06309.2002
Graves, J. D., Draves, K. E., Gotoh, Y., Krebs, E. G., & Clark, E. A. (2001). Both Phosphorylation and Caspase-mediated Cleavage Contribute to Regulation of the Ste20-like Protein Kinase Mst1 during CD95/Fas-induced Apoptosis. *Journal of Biological Chemistry*, *276*(18), 14909–14915. https://doi.org/10.1074/jbc.M010905200
Guo, H., Hong, S., Jin, X.-L., Chen, R.-S., Avasthi, P. P., Tu, Y.-T., Ivanco, T. L., & Li, Y. (2000). Specificity and Efficiency of Cre-Mediated Recombination in Emx1–cre Knock-in Mice. *Biochemical and Biophysical Research Communications*, *273*(2), 661–665. https://doi.org/10.1006/bbrc.2000.2870
Halder, G., & Johnson, R. L. (2011). Hippo signaling: Growth control and beyond. *Development*, *138*(1), 9–22. https://doi.org/10.1242/dev.045500
Hammad, H., Vanderkerken, M., Pouliot, P., Deswarte, K., Toussaint, W., Vergote, K., Vandersarren, L., Janssens, S., Ramou, I., Savvides, S. N., Haigh, J. J., Hendriks, R., Kopf, M., Craessaerts, K., de Strooper, B., Kearney, J. F., Conrad, D. H., & Lambrecht, B. N. (2017). Transitional B cells commit to marginal zone

B cell fate by Taok3-mediated surface expression of ADAM10. *Nature Immunology*, *18*(3), 313–320. https://doi.org/10.1038/ni.3657
Han, D., Byun, S.-H., Park, S., Kim, J., Kim, I., Ha, S., Kwon, M., & Yoon, K. (2015). YAP/TAZ enhance mammalian embryonic neural stem cell characteristics in a Tead-dependent manner. *Biochemical and Biophysical Research Communications*, *458*(1), 110–116. https://doi.org/10.1016/j.bbrc.2015.01.077
Han, D., Lee, S. M., Kwon, M., Noh, H., Lee, J. H., Yoon, Y., Cho, J. Y., & Yoon, K. (2020). YAP Enhances FGF2-Dependent Neural Stem Cell Proliferation by Induction of FGF Receptor Expression. *Stem Cells and Development*, *29*(18), 1240–1246. https://doi.org/10.1089/scd.2019.0281
Han, Y. (2019). Analysis of the role of the Hippo pathway in cancer. *Journal of Translational Medicine*, *17*(1), 116. https://doi.org/10.1186/s12967-019-1869-4
Hansen, C. G., Moroishi, T., & Guan, K.-L. (2015). YAP and TAZ: A nexus for Hippo signaling and beyond. *Trends in Cell Biology*, *25*(9), 499–513. https://doi.org/10.1016/j.tcb.2015.05.002
Hao, Y., Chun, A., Cheung, K., Rashidi, B., & Yang, X. (2008). Tumor Suppressor LATS1 Is a Negative Regulator of Oncogene YAP. *Journal of Biological Chemistry*, *283*(9), 5496–5509. https://doi.org/10.1074/jbc.M709037200
Happé, H., van der Wal, A. M., Leonhard, W. N., Kunnen, S. J., Breuning, M. H., de Heer, E., & Peters, D. J. M. (2011). Altered Hippo Signaling in polycystic kidney disease. *The Journal of Pathology*, *224*(1), 133–142. https://doi.org/10.1002/path.2856
Haque, R. U., & Levey, A. I. (2019). Alzheimer's disease: A clinical perspective and future nonhuman primate research opportunities. *Proceedings of the National Academy of Sciences of the United States of America*. https://doi.org/10.1073/pnas.1912954116
Hauri, S., Wepf, A., Drogen, A., Varjosalo, M., Tapon, N., Aebersold, R., & Gstaiger, M. (2013). Interaction proteome of human Hippo signaling: Modular control of the co-activator YAP1. *Molecular Systems Biology*, *9*(1), 713. https://doi.org/10.1002/msb.201304750
Hergovich, A., Schmitz, D., & Hemmings, B. A. (2006). The human tumour suppressor LATS1 is activated by human MOB1 at the membrane. *Biochemical and Biophysical Research Communications*, *345*(1), 50–58. https://doi.org/10.1016/j.bbrc.2006.03.244
Herholt, A., Brankatschk, B., Kannaiyan, N., Papiol, S., Wichert, S. P., Wehr, M. C., & Rossner, M. J. (2018). Pathway sensor-based functional genomics screening identifies modulators of neuronal activity. *Scientific Reports*, *8*(1), 17597. https://doi.org/10.1038/s41598-018-36008-9
Hiemer, S. E., & Varelas, X. (2013). Stem cell regulation by the Hippo pathway. *Biochimica et Biophysica Acta (BBA) - General Subjects*, *1830*(2), 2323–2334. https://doi.org/10.1016/j.bbagen.2012.07.005
Hirabayashi, S., Nakagawa, K., Sumita, K., Hidaka, S., Kawai, T., Ikeda, M., Kawata, A., Ohno, K., & Hata, Y. (2008). Threonine 74 of MOB1 is a putative key phosphorylation site by MST2 to form the scaffold to activate nuclear Dbf2-related kinase 1. *Oncogene*, *27*(31), 4281–4292. https://doi.org/10.1038/onc.2008.66
Huang, J., Wu, S., Barrera, J., Matthews, K., & Pan, D. (2005). The Hippo signaling pathway coordinately regulates cell proliferation and apoptosis by inactivating Yorkie, the Drosophila Homolog of YAP. *Cell*, *122*(3), 421–434. https://doi.org/10.1016/j.cell.2005.06.007
Hughes, L. J., Park, R., Lee, M. J., Terry, B. K., Lee, D. J., Kim, H., Cho, S.-H., & Kim, S. (2020). Yap/Taz are required for establishing the cerebellar radial glia scaffold and proper foliation. *Developmental Biology*, *457*(1), 150–162. https://doi.org/10.1016/j.ydbio.2019.10.002
Hutchison, M., Berman, K. S., & Cobb, M. H. (1998). Isolation of TAO1, a Protein Kinase That Activates MEKs in Stress-activated Protein Kinase Cascades. *Journal of Biological Chemistry*, *273*(44), 28625–28632. https://doi.org/10.1074/jbc.273.44.28625
Insel, T., Cuthbert, B., Garvey, M., Heinssen, R., Pine, D. S., Quinn, K., Sanislow, C., & Wang, P. (2010). Research Domain Criteria (RDoC): Toward a New Classification Framework for Research on Mental Disorders. *American Journal of Psychiatry*, *167*(7), 748–751. https://doi.org/10.1176/appi.ajp.2010.09091379
Jan, Y.-N., & Jan, L. Y. (2010). Branching out: Mechanisms of dendritic arborization. *Nature Reviews Neuroscience*, *11*(5), 316–328. https://doi.org/10.1038/nrn2836
Jiang, Q., Liu, D., Gong, Y., Wang, Y., Sun, S., Gui, Y., & Song, H. (2009). Yap is required for the development of brain, eyes, and neural crest in zebrafish. *Biochemical and Biophysical Research Communications*, *384*(1), 114–119. https://doi.org/10.1016/j.bbrc.2009.04.070
Kandilya, D., Shyamasundar, S., Singh, D. K., Banik, A., Hande, M. P., Stünkel, W., Chong, Y. S., & Dheen, S. T. (2020). High glucose alters the DNA methylation pattern of neurodevelopment associated genes in

human neural progenitor cells in vitro. *Scientific Reports*, *10*(1), 15676. https://doi.org/10.1038/s41598-020-72485-7
Kapfhamer, D., King, I., Zou, M. E., Lim, J. P., Heberlein, U., & Wolf, F. W. (2012). JNK Pathway Activation Is Controlled by Tao/TAOK3 to Modulate Ethanol Sensitivity. *PLoS ONE*, *7*(12), e50594. https://doi.org/10.1371/journal.pone.0050594
Kapfhamer, D., Taylor, S., Zou, M. E., Lim, J. P., Kharazia, V., & Heberlein, U. (2013). Taok2 controls behavioral response to ethanol in mice: Taok2 and ethanol behaviors. *Genes, Brain and Behavior*, *12*(1), 87–97. https://doi.org/10.1111/j.1601-183X.2012.00834.x
Karl, T., & Arnold, J. C. (2014). Schizophrenia: A consequence of gene-environment interactions? *Frontiers in Behavioral Neuroscience*, *8*. https://doi.org/10.3389/fnbeh.2014.00435
Kim, E., Kang, J. G., Kang, M. J., Park, J. H., Kim, Y. J., Kweon, T. H., Lee, H.-W., Jho, E.-H., Lee, Y.-H., Kim, S.-I., Yi, E. C., Park, H. W., Yang, W. H., & Cho, J. W. (2020). O-GlcNAcylation on LATS2 disrupts the Hippo pathway by inhibiting its activity. *Proceedings of the National Academy of Sciences of the United States of America*, *117*(25), 14259–14269. https://doi.org/10.1073/pnas.1913469117
Kim, H., Kim, M., Im, S.-K., & Fang, S. (2018). Mouse Cre-LoxP system: General principles to determine tissue-specific roles of target genes. *Laboratory Animal Research*, *34*(4), 147–159. https://doi.org/10.5625/lar.2018.34.4.147
Kim, W., Khan, S. K., Liu, Y., Xu, R., Park, O., He, Y., Cha, B., Gao, B., & Yang, Y. (2018). Hepatic Hippo signaling inhibits protumoural microenvironment to suppress hepatocellular carcinoma. *Gut*, *67*(9), 1692–1703. https://doi.org/10.1136/gutjnl-2017-314061
Kim, W., Khan, S. K., & Yang, Y. (2017). Interacting network of Hippo, Wnt/β-catenin and Notch signaling represses liver tumor formation. *BMB Reports*, *50*(1), 1–2. https://doi.org/10.5483/BMBRep.2017.50.1.196
King, I., Tsai, L. T.-Y., Pflanz, R., Voigt, A., Lee, S., Jackle, H., Lu, B., & Heberlein, U. (2011). Drosophila tao Controls Mushroom Body Development and Ethanol-Stimulated Behavior through par-1. *Journal of Neuroscience*, *31*(3), 1139–1148. https://doi.org/10.1523/JNEUROSCI.4416-10.2011
Labbadia, J., & Morimoto, R. I. (2013). Huntington's disease: Underlying molecular mechanisms and emerging concepts. *Trends in Biochemical Sciences*, *38*(8), 378–385. https://doi.org/10.1016/j.tibs.2013.05.003
Lavado, A., Park, J. Y., Paré, J., Finkelstein, D., Pan, H., Xu, B., Fan, Y., Kumar, R. P., Neale, G., Kwak, Y. D., McKinnon, P. J., Johnson, R. L., & Cao, X. (2018). The Hippo Pathway Prevents YAP/TAZ-Driven Hypertranscription and Controls Neural Progenitor Number. *Developmental Cell*, *47*(5), 576-591.e8. https://doi.org/10.1016/j.devcel.2018.09.021
Lee, J.-H., Kim, T.-S., Yang, T.-H., Koo, B.-K., Oh, S.-P., Lee, K.-P., Oh, H.-J., Lee, S.-H., Kong, Y.-Y., Kim, J.-M., & Lim, D.-S. (2008). A crucial role of WW45 in developing epithelial tissues in the mouse. *The EMBO Journal*, *27*(8), 1231–1242. https://doi.org/10.1038/emboj.2008.63
Lee, K.-K., Ohyama, T., Yajima, N., Tsubuki, S., & Yonehara, S. (2001). MST, a Physiological Caspase Substrate, Highly Sensitizes Apoptosis Both Upstream and Downstream of Caspase Activation. *Journal of Biological Chemistry*, *276*(22), 19276–19285. https://doi.org/10.1074/jbc.M005109200
Lei, Q.-Y., Zhang, H., Zhao, B., Zha, Z.-Y., Bai, F., Pei, X.-H., Zhao, S., Xiong, Y., & Guan, K.-L. (2008). TAZ promotes cell proliferation and epithelial-mesenchymal transition and is inhibited by the hippo pathway. *Molecular and Cellular Biology*, *28*(7), 2426–2436. https://doi.org/10.1128/MCB.01874-07
Li, J., Wilkinson, B., Clementel, V. A., Hou, J., O'Dell, T. J., & Coba, M. P. (2016). Long-term potentiation modulates synaptic phosphorylation networks and reshapes the structure of the postsynaptic interactome. *Science Signaling*, *9*(440), rs8–rs8. https://doi.org/10.1126/scisignal.aaf6716
Li, Q., Nirala, N. K., Nie, Y., Chen, H.-J., Ostroff, G., Mao, J., Wang, Q., Xu, L., & Ip, Y. T. (2018). Ingestion of Food Particles Regulates the Mechanosensing Misshapen-Yorkie Pathway in Drosophila Intestinal Growth. *Developmental Cell*, *45*(4), 433-449.e6. https://doi.org/10.1016/j.devcel.2018.04.014
Li, Y., He, C.-L., Li, W.-X., Zhang, R.-X., & Duan, Y. (2020). Transcriptome analysis reveals gender-specific differences in overall metabolic response of male and female patients in lung adenocarcinoma. *PLOS ONE*, *15*(4), e0230796. https://doi.org/10.1371/journal.pone.0230796
Li, Y., Zhou, H., Li, F., Chan, S. W., Lin, Z., Wei, Z., Yang, Z., Guo, F., Lim, C. J., Xing, W., Shen, Y., Hong, W., Long, J., & Zhang, M. (2015). Angiomotin binding-induced activation of Merlin/NF2 in the Hippo pathway. *Cell Research*, *25*(7), 801–817. https://doi.org/10.1038/cr.2015.69

Lin, K. C., Moroishi, T., Meng, Z., Jeong, H.-S., Plouffe, S. W., Sekido, Y., Han, J., Park, H. W., & Guan, K.-L. (2017). Regulation of Hippo pathway transcription factor TEAD by p38 MAPK-induced cytoplasmic translocation. *Nature Cell Biology*, *19*(8), 996–1002. https://doi.org/10.1038/ncb3581
Liu, S., Zhou, L., Yuan, H., Vieira, M., Sanz-Clemente, A., Badger, J. D., Lu, W., Traynelis, S. F., & Roche, K. W. (2017). A Rare Variant Identified Within the GluN2B C-Terminus in a Patient with Autism Affects NMDA Receptor Surface Expression and Spine Density. *The Journal of Neuroscience*, *37*(15), 4093–4102. https://doi.org/10.1523/JNEUROSCI.0827-16.2017
Love, M. I., Huber, W., & Anders, S. (2014). Moderated estimation of fold change and dispersion for RNA-seq data with DESeq2. *Genome Biology*, *15*(12), 550. https://doi.org/10.1186/s13059-014-0550-8
Ma, B., Chen, Y., Chen, L., Cheng, H., Mu, C., Li, J., Gao, R., Zhou, C., Cao, L., Liu, J., Zhu, Y., Chen, Q., & Wu, S. (2015). Hypoxia regulates Hippo Signaling through the SIAH2 ubiquitin E3 ligase. *Nature Cell Biology*, *17*(1), 95–103. https://doi.org/10.1038/ncb3073
Ma, S., Zhang, B., LaFave, L. M., Earl, A. S., Chiang, Z., Hu, Y., Ding, J., Brack, A., Kartha, V. K., Tay, T., Law, T., Lareau, C., Hsu, Y.-C., Regev, A., & Buenrostro, J. D. (2020). Chromatin Potential Identified by Shared Single-Cell Profiling of RNA and Chromatin. *Cell*, *183*(4), 1103-1116.e20. https://doi.org/10.1016/j.cell.2020.09.056
MacKeigan, J. P., Murphy, L. O., & Blenis, J. (2005). Sensitized RNAi screen of human kinases and phosphatases identifies new regulators of apoptosis and chemoresistance. *Nature Cell Biology*, *7*(6), 591–600. https://doi.org/10.1038/ncb1258
Maillard, A. M., Ruef, A., Pizzagalli, F., Migliavacca, E., Hippolyte, L., Adaszewski, S., Dukart, J., Ferrari, C., Conus, P., Männik, K., Zazhytska, M., Siffredi, V., Maeder, P., Kutalik, Z., Kherif, F., Hadjikhani, N., Beckmann, J. S., Reymond, A., Draganski, B., … 16p11.2 European Consortium. (2015). The 16p11.2 locus modulates brain structures common to autism, schizophrenia and obesity. *Molecular Psychiatry*, *20*(1), 140–147. https://doi.org/10.1038/mp.2014.145
Manderfield, L. J., Aghajanian, H., Engleka, K. A., Lim, L. Y., Liu, F., Jain, R., Li, L., Olson, E. N., & Epstein, J. A. (2015). Hippo signaling is required for Notch-dependent smooth muscle differentiation of neural crest. *Development*, *142*(17), 2962–2971. https://doi.org/10.1242/dev.125807
Matallanas, D., Romano, D., Yee, K., Meissl, K., Kucerova, L., Piazzolla, D., Baccarini, M., Vass, J. K., Kolch, W., & O'Neill, E. (2007). RASSF1A Elicits Apoptosis through an MST2 Pathway Directing Proapoptotic Transcription by the p73 Tumor Suppressor Protein. *Molecular Cell*, *27*(6), 962–975. https://doi.org/10.1016/j.molcel.2007.08.008
Matsuzaki, M., Ellis-Davies, G. C. R., Nemoto, T., Miyashita, Y., Iino, M., & Kasai, H. (2001). Dendritic spine geometry is critical for AMPA receptor expression in hippocampal CA1 pyramidal neurons. *Nature Neuroscience*, *4*(11), 1086–1092. https://doi.org/10.1038/nn736
Matsuzaki, M., Honkura, N., Ellis-Davies, G. C. R., & Kasai, H. (2004). Structural basis of long-term potentiation in single dendritic spines. *Nature*, *429*(6993), 761–766. https://doi.org/10.1038/nature02617
McCarthy, S. E., Makarov, V., Kirov, G., Addington, A. M., McClellan, J., Yoon, S., Perkins, D. O., Dickel, D. E., Kusenda, M., Krastoshevsky, O., Krause, V., Kumar, R. A., Grozeva, D., Malhotra, D., Walsh, T., Zackai, E. H., Kaplan, P., Ganesh, J., Krantz, I. D., … Sebat, J. (2009). Microduplications of 16p11.2 are associated with schizophrenia. *Nature Genetics*, *41*(11), 1223–1227. https://doi.org/10.1038/ng.474
Meng, Z., Moroishi, T., & Guan, K.-L. (2016). Mechanisms of Hippo pathway regulation. *Genes & Development*, *30*(1), 1–17. https://doi.org/10.1101/gad.274027.115
Meng, Z., Moroishi, T., Mottier-Pavie, V., Plouffe, S. W., Hansen, C. G., Hong, A. W., Park, H. W., Mo, J.-S., Lu, W., Lu, S., Flores, F., Yu, F.-X., Halder, G., & Guan, K.-L. (2015). MAP4K family kinases act in parallel to MST1/2 to activate LATS1/2 in the Hippo pathway. *Nature Communications*, *6*(1), 8357. https://doi.org/10.1038/ncomms9357
Milewski, R. C., Chi, N. C., Li, J., Brown, C., Lu, M. M., & Epstein, J. A. (2004). Identification of minimal enhancer elements sufficient for Pax3 expression in neural crest and implication of Tead2 as a regulator of Pax3. *Development (Cambridge, England)*, *131*(4), 829–837. https://doi.org/10.1242/dev.00975
Misra, J. R., & Irvine, K. D. (2018). The Hippo Signaling Network and Its Biological Functions. *Annual Review of Genetics*, *52*(1), 65–87. https://doi.org/10.1146/annurev-genet-120417-031621
Mitsopoulos, C., Zihni, C., Garg, R., Ridley, A. J., & Morris, J. D. H. (2003). The Prostate-derived Sterile 20-like Kinase (PSK) Regulates Microtubule Organization and Stability. *Journal of Biological Chemistry*, *278*(20), 18085–18091. https://doi.org/10.1074/jbc.M213064200

Mo, J.-S., Yu, F.-X., Gong, R., Brown, J. H., & Guan, K.-L. (2012). Regulation of the Hippo-YAP pathway by protease-activated receptors (PARs). *Genes & Development*, *26*(19), 2138–2143. https://doi.org/10.1101/gad.197582.112
Moon, S., Yeon Park, S., & Woo Park, H. (2018). Regulation of the Hippo pathway in cancer biology. *Cellular and Molecular Life Sciences: CMLS*, *75*(13), 2303–2319. https://doi.org/10.1007/s00018-018-2804-1
Moore, T. M., Garg, R., Johnson, C., Coptcoat, M. J., Ridley, A. J., & Morris, J. D. H. (2000). PSK, a Novel STE20-like Kinase Derived from Prostatic Carcinoma That Activates the c-Jun N-terminal Kinase Mitogen-activated Protein Kinase Pathway and Regulates Actin Cytoskeletal Organization. *Journal of Biological Chemistry*, *275*(6), 4311–4322. https://doi.org/10.1074/jbc.275.6.4311
Morris, S. E., & Cuthbert, B. N. (2012). Research Domain Criteria: Cognitive systems, neural circuits, and dimensions of behavior. *Dialogues in Clinical Neuroscience*, *14*(1), 29–37.
Moya, I. M., & Halder, G. (2014). Discovering the Hippo pathway protein-protein interactome. *Cell Research*, *24*(2), 137–138. https://doi.org/10.1038/cr.2014.6
Mueller, K. A., Glajch, K. E., Huizenga, M. N., Wilson, R. A., Granucci, E. J., Dios, A. M., Tousley, A. R., Iuliano, M., Weisman, E., LaQuaglia, M. J., DiFiglia, M., Kegel-Gleason, K., Vakili, K., & Sadri-Vakili, G. (2018). Hippo Signaling Pathway Dysregulation in Human Huntington's Disease Brain and Neuronal Stem Cells. *Scientific Reports*, *8*(1), 11355. https://doi.org/10.1038/s41598-018-29319-4
Nishimoto, M., Uranishi, K., Asaka, M. N., Suzuki, A., Mizuno, Y., Hirasaki, M., & Okuda, A. (2019). Transformation of normal cells by aberrant activation of YAP via cMyc with TEAD. *Scientific Reports*, *9*(1), 10933. https://doi.org/10.1038/s41598-019-47301-6
Orchard, S., Ammari, M., Aranda, B., Breuza, L., Briganti, L., Broackes-Carter, F., Campbell, N. H., Chavali, G., Chen, C., del-Toro, N., Duesbury, M., Dumousseau, M., Galeota, E., Hinz, U., Iannuccelli, M., Jagannathan, S., Jimenez, R., Khadake, J., Lagreid, A., … Hermjakob, H. (2014). The MIntAct project—IntAct as a common curation platform for 11 molecular interaction databases. *Nucleic Acids Research*, *42*(D1), D358–D363. https://doi.org/10.1093/nar/gkt1115
Ormonde, J. V. S., Li, Z., Stegen, C., & Madrenas, J. (2018). TAOK3 Regulates Canonical TCR Signaling by Preventing Early SHP-1–Mediated Inactivation of LCK. *The Journal of Immunology*, *201*(11), 3431–3442. https://doi.org/10.4049/jimmunol.1800284
Ouyang, T., Meng, W., Li, M., Hong, T., & Zhang, N. (2020). Recent Advances of the Hippo/YAP Signaling Pathway in Brain Development and Glioma. *Cellular and Molecular Neurobiology*, *40*(4), 495–510. https://doi.org/10.1007/s10571-019-00762-9
Pan, D. (2010). The Hippo Signaling Pathway in Development and Cancer. *Developmental Cell*, *19*(4), 491–505. https://doi.org/10.1016/j.devcel.2010.09.011
Panciera, T., Azzolin, L., Fujimura, A., Di Biagio, D., Frasson, C., Bresolin, S., Soligo, S., Basso, G., Bicciato, S., Rosato, A., Cordenonsi, M., & Piccolo, S. (2016). Induction of Expandable Tissue-Specific Stem/Progenitor Cells through Transient Expression of YAP/TAZ. *Cell Stem Cell*, *19*(6), 725–737. https://doi.org/10.1016/j.stem.2016.08.009
Paramasivam, M., Sarkeshik, A., Yates, J. R., Fernandes, M. J. G., & McCollum, D. (2011). Angiomotin family proteins are novel activators of the LATS2 kinase tumor suppressor. *Molecular Biology of the Cell*, *22*(19), 3725–3733. https://doi.org/10.1091/mbc.e11-04-0300
Pardiñas, A. F., Holmans, P., Pocklington, A. J., Escott-Price, V., Ripke, S., Carrera, N., Legge, S. E., Bishop, S., Cameron, D., Hamshere, M. L., Han, J., Hubbard, L., Lynham, A., Mantripragada, K., Rees, E., MacCabe, J. H., McCarroll, S. A., Baune, B. T., Breen, G., … Walters, J. T. R. (2018). Common schizophrenia alleles are enriched in mutation-intolerant genes and in regions under strong background selection. *Nature Genetics*, *50*(3), 381–389. https://doi.org/10.1038/s41588-018-0059-2
Park, R., Moon, U. Y., Park, J. Y., Hughes, L. J., Johnson, R. L., Cho, S.-H., & Kim, S. (2016). Yap is required for ependymal integrity and is suppressed in LPA-induced hydrocephalus. *Nature Communications*, *7*(1), 10329. https://doi.org/10.1038/ncomms10329
Pearson, G., Robinson, F., Beers Gibson, T., Xu, B., Karandikar, M., Berman, K., & Cobb, M. H. (2001). Mitogen-Activated Protein (MAP) Kinase Pathways: Regulation and Physiological Functions*. *Endocrine Reviews*, *22*(2), 153–183. https://doi.org/10.1210/edrv.22.2.0428
Plouffe, S. W., Meng, Z., Lin, K. C., Lin, B., Hong, A. W., Chun, J. V., & Guan, K.-L. (2016). Characterization of Hippo Pathway Components by Gene Inactivation. *Molecular Cell*, *64*(5), 993–1008. https://doi.org/10.1016/j.molcel.2016.10.034

Poon, C. L. C., Lin, J. I., Zhang, X., & Harvey, K. F. (2011). The Sterile 20-like Kinase Tao-1 Controls Tissue Growth by Regulating the Salvador-Warts-Hippo Pathway. *Developmental Cell*, *21*(5), 896–906. https://doi.org/10.1016/j.devcel.2011.09.012
Praskova, M., Xia, F., & Avruch, J. (2008). MOBKL1A/MOBKL1B phosphorylation by MST1 and MST2 inhibits cell proliferation. *Current Biology: CB*, *18*(5), 311–321. https://doi.org/10.1016/j.cub.2008.02.006
Raman, M., Earnest, S., Zhang, K., Zhao, Y., & Cobb, M. H. (2007). TAO kinases mediate activation of p38 in response to DNA damage. *The EMBO Journal*, *26*(8), 2005–2014. https://doi.org/10.1038/sj.emboj.7601668
Rayon, T., Menchero, S., Nieto, A., Xenopoulos, P., Crespo, M., Cockburn, K., Cañon, S., Sasaki, H., Hadjantonakis, A.-K., de la Pompa, J. L., Rossant, J., & Manzanares, M. (2014). Notch and Hippo Converge on Cdx2 to Specify the Trophectoderm Lineage in the Mouse Blastocyst. *Developmental Cell*, *30*(4), 410–422. https://doi.org/10.1016/j.devcel.2014.06.019
Richter, M., Murtaza, N., Scharrenberg, R., White, S. H., Johanns, O., Walker, S., Yuen, R. K. C., Schwanke, B., Bedürftig, B., Henis, M., Scharf, S., Kraus, V., Dörk, R., Hellmann, J., Lindenmaier, Z., Ellegood, J., Hartung, H., Kwan, V., Sedlacik, J., … Calderon de Anda, F. (2019). Altered TAOK2 activity causes autism-related neurodevelopmental and cognitive abnormalities through RhoA signaling. *Molecular Psychiatry*, *24*(9), 1329–1350. https://doi.org/10.1038/s41380-018-0025-5
Rong, X., Han, Q., Lin, X., Kremerskothen, J., & Wang, E. (2019). FRMPD1 activates the Hippo pathway via interaction with WWC3 to suppress the proliferation and invasiveness of lung cancer cells. *Cancer Management and Research*, *Volume 11*, 3395–3410. https://doi.org/10.2147/CMAR.S194512
Sabatini, B. L., Oertner, T. G., & Svoboda, K. (2002). The Life Cycle of Ca2+ Ions in Dendritic Spines. *Neuron*, *33*(3), 439–452. https://doi.org/10.1016/S0896-6273(02)00573-1
Sánchez-Sanz, G., Matallanas, D., Nguyen, L. K., Kholodenko, B. N., Rosta, E., Kolch, W., & Buchete, N.-V. (2016). MST2-RASSF protein–protein interactions through SARAH domains. *Briefings in Bioinformatics*, *17*(4), 593–602. https://doi.org/10.1093/bib/bbv070
Sanphui, P., & Biswas, S. C. (2013). FoxO3a is activated and executes neuron death via Bim in response to β-amyloid. *Cell Death & Disease*, *4*, e625. https://doi.org/10.1038/cddis.2013.148
Schlegelmilch, K., Mohseni, M., Kirak, O., Pruszak, J., Rodriguez, J. R., Zhou, D., Kreger, B. T., Vasioukhin, V., Avruch, J., Brummelkamp, T. R., & Camargo, F. D. (2011). Yap1 Acts Downstream of α-Catenin to Control Epidermal Proliferation. *Cell*, *144*(5), 782–795. https://doi.org/10.1016/j.cell.2011.02.031
Sharma, R., Fedorenko, I., Spence, P. T., Sondak, V. K., Smalley, K. S. M., & Koomen, J. M. (2016). Activity-Based Protein Profiling Shows Heterogeneous Signaling Adaptations to BRAF Inhibition. *Journal of Proteome Research*, *15*(12), 4476–4489. https://doi.org/10.1021/acs.jproteome.6b00613
Shemesh, O. A., Linghu, C., Piatkevich, K. D., Goodwin, D., Celiker, O. T., Gritton, H. J., Romano, M. F., Gao, R., Yu, C.-C. (Jay), Tseng, H.-A., Bensussen, S., Narayan, S., Yang, C.-T., Freifeld, L., Siciliano, C. A., Gupta, I., Wang, J., Pak, N., Yoon, Y.-G., … Boyden, E. S. (2020). Precision Calcium Imaging of Dense Neural Populations via a Cell-Body-Targeted Calcium Indicator. *Neuron*, *107*(3), 470-486.e11. https://doi.org/10.1016/j.neuron.2020.05.029
Shepherd, G. M. (1996). The dendritic spine: A multifunctional integrative unit. *Journal of Neurophysiology*, *75*(6), 2197–2210. https://doi.org/10.1152/jn.1996.75.6.2197
Silvis, M. R., Kreger, B. T., Lien, W.-H., Klezovitch, O., Rudakova, G. M., Camargo, F. D., Lantz, D. M., Seykora, J. T., & Vasioukhin, V. (2011). -Catenin Is a Tumor Suppressor That Controls Cell Accumulation by Regulating the Localization and Activity of the Transcriptional Coactivator Yap1. *Science Signaling*, *4*(174), ra33–ra33. https://doi.org/10.1126/scisignal.2001823
Stark, C. (2006). BioGRID: A general repository for interaction datasets. *Nucleic Acids Research*, *34*(90001), D535–D539. https://doi.org/10.1093/nar/gkj109
Steinberg, S., de Jong, S., Mattheisen, M., Costas, J., Demontis, D., Jamain, S., Pietiläinen, O. P. H., Lin, K., Papiol, S., Huttenlocher, J., Sigurdsson, E., Vassos, E., Giegling, I., Breuer, R., Fraser, G., Walker, N., Melle, I., Djurovic, S., Agartz, I., … Stefansson, K. (2014). Common variant at 16p11.2 conferring risk of psychosis. *Molecular Psychiatry*, *19*(1), 108–114. https://doi.org/10.1038/mp.2012.157
Steinman, K. J., Spence, S. J., Ramocki, M. B., Proud, M. B., Kessler, S. K., Marco, E. J., Green Snyder, L., D'Angelo, D., Chen, Q., Chung, W. K., Sherr, E. H., & on behalf of the Simons VIP Consortium. (2016). 16p11.2 deletion and duplication: Characterizing neurologic phenotypes in a large clinically ascertained cohort. *American Journal of Medical Genetics Part A*, *170*(11), 2943–2955. https://doi.org/10.1002/ajmg.a.37820

Stephan, M., Volkmann, P., & Rossner, M. J. (2019). Assessing behavior and cognition in rodents, nonhuman primates, and humans: Where are the limits of translation? *Dialogues in Clinical Neuroscience*, *21*(3), 249–259. https://doi.org/10.31887/DCNS.2019.21.3/mrossner
Stephenson, J. R., Wang, X., Perfitt, T. L., Parrish, W. P., Shonesy, B. C., Marks, C. R., Mortlock, D. P., Nakagawa, T., Sutcliffe, J. S., & Colbran, R. J. (2017). A Novel Human *CAMK2A* Mutation Disrupts Dendritic Morphology and Synaptic Transmission, and Causes ASD-Related Behaviors. *The Journal of Neuroscience*, *37*(8), 2216–2233. https://doi.org/10.1523/JNEUROSCI.2068-16.2017
Strano, S., Monti, O., Pediconi, N., Baccarini, A., Fontemaggi, G., Lapi, E., Mantovani, F., Damalas, A., Citro, G., Sacchi, A., Del Sal, G., Levrero, M., & Blandino, G. (2005). The Transcriptional Coactivator Yes-Associated Protein Drives p73 Gene-Target Specificity in Response to DNA Damage. *Molecular Cell*, *18*(4), 447–459. https://doi.org/10.1016/j.molcel.2005.04.008
Sukumaran, S. K., Stumpf, M., Salamon, S., Ahmad, I., Bhattacharya, K., Fischer, S., Müller, R., Altmüller, J., Budde, B., Thiele, H., Tariq, M., Malik, N. A., Nürnberg, P., Baig, S. M., Hussain, M. S., & Noegel, A. A. (2017). CDK5RAP2 interaction with components of the Hippo signaling pathway may play a role in primary microcephaly. *Molecular Genetics and Genomics*, *292*(2), 365–383. https://doi.org/10.1007/s00438-016-1277-x
Sun, G., & Irvine, K. D. (2013). Ajuba Family Proteins Link JNK to Hippo Signaling. *Science Signaling*, *6*(292), ra81–ra81. https://doi.org/10.1126/scisignal.2004324
Swistowski, A., Zhang, Q., Orcholski, M. E., Crippen, D., Vitelli, C., Kurakin, A., & Bredesen, D. E. (2009). Novel Mediators of Amyloid Precursor Protein Signaling. *Journal of Neuroscience*, *29*(50), 15703–15712. https://doi.org/10.1523/JNEUROSCI.4351-09.2009
Takumi, Y., Ramírez-León, V., Laake, P., Rinvik, E., & Ottersen, O. P. (1999). Different modes of expression of AMPA and NMDA receptors in hippocampal synapses. *Nature Neuroscience*, *2*(7), 618–624. https://doi.org/10.1038/10172
Tassi, E., Biesova, Z., Di Fiore, P. P., Gutkind, J. S., & Wong, W. T. (1999). Human JIK, a Novel Member of the STE20 Kinase Family That Inhibits JNK and Is Negatively Regulated by Epidermal Growth Factor. *Journal of Biological Chemistry*, *274*(47), 33287–33295. https://doi.org/10.1074/jbc.274.47.33287
Tavares, I. A., Touma, D., Lynham, S., Troakes, C., Schober, M., Causevic, M., Garg, R., Noble, W., Killick, R., Bodi, I., Hanger, D. P., & Morris, J. D. H. (2013). Prostate-derived Sterile 20-like Kinases (PSKs/TAOKs) Phosphorylate Tau Protein and Are Activated in Tangle-bearing Neurons in Alzheimer Disease. *Journal of Biological Chemistry*, *288*(21), 15418–15429. https://doi.org/10.1074/jbc.M112.448183
Thakore, P. I., D'Ippolito, A. M., Song, L., Safi, A., Shivakumar, N. K., Kabadi, A. M., Reddy, T. E., Crawford, G. E., & Gersbach, C. A. (2015). Highly specific epigenome editing by CRISPR-Cas9 repressors for silencing of distal regulatory elements. *Nature Methods*, *12*(12), 1143–1149. https://doi.org/10.1038/nmeth.3630
Toloczko, A., Guo, F., Yuen, H.-F., Wen, Q., Wood, S. A., Ong, Y. S., Chan, P. Y., Shaik, A. A., Gunaratne, J., Dunne, M. J., Hong, W., & Chan, S. W. (2017). Deubiquitinating Enzyme USP9X Suppresses Tumor Growth via LATS Kinase and Core Components of the Hippo Pathway. *Cancer Research*, *77*(18), 4921–4933. https://doi.org/10.1158/0008-5472.CAN-16-3413
Torrini, C., Cubero, R. J., Dirkx, E., Braga, L., Ali, H., Prosdocimo, G., Gutierrez, M. I., Collesi, C., Licastro, D., Zentilin, L., Mano, M., Zacchigna, S., Vendruscolo, M., Marsili, M., Samal, A., & Giacca, M. (2019). Common Regulatory Pathways Mediate Activity of MicroRNAs Inducing Cardiomyocyte Proliferation. *Cell Reports*, *27*(9), 2759-2771.e5. https://doi.org/10.1016/j.celrep.2019.05.005
Tschaharganeh, D. F., Chen, X., Latzko, P., Malz, M., Gaida, M. M., Felix, K., Ladu, S., Singer, S., Pinna, F., Gretz, N., Sticht, C., Tomasi, M. L., Delogu, S., Evert, M., Fan, B., Ribback, S., Jiang, L., Brozzetti, S., Bergmann, F., … Breuhahn, K. (2013). Yes-Associated Protein Up-regulates Jagged-1 and Activates the NOTCH Pathway in Human Hepatocellular Carcinoma. *Gastroenterology*, *144*(7), 1530-1542.e12. https://doi.org/10.1053/j.gastro.2013.02.009
Ultanir, S. K., Yadav, S., Hertz, N. T., Oses-Prieto, J. A., Claxton, S., Burlingame, A. L., Shokat, K. M., Jan, L. Y., & Jan, Y.-N. (2014). MST3 Kinase Phosphorylates TAO1/2 to Enable Myosin Va Function in Promoting Spine Synapse Development. *Neuron*, *84*(5), 968–982. https://doi.org/10.1016/j.neuron.2014.10.025
Varelas, X., Miller, B. W., Sopko, R., Song, S., Gregorieff, A., Fellouse, F. A., Sakuma, R., Pawson, T., Hunziker, W., McNeill, H., Wrana, J. L., & Attisano, L. (2010). The Hippo Pathway Regulates Wnt/β-Catenin Signaling. *Developmental Cell*, *18*(4), 579–591. https://doi.org/10.1016/j.devcel.2010.03.007

Volkmann, P., Stephan, M., Krackow, S., Jensen, N., & Rossner, M. J. (2021). PsyCoP – A Platform for Systematic Semi-Automated Behavioral and Cognitive Profiling Reveals Gene and Environment Dependent Impairments of Tcf4 Transgenic Mice Subjected to Social Defeat. *Frontiers in Behavioral Neuroscience*, *14*, 618180. https://doi.org/10.3389/fnbeh.2020.618180
Wakabayashi, T., Kosaka, J., & Oshika, T. (2005). JNK inhibitory kinase is up-regulated in retinal ganglion cells after axotomy and enhances BimEL expression level in neuronal cells. *Journal of Neurochemistry*, *95*(2), 526–536. https://doi.org/10.1111/j.1471-4159.2005.03389.x
Wang, Z., Liu, P., Zhou, X., Wang, T., Feng, X., Sun, Y.-P., Xiong, Y., Yuan, H.-X., & Guan, K.-L. (2017). Endothelin Promotes Colorectal Tumorigenesis by Activating YAP/TAZ. *Cancer Research*, *77*(9), 2413–2423. https://doi.org/10.1158/0008-5472.CAN-16-3229
Watson, C. T., Tomas, M.-B., Sharp, A. J., & Mefford, H. C. (2014). The Genetics of Microdeletion and Microduplication Syndromes: An Update. *Annual Review of Genomics and Human Genetics*, *15*(1), 215–244. https://doi.org/10.1146/annurev-genom-091212-153408
Wehr, M. C., Hinrichs, W., Brzózka, M. M., Unterbarnscheidt, T., Herholt, A., Wintgens, J. P., Papiol, S., Soto-Bernardini, M. C., Kravchenko, M., Zhang, M., Nave, K., Wichert, S. P., Falkai, P., Zhang, W., Schwab, M. H., & Rossner, M. J. (2017). Spironolactone is an antagonist of NRG 1-ERBB4 signaling and schizophrenia-relevant endophenotypes in mice. *EMBO Molecular Medicine*, *9*(10), 1448–1462. https://doi.org/10.15252/emmm.201707691
Wehr, M. C., Holder, M. V., Gailite, I., Saunders, R. E., Maile, T. M., Ciirdaeva, E., Instrell, R., Jiang, M., Howell, M., Rossner, M. J., & Tapon, N. (2013). Salt-inducible kinases regulate growth through the Hippo Signaling pathway in Drosophila. *Nature Cell Biology*, *15*(1), 61–71. https://doi.org/10.1038/ncb2658
Wehr, M. C., Laage, R., Bolz, U., Fischer, T. M., Grünewald, S., Scheek, S., Bach, A., Nave, K.-A., & Rossner, M. J. (2006). Monitoring regulated protein-protein interactions using split TEV. *Nature Methods*, *3*(12), 985–993. https://doi.org/10.1038/nmeth967
Weiss, L. A., Shen, Y., Korn, J. M., Arking, D. E., Miller, D. T., Fossdal, R., Saemundsen, E., Stefansson, H., Ferreira, M. A. R., Green, T., Platt, O. S., Ruderfer, D. M., Walsh, C. A., Altshuler, D., Chakravarti, A., Tanzi, R. E., Stefansson, K., Santangelo, S. L., Gusella, J. F., … Daly, M. J. (2008). Association between Microdeletion and Microduplication at 16p11.2 and Autism. *New England Journal of Medicine*, *358*(7), 667–675. https://doi.org/10.1056/NEJMoa075974
Wennmann, D. O., Schmitz, J., Wehr, M. C., Krahn, M. P., Koschmal, N., Gromnitza, S., Schulze, U., Weide, T., Chekuri, A., Skryabin, B. V., Gerke, V., Pavenstädt, H., Duning, K., & Kremerskothen, J. (2014). Evolutionary and molecular facts link the WWC protein family to Hippo signaling. *Molecular Biology and Evolution*, *31*(7), 1710–1723. https://doi.org/10.1093/molbev/msu115
Williamson, K. A., Rainger, J., Floyd, J. A. B., Ansari, M., Meynert, A., Aldridge, K. V., Rainger, J. K., Anderson, C. A., Moore, A. T., Hurles, M. E., Clarke, A., van Heyningen, V., Verloes, A., Taylor, M. S., Wilkie, A. O. M., & FitzPatrick, D. R. (2014). Heterozygous Loss-of-Function Mutations in YAP1 Cause Both Isolated and Syndromic Optic Fissure Closure Defects. *The American Journal of Human Genetics*, *94*(2), 295–302. https://doi.org/10.1016/j.ajhg.2014.01.001
Wintgens, J. P., Rossner, M. J., & Wehr, M. C. (2017). Characterizing Dynamic Protein–Protein Interactions Using the Genetically Encoded Split Biosensor Assay Technique Split TEV. In V. Stein (Ed.), *Synthetic Protein Switches* (Vol. 1596, pp. 219–238). Springer New York. https://doi.org/10.1007/978-1-4939-6940-1_14
Wojtala, R. L., Tavares, I. A., Morton, P. E., Valderrama, F., Thomas, N. S. B., & Morris, J. D. H. (2011). Prostate-derived Sterile 20-like Kinases (PSKs/TAOKs) Are Activated in Mitosis and Contribute to Mitotic Cell Rounding and Spindle Positioning. *Journal of Biological Chemistry*, *286*(34), 30161–30170. https://doi.org/10.1074/jbc.M111.228320
Wu, D., Wu, F., Lin, R., Meng, Y., Wei, W., Sun, Q., & Jia, L. (2020). Impairment of learning and memory induced by perinatal exposure to BPA is associated with ERα-mediated alterations of synaptic plasticity and PKC/ERK/CREB signaling pathway in offspring rats. *Brain Research Bulletin*, *161*, 43–54. https://doi.org/10.1016/j.brainresbull.2020.04.023
Xiong, S., Couzens, A. L., Kean, M. J., Mao, D. Y., Guettler, S., Kurinov, I., Gingras, A.-C., & Sicheri, F. (2017). Regulation of Protein Interactions by Mps One Binder (MOB1) Phosphorylation. *Molecular & Cellular Proteomics*, *16*(6), 1111–1125. https://doi.org/10.1074/mcp.M117.068130

Xu, T., Wang, W., Zhang, S., Stewart, R. A., & Yu, W. (1995). Identifying tumor suppressors in genetic mosaics: The Drosophila lats gene encodes a putative protein kinase. *Development (Cambridge, England)*, *121*(4), 1053–1063.
Yadav, S., Oses-Prieto, J. A., Peters, C. J., Zhou, J., Pleasure, S. J., Burlingame, A. L., Jan, L. Y., & Jan, Y.-N. (2017). TAOK2 Kinase Mediates PSD95 Stability and Dendritic Spine Maturation through Septin7 Phosphorylation. *Neuron*, *93*(2), 379–393. https://doi.org/10.1016/j.neuron.2016.12.006
Yan, Z., Kim, E., Datta, D., Lewis, D. A., & Soderling, S. H. (2016). Synaptic Actin Dysregulation, a Convergent Mechanism of Mental Disorders? *The Journal of Neuroscience*, *36*(45), 11411–11417. https://doi.org/10.1523/JNEUROSCI.2360-16.2016
Yang, G., Pan, F., & Gan, W.-B. (2009). Stably maintained dendritic spines are associated with lifelong memories. *Nature*, *462*(7275), 920–924. https://doi.org/10.1038/nature08577
Yao, M., Wang, Y., Zhang, P., Chen, H., Xu, Z., Jiao, J., & Yuan, Z. (2014). BMP2-SMAD Signaling Represses the Proliferation of Embryonic Neural Stem Cells through YAP. *Journal of Neuroscience*, *34*(36), 12039–12048. https://doi.org/10.1523/JNEUROSCI.0486-14.2014
Yasuda, S., Tanaka, H., Sugiura, H., Okamura, K., Sakaguchi, T., Tran, U., Takemiya, T., Mizoguchi, A., Yagita, Y., Sakurai, T., De Robertis, E. M., & Yamagata, K. (2007). Activity-Induced Protocadherin Arcadlin Regulates Dendritic Spine Number by Triggering N-Cadherin Endocytosis via TAO2β and p38 MAP Kinases. *Neuron*, *56*(3), 456–471. https://doi.org/10.1016/j.neuron.2007.08.020
Ye, J., Shi, M., Chen, W., Zhu, F., & Duan, Q. (2020). Research Advances in the Molecular Functions and Relevant Diseases of TAOKs, Novel STE20 Kinase Family Members. *Current Pharmaceutical Design*, *26*(26), 3122–3133. https://doi.org/10.2174/1381612826666200203115458
Yimlamai, D., Christodoulou, C., Galli, G. G., Yanger, K., Pepe-Mooney, B., Gurung, B., Shrestha, K., Cahan, P., Stanger, B. Z., & Camargo, F. D. (2014). Hippo Pathway Activity Influences Liver Cell Fate. *Cell*, *157*(6), 1324–1338. https://doi.org/10.1016/j.cell.2014.03.060
Yin, F., Yu, J., Zheng, Y., Chen, Q., Zhang, N., & Pan, D. (2013). Spatial Organization of Hippo Signaling at the Plasma Membrane Mediated by the Tumor Suppressor Merlin/NF2. *Cell*, *154*(6), 1342–1355. https://doi.org/10.1016/j.cell.2013.08.025
Yip, Z. C., & Heiman, M. G. (2016). Duplication of a Single Neuron in C. elegans Reveals a Pathway for Dendrite Tiling by Mutual Repulsion. *Cell Reports*, *15*(10), 2109–2117. https://doi.org/10.1016/j.celrep.2016.05.003
Yoneda, T., Imaizumi, K., Oono, K., Yui, D., Gomi, F., Katayama, T., & Tohyama, M. (2001). Activation of Caspase-12, an Endoplastic Reticulum (ER) Resident Caspase, through Tumor Necrosis Factor Receptor-associated Factor 2-dependent Mechanism in Response to the ER Stress. *Journal of Biological Chemistry*, *276*(17), 13935–13940. https://doi.org/10.1074/jbc.M010677200
Yu, F.-X., & Guan, K.-L. (2013). The Hippo pathway: Regulators and regulations. *Genes & Development*, *27*(4), 355–371. https://doi.org/10.1101/gad.210773.112
Yu, F.-X., Zhao, B., & Guan, K.-L. (2015). Hippo Pathway in Organ Size Control, Tissue Homeostasis, and Cancer. *Cell*, *163*(4), 811–828. https://doi.org/10.1016/j.cell.2015.10.044
Yu, F.-X., Zhao, B., Panupinthu, N., Jewell, J. L., Lian, I., Wang, L. H., Zhao, J., Yuan, H., Tumaneng, K., Li, H., Fu, X.-D., Mills, G. B., & Guan, K.-L. (2012). Regulation of the Hippo-YAP Pathway by G-Protein-Coupled Receptor Signaling. *Cell*, *150*(4), 780–791. https://doi.org/10.1016/j.cell.2012.06.037
Yu, J., Zheng, Y., Dong, J., Klusza, S., Deng, W.-M., & Pan, D. (2010). Kibra Functions as a Tumor Suppressor Protein that Regulates Hippo Signaling in Conjunction with Merlin and Expanded. *Developmental Cell*, *18*(2), 288–299. https://doi.org/10.1016/j.devcel.2009.12.012
Yuste, R., & Denk, W. (1995). Dendritic spines as basic functional units of neuronal integration. *Nature*, *375*(6533), 682–684. https://doi.org/10.1038/375682a0
Yustein, J. T., Xia, L., Kahlenburg, J. M., Robinson, D., Templeton, D., & Kung, H.-J. (2003). Comparative studies of a new subfamily of human Ste20-like kinases: Homodimerization, subcellular localization, and selective activation of MKK3 and p38. *Oncogene*, *22*(40), 6129–6141. https://doi.org/10.1038/sj.onc.1206605
Zhang, H., Deo, M., Thompson, R. C., Uhler, M. D., & Turner, D. L. (2012). Negative regulation of Yap during neuronal differentiation. *Developmental Biology*, *361*(1), 103–115. https://doi.org/10.1016/j.ydbio.2011.10.017

Zhang, J., Smolen, G. A., & Haber, D. A. (2008). Negative Regulation of YAP by LATS1 Underscores Evolutionary Conservation of the Drosophila Hippo Pathway. *Cancer Research*, *68*(8), 2789–2794. https://doi.org/10.1158/0008-5472.CAN-07-6205
Zhang, W., Chen, T., Wan, T., He, L., Li, N., Yuan, Z., & Cao, X. (2000). Cloning of DPK, a Novel Dendritic Cell-Derived Protein Kinase Activating the ERK1/ERK2 and JNK/SAPK Pathways. *Biochemical and Biophysical Research Communications*, *274*(3), 872–879. https://doi.org/10.1006/bbrc.2000.3244
Zhang, Z., Tang, Z., Ma, X., Sun, K., Fan, L., Fang, J., Pan, J., Wang, X., An, H., & Zhou, J. (2018). TAOK1 negatively regulates IL-17-mediated signaling and inflammation. *Cellular & Molecular Immunology*, *15*(8), 794–802. https://doi.org/10.1038/cmi.2017.158
Zhao, B., Li, L., & Guan, K.-L. (2010). Hippo signaling at a glance. *Journal of Cell Science*, *123*(Pt 23), 4001–4006. https://doi.org/10.1242/jcs.069070
Zhao, B., Li, L., Lu, Q., Wang, L. H., Liu, C.-Y., Lei, Q., & Guan, K.-L. (2011). Angiomotin is a novel Hippo pathway component that inhibits YAP oncoprotein. *Genes & Development*, *25*(1), 51–63. https://doi.org/10.1101/gad.2000111
Zhao, B., Li, L., Tumaneng, K., Wang, C.-Y., & Guan, K.-L. (2010a). A coordinated phosphorylation by Lats and CK1 regulates YAP stability through SCF(beta-TRCP). *Genes & Development*, *24*(1), 72–85. https://doi.org/10.1101/gad.1843810
Zhao, B., Li, L., Tumaneng, K., Wang, C.-Y., & Guan, K.-L. (2010b). A coordinated phosphorylation by Lats and CK1 regulates YAP stability through SCF(beta-TRCP). *Genes & Development*, *24*(1), 72–85. https://doi.org/10.1101/gad.1843810
Zhao, B., Wei, X., Li, W., Udan, R. S., Yang, Q., Kim, J., Xie, J., Ikenoue, T., Yu, J., Li, L., Zheng, P., Ye, K., Chinnaiyan, A., Halder, G., Lai, Z.-C., & Guan, K.-L. (2007). Inactivation of YAP oncoprotein by the Hippo pathway is involved in cell contact inhibition and tissue growth control. *Genes & Development*, *21*(21), 2747–2761. https://doi.org/10.1101/gad.1602907
Zhao, B., Ye, X., Yu, J., Li, L., Li, W., Li, S., Yu, J., Lin, J. D., Wang, C.-Y., Chinnaiyan, A. M., Lai, Z.-C., & Guan, K.-L. (2008). TEAD mediates YAP-dependent gene induction and growth control. *Genes & Development*, *22*(14), 1962–1971. https://doi.org/10.1101/gad.1664408
Zhou, D., Zhang, Y., Wu, H., Barry, E., Yin, Y., Lawrence, E., Dawson, D., Willis, J. E., Markowitz, S. D., Camargo, F. D., & Avruch, J. (2011). Mst1 and Mst2 protein kinases restrain intestinal stem cell proliferation and colonic tumorigenesis by inhibition of Yes-associated protein (Yap) overabundance. *Proceedings of the National Academy of Sciences*, *108*(49), E1312–E1320. https://doi.org/10.1073/pnas.1110428108
Zhou, Q., Homma, K. J., & Poo, M. (2004). Shrinkage of Dendritic Spines Associated with Long-Term Depression of Hippocampal Synapses. *Neuron*, *44*(5), 749–757. https://doi.org/10.1016/j.neuron.2004.11.011
Zhou, X., Wang, S., Wang, Z., Feng, X., Liu, P., Lv, X.-B., Li, F., Yu, F.-X., Sun, Y., Yuan, H., Zhu, H., Xiong, Y., Lei, Q.-Y., & Guan, K.-L. (2015). Estrogen regulates Hippo signaling via GPER in breast cancer. *Journal of Clinical Investigation*, *125*(5), 2123–2135. https://doi.org/10.1172/JCI79573
Zhou, Y., Kaiser, T., Monteiro, P., Zhang, X., Van der Goes, Marie. S., Wang, D., Barak, B., Zeng, M., Li, C., Lu, C., Wells, M., Amaya, A., Nguyen, S., Lewis, M., Sanjana, N., Zhou, Y., Zhang, M., Zhang, F., Fu, Z., & Feng, G. (2016). Mice with Shank3 Mutations Associated with ASD and Schizophrenia Display Both Shared and Distinct Defects. *Neuron*, *89*(1), 147–162. https://doi.org/10.1016/j.neuron.2015.11.023
Zihni, C., Mitsopoulos, C., Tavares, I. A., Baum, B., Ridley, A. J., & Morris, J. D. H. (2007). Prostate-derived Sterile 20-like Kinase 1-α Induces Apoptosis: JNK- AND CASPASE-DEPENDENT NUCLEAR LOCALIZATION IS A REQUIREMENT FOR MEMBRANE BLEBBING. *Journal of Biological Chemistry*, *282*(9), 6484–6493. https://doi.org/10.1074/jbc.M608336200
Zihni, C., Mitsopoulos, C., Tavares, I. A., Ridley, A. J., & Morris, J. D. H. (2006). Prostate-derived Sterile 20-like Kinase 2 (PSK2) Regulates Apoptotic Morphology via C-Jun N-terminal Kinase and Rho Kinase-1. *Journal of Biological Chemistry*, *281*(11), 7317–7323. https://doi.org/10.1074/jbc.M513769200
Zygulska, A. L., Krzemieniecki, K., & Pierzchalski, P. (2017). Hippo pathway—Brief overview of its relevance in cancer. *Journal of Physiology and Pharmacology: An Official Journal of the Polish Physiological Society*, *68*(3), 311–335.

Appendix A: Supplementary Tables

Table S1: Oligos for Gateway-based BP cloning of ORF

No	Component	Oligo se (incl. ACCATG) for BP cloning into pDONR-Zeo	Oligo as (no stop codon) for BP cloning into pDONR-Zeo
1	YAP1	GGGGACAAGTTTGTACAAAAAAGCAGGCTCTACCATGGATCCCGGGCAGCAGCC	GGGGACCACTTTGTACAAGAAAGCTGGGTCTAACCATGTAAGAAAGCTTTCTTTATCTAGCTTGG
2	LATS1	GGGGACAAGTTTGTACAAAAAAGCAGGCTCCACCATGAAGAGGAGTGAAAAGCCAGAAGG	GGGGACCACTTTGTACAAGAAAGCTGGGTCAACATATACTAGATCGCGATTTTTAATCTCTGAG
3	LATS2	GGGGACAAGTTTGTACAAAAAAGCAGGCTCTACCATGAGGCCAAAGACTTTTCCTGCCAC	GGGGACCACTTTGTACAAGAAAGCTGGGTCCACGTACACAGGCTGGCAGCC
4	STK4	GGGGACAAGTTTGTACAAAAAAGCAGGCTCTACCATGGAGACGGTACAGCTGAGGAAC	GGGGACCACTTTGTACAAGAAAGCTGGGTCGAAGTTTTGTTGCCGTCTCTTCTTAGCC
5	STK3	GGGGACAAGTTTGTACAAAAAAGCAGGCTCTACCATGGAGCAGCCGCCGGCG	GGGGACCACTTTGTACAAGAAAGCTGGGTCAAAGTTTTGCTGCCTTCTTTTCTTTGCATCC
6	SAV1	GGGGACAAGTTTGTACAAAAAAGCAGGCTCTACCATGCTGTCCCGAAAGAAAACCAAAAACGAAG	GGGGACCACTTTGTACAAGAAAGCTGGGTCAAAATTTTTTCCATGTTGTTGGGCATACCACTG
7	MOB1A	GGGGACAAGTTTGTACAAAAAAGCAGGCTCCACCATGAGCTTCCTCTTCAGCAGCCG	GGGGACCACTTTGTACAAGAAAGCTGGGTCTCTGTCTTTTGATCCAAGTTTCTCTATTAATTCTTG
8	RASSF1	GGGGACAAGTTTGTACAAAAAAGCAGGCTCTACCATGTCGGGGGAGCCTGAGCTC	GGGGACCACTTTGTACAAGAAAGCTGGGTCCCCAAGGGGGCAGGCGTG
9	RASSF2	GGGGACAAGTTTGTACAAAAAAGCAGGCTCTACCATGGACTACAGCCACCAAACGTCC	GGGGACCACTTTGTACAAGAAAGCTGGGTCGATTGTTGCTGGGGTCTCGGCTATC
10	RASSF6	GGGGACAAGTTTGTACAAAAAAGCAGGCTCTACCATGACTATGATGGCTCACCAGTACCC	GGGGACCACTTTGTACAAGAAAGCTGGGTCAACTGTTGTCTCTGTTTTTATTACTAGTTTATTTTGAAGAC
11	NF2	GGGGACAAGTTTGTACAAAAAAGCAGGCTCTACCATGGCCGGGGCCATCGCTTC	GGGGACCACTTTGTACAAGAAAGCTGGGTCGAGCTCTTCAAAGAAGGCCACTCG
12	WWC1	GGGGACAAGTTTGTACAAAAAAGCAGGCTCTACCATGCCCCGGCCGGAGCTG	GGGGACCACTTTGTACAAGAAAGCTGGGTCGACGTCATCTGCAGAGAGAGCTG
13	WWC2	GGGGACAAGTTTGTACAAAAAAGCAGGCTCCACCATGCCTAGGAGGGCCGGGAG	GGGGACCACTTTGTACAAGAAAGCTGGGTCCACATCATCAGCTGGCAGGGATG
14	WWC3	GGGGACAAGTTTGTACAAAAAAGCAGGCTCCACCATGCCTTGGCTGAGCGGCG	GGGGACCACTTTGTACAAGAAAGCTGGGTCGACGTCGTCGGCTGGGAGAG
15	FRMD6	GGGGACAAGTTTGTACAAAAAAGCAGGCTCTACCATGAACAAATTGAATTTTCATAACAACAGAGTCATGCAAG	GGGGACCACTTTGTACAAGAAAGCTGGGTCCACAACAAACTCTGGAACTTCATCATGAG
16	AMOT	GGGGACAAGTTTGTACAAAAAAGCAGGCTCCACCATGAGAAATTCTGAAGAACAGCCAAGTGG	GGGGACCACTTTGTACAAGAAAGCTGGGTCGATGAGATATTCCACCATCTCTGCATC

17	AMOTL1	GGGGACAAGTTTGTACAAAAAAGCAGGCTCCACCATGTGGAGGGCAAAGTTGCGCC	GGGGACCACTTTGTACAAGAAAGCTGGGTCGATGAGGACTTCCATCATCTCTCCATC
18	AMOTL2	GGGGACAAGTTTGTACAAAAAAGCAGGCTCCACCATGAGGACACTGGAAGACTCCTCG	GGGGACCACTTTGTACAAGAAAGCTGGGTCGATCAGTATCTCCACCATGTCTGAC
19	PTPN14	Plasmid ID, HsCD00379266	
20	AJUBA	GGGGACAAGTTTGTACAAAAAAGCAGGCTCCACCATGGAGCGGTTAGGAGAGAAAGCC	GGGGACCACTTTGTACAAGAAAGCTGGGTCGATATAGTTGGCAGGGGGTTGTCG
21	WTIP	GGGGACAAGTTTGTACAAAAAAGCAGGCTCCACCATGCAGCGCTCCAGGGCG	GGGGACCACTTTGTACAAGAAAGCTGGGTCGAGCTCAGTGACGTGCACAGTG
22	TAOK1	GGGGACAAGTTTGTACAAAAAAGCAGGCTCCACCATGCCATCAACTAACAGAGCAGGC	GGGGACCACTTTGTACAAGAAAGCTGGGTCTGTATAAGACATGTGTGACCCATTGG
23	TAOK2	GGGGACAAGTTTGTACAAAAAAGCAGGCTCCACCATGCCAGCTGGGGGCCGG	GGGGACCACTTTGTACAAGAAAGCTGGGTCCCTCCAGGGGGGCAGGG
24	TAOK3	GGGGACAAGTTTGTACAAAAAAGCAGGCTCCACCATGCGTAAAGGGGTGCTGAAGGAC	GGGGACCACTTTGTACAAGAAAGCTGGGTCTCTGTAGTCCTCCTTAGGAAAATCTAATGTAAC
25	PARD3	GGGGACAAGTTTGTACAAAAAAGCAGGCTCCACCATGAAAGTGACCGTGTGCTTCGGAC	GGGGACCACTTTGTACAAGAAAGCTGGGTCGGAATAGAAGGGCCTCCCTTTCTC
26	PARD6A	GGGGACAAGTTTGTACAAAAAAGCAGGCTCCACCATGGCCCGGCCGCAGAGG	GGGGACCACTTTGTACAAGAAAGCTGGGTCGAGGCTGAAGCCACTACCATCTC
27	PRKCZ	GGGGACAAGTTTGTACAAAAAAGCAGGCTCTACCATGCCCAGCAGGACCGGCC	GGGGACCACTTTGTACAAGAAAGCTGGGTCCACCGACTCCTCGGTGGACAG
28	ERBB4	GGGGACAAGTTTGTACAAAAAAGCAGGCTCTACCATGAAGCCGGCGACAGGACTTTGG	GGGGACCACTTTGTACAAGAAAGCTGGGTCCACCACAGTATTCCGGTGTCTGTAAG
29	R1-noSARAH	GGGGACAAGTTTGTACAAAAAAGCAGGCTCTACCATGTCGGGGGAGCCTGAGCTC	GGGGACCACTTTGTACAAGAAAGCTGGGTCCCCAGAGTCATTTTCCTTCAGGACAAAG

Table S2: Screening data (fold change values and log2-transformed values for all bait-prey interactions measured)

PPI No	Bait (HGNC)	Prey (HGNC)	Fold change sTEV	Fold change (log2) sTEV
1	LATS1	YAP1	4.94	2.31
2	LATS1	LATS1	1.84	0.88
3	LATS1	LATS2	1.79	0.84
4	LATS1	STK4	2.97	1.57
5	LATS1	STK3	2.83	1.50
6	LATS1	SAV1	1.14	0.18
7	LATS1	MOB1A	15.09	3.92
8	LATS1	RASSF1	1.04	0.05

9	LATS1	RASSF2	2.10	1.07
10	LATS1	RASSF6	1.55	0.63
11	LATS1	NF2	3.36	1.75
12	LATS1	WWC1	2.02	1.01
13	LATS1	WWC2	1.62	0.69
14	LATS1	WWC3	1.56	0.65
15	LATS1	FRMD6	1.82	0.86
16	LATS1	AMOT	3.69	1.88
17	LATS1	AMOTL1	1.29	0.36
18	LATS1	AMOTL2	1.94	0.95
19	LATS1	PTPN14	1.13	0.17
20	LATS1	AJUBA	2.06	1.04
21	LATS1	WTIP	2.65	1.40
22	LATS1	TAOK1	5.34	2.42
23	LATS1	TAOK2	1.66	0.73
24	LATS1	TAOK3	1.78	0.84
25	LATS1	PARD3	1.00	0.00
26	LATS1	PARD6A	1.00	0.00
27	LATS1	PRKCZ	1.05	0.07
28	LATS1	ERBB4	1.00	0.00
29	LATS2	YAP1	8.46	3.08
30	LATS2	LATS1	1.96	0.97
31	LATS2	LATS2	4.32	2.11
32	LATS2	STK4	7.34	2.88
33	LATS2	STK3	2.14	1.10
34	LATS2	SAV1	1.80	0.85
35	LATS2	MOB1A	41.29	5.37
36	LATS2	RASSF1	1.38	0.46
37	LATS2	RASSF2	2.48	1.31
38	LATS2	RASSF6	1.53	0.62
39	LATS2	NF2	7.91	2.98
40	LATS2	WWC1	10.90	3.45
41	LATS2	WWC2	4.15	2.05
42	LATS2	WWC3	4.22	2.08
43	LATS2	FRMD6	1.24	0.32
44	LATS2	AMOT	5.22	2.38
45	LATS2	AMOTL1	3.73	1.90
46	LATS2	AMOTL2	6.05	2.60

47	LATS2	PTPN14	7.17	2.84
48	LATS2	AJUBA	5.93	2.57
49	LATS2	WTIP	11.30	3.50
50	LATS2	TAOK1	1.85	0.89
51	LATS2	TAOK2	2.13	1.09
52	LATS2	TAOK3	3.94	1.98
53	LATS2	PARD3	1.00	0.00
54	LATS2	PARD6A	1.36	0.44
55	LATS2	PRKCZ	1.00	0.00
56	LATS2	ERBB4	1.00	0.00
57	STK3	YAP1	2.66	1.41
58	STK3	LATS1	4.49	2.17
59	STK3	LATS2	3.33	1.74
60	STK3	STK4	4.86	2.28
61	STK3	STK3	4.97	2.31
62	STK3	SAV1	4.97	2.31
63	STK3	MOB1A	2.92	1.54
64	STK3	RASSF1	7.13	2.83
65	STK3	RASSF2	5.74	2.52
66	STK3	RASSF6	5.75	2.52
67	STK3	NF2	1.35	0.44
68	STK3	WWC1	2.53	1.34
69	STK3	WWC2	2.28	1.19
70	STK3	WWC3	1.66	0.73
71	STK3	FRMD6	1.81	0.85
72	STK3	AMOT	4.87	2.29
73	STK3	AMOTL1	2.30	1.20
74	STK3	AMOTL2	2.61	1.39
75	STK3	PTPN14	2.63	1.40
76	STK3	AJUBA	1.91	0.94
77	STK3	WTIP	1.83	0.87
78	STK3	TAOK1	1.00	0.00
79	STK3	TAOK2	1.00	0.00
80	STK3	TAOK3	2.49	1.32
81	STK3	PARD3	1.00	0.00
82	STK3	PARD6A	1.00	0.00
83	STK3	PRKCZ	2.36	1.24
84	STK3	ERBB4	3.28	1.71

85	SAV1	YAP1	1.40	0.48
86	SAV1	LATS1	1.00	0.00
87	SAV1	LATS2	1.00	0.00
88	SAV1	STK4	15.59	3.96
89	SAV1	STK3	14.60	3.87
90	SAV1	SAV1	1.29	0.37
91	SAV1	MOB1A	1.64	0.71
92	SAV1	RASSF1	1.00	0.00
93	SAV1	RASSF2	1.16	0.22
94	SAV1	RASSF6	1.33	0.42
95	SAV1	NF2	1.00	0.00
96	SAV1	WWC1	1.00	0.00
97	SAV1	WWC2	1.08	0.11
98	SAV1	WWC3	1.54	0.62
99	SAV1	FRMD6	1.37	0.46
100	SAV1	AMOT	2.25	1.17
101	SAV1	AMOTL1	1.58	0.66
102	SAV1	AMOTL2	1.19	0.25
103	SAV1	PTPN14	1.48	0.57
104	SAV1	AJUBA	1.01	0.01
105	SAV1	WTIP	1.41	0.49
106	SAV1	TAOK1	2.56	1.36
107	SAV1	TAOK2	1.70	0.77
108	SAV1	TAOK3	1.00	0.00
109	SAV1	PARD3	1.00	0.00
110	SAV1	PARD6A	1.00	0.00
111	SAV1	PRKCZ	1.00	0.00
112	SAV1	ERBB4	1.00	0.00
113	MOB1A	YAP1	1.07	0.10
114	MOB1A	LATS1	3.97	1.99
115	MOB1A	LATS2	8.03	3.01
116	MOB1A	STK4	4.16	2.05
117	MOB1A	STK3	3.02	1.59
118	MOB1A	SAV1	1.60	0.68
119	MOB1A	MOB1A	1.58	0.66
120	MOB1A	RASSF1	1.26	0.33
121	MOB1A	RASSF2	1.78	0.83
122	MOB1A	RASSF6	1.70	0.76

123	MOB1A	NF2	1.00	0.00
124	MOB1A	WWC1	1.12	0.16
125	MOB1A	WWC2	1.29	0.37
126	MOB1A	WWC3	1.58	0.66
127	MOB1A	FRMD6	1.34	0.42
128	MOB1A	AMOT	2.64	1.40
129	MOB1A	AMOTL1	1.43	0.51
130	MOB1A	AMOTL2	1.28	0.35
131	MOB1A	PTPN14	1.58	0.66
132	MOB1A	AJUBA	1.02	0.03
133	MOB1A	WTIP	1.65	0.73
134	MOB1A	TAOK1	1.00	0.00
135	MOB1A	TAOK2	1.71	0.77
136	MOB1A	TAOK3	2.19	1.13
137	MOB1A	PARD3	1.00	0.00
138	MOB1A	PARD6A	1.00	0.00
139	MOB1A	PRKCZ	1.00	0.00
140	MOB1A	ERBB4	1.00	0.00
141	RASSF1	YAP1	1.64	0.71
142	RASSF1	LATS1	1.33	0.41
143	RASSF1	LATS2	1.58	0.66
144	RASSF1	STK4	42.45	5.41
145	RASSF1	STK3	33.88	5.08
146	RASSF1	SAV1	1.32	0.40
147	RASSF1	MOB1A	1.28	0.35
148	RASSF1	RASSF1	2.81	1.49
149	RASSF1	RASSF2	2.03	1.02
150	RASSF1	RASSF6	1.93	0.95
151	RASSF1	NF2	1.27	0.34
152	RASSF1	WWC1	1.36	0.44
153	RASSF1	WWC2	1.07	0.09
154	RASSF1	WWC3	1.00	0.00
155	RASSF1	FRMD6	1.04	0.06
156	RASSF1	AMOT	2.68	1.42
157	RASSF1	AMOTL1	1.00	0.00
158	RASSF1	AMOTL2	1.00	0.00
159	RASSF1	PTPN14	1.38	0.46
160	RASSF1	AJUBA	1.00	0.00

161	RASSF1	WTIP	1.17	0.22
162	RASSF1	TAOK1	1.00	0.00
163	RASSF1	TAOK2	1.00	0.00
164	RASSF1	TAOK3	1.00	0.00
165	RASSF1	PARD3	1.15	0.21
166	RASSF1	PARD6A	1.00	0.00
167	RASSF1	PRKCZ	1.00	0.00
168	RASSF1	ERBB4	1.00	0.00
169	RASSF2	YAP1	1.79	0.84
170	RASSF2	LATS1	1.49	0.58
171	RASSF2	LATS2	1.30	0.37
172	RASSF2	STK4	40.17	5.33
173	RASSF2	STK3	27.00	4.76
174	RASSF2	SAV1	1.45	0.54
175	RASSF2	MOB1A	1.38	0.46
176	RASSF2	RASSF1	1.17	0.23
177	RASSF2	RASSF2	1.84	0.88
178	RASSF2	RASSF6	1.97	0.97
179	RASSF2	NF2	1.45	0.53
180	RASSF2	WWC1	1.44	0.53
181	RASSF2	WWC2	1.55	0.63
182	RASSF2	WWC3	1.00	0.00
183	RASSF2	FRMD6	1.82	0.86
184	RASSF2	AMOT	2.57	1.36
185	RASSF2	AMOTL1	1.41	0.49
186	RASSF2	AMOTL2	1.38	0.47
187	RASSF2	PTPN14	1.45	0.53
188	RASSF2	AJUBA	1.00	0.00
189	RASSF2	WTIP	1.24	0.31
190	RASSF2	TAOK1	1.00	0.00
191	RASSF2	TAOK2	1.06	0.08
192	RASSF2	TAOK3	1.80	0.84
193	RASSF2	PARD3	1.00	0.00
194	RASSF2	PARD6A	1.00	0.00
195	RASSF2	PRKCZ	1.00	0.00
196	RASSF2	ERBB4	1.00	0.00
197	RASSF6	YAP1	1.26	0.33
198	RASSF6	LATS1	1.28	0.36

199	RASSF6	LATS2	1.00	0.00
200	RASSF6	STK4	8.81	3.14
201	RASSF6	STK3	7.97	3.00
202	RASSF6	SAV1	1.68	0.75
203	RASSF6	MOB1A	1.80	0.84
204	RASSF6	RASSF1	1.29	0.36
205	RASSF6	RASSF2	1.44	0.52
206	RASSF6	RASSF6	1.67	0.74
207	RASSF6	NF2	1.00	0.00
208	RASSF6	WWC1	1.00	0.00
209	RASSF6	WWC2	1.00	0.00
210	RASSF6	WWC3	1.00	0.00
211	RASSF6	FRMD6	1.22	0.29
212	RASSF6	AMOT	1.36	0.45
213	RASSF6	AMOTL1	1.47	0.56
214	RASSF6	AMOTL2	1.32	0.40
215	RASSF6	PTPN14	1.08	0.11
216	RASSF6	AJUBA	1.55	0.64
217	RASSF6	WTIP	1.17	0.23
218	RASSF6	TAOK1	1.00	0.00
219	RASSF6	TAOK2	1.00	0.00
220	RASSF6	TAOK3	2.22	1.15
221	RASSF6	PARD3	1.17	0.23
222	RASSF6	PARD6A	1.00	0.00
223	RASSF6	PRKCZ	1.00	0.00
224	RASSF6	ERBB4	1.00	0.00
225	NF2	YAP1	4.32	2.11
226	NF2	LATS1	6.35	2.67
227	NF2	LATS2	4.93	2.30
228	NF2	STK4	4.01	2.00
229	NF2	STK3	2.04	1.03
230	NF2	SAV1	1.89	0.92
231	NF2	MOB1A	1.61	0.69
232	NF2	RASSF1	1.92	0.94
233	NF2	RASSF2	4.40	2.14
234	NF2	RASSF6	2.04	1.03
235	NF2	NF2	24.11	4.59
236	NF2	WWC1	14.58	3.87

237	NF2	WWC2	5.05	2.34
238	NF2	WWC3	2.50	1.32
239	NF2	FRMD6	1.09	0.12
240	NF2	AMOT	14.23	3.83
241	NF2	AMOTL1	13.97	3.80
242	NF2	AMOTL2	19.72	4.30
243	NF2	PTPN14	8.23	3.04
244	NF2	AJUBA	1.09	0.13
245	NF2	WTIP	1.16	0.21
246	NF2	TAOK1	9.75	3.29
247	NF2	TAOK2	15.74	3.98
248	NF2	TAOK3	1.00	0.00
249	NF2	PARD3	1.00	0.00
250	NF2	PARD6A	1.00	0.00
251	NF2	PRKCZ	1.00	0.00
252	NF2	ERBB4	1.00	0.00
253	WWC1	YAP1	4.79	2.26
254	WWC1	LATS1	6.09	2.61
255	WWC1	LATS2	5.15	2.36
256	WWC1	STK4	6.58	2.72
257	WWC1	STK3	2.72	1.44
258	WWC1	SAV1	2.09	1.06
259	WWC1	MOB1A	1.59	0.67
260	WWC1	RASSF1	1.88	0.91
261	WWC1	RASSF2	4.50	2.17
262	WWC1	RASSF6	1.94	0.96
263	WWC1	NF2	6.52	2.70
264	WWC1	WWC1	18.01	4.17
265	WWC1	WWC2	22.13	4.47
266	WWC1	WWC3	7.74	2.95
267	WWC1	FRMD6	1.83	0.87
268	WWC1	AMOT	20.36	4.35
269	WWC1	AMOTL1	10.87	3.44
270	WWC1	AMOTL2	12.40	3.63
271	WWC1	PTPN14	12.27	3.62
272	WWC1	AJUBA	1.02	0.03
273	WWC1	WTIP	2.15	1.10
274	WWC1	TAOK1	21.12	4.40

275	WWC1	TAOK2	10.89	3.45
276	WWC1	TAOK3	1.00	0.00
277	WWC1	PARD3	19.46	4.28
278	WWC1	PARD6A	46.63	5.54
279	WWC1	PRKCZ	127.65	7.00
280	WWC1	ERBB4	13.12	3.71
281	WWC2	YAP1	3.17	1.67
282	WWC2	LATS1	3.10	1.63
283	WWC2	LATS2	2.34	1.23
284	WWC2	STK4	5.39	2.43
285	WWC2	STK3	1.03	0.05
286	WWC2	SAV1	1.00	0.00
287	WWC2	MOB1A	1.51	0.59
288	WWC2	RASSF1	1.00	0.00
289	WWC2	RASSF2	2.61	1.39
290	WWC2	RASSF6	1.10	0.13
291	WWC2	NF2	6.83	2.77
292	WWC2	WWC1	22.37	4.48
293	WWC2	WWC2	26.56	4.73
294	WWC2	WWC3	10.75	3.43
295	WWC2	FRMD6	2.58	1.37
296	WWC2	AMOT	44.49	5.48
297	WWC2	AMOTL1	24.89	4.64
298	WWC2	AMOTL2	21.84	4.45
299	WWC2	PTPN14	13.26	3.73
300	WWC2	AJUBA	1.72	0.79
301	WWC2	WTIP	1.58	0.66
302	WWC2	TAOK1	2.91	1.54
303	WWC2	TAOK2	1.00	0.00
304	WWC2	TAOK3	1.00	0.00
305	WWC2	PARD3	11.35	3.50
306	WWC2	PARD6A	7.53	2.91
307	WWC2	PRKCZ	1.00	0.00
308	WWC2	ERBB4	1.29	0.37
309	WWC3	YAP1	11.00	3.46
310	WWC3	LATS1	7.31	2.87
311	WWC3	LATS2	6.82	2.77
312	WWC3	STK4	10.17	3.35

313	WWC3	STK3	5.08	2.34
314	WWC3	SAV1	3.63	1.86
315	WWC3	MOB1A	1.58	0.66
316	WWC3	RASSF1	3.17	1.66
317	WWC3	RASSF2	5.17	2.37
318	WWC3	RASSF6	1.97	0.98
319	WWC3	NF2	3.50	1.81
320	WWC3	WWC1	9.84	3.30
321	WWC3	WWC2	15.15	3.92
322	WWC3	WWC3	3.65	1.87
323	WWC3	FRMD6	1.07	0.10
324	WWC3	AMOT	22.80	4.51
325	WWC3	AMOTL1	8.35	3.06
326	WWC3	AMOTL2	32.33	5.01
327	WWC3	PTPN14	12.53	3.65
328	WWC3	AJUBA	1.26	0.34
329	WWC3	WTIP	1.37	0.46
330	WWC3	TAOK1	1.00	0.00
331	WWC3	TAOK2	2.72	1.44
332	WWC3	TAOK3	10.60	3.41
333	WWC3	PARD3	1.00	0.00
334	WWC3	PARD6A	1.00	0.00
335	WWC3	PRKCZ	13.61	3.77
336	WWC3	ERBB4	2.43	1.28
337	FRMD6	YAP1	1.84	0.88
338	FRMD6	LATS1	1.79	0.84
339	FRMD6	LATS2	1.65	0.72
340	FRMD6	STK4	1.26	0.33
341	FRMD6	STK3	1.17	0.23
342	FRMD6	SAV1	1.89	0.92
343	FRMD6	MOB1A	1.20	0.26
344	FRMD6	RASSF1	1.06	0.09
345	FRMD6	RASSF2	1.15	0.20
346	FRMD6	RASSF6	1.86	0.90
347	FRMD6	NF2	1.31	0.38
348	FRMD6	WWC1	1.54	0.62
349	FRMD6	WWC2	1.00	0.00
350	FRMD6	WWC3	1.00	0.00

351	FRMD6	FRMD6	1.59	0.67
352	FRMD6	AMOT	2.74	1.45
353	FRMD6	AMOTL1	1.00	0.00
354	FRMD6	AMOTL2	1.17	0.22
355	FRMD6	PTPN14	1.11	0.15
356	FRMD6	AJUBA	1.41	0.49
357	FRMD6	WTIP	1.09	0.13
358	FRMD6	TAOK1	1.00	0.00
359	FRMD6	TAOK2	1.00	0.00
360	FRMD6	TAOK3	1.40	0.48
361	FRMD6	PARD3	2.44	1.28
362	FRMD6	PARD6A	1.00	0.00
363	FRMD6	PRKCZ	1.00	0.00
364	FRMD6	ERBB4	1.00	0.00
365	AMOT	YAP1	7.43	2.89
366	AMOT	LATS1	4.22	2.08
367	AMOT	LATS2	5.34	2.42
368	AMOT	STK4	6.10	2.61
369	AMOT	STK3	2.21	1.15
370	AMOT	SAV1	1.05	0.07
371	AMOT	MOB1A	1.02	0.03
372	AMOT	RASSF1	1.25	0.32
373	AMOT	RASSF2	5.06	2.34
374	AMOT	RASSF6	1.21	0.28
375	AMOT	NF2	20.72	4.37
376	AMOT	WWC1	14.26	3.83
377	AMOT	WWC2	14.68	3.88
378	AMOT	WWC3	7.22	2.85
379	AMOT	FRMD6	1.16	0.22
380	AMOT	AMOT	85.61	6.42
381	AMOT	AMOTL1	35.14	5.14
382	AMOT	AMOTL2	24.14	4.59
383	AMOT	PTPN14	9.04	3.18
384	AMOT	AJUBA	4.45	2.16
385	AMOT	WTIP	2.04	1.03
386	AMOT	TAOK1	1.32	0.40
387	AMOT	TAOK2	2.75	1.46
388	AMOT	TAOK3	3.97	1.99

389	AMOT	PARD3	1.42	0.51
390	AMOT	PARD6A	2.90	1.54
391	AMOT	PRKCZ	5.54	2.47
392	AMOT	ERBB4	1.35	0.44
393	AMOTL1	YAP1	6.92	2.79
394	AMOTL1	LATS1	2.68	1.42
395	AMOTL1	LATS2	3.20	1.68
396	AMOTL1	STK4	4.16	2.06
397	AMOTL1	STK3	1.87	0.90
398	AMOTL1	SAV1	1.16	0.21
399	AMOTL1	MOB1A	1.00	0.00
400	AMOTL1	RASSF1	1.00	0.00
401	AMOTL1	RASSF2	2.94	1.56
402	AMOTL1	RASSF6	1.54	0.62
403	AMOTL1	NF2	11.61	3.54
404	AMOTL1	WWC1	11.14	3.48
405	AMOTL1	WWC2	11.98	3.58
406	AMOTL1	WWC3	5.01	2.33
407	AMOTL1	FRMD6	1.60	0.68
408	AMOTL1	AMOT	59.31	5.89
409	AMOTL1	AMOTL1	21.19	4.41
410	AMOTL1	AMOTL2	7.62	2.93
411	AMOTL1	PTPN14	5.44	2.44
412	AMOTL1	AJUBA	2.82	1.50
413	AMOTL1	WTIP	1.93	0.95
414	AMOTL1	TAOK1	2.66	1.41
415	AMOTL1	TAOK2	1.00	0.00
416	AMOTL1	TAOK3	1.00	0.00
417	AMOTL1	PARD3	4.56	2.19
418	AMOTL1	PARD6A	1.00	0.00
419	AMOTL1	PRKCZ	1.00	0.00
420	AMOTL1	ERBB4	1.00	0.00
421	AMOTL2	YAP1	8.55	3.10
422	AMOTL2	LATS1	3.01	1.59
423	AMOTL2	LATS2	3.64	1.86
424	AMOTL2	STK4	5.93	2.57
425	AMOTL2	STK3	3.12	1.64
426	AMOTL2	SAV1	1.55	0.63

427	AMOTL2	MOB1A	1.41	0.49
428	AMOTL2	RASSF1	1.37	0.45
429	AMOTL2	RASSF2	3.73	1.90
430	AMOTL2	RASSF6	2.16	1.11
431	AMOTL2	NF2	20.80	4.38
432	AMOTL2	WWC1	7.43	2.89
433	AMOTL2	WWC2	15.39	3.94
434	AMOTL2	WWC3	12.40	3.63
435	AMOTL2	FRMD6	2.02	1.02
436	AMOTL2	AMOT	33.92	5.08
437	AMOTL2	AMOTL1	10.58	3.40
438	AMOTL2	AMOTL2	22.84	4.51
439	AMOTL2	PTPN14	4.89	2.29
440	AMOTL2	AJUBA	2.36	1.24
441	AMOTL2	WTIP	1.89	0.92
442	AMOTL2	TAOK1	4.76	2.25
443	AMOTL2	TAOK2	8.89	3.15
444	AMOTL2	TAOK3	5.22	2.38
445	AMOTL2	PARD3	1.00	0.00
446	AMOTL2	PARD6A	1.00	0.00
447	AMOTL2	PRKCZ	9.41	3.23
448	AMOTL2	ERBB4	1.00	0.00
449	PTPN14	YAP1	14.73	3.88
450	PTPN14	LATS1	6.43	2.68
451	PTPN14	LATS2	9.76	3.29
452	PTPN14	STK4	9.29	3.22
453	PTPN14	STK3	2.67	1.41
454	PTPN14	SAV1	2.26	1.17
455	PTPN14	MOB1A	1.62	0.70
456	PTPN14	RASSF1	2.42	1.28
457	PTPN14	RASSF2	6.17	2.63
458	PTPN14	RASSF6	1.83	0.87
459	PTPN14	NF2	15.49	3.95
460	PTPN14	WWC1	20.19	4.34
461	PTPN14	WWC2	29.15	4.87
462	PTPN14	WWC3	14.12	3.82
463	PTPN14	FRMD6	3.66	1.87
464	PTPN14	AMOT	15.93	3.99

465	PTPN14	AMOTL1	7.14	2.84
466	PTPN14	AMOTL2	10.31	3.37
467	PTPN14	PTPN14	8.71	3.12
468	PTPN14	AJUBA	7.19	2.85
469	PTPN14	WTIP	2.40	1.26
470	PTPN14	TAOK1	1.00	0.00
471	PTPN14	TAOK2	1.00	0.00
472	PTPN14	TAOK3	12.10	3.60
473	PTPN14	PARD3	1.00	0.00
474	PTPN14	PARD6A	1.00	0.00
475	PTPN14	PRKCZ	15.95	4.00
476	PTPN14	ERBB4	1.00	0.00
477	AJUBA	YAP1	1.67	0.74
478	AJUBA	LATS1	3.81	1.93
479	AJUBA	LATS2	2.92	1.54
480	AJUBA	STK4	1.58	0.66
481	AJUBA	STK3	1.35	0.44
482	AJUBA	SAV1	1.27	0.34
483	AJUBA	MOB1A	1.03	0.04
484	AJUBA	RASSF1	1.22	0.28
485	AJUBA	RASSF2	2.12	1.08
486	AJUBA	RASSF6	1.45	0.54
487	AJUBA	NF2	3.33	1.74
488	AJUBA	WWC1	3.16	1.66
489	AJUBA	WWC2	4.51	2.17
490	AJUBA	WWC3	2.04	1.03
491	AJUBA	FRMD6	4.32	2.11
492	AJUBA	AMOT	9.82	3.30
493	AJUBA	AMOTL1	4.01	2.00
494	AJUBA	AMOTL2	4.16	2.06
495	AJUBA	PTPN14	3.18	1.67
496	AJUBA	AJUBA	2.39	1.26
497	AJUBA	WTIP	2.15	1.11
498	AJUBA	TAOK1	1.00	0.00
499	AJUBA	TAOK2	1.92	0.94
500	AJUBA	TAOK3	3.46	1.79
501	AJUBA	PARD3	1.00	0.00
502	AJUBA	PARD6A	1.00	0.00

503	AJUBA	PRKCZ	2.55	1.35
504	AJUBA	ERBB4	1.07	0.10
505	WTIP	YAP1	5.81	2.54
506	WTIP	LATS1	12.92	3.69
507	WTIP	LATS2	14.58	3.87
508	WTIP	STK4	8.13	3.02
509	WTIP	STK3	2.73	1.45
510	WTIP	SAV1	2.42	1.28
511	WTIP	MOB1A	1.37	0.45
512	WTIP	RASSF1	2.65	1.41
513	WTIP	RASSF2	4.94	2.30
514	WTIP	RASSF6	1.99	0.99
515	WTIP	NF2	2.82	1.50
516	WTIP	WWC1	9.64	3.27
517	WTIP	WWC2	7.06	2.82
518	WTIP	WWC3	3.96	1.99
519	WTIP	FRMD6	1.98	0.99
520	WTIP	AMOT	10.15	3.34
521	WTIP	AMOTL1	7.08	2.82
522	WTIP	AMOTL2	8.07	3.01
523	WTIP	PTPN14	6.82	2.77
524	WTIP	AJUBA	3.84	1.94
525	WTIP	WTIP	3.67	1.88
526	WTIP	TAOK1	1.26	0.33
527	WTIP	TAOK2	2.34	1.23
528	WTIP	TAOK3	6.48	2.70
529	WTIP	PARD3	9.23	3.21
530	WTIP	PARD6A	1.00	0.00
531	WTIP	PRKCZ	5.49	2.46
532	WTIP	ERBB4	1.00	0.00
533	TAOK1	YAP1	1.73	0.79
534	TAOK1	LATS1	1.00	0.00
535	TAOK1	LATS2	1.00	0.00
536	TAOK1	STK4	1.35	0.43
537	TAOK1	STK3	1.83	0.87
538	TAOK1	SAV1	1.00	0.00
539	TAOK1	MOB1A	1.14	0.19
540	TAOK1	RASSF1	1.00	0.00

541	TAOK1	RASSF2	1.00	0.00
542	TAOK1	RASSF6	1.03	0.05
543	TAOK1	NF2	1.27	0.34
544	TAOK1	WWC1	1.00	0.00
545	TAOK1	WWC2	1.09	0.12
546	TAOK1	WWC3	1.00	0.00
547	TAOK1	FRMD6	1.00	0.00
548	TAOK1	AMOT	2.21	1.15
549	TAOK1	AMOTL1	1.02	0.02
550	TAOK1	AMOTL2	1.43	0.52
551	TAOK1	PTPN14	1.13	0.17
552	TAOK1	AJUBA	1.00	0.00
553	TAOK1	WTIP	1.10	0.14
554	TAOK1	TAOK1	1.88	0.91
555	TAOK1	TAOK2	4.30	2.11
556	TAOK1	TAOK3	1.25	0.33
557	TAOK1	PARD3	1.00	0.00
558	TAOK1	PARD6A	1.36	0.44
559	TAOK1	PRKCZ	1.00	0.00
560	TAOK1	ERBB4	1.00	0.00
561	TAOK2	YAP1	2.64	1.40
562	TAOK2	LATS1	5.14	2.36
563	TAOK2	LATS2	2.75	1.46
564	TAOK2	STK4	12.32	3.62
565	TAOK2	STK3	5.21	2.38
566	TAOK2	SAV1	2.32	1.21
567	TAOK2	MOB1A	4.13	2.05
568	TAOK2	RASSF1	4.06	2.02
569	TAOK2	RASSF2	8.09	3.02
570	TAOK2	RASSF6	2.71	1.44
571	TAOK2	NF2	2.06	1.04
572	TAOK2	WWC1	6.13	2.62
573	TAOK2	WWC2	2.39	1.26
574	TAOK2	WWC3	1.25	0.32
575	TAOK2	FRMD6	2.73	1.45
576	TAOK2	AMOT	14.80	3.89
577	TAOK2	AMOTL1	2.58	1.37
578	TAOK2	AMOTL2	1.67	0.74

579	TAOK2	PTPN14	4.03	2.01
580	TAOK2	AJUBA	2.13	1.09
581	TAOK2	WTIP	1.36	0.44
582	TAOK2	TAOK1	18.25	4.19
583	TAOK2	TAOK2	14.82	3.89
584	TAOK2	TAOK3	1.00	0.00
585	TAOK2	PARD3	1.00	0.00
586	TAOK2	PARD6A	2.15	1.11
587	TAOK2	PRKCZ	3.33	1.73
588	TAOK2	ERBB4	1.00	0.00
589	TAOK3	YAP1	2.00	1.00
590	TAOK3	LATS1	1.67	0.74
591	TAOK3	LATS2	2.29	1.20
592	TAOK3	STK4	2.50	1.32
593	TAOK3	STK3	1.75	0.81
594	TAOK3	SAV1	1.41	0.49
595	TAOK3	MOB1A	1.49	0.57
596	TAOK3	RASSF1	1.27	0.35
597	TAOK3	RASSF2	2.35	1.23
598	TAOK3	RASSF6	1.53	0.61
599	TAOK3	NF2	1.00	0.00
600	TAOK3	WWC1	1.00	0.00
601	TAOK3	WWC2	1.00	0.00
602	TAOK3	WWC3	1.00	0.00
603	TAOK3	FRMD6	1.02	0.03
604	TAOK3	AMOT	1.71	0.78
605	TAOK3	AMOTL1	1.00	0.00
606	TAOK3	AMOTL2	1.00	0.00
607	TAOK3	PTPN14	1.00	0.00
608	TAOK3	AJUBA	1.00	0.00
609	TAOK3	WTIP	1.00	0.00
610	TAOK3	TAOK1	3.92	1.97
611	TAOK3	TAOK2	1.77	0.83
612	TAOK3	TAOK3	1.00	0.00
613	TAOK3	PARD3	1.00	0.00
614	TAOK3	PARD6A	1.00	0.00
615	TAOK3	PRKCZ	1.97	0.98
616	TAOK3	ERBB4	1.00	0.00

617	PARD3	YAP1	6.94	2.79
618	PARD3	LATS1	7.34	2.88
619	PARD3	LATS2	4.30	2.10
620	PARD3	STK4	13.62	3.77
621	PARD3	STK3	3.21	1.68
622	PARD3	SAV1	1.72	0.78
623	PARD3	MOB1A	1.33	0.41
624	PARD3	RASSF1	2.61	1.38
625	PARD3	RASSF2	7.08	2.82
626	PARD3	RASSF6	1.56	0.64
627	PARD3	NF2	2.17	1.12
628	PARD3	WWC1	4.46	2.16
629	PARD3	WWC2	3.46	1.79
630	PARD3	WWC3	3.16	1.66
631	PARD3	FRMD6	3.57	1.84
632	PARD3	AMOT	2.90	1.54
633	PARD3	AMOTL1	1.00	0.00
634	PARD3	AMOTL2	1.59	0.67
635	PARD3	PTPN14	1.82	0.87
636	PARD3	AJUBA	1.72	0.78
637	PARD3	WTIP	1.22	0.29
638	PARD3	TAOK1	1.00	0.00
639	PARD3	TAOK2	1.00	0.00
640	PARD3	TAOK3	8.70	3.12
641	PARD3	PARD3	5.34	2.42
642	PARD3	PARD6A	1.00	0.00
643	PARD3	PRKCZ	1.00	0.00
644	PARD3	ERBB4	3.76	1.91
645	PARD6A	YAP1	2.69	1.43
646	PARD6A	LATS1	2.19	1.13
647	PARD6A	LATS2	2.43	1.28
648	PARD6A	STK4	3.57	1.84
649	PARD6A	STK3	1.57	0.65
650	PARD6A	SAV1	1.75	0.80
651	PARD6A	MOB1A	1.38	0.47
652	PARD6A	RASSF1	1.55	0.63
653	PARD6A	RASSF2	2.89	1.53
654	PARD6A	RASSF6	2.05	1.04

655	PARD6A	NF2	1.41	0.49
656	PARD6A	WWC1	2.64	1.40
657	PARD6A	WWC2	1.75	0.81
658	PARD6A	WWC3	1.52	0.60
659	PARD6A	FRMD6	1.11	0.16
660	PARD6A	AMOT	2.54	1.35
661	PARD6A	AMOTL1	1.21	0.28
662	PARD6A	AMOTL2	1.41	0.50
663	PARD6A	PTPN14	1.64	0.71
664	PARD6A	AJUBA	1.20	0.26
665	PARD6A	WTIP	1.45	0.54
666	PARD6A	TAOK1	1.00	0.00
667	PARD6A	TAOK2	1.00	0.00
668	PARD6A	TAOK3	13.46	3.75
669	PARD6A	PARD3	5.46	2.45
670	PARD6A	PARD6A	1.00	0.00
671	PARD6A	PRKCZ	13.78	3.78
672	PARD6A	ERBB4	1.00	0.00
673	PRKCZ	YAP1	3.87	1.95
674	PRKCZ	LATS1	2.45	1.29
675	PRKCZ	LATS2	2.88	1.53
676	PRKCZ	STK4	4.34	2.12
677	PRKCZ	STK3	1.47	0.56
678	PRKCZ	SAV1	1.68	0.75
679	PRKCZ	MOB1A	1.16	0.21
680	PRKCZ	RASSF1	1.41	0.50
681	PRKCZ	RASSF2	2.79	1.48
682	PRKCZ	RASSF6	1.64	0.71
683	PRKCZ	NF2	1.92	0.94
684	PRKCZ	WWC1	7.39	2.89
685	PRKCZ	WWC2	3.38	1.76
686	PRKCZ	WWC3	2.19	1.13
687	PRKCZ	FRMD6	1.44	0.52
688	PRKCZ	AMOT	4.24	2.09
689	PRKCZ	AMOTL1	1.80	0.85
690	PRKCZ	AMOTL2	1.67	0.74
691	PRKCZ	PTPN14	2.49	1.32
692	PRKCZ	AJUBA	1.00	0.00

693	PRKCZ	WTIP	1.43	0.52
694	PRKCZ	TAOK1	1.00	0.00
695	PRKCZ	TAOK2	5.41	2.44
696	PRKCZ	TAOK3	19.04	4.25
697	PRKCZ	PARD3	3.91	1.97
698	PRKCZ	PARD6A	1.00	0.00
699	PRKCZ	PRKCZ	154.79	7.27
700	PRKCZ	ERBB4	2.19	1.13
701	ERBB4	YAP1	19.03	4.25
702	ERBB4	LATS1	13.01	3.70
703	ERBB4	LATS2	11.00	3.46
704	ERBB4	STK4	24.80	4.63
705	ERBB4	STK3	4.63	2.21
706	ERBB4	SAV1	4.54	2.18
707	ERBB4	MOB1A	1.09	0.13
708	ERBB4	RASSF1	4.53	2.18
709	ERBB4	RASSF2	15.00	3.91
710	ERBB4	RASSF6	1.78	0.83
711	ERBB4	NF2	28.59	4.84
712	ERBB4	WWC1	34.54	5.11
713	ERBB4	WWC2	23.04	4.53
714	ERBB4	WWC3	11.23	3.49
715	ERBB4	FRMD6	12.23	3.61
716	ERBB4	AMOT	5.04	2.33
717	ERBB4	AMOTL1	1.47	0.55
718	ERBB4	AMOTL2	4.43	2.15
719	ERBB4	PTPN14	13.59	3.76
720	ERBB4	AJUBA	7.67	2.94
721	ERBB4	WTIP	2.02	1.01
722	ERBB4	TAOK1	1.00	0.00
723	ERBB4	TAOK2	1.00	0.00
724	ERBB4	TAOK3	6.21	2.63
725	ERBB4	PARD3	13.92	3.80
726	ERBB4	PARD6A	1.00	0.00
727	ERBB4	PRKCZ	1.00	0.00
728	ERBB4	ERBB4	17.49	4.13

Table S3: Detailed information of cis-regulatory sensors

Response Element (RE) name	full RE / promoter name	Category	Pathway
UPRE-v2-MLP	Unfolded protein RE	Cellular stress	Unfolded protein response
sEGFP-hIL6p	Interleukin 6 promoter	Immune response	cytokine Signaling, immune response
sEGFP-hIL8p	Interleukin 8 promoter	Immune response	cytokine Signaling, immune response
NFkB-RE-v2-MLP	nuclear factor of kappa light polypeptide gene enhancer in B-cells RE	Immune response	NFkB / cytokines; also MAPK / DEG response…
CRE-MLP	cAMP RE	Synaptic activity, calcium Signaling	cAMP - PKA
SARE-MLP	Synaptic activity RE	Synaptic activity, calcium Signaling / IEG	Ca2+, cAMP Signaling
SRE-MLP	Serum RE	IEG response (in neurons: synaptic activity)	MAPK / IEG response
AP1-v1-MLP	activator protein 1 RE	IEG response (in neurons: synaptic activity)	MAPK / IEG response
sEGFP-hDUSP5p	Dual specificity phosphatase 5 promoter	IEG response (in neurons: synaptic activity)	MAPK / IEG response
sEGFP-hEGR1p	Early growth response 1 promoter	IEG response (in neurons: synaptic activity)	MAPK / IEG response
sEGFP-hEGR2p	Early growth response 2 promoter	IEG response (in neurons: synaptic activity)	MAPK / IEG response
sEGFP-hFOSBp	FBJ murine osteosarcoma viral oncogene homolog B promoter	IEG response (in neurons: synaptic activity)	MAPK / IEG response
sEGFP-hFOSp	FBJ murine osteosarcoma viral oncogene homolog promoter	IEG response (in neurons: synaptic activity)	MAPK / IEG response
sEGFP-hNR4A1p	Nuclear receptor subfamily 4, group A, member 1 promoter	IEG response (in neurons: synaptic activity)	MAPK / IEG response
sEGFP-MLP	Adenoviral major late promoter	background control	
MRE-MLP	Metal RE	Cellular stress	metal homeostasis
SREBP-RE-v2-MLP	sterol regulatory element-binding protein RE	Metabolism	cholesterol, insulin
CEBP-RE-v1-MLP	CCAAT/enhancer binding protein RE	Metabolism	general regulation of metabolism
E2F-RE-v2-MLP	E2F (family) transcription factor RE	Cell fate	G1/S Check Point

TEAD4-RE-v4-MLP	TEA domain family member RE	Cell fate	Hippo - YAP/TAZ
sEGFP-hEIF2AK2p	Eukaryotic translation initiation factor 2-alpha kinase 2 promoter	Immune response	JAK - STAT1, interferon
sEGFP-hTNFAp	Tumour necrosis factor alpha promoter	Synaptic activity, calcium Signaling	CREB, PKA, other
sEGFP-hDUSP1p	Dual specificity phosphatase 1 promoter	IEG response (in neurons: synaptic activity)	MAPK / IEG response

Table S4: Univariate ANOVA Type II Wilk's

variable	term	F	p	annot	p_adj	annot_adj
Meanspeed	G	3.726548	0.057665	p<0.1	0.313398	n.s.
Meanspeed	E	8.018176	0.006064	**	0.065841	p<0.1
Meanspeed	G:E	0.270271	0.604814	n.s.	0.969312	n.s.
Rotations	G	2.692561	0.105369	n.s.	0.429001	n.s.
Rotations	E	8.888845	0.003961	**	0.057118	p<0.1
Rotations	G:E	0.199964	0.656151	n.s.	0.969312	n.s.
Center	G	3.642573	0.06048	p<0.1	0.313398	n.s.
Center	E	0.007885	0.929502	n.s.	0.969312	n.s.
Center	G:E	0.102472	0.74985	n.s.	0.969312	n.s.
Alternations	G	0.307648	0.580921	n.s.	0.969312	n.s.
Alternations	E	1.127427	0.292027	n.s.	0.756616	n.s.
Alternations	G:E	0.962767	0.329919	n.s.	0.817624	n.s.
Choices	G	9.064249	0.003639	**	0.057118	p<0.1
Choices	E	0.041979	0.838263	n.s.	0.969312	n.s.
Choices	G:E	0.149064	0.70062	n.s.	0.969312	n.s.
Context	G	0.009845	0.921249	n.s.	0.969312	n.s.
Context	E	0.356614	0.552347	n.s.	0.969312	n.s.
Context	G:E	0.105283	0.746562	n.s.	0.969312	n.s.
Cue	G	0.016047	0.899565	n.s.	0.969312	n.s.
Cue	E	2.405426	0.12549	n.s.	0.476863	n.s.
Cue	G:E	0.008513	0.926756	n.s.	0.969312	n.s.
FreezeBase	G	0.001927	0.965115	n.s.	0.969312	n.s.
FreezeBase	E	1.570028	0.214433	n.s.	0.611133	n.s.
FreezeBase	G:E	0.01303	0.909451	n.s.	0.969312	n.s.
Timeimmobile	G	0.007023	0.933455	n.s.	0.969312	n.s.
Timeimmobile	E	0.1813	0.671584	n.s.	0.969312	n.s.
Timeimmobile	G:E	2.294269	0.13442	n.s.	0.478872	n.s.
SucPref	G	0.088839	0.766554	n.s.	0.969312	n.s.
SucPref	E	7.748425	0.006931	**	0.065841	p<0.1

SucPref	G:E	0.206925	0.650616	n.s.	0.969312	n.s.
PlacePref	G	3.763424	0.056473	p<0.1	0.313398	n.s.
PlacePref	E	36.15976	7.73E-08	***	4.41E-06	***
PlacePref	G:E	0.340255	0.561584	n.s.	0.969312	n.s.
ReversalLearn	G	1.645456	0.203871	n.s.	0.611133	n.s.
ReversalLearn	E	0.001491	0.969312	n.s.	0.969312	n.s.
ReversalLearn	G:E	1.331804	0.252466	n.s.	0.685265	n.s.
SerialLearn	G	0.016104	0.899388	n.s.	0.969312	n.s.
SerialLearn	E	4.469882	0.038113	*	0.271557	n.s.
SerialLearn	G:E	0.635065	0.428237	n.s.	0.904056	n.s.
Activity	G	0.184632	0.668761	n.s.	0.969312	n.s.
Activity	E	8.86458	0.004008	**	0.057118	p<0.1
Activity	G:E	3.2996	0.07364	p<0.1	0.331826	n.s.
Nocturnal	G	0.865045	0.355573	n.s.	0.841676	n.s.
Nocturnal	E	0.239444	0.62616	n.s.	0.969312	n.s.
Nocturnal	G:E	0.006437	0.936288	n.s.	0.969312	n.s.
Baseline	G	3.252517	0.07568	p<0.1	0.331826	n.s.
Baseline	E	0.066903	0.796671	n.s.	0.969312	n.s.
Baseline	G:E	0.005689	0.940097	n.s.	0.969312	n.s.
inhibition70	G	0.109486	0.741733	n.s.	0.969312	n.s.
inhibition70	E	0.006347	0.936734	n.s.	0.969312	n.s.
inhibition70	G:E	4.628874	0.034941	*	0.271557	n.s.
inhibition75	G	0.817164	0.369156	n.s.	0.841676	n.s.
inhibition75	E	0.309711	0.579658	n.s.	0.969312	n.s.
inhibition75	G:E	2.103883	0.151456	n.s.	0.479612	n.s.
inhibition80	G	2.185464	0.14387	n.s.	0.479612	n.s.
inhibition80	E	0.722629	0.398223	n.s.	0.873028	n.s.
inhibition80	G:E	0.083067	0.774047	n.s.	0.969312	n.s.

Acknowledgements

First, I would like to show my greatest appreciation to PD Dr. Michael Wehr. I feel so lucky to have you as my supervisor during my PhD phase. I feel very grateful for your supervision and support in the last few years. I am always impressed by your meticulous attitude toward research work, your diligence, your excellent time management ability and your extremely high emotional intelligence. Also, I am always enlightened by the ideas and suggestions you give to me. You not only teach me how to perform scientific research, but also guide me to surpass myself and achieve my goals in life. You encouraged me to express myself freely and helped me to reshape my confidence, which benefits me a lot. Of course, sometimes you may be a bit strict to me and I feel a little overwhelmed. But it is just this kind of practice that makes me realize I have more potentials than what I expected.

Then I would like to express my great thanks to Prof. Moritz Rossner. Thank you for always giving me very useful suggestions for my projects and inspiring me to look at my research work in a different way.

In addition, I really need to thank Vivek Sahoo for sharing your experience on science with me and comforting me in my depression time. I feel really very appreciated to have you as my colleague and friend. Specially, I would like to express my gratitude to Nirmal Kannaiyan and Marius Stephan for help me process my data and give me suggestions to show my results in a more professional way. Also I must convey my sincere thanks to Barbara Meisel, Monika Rübekeil and Johanna Zahn for their help of lab work, to Beate Kauschat for the primary neuron cultures, to Dr. Ben Brankatschk, Dr. Sven Wichert, Karin Neumeier, and Stefanie Behrens for helping me finish the cisProlifer assay.

Last but not least, I need to express my sincerest thanks to my husband, Dr. Jiajun Qiu. Thank you very much for your consistent support and love for the last few years. Thank you for accompanying me to go through the ups and downs of life. Thank you for the patience and consideration you give to me. And thank you for always take my demand as your first consideration. I think going abroad to pursue a doctor degree together with you is the best thing that I have done.